Development of cell-based assays for testing Clostridial Neurotoxins

By:

Deniz Simsek

A thesis submitted in partial fulfilment of the requirements for the degree of Doctor of Philosophy

March 2023

The University of Sheffield

Faculty of Science

School of Bioscience

Abstract

Clostridial neurotoxins are protein structures generated by a bacterium. Clostridial neurotoxins consist of botulinum neurotoxin, with its serotypes, and tetanus neurotoxin. A small amount of these proteins is lethal as they cause muscle paralysis. However, safe doses are used for cosmetic and medical purposes. Due to their potency, it is essential to develop a sensitive assay to detect small amounts of the neurotoxins for several reasons. Firstly, safe doses should be determined before releasing them as medical or cosmetic treatments. Secondly, it is important to test food products in order to prevent food poisoning. Thirdly, neurotoxins could be used as a bioweapon, so detection of small amounts is necessary for security. Currently, the mouse bioassay is the international gold standard test. However, it has many drawbacks. The test is expensive, time-consuming, requires advanced facilities and skills, and, most importantly, raises ethical issues in relation to animal welfare. Approximately 100 mice are killed in every test and experience significant suffering. Therefore, developing a fast, cheap, and sensitive replacement assay which adheres to 3Rs (Replace, Refine, and Reduce animals in research) principles is essential. A main aim of this project is to develop a replacement assay for sensitive detection of clostridial neurotoxins to fulfil this gap. In this project, neuroblastoma cells are mainly used to test clostridial toxin activity, and this involves 3Rs principles. Several neuroblastoma cell lines are generated through the project to get better results for toxin sensitivity. The neurotoxins are first tested by immunoblotting whether the toxin could cleave target proteins in neuroblastoma cell lines. However, a one-step ELISA method is developed to measure toxin level in a faster and more practical way. Immunocytochemistry and immunoblotting techniques are used to characterise neuroblastoma cell lines to confirm why they are sensitive to the clostridial neurotoxins. It was found that neuroblastoma cell lines are quite sensitive for testing most of the clostridial neurotoxins. In particular, BoNT/A, BoNT/B, BoNT/C, BoNT/DC, and TeNT activities could be measured quickly and sensitively in neuroblastoma cell lines. Neuroblastoma cells are promising for developing a cell-based assay to replace the mouse assay for most of the clostridial neurotoxins. The cell-based assay developed in this research is quite sensitive, however there is still room to improve sensitivity. Moreover, this assay allows for the detection of all steps of clostridial intoxication: Toxin-receptor binding, translocation of toxin inside cells and SNARE cleavage by toxin. Previous studies use SiMa human neuroblastoma cell line for botulinum neurotoxin A and botulinum neurotoxin B activities. However, this research has introduced a new sensitive neuroblastoma cell line for clostridial neurotoxins, the LAN-5 human neuroblastoma cell. My research has contributed more knowledge about the relationship between neuroblastoma cells and clostridial neurotoxins. I have also introduced other cell type, HeLa cells, for

BoNT/B potency. To conclude, this PhD study discovered new sensitive cell lines to test clostridial neurotoxin potency. This is promising for the development of sensitive replacement cell-based assays.

Table of Contents

Tables and Figures

List of abbreviations

3Rs	Refine, reduce, and replace animal use in research
AA	Amino acid
ANOVA	Analysis of Variance
BiTox/A	SNARE-stapled chimera constructed from LcTd/A conjugated to Rbd/A
BiTox/C	SNARE-stapled chimera constructed from LcTd/A conjugated to Rbd/C
BiTox/D	SNARE-stapled chimera constructed from LcTd/A conjugated to Rbd/D
BiTox/E	SNARE-stapled chimera constructed from LcTd/A conjugated to Rbd/E
BoNT	Botulinum Neurotoxin
BoNT/A	Botulinum Neurotoxin, Serotype A
BoNT/B	Botulinum Neurotoxin, Serotype B
BoNT/C	Botulinum Neurotoxin, Serotype C
BoNT/D	Botulinum Neurotoxin, Serotype D
BoNT/DC	Botulinum Neurotoxin, Serotype DC
BSA	Bovine serum albumin
CI	Confidence interval
CNS	Central nervous system
CNT	Clostridial neurotoxins
c-VAMP	Cytosolic VAMP
DAPI	4’,6-diamidino-2-phenylindole
DMEM	Dulbecco’s modified Eagle medium
EC50	Half maximal effective concentration
ECL	Electrochemiluminescence
EDTA	Ethylenediaminetetraacetic acid
EGF	Epidermal growth factor
ELISA	Enzyme-linked immunosorbent assay
ESC	Embryonic stem cells
FBS	Foetal bovine serum
FDA	Food and drug administration
GABA	Gamma-aminobutyric acid
GBS	Ganglioside binding site
H_2O	Deionized water
H_C	Binding domain

HC	Heavy chain
H_N	Translocation domain
hiPSC	Human induced pluripotent stem cells
ICC	Immunocytochemistry
LC	Light chain
Lc-H_N	Light chain and translocation domain
LcTd	Light chain and translocation domain
LD50	The dosage at which 50% of mice are expected to die
M	Molar concentration per litre
MBA	Mouse bioassay
MES	2-(N-morpholino) ethane sulfonic acid
$MgCl_2$	Magnesium Chloride
mL	Millilitre
msec	Millisecond
MSC	Mouse spinal cords
mV	Millivolts
n	Number of repeats within an experiment
N	Number of separate experiments
NGF	Nerve growth factor
NMJ	Neuromuscular junction
NS	Not significant
PBS	Phosphate-buffered saline
PCR	Polymerase chain reaction
PDB	Protein data bank
PEI	Polyethyleneimine
PFA	Paraformaldehyde
R^2	Goodness of fit
RA	Retinoic acid
Rbd	Receptor binding domain
RCF	Relative centrifugal force
RSC	Rat spinal cords
SDS	Sodium dodecyl sulphate
S.E.M.	Standard error of mean
SNAP23	Synaptosomal-associated protein 23

SNAP25	Synaptosomal-associated protein 25
SNARE	Soluble N-ethylmaleimide sensitive factor attachment protein receptor
SV2	Synaptic vesicle protein 2
SV2A	Synaptic vesicle protein 2 Isoform A
SV2B	Synaptic vesicle protein 2 Isoform B
SV2C	Synaptic vesicle protein 2 Isoform C
SYT	Synaptotagmin
SYTI	Synaptotagmin I
SYTII	Synaptotagmin II
TeNT	Tetanus Neurotoxin
Tet-Bot	SNARE-stapled chimera constructed from LcTd/A conjugated to Rbd/TeNT
Td	Translocation domain
U	Units of CNT potency: 1U corresponds to one LD50 in mouse bioassay
v/v	Volume/Volume percentage
v-VAMP	Vesicular VAMP
VAMP	Vesicle associated membrane protein
vATPase	Vacuolar (H+) adenosine triphosphatase
VSV-G	Vesicular stomatitis virus G
WB	Western blot
w/v	Weight/Volume percentage

Acknowledgements 1

Öncelikle İngiltere'de doktora yapma imkânını bana veren Türkiye Cumhuriyeti Devleti'ne sonsuz teşekkürlerimi sunarım. Doktora suresince çalışmalarımın tümü Türkiye Cumhuriyeti Devleti'nin sponsorluğu ve desteği ile yapılmıştır. Bana verilen bu imkânı en iyi şekilde değerlendirmiş olmayı umuyorum ve sonsuz teşekkürlerimi sunuyorum.

First and foremost, I would like to express my deepest gratitude to the Government of the Republic of Turkey for giving me the opportunity to do my PhD in the UK. All of my studies during my PhD were carried out with the sponsorship and support of the Republic of Turkey. I hope to have made the best use of this opportunity given to me and I express my endless thanks.

Deniz Simsek

01.03.2023

Acknowledgements 2

I would like to acknowledge my previous supervisor, Bazbek Davletov, for allowing me to work in his lab and project, and for his support during this time. My sincere gratitude reaches out to all the members of the Davletov lab, who are always happy to share their knowledge and experiences with me. Thank you to Charlotte Leese for teaching me cell culture techniques, western blot and for your endless support and patience over the years. Thank you to Ciara Doran for your cell culture advice. Thank you to Ceyda Caliskan for teaching me various cell culture techniques and suggestions and for friendship.

I would like to thank my advisor Andrew Peden for his invaluable advice and guidance, as well as for donating antibodies and cell lines. I would also want to acknowledge his lab members for always helping to troubleshoot and sharing their reagents and equipment. I would like to thank Liz Seward, my advisor, and also my supervisor during my final year, for her helpful support and reassurance.

Thank you to my thesis mentor, Rhiannon Jones, for her support and help to start writing my thesis during my final year.

A massive thank to my friends and family for their constant support and love during the project. Thank you to my mother, Kubra Simsek, and my father Mehmet Simsek, for always believing in me and encouraging me. I have always felt your constant love and support even though you are miles away from me. I love you both. Thank you to my sister Esra Simsek, for your endless encouragement and support throughout my life. Our phone calls including Firat Ocal and our lovely cat Benji consistently kept me entertained and made me feel at home after tiring lab days. I love all of you. Thank you to my boyfriend Sam Walker for his endless support. You always believe in and encourage me, not just for my project but also for all other aspects of my life. Our adventures and laughs together made me alive and happy during this project. I love you.

In closing, I would like to thank everyone who has supported me throughout this journey.

Declaration

I declare that all data of this thesis have been completed by me, the author. Some stable cell lines, proteins, plasmids, and reagents that are helpfully provided by others. A thorough reference and acknowledgment of any work carried out by others has been included throughout the text.

1 Chapter 1: Introduction

1.1 Clostridial neurotoxins

The clostridial neurotoxins (CNTs), protein structures produced by anaerobic bacteria, consist of tetanus neurotoxin (TeNT) and seven main serotypes of botulinum neurotoxin (BoNTs) named from A to G (Montecucco and Schiavo, 1995). BoNTs and TeNT are produced by *Clostridium botulinum* and *Clostridium tetani*, respectively. *Clostridium butyricum* and *Clostridium barati* are also found to synthesize some of the BoNT serotypes (Rasetti-Escargueil and Popoff, 2022). BoNT and TeNT both cause cell intoxication by inhibiting neurotransmitter release (Lacy and Stevens, 1999) and, as a result of their absolute neurospecificity and catalytic activity, are the most poisonous toxins known to man. Specifically, they attach to the presynaptic terminals of motor neurons at the neuromuscular junctions (NMJs). In addition, they can bind to the synaptic terminals of sensory and adrenergic neurons (Montecucco and Schiavo, 1995). Upon entering the neuronal cells from the presynaptic terminal, BoNTs inhibit acetylcholine (Ach) release which results in flaccid muscle paralysis, causing a lethal disease called botulism. In the case of TeNT, after binding to the presynaptic terminal, it travels via retrograde transport up the axon and enters inhibitory interneurons to affect the central nervous system (CNS). There, it blocks the release of inhibitory (gamma-aminobutyric acid (GABA) and glycine) neurotransmitters, causing spastic paralysis (hypercontraction of skeletal muscles), which leads to tetanus (Montecucco and Schiavo, 1995, Lacy and Stevens, 1999, Dong et al., 2019). The intracellular pathway of BoNT and TeNT is shown schematically in Figure 1.1. As a result of these differing pathways, the peripheral site of action of BoNT and the central site of action of TeNT cause opposite clinical symptoms. While BoNTs and TeNT present different clinical symptoms, both share a common mechanism of action and a high degree of sequence and structural homology (Turton et al., 2002).

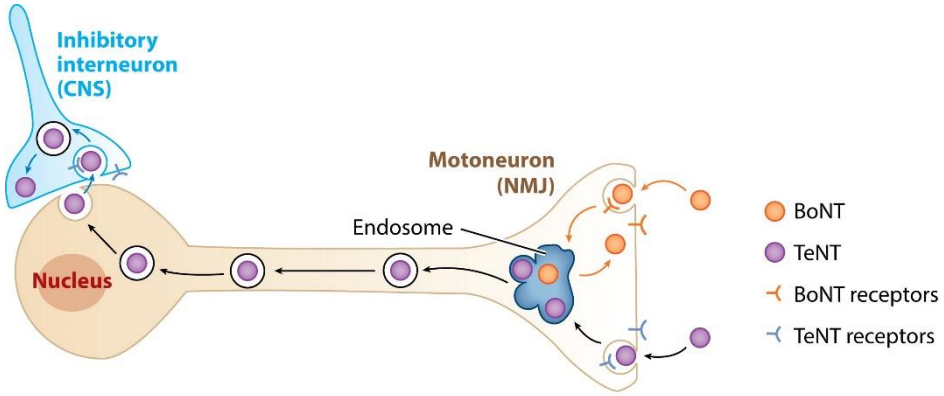

Figure 1.1 Different intracellular routes followed by BoNT and TeNT cause opposite clinical symptoms.

BoNT and TeNT bind to specific receptors to enter neurons from the presynaptic terminal at the NMJs. BoNT causes flaccid muscle paralysis by blocking Ach release at the NMJs, causing toxicity in peripheral neurons. In contrast, TeNT moves via retrograde transport through the axon, reaches the soma, and transfers to inhibitory interneurons by transcytosis. It shows the toxicity on central neurons by preventing the release of inhibitory neurotransmitters, GABA, and glycine, which results in spastic paralysis (hypercontraction of skeletal muscles). From Dong et al. (2019) (copyright clearance: order license ID 1382211-1).

1.1.1 Molecular structure

CNTs are generated as inactive single chain proteins with a molecular size of ~150 kDa. Subsequently, the protein is post-translationally cleaved to create an active di-chain molecule (Figure 1.2 A). The di-chain molecule consists of a light chain (LC) around 50 kDa in size and heavy chain (HC) around 100 kDa in size, which are connected by a conserved single disulphide bond (Figure 1.2 B) (Lacy and Stevens, 1999, Turton et al., 2002, Pirazzini et al., 2016). The active di-chain molecule consists of three functional domains that provide binding, translocation, and proteolytic activity. As a catalytic domain, the LC is a zinc endopeptidase which cleaves soluble N-ethylmaleimide sensitive factor attachment protein receptors (SNAREs), the substrates of CNTs. The HC has two functional domains, each of which is 50 kDa in molecular size: the N-terminal half is the translocation domain (H_N), which forms ion channels in lipid bilayers, and assists the translocation of the LC from the intracellular lumen to the cytosol; the C-terminal half is the binding domain (H_C), which is responsible for binding to specific cell surface receptors and endocytosis into neurons (Turton et al., 2002, Pirazzini et al., 2016).

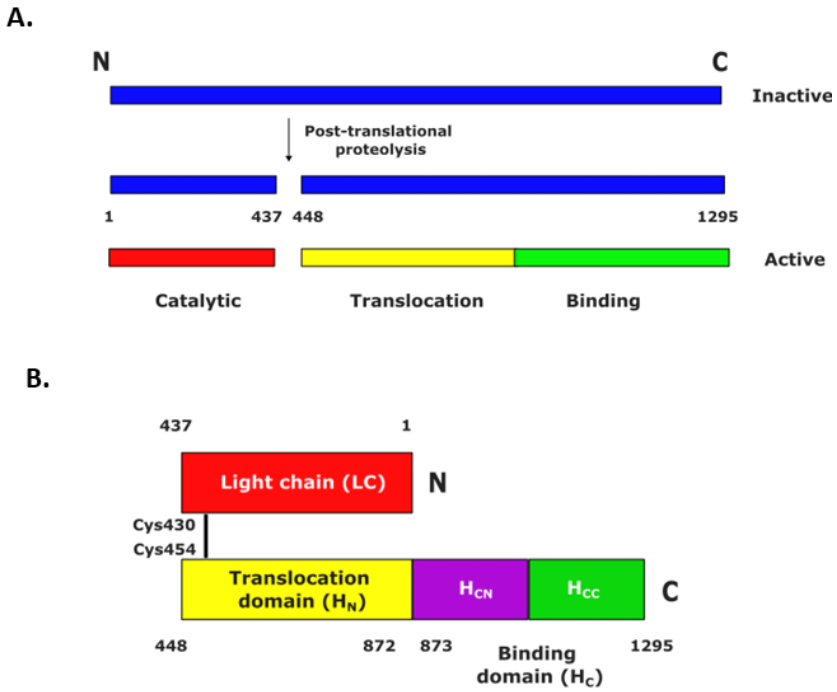

Figure 1.2 Schematic description of CNT generation and its structure.

A) *CNT are generated as a single inactive protein chain (150 kDa). After post-translational proteolysis, the di-chain active form of the protein occurs, and the two chains are connected by a disulphide bond.* ***B)*** *A detailed di-chain structure of CNT is demonstrated. The active CNT has three functional domains. The catalytic domain (LC), which consists of a zinc-endopeptidase (50 kDa) is displayed in red. The H_N is responsible for translocating LC to the cytosol (50 kDa) and is coloured in yellow. The binding domain (H_C), consisting of two subdomains, binds to specific receptors on the neuronal cell membrane for entry (50 kDa) and is coloured in purple and green. Figures were created by using Inkscape.*

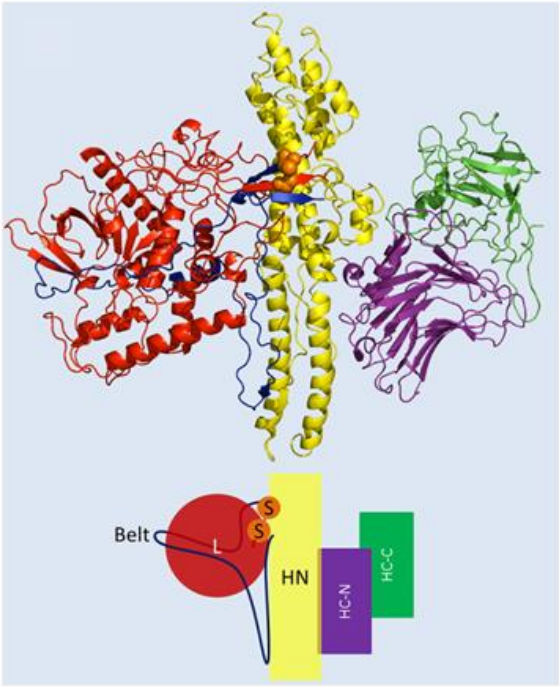

Figure 1.3 The crystallographic structure of CNTs.

The crystal structure of BoNT/A is shown as a representative example. The lower panel shows a summary of the molecular organisation of the four domains, labelled with the same colour as in the crystal structure. L (red) is the catalytic domain, comprising a catalytic zinc atom and the conserved zinc-binding HExxH motif. HN (yellow) is the translocation domain, consisting of a pair of long amphipathic helices and the translocation belt (blue), which wraps around the LC. The L is connected to the HN by a disulphide bridge (orange). The binding domain has two subdomains, HC-N (purple) and HC-C (green), with a mainly B-sheet topology. From Pirazzini et al. (2016) (Copyright clearance: Elsevier license number 5600830745246).

The crystal structure of BoNT/A has been shown in Figure 1.3 as a representative three-dimensional structure of CNTs. The H_C comprises two sub-domains, H_{CN} and H_{CC}, which are roughly the same size and mainly formed by B-sheet structures. The H_{CC} is involved in the specific binding of toxin to the neuronal membrane, whereas there is evidence that the H_{CN} may bind to membrane lipids (Turton et al., 2002, Pirazzini et al., 2016). The H_C rotates away from the central H_N to make its surface loop reachable for binding. The H_N has a pair of long amphipathic helices and a long loop known as the translocation belt, which wraps around the LC. The LC contains a catalytic zinc atom and the conserved zinc-binding HExxH motif, which is typical of zinc proteases. It is located in a deep cleft on the surface of the protein, accessible via a channel. Although each CNT has three functional domains, which define the mode of action for CNTs, the arrangement and relations of domains differ for each CNT. As compared with other domains, the LC and H_{CC} domains possess a more diverse variety of amino acids

(AA) (Tian et al., 2022). The highly variable AAs are placed on the exterior or surface of the folded protein, while the conserved AAs are found interior. As a consequence, these two sites on the protein are the main sources that determine the toxin type.

1.1.2 Mechanism of action

1.1.2.1 SNARE regulated mediated exocytosis and endocytosis

Eukaryotes have a well-conserved cellular process called exocytosis, which enables trafficking of biomolecules between intracellular compartments for proper maintenance of those organelles (Gerst, 1999). Appropriate regulation of exocytosis is essential for the release of neurotransmitters, hormones, cytokines, enzymes as well as balancing the amount of lipids, receptors, and transporters in the plasma membrane. Exocytosis provides a continuation link between intravesicular space and extracellular space as a result of the fusion of vesicle membrane to plasma membrane. Consequently, vesicle content is released from the cell to the outside (Lin and Scheller, 2000). In order to deliver biomolecules are to their correct destinations, trafficking of vesicles must be occurring organelle-specific, which requires SNARE proteins with the following steps: development of transport vesicles from a donor organelle, target selection, docking and fusion with an acceptor organelle (Gerst, 1999, Lin and Scheller, 2000). Proteins known as SNAREs play an essential role in intracellular membrane fusion events, ensuring specificity. SNAREs are divided into 2 categories. SNAREs present on the vesicle membrane are called v-SNAREs and those on the target membrane are t-SNAREs (Gerst, 1999).

Neuronal communication occurs through chemical synaptic transmission and the synaptic vesicle cycle. Upon stimulation of the presynaptic neuron, Ca^{+2} enters the cells. Ca^{+2} influx induces membrane fusion between synaptic vesicle membrane consisting of neurotransmitters and presynaptic membrane (Duman and Forte, 2003). Following release of neurotransmitters into the synaptic cleft, neurotransmitters pass through to postsynaptic neurons. After neurotransmitter release, vesicle membrane proteins are recycled via endocytosis mediated by clathrin and dynamin into presynaptic neurons to be reused (Lin and Scheller, 2000).

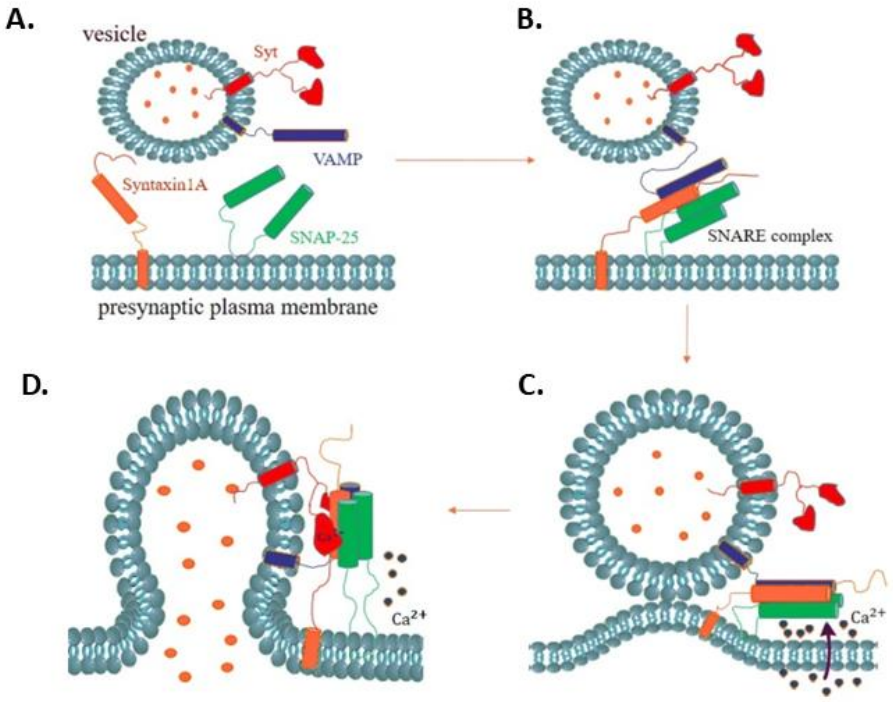

Figure 1.4 SNAREs mediate vesicle exocytosis in the presynaptic plasma membrane.

SNARE proteins, VAMP2, syntaxin-1, SNAP25, mediate vesicle exocytosis in neurones. A) Syntaxin-1 is initially not binding to SNAP25 or VAMP2. B) Following conformational changes, VAMP2 binds to syntaxin-1 and SNAP25 in a parallel arrangement, which forms the core complex. C) Ca^{+2} induces further zippering of parallel helices, which provides interaction between vesicle and plasma membrane. D) With binding of Ca^{+2} molecules to SYTI, the fusion occurs, and neurotransmitters are released into the synaptic cleft. From Wang et al. (2019) (Copyright clearance: Springer Nature license number 5605330491434).

Exocytosis of neurotransmitters from presynaptic neuronal cells requires neuronal SNARE proteins, which are vesicle associated membrane protein (VAMP), Synaptosomal-associated protein 25 (SNAP25), and syntaxin 1 (Figure 1.4) (Wang et al., 2019). VAMP2, v-SNARE, located on the vesicle membrane fuses with syntaxin 1 and SNAP25, t-SNAREs, resident on the plasma membrane, forming the stable ternary complex, also called the core complex (Lin and Scheller, 2000). The core complex consists of four parallel helices: the H3 domain of syntaxin 1, one coiled-coil domain of VAMP2, and two coiled-coils of SNAP25. Syntaxin is initially in its closed form (Figure 1.4 A). Syntaxin, SNAP25, and VAMP domains are all positioned in parallel and form a connection during nucleation (Figure 1.4 B). The symmetric arrangement of the helices in the core complex allows for the stable association of the two membranes. Ca^{+2} triggers the subsequent zippering of parallel helices, which enables vesicle

membrane contact with the plasma membrane (Figure 1.4 C). Upon Ca^{+2} binding to SYTI, membrane fusion occurs, and the neurotransmitters are released into the synaptic cleft (Figure 1.4 D) (Lin and Scheller, 2000, Chen and Scheller, 2001, Wang et al., 2019).

Several SNARE regulator proteins participate in vesicle exocytosis along with SNARE proteins. n-Sec1, synaptophysin, synaptotagmin (SYT), synaptic vesicle protein 2 (SV2) (Gerst, 1999). n-Sec1, also known as Munc-18, is a t-SNARE regulator, which binds to the amino terminal of the syntaxin, when the syntaxin is in close form. As it stabilises closed syntaxin formation, this interaction prevents the assembly of syntaxin and SNAP25 into binary forms. Following conformational changes, the structure opens to facilitate SNARE formation (Gerst, 1999, Chen and Scheller, 2001). Synaptophysin I and synaptophysin II are v-SNARE regulators, found at synaptic vesicle membranes. They form complexes with the VAMP family. The synaptophysin-VAMP interaction prevents VAMP from assembly with t-SNAREs at the early stages of the process. SYTI is a synaptic vesicle protein, necessary for SNARE-mediated exocytosis. As it binds to Ca^{+2}, SNAREs, and phospholipids, it is recognised as a Ca^{+2} sensor in neuronal exocytosis (Chen and Scheller, 2001). Thus, it has been suggested that SYTI binds to the SNARE complex in a Ca^{+2} dependent manner. However, Rickman and Davletov (2003) found that SYTI attaches to the SNAP25-syntaxin heterodimer in the absence of Ca^{+2}. Since VAMP is inhibited on the synaptic vesicle membrane, synaptotagmin interaction with the SNAP25-syntaxin heterodimer might contribute to and be a facilitator of the additional integration of VAMP2 into the SNARE complex. Additionally, SV2 isoforms, SV2A and SV2B, interact with SYTI to regulate neurotransmitter release in exocytosis (Ciruelas et al., 2019, Rossi et al., 2022). SV2 loss leads to a decline in the level of SNARE complexes (Ciruelas et al., 2019). The presence of SV2 appears to facilitate the transition from a vesicle docking state to a release-competent state once vesicles dock at the plasma membrane.

There is a remarkable fact that SYTI and SV2, besides playing a vital role in synaptic vesicle exocytosis, are also used by CNTs to enter neuronal cells by acting as receptors (Dong et al., 2019, Rossi et al., 2022). After vesicle fusion, SYTI and SV2 are present on the transmembrane and become plasma membrane proteins until recycled inside cells via endocytosis. This makes SYTI and SV2 proteins accessible for CNTs to interact with, and CNTs can bind them during vesicle recycling. Apparently, CNTs are taking advantage of the vesicle recycling mechanism to enter neurons.

1.1.2.2 Steps of the intoxication

The CNTs intoxicate the cells in a multistep mechanism that involves binding, internalization, translocation, and cleavage of SNAREs (Figure 1.4). During each stage of intoxication, CNT utilizes the relevant functional domain. In presynaptic nerve terminals, the toxin first binds to specific receptors expressed on the neuronal cell membrane through its HC domain. Toxins recognize two different types of receptors, ganglioside and protein receptors, and enter neuronal cells via the dual receptor model (Turton et al., 2002). A ganglioside is a type of glycosphingolipid that consists of two parts, a ceramide tail, and a carbohydrate head group that contains a variety of sialic acids attached. Gangliosides are abundantly expressed on the neuronal surface and exist in a variety of species (Dong et al., 2019). The protein receptors used by CNTs are the synaptic vesicle membrane proteins, SV2 and synaptotagmin. Each CNT binds to different types of gangliosides and protein receptor with varying affinities (Table 1.1). In addition to gangliosides and protein receptors, CNTs interacts with the lipid membrane which contributes to the overall affinity of the toxin to the cell membrane. The lipid binding loop is located between the Ganglioside Binding Site (GBS) and protein receptor binding site and interacts with lipid layers hydrophobically. According to the dual-receptor model, the toxin initially binds to gangliosides with a low affinity. The toxin subsequently binds to a protein receptor and adheres strongly to the cell membrane, allowing it to be internalized via endocytosis (Dong et al., 2019). Although the dual-receptor model is established for most CNTs, it is not clear for TeNT and BoNT/C because their receptor protein has not been identified. However, it has been suggested that TeNT enters the cells using two gangliosides simultaneously (Rummel, 2017).

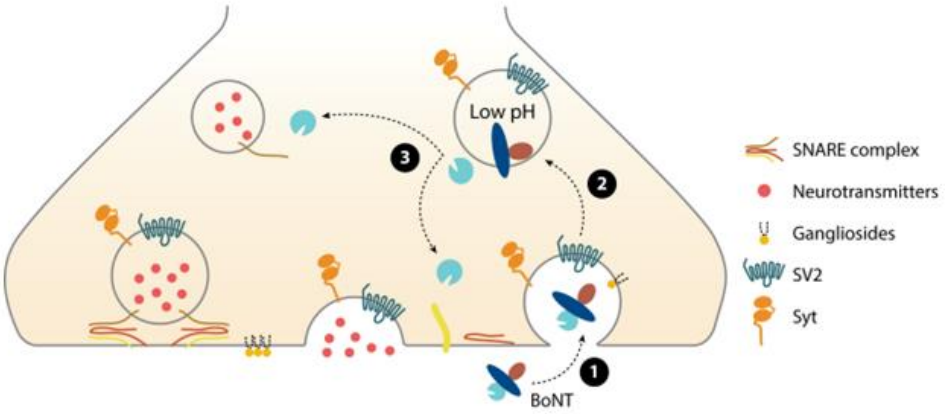

Figure 1.5 The mode of action of CNTs.

The intoxication of CNT has multiple steps. (1) CNT enters neurons from the presynaptic nerve terminal by the dual receptor model. The toxin first binds to the gangliosides, expressed extensively on the neuronal surface, with a low affinity. Then it binds to specific receptor proteins, SV2 or SYT, with a strong affinity to be internalised into cells. (2) Reduction of pH in the endosome triggers a conformational change in H_N domain, which assists the translocation of LC from the endosome lumen to the cytosol. (3) The released LC cleaves specific SNARE, which disrupts the SNARE complex and thus prevents synaptic vesicle exocytosis. From Dong et al. (2019) (copyright clearance: order license ID 1382211-1).

Clostridium Neurotoxins	Ganglioside Receptor	Protein Receptor
BoNT/A	GT1b>GD1a=GD1b>GM1	SV2C>SV2A>SV2B
BoNT/B	GT1b>GD1a>GD1b	SYTII*>SYTI
BoNT/C	GD1b>GT1b>GD1a>GM1a	
BoNT/D	GD2>GT1b=GD1b	SV2B>SV2C>SV2A
BoNT/DC	**GM1a>GD1a>GD1b=GT1b>**	SYTII*>SYTI
TeNT	*Conserved GBS*: GM1a>GD1a>GT1b=GD1b	Nidogen1/2; SV2
	Sialic acid site: GT1b>GD1b>GD1a>GM1a	

Table 1.1 Specific gangliosides and protein receptors for each CNT.

**Human and primate SYTII protein receptors show low affinity to BoNT/B and BoNT/DC due to the mutation.*

After endocytosis, the LC is translocated from the endosomal lumen to the cytosol with the assistance of the H_N and HC domains. The reduction of pH level within the endosome leads to conformational variations in the H_N domain, increasing hydrophobicity and its ability to interact with the lipid layer (Turton et al., 2002). After insertion of HN into the membrane, a transmembrane channel forms, made up of six α-helices (Pirazzini et al., 2016). At the same time, HN-belt-HC can form a channel with the same conductivity and serves as a transmembrane chaperone for LC translocation into the cytosol (Montal, 2009, Pirazzini et al., 2016). The channel diameter is predicted at 15 Å, which could not permit delivery of the globular LC with 55 Å × 55 Å × 62 Å dimensions. Therefore, LC becomes unfolded at the acidic endosomal pH, enters the channel and remains unfolded during translocation (Koriazova and Montal, 2003). The attachment of HC-LC complex to the membrane prevents LC assembly and LC translocation occurs in the N to C terminus direction (Fischer and Montal, 2007). LC blocks the HC channel during the process. As soon as LC is exposed to the cytosol, the disulphide bond between LC and HN is reduced by the NADPH-thioredoxin reductase-thioredoxin complex (Dong et al., 2019). When LC is released from the trans compartment into the neutral cytosol, it refolds and regains its proteolytic activity, and HC channel is then unblocked (Fischer and Montal, 2007, Pirazzini et al., 2016). Depending on the toxin, the released LC cleaves the target SNARE (Figure 1.5). Normally the SNAREs, VAMP, SNAP25, and syntaxin initiate membrane fusion by forming a protein complex between vesicles and the cell membrane, allowing vesicle exocytosis to occur (Chen and Scheller, 2001). However, the cleavage of any of the three SNAREs by CNTs is enough to disrupt the formation of the SNARE complex, which prevents vesicle exocytosis and thus neurotransmitter release. BoNT/A, BoNT/C, and BoNT/E cleave SNAP25 at different cleavage sites. Additionally, BoNT/C also cleaves Syntaxin 1. BoNT/B, BoNT/D, BoNT/F, BoNT/G, and TeNT cleave VAMP1, VAMP2, and VAMP3 (Turton et al., 2002). TeNT and BoNT/B cleave VAMP2 at the same site, which is Q76-77F (Schenke et al., 2020). BoNT/D and BoNT/DC cleave VAMP2 at the same site, K59-60L.

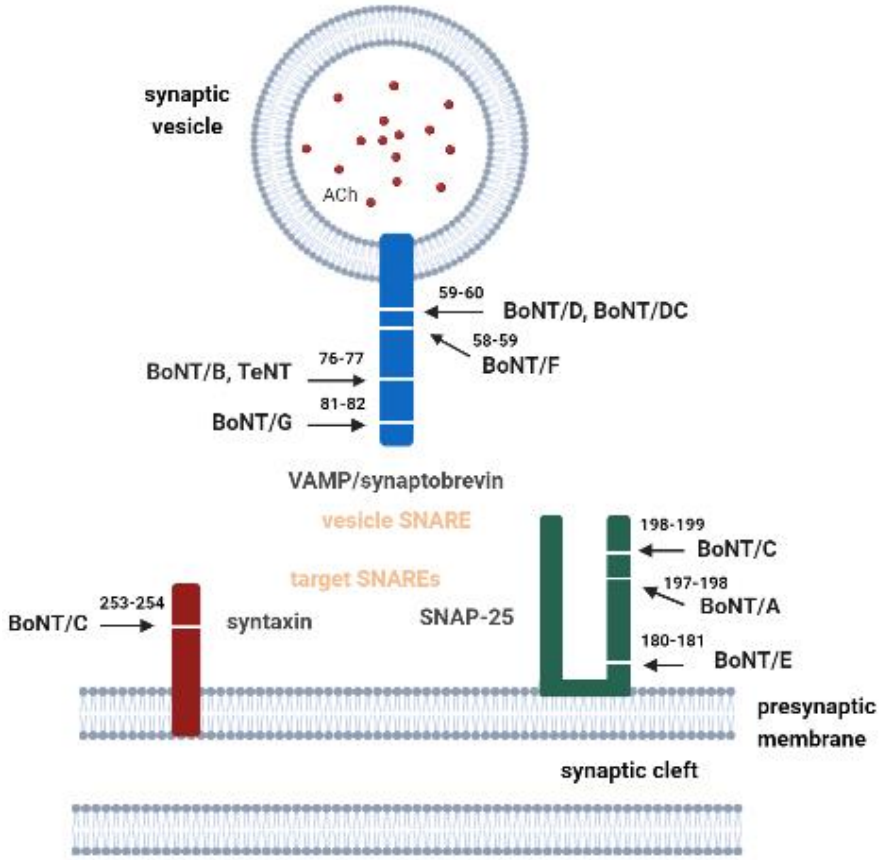

Figure 1.6 CNTs cleave SNAREs.

Vesicle SNARE, VAMP, and target SNAREs, SNAP25 and Syntaxin, form a highly stable SNARE complex. The CNTs cleave SNAREs and damage the formation of the SNARE complex, which inhibits vesicle exocytosis. BoNT/A, BoNT/C, BoNT/E cleave SNAP25 at different sites. Additionally, BoNT/C cleaves Syntaxin. BoNT/B, BoNT/D, BoNT/F, BoNT/G, and TeNT cleave VAMP. BoNT/B and TeNT cleave VAMP at the same site (76-77). BoNT/D and BoNT/DC cleave VAMP at the same site (59-60). Figures were created by using BioRender.

1.1.3 Botulinum neurotoxin serotypes

Until 1970, BoNT was classified into serotypes, from A to G, based on different serological properties after being identified for the first time in 1897 (Dong et al., 2019, Dong and Stenmark, 2021). Then naturally formed chimeric toxins BoNT/DC and BoNT/CD were characterized. They are a mixture of BoNT/D and BoNT/C serotypes. BoNT/CD consists of LC-H_N domains of BoNT/C and H_C domain of BoNT/D, whereas BoNT/DC comprises of LC-H_N domains of BoNT/D and H_C domain of BoNT/C. With advances in sequencing, several subtypes within the same serotype have also been found. A novel serotype, BoNT/H, was discovered in an infant botulism case. Moreover, BoNT-like toxins, BoNT/X and BoNT/En, have been recently discovered. BoNT/Wo has been described as a distant homolog of BoNT. As shown in Figure 1.6, a phylogenetic split network of CNTs and BoNT-like toxins shows the potential

evolutionary relationships between toxins based on comparisons of their protein sequences (Dong et al., 2019).

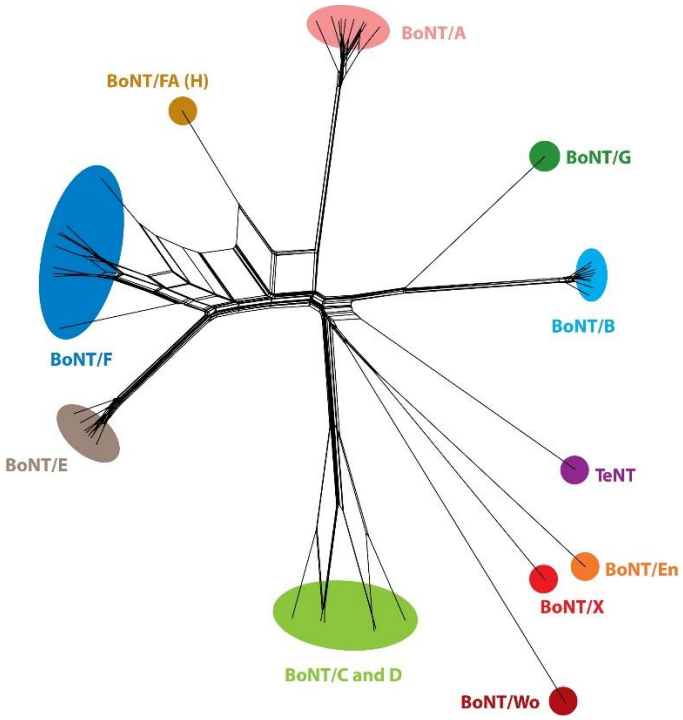

Figure 1.7 A phylogenetic split network of CNTs and BoNT-like toxins.

The diagram illustrates the evolutionary relationship between BoNT serotypes, TeNT, chimeric toxins, BoNT-Like toxins, and homolog toxin BoNT/Wo, based on their protein sequences. From Dong et al. (2019) (copyright clearance: order license ID 1382211-1).

The following sections will mainly focus on BoNT/A, BoNT/B, BoNT/C, BoNT/D, BoNT/DC, and TeNT, as these were the toxins studied during this research.

1.1.3.1 Botulinum neurotoxin A

The generation of serologically different BoNTs from different strains of *Clostridia* was first detected in 1910, and designated as BoNT/A and BoNT/B (Burke, 1919). It was observed that type A strains produced stronger toxins than type B strains under the same cultural conditions. Since then, BoNT/A, also known as BOTOX, has gained extensive use for medical and cosmetic purposes. BoNT/A received the first FDA approval for the treatment of crossed eye condition and hemifacial spasm in 1989. It has been used for a variety of medical conditions in a short period of time, such as dystonia, hyperhidrosis, digestive and urinary disorders, and migraine (Davletov et al., 2005). In comparison with other serotypes, BoNT/A toxicity is exceptional since only one microgram is capable of killing an adult

human. While the muscle paralysis effect of all BoNTs are reversible, BoNT/A has the longest paralytic effect of the known serotypes, which makes it more practical for medical uses (Pirazzini et al., 2017).

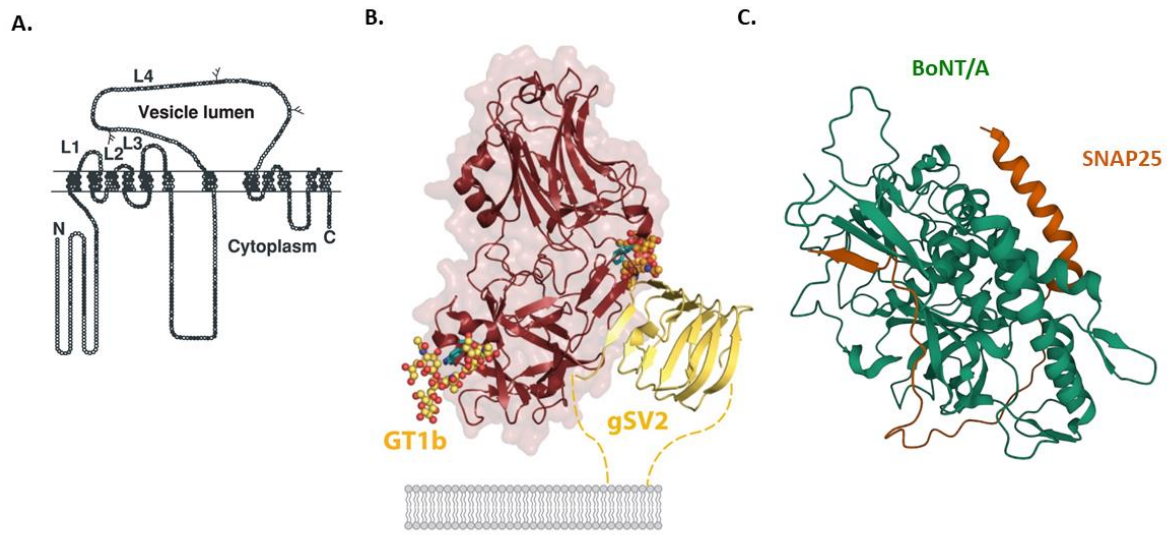

Figure 1.8 Interaction of BoNT/A with its receptors and substrate based on crystallographic analysis.

A) *Linear description of SV2, which BoNT/A uses as a receptor molecule. It has 12 transmembrane helices. C- and N-terminus sites are both present in the cytosol. BoNT/A binds to a major luminal domain, SV2-L4. From Peng et. al (2011) (copyright notice: Attribution 4.0 International (CC BY 4.0)).* ***B)*** *BoNT/A (red) interacts with the glycosylated SV2 (yellow) and GT1b (yellow dots). Conserved GBS residues and F953 are depicted in cyan. Orange dashes show the glycan linked to SV2C. From Dong et al. (2019) (copyright clearance: order license ID 1382211-1).* ***C)*** *BoNT/A-LC (green) and its interaction with the target protein, SNAP25 (red). SNAP25 is extensively wrapped around BoNT/A-LC. From Protein Data Bank (PDB): 1XTG.*

BoNT/A has a crystal structure with 3.3 Å resolution. It displays a linear organization of three functional domains, where the catalytic and binding domains do not interact (Lacy et al., 1998). As a result of its unique structural properties, BoNT/A enters neuronal cells using specific receptors with varying affinities and specifically cleaves its substrate, SNAP25. The H_C domain of BoNT/A has a GBS with the conserved residues of SxWY (lactose binding site), which is also found in BoNT/B, BoNT/E, BoNT/F, BoNT/G, and TeNT (Rummel, 2017). The conserved GBS with the SxWY motif interacts with the terminal NAcGalβ3–1Galβ moiety of gangliosides (Strotmeier et al., 2010). The conserved GBS of BoNT/A binds to GT1b strongly, to GD1a and GD1b with middling affinity, and it's lowest preference is for GM1 (Rummel, 2017). BoNT/A utilises all SV2 isoforms, SV2A, SV2B and SV2C, as protein receptors. SV2 consists of 12 transmembrane helices, and both C-terminus and N-terminus sites are found on the cytosol (Peng et al., 2011, Dong et al., 2019). It has only one major luminal domain, the fourth luminal domain (SV2-L4), which BoNT/A recognises (Figure 1.7 A). BoNT/A specifically and strongly binds to SV2C-L4 and weakly binds to SV2A-L4 and SV2B-L4. Moreover, N-glycosylating each

SV2 isoform enhances the efficacy of BoNT/A binding and F953 is a key AA of the protein binding site as mutation in F953 of BoNT/A leads to its loss of toxicity (Rummel, 2017, Dong et al., 2019). The binding of SV2C and GT1b to BoNT/A is schematically illustrated in Figure 1.7 B. In all BoNT serotypes, LC has a conserved catalytic site with the signature motif HEXXH. Therefore, the specific recognition and cleavage of substrates results from protein regions outside the catalytic site. Based on the crystal structure of the LC of BoNT/A and its substrate SNAP25, it is found that SNAP25 interacts extensively with LC-A via binding both the N-terminal and C-terminal sites of SNAP25. The unique interaction with LC-A might require the 'long stretch' of SNAP25 , where SNAP25 surrounds the LC from N-terminal via a-exosite bound to C-terminal of SNAP25 b-exosite bound (Figure 1.7 C) (Dong and Stenmark, 2021).

1.1.3.2 Botulinum neurotoxin B

BoNT, which was first isolated in 1895 by Emile van Ermengem, was later referred to as BoNT/B. In the 1910s, they were designated as BoNT/A and BoNT/B (Rummel, 2017). It has been used for a variety of medical conditions, mostly in the same areas as BoNT/A, since 1999 under the name MyoBloc (Dressler and Eleopra, 2006). The immune system can develop an immune response against any BoNT serotype as a bacterial toxin, so BoNT/B is an efficient alternative when patients develop a resistance to BoNT/A and no longer develop muscle paralysis in response to it (Callaway, 2004). However, BoNT/A and BoNT/B have different motor and autonomic effects when they are injected. BoNT/B causes relatively stronger autonomic effects and relatively weaker motor effects when compared to BoNT/A. This might be due to the different receptor densities of BoNT/A and BoNT/B on autonomic and motor synapses (Dressler and Eleopra, 2006). Therefore, BoNT/B should be used carefully in patients with autonomic disorders. Moreover, BoNT/B is the serotype that causes the third longest duration of muscle paralysis, after BoNT/A and BoNT/C (Pirazzini et al., 2017).

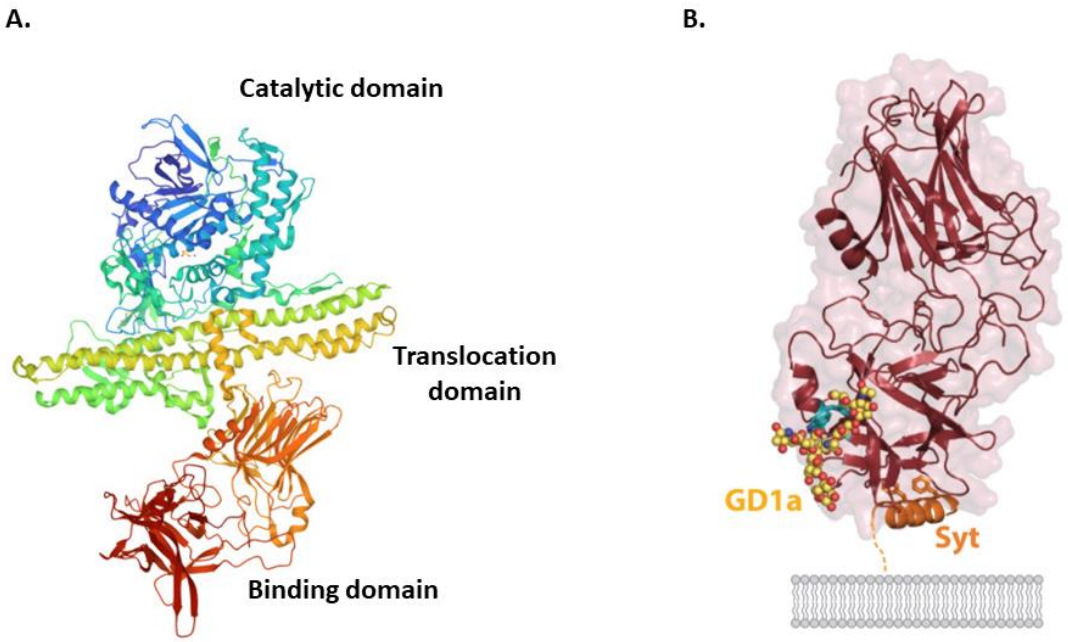

Figure 1.9 Crystal structure of BoNT/B and its interaction with receptors.

A) *Three main domains of BoNT/B are linearly arranged. The catalytic domain (blue) and binding domain (red-orange) are isolated by the translocation domain (yellow). From PDB: 1EPW.* ***B)*** *BoNT/B interacts with its receptors on the cell membrane. BoNT/B (red) binds to SYTII (orange) and GD1a (dots). Conserved GBS is shown as cyan; F47 and F54 hydrophobic residues of SYTII are demonstrated as sticks. From Dong et al. (2019) (copyright clearance: order license ID 1382211-1).*

The crystal structure of BoNT/B has been determined at 1.8 Å. It has a linear arrangement of its three main domains, and the H_c domain and LC domain do not interact, similar to BoNT/A (Figure 1.8 A) (Swaminathan and Eswaramoorthy, 2000). However, the H_C of BoNT/A angles away from the HN by 25° more than the H_C of BoNT/B. BoNT/B has the conserved GBS (SxWY motif) in the H_C domain and binds to GT1b and GD1a with highest affinity, and less preferentially to GD1b (Figure 1.8 B). BoNT/B uses SYTI and SYTII as protein receptors, and the GBS and SYT binding sites are separated from each other. Hydrophobic F47 and F54 residues in SYTII bind to the H_C and are responsible for the major interaction. In humans and primates, the SYTII gene has a mutation related to these hydrophobic residues, which causes low affinity for BoNT/B (Rummel, 2017, Dong et al., 2019). This might explain why BoNT/B is less toxic to humans than BoNT/A. As a part of the HN, the belt region of BoNT/B does not shield the zinc ion in the catalytic region, whereas it is covered by the belt in BoNT/A (Swaminathan and Eswaramoorthy, 2000). The belt region in BoNT/B is shorter than BoNT/A, which causes conformational differences. The catalytic region is thus more accessible to its substrate or inhibitors in the BoNT/B structure.

1.1.3.3 Botulinum neurotoxin C

In 1922, Botulinum type C, causing botulism in birds, was identified as the third serotype. Although Botulinum C does not lead to food-borne botulism, it is capable of paralyzing human muscles (Davletov et al., 2005). BoNT/C cannot traverse the human gut, which could explain this contradiction. Unlike other serotypes, BoNT/C is the only serotype that causes axon retractions and neuronal death. Apoptosis was demonstrated by Rust et al. (2016) in differentiated SiMa neuroblastomas treated with BoNT/C. The BoNT/C serotype has the second longest duration of paralysis in human and mouse muscles when injected (Pirazzini et al., 2017). It is found to be an effective alternative for the treatment of focal dystonia (Eleopra et al., 2006). It is advantageous as a clinical use because it has a longer duration of action and appears to be safe in humans as it does not affect motor function.

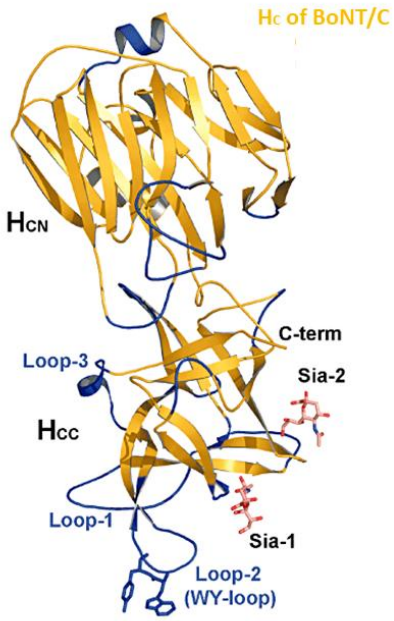

Figure 1.10 Crystal structure of H_C fragment of BoNT/C.

The H_C domain of BoNT/C (yellow) has several regions that interact with gangliosides. In the H_{CC}, there are three loops and two sialic acid binding sites, Sia-1 and Sia-2. The major binding activity with gangliosides is undertaken by Sia-1, whereas Sia-2 does not involve binding. Conserved GBS is not present in the H_{CC}, but Loop-1 and Loop-3 correspond to it. The conformational changes in the structure are shown in blue when compared to the H_{CC} domains of BoNT/A and BoNT/B. Loop-2, also called WY-loop, and Sia-1 site are the essential ganglioside binding sites of BoNT/C. From Strotmeier et al. (2011) (copyright clearance: order license ID 1382464-1).

In contrast to other BoNT serotypes, the H_C domain of BoNT/C failed to bind synaptic vesicle proteins, and the protein receptor for BoNT/C has not been identified so far (Rummel, 2017). BoNT/C can enter cells via two ganglioside binding sites. BoNT/C binds to GD1b and GT1b most preferentially and attaches to GD1a and GM1a with less affinity. The conserved GBS (SXWY motif) is not preserved in BoNT/C but loop 1 and loop 3 (S1281) regions correspond to the conserved GBS site in other serotypes (Figure 1.9) (Strotmeier et al., 2011). Blue coloured lines in the figure indicates the large conformational differences in the structure compared to BoNT/A and BoNT/B. Moreover, BoNT/C has a WY-loop (W1258, Y1259) and a unique sialic acid binding site (Y1179 in the Sia-1 site). BoNT/C has a reduced affinity for gangliosides when mutated at these three regions, confirming that they all participate in ganglioside interaction. However, the WY loop and Sia-1 site play a crucial role in this interaction because mutation of either region decreases toxicity by ~200 fold. In addition, the Sia-2 site does not involve binding. BoNT/C also differs from other serotypes by having two zinc atoms in the LC domain (Swaminathan and Eswaramoorthy, 2000). Due to the proximity of the cleavage sites, it is highly likely that BoNT/C cleaves SNAP25-Syntaxin dimers simultaneously (Davletov et al., 2005).

1.1.3.4 Botulinum neurotoxin D

Botulinum D, first discovered in 1929, causes botulism in cattle (Davletov et al., 2005). Compared to the human pathogenic BoNT/A and BoNT/B, BoNT/D shows the lowest AA sequence homology at ~ 25% (Strotmeier et al., 2010). BoNT/D is not toxic to humans, but it is the most potent toxin to mice (Pirazzini et al., 2017). There is a difference between human and mouse VAMP1 at residue 48, which might explain the lower sensitivity of BoNT/D in humans (Dong et al., 2019). As a result, BoNT/D cannot cleave human VAMP1, but it can cleave human VAMP2. Therefore, BoNT/D can enter human neurons and display neurotoxicity by cleaving VAMP2 (Pellett et al., 2015). The sensitivity of BoNT/D to human neurons is still lower than that of BoNT/A. However, if it is exposed to humans in large quantities, it might cause botulism in humans. Thus, botulinum D should also be considered a potential human pathogen. Additionally, as BoNT/D binds with high selectivity to target cells, it can be used as a transport vehicle for the delivery of cargo proteins from the cytosol to neurons (Bade et al., 2004).

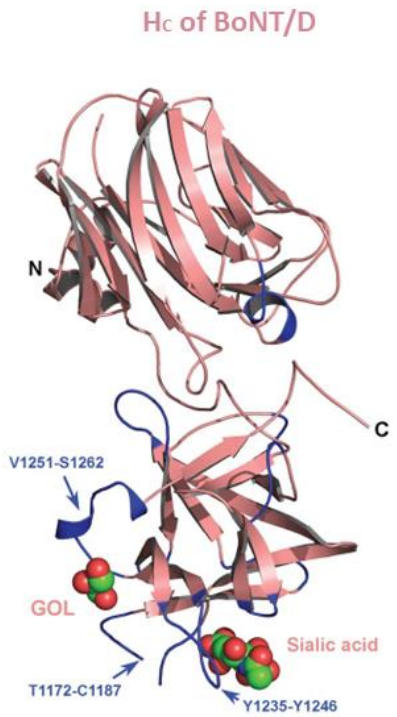

Figure 1.11 Crystal structure of H_C domain of BoNT/D.

The glycerol molecule and sialic acid bind to the H_C domain of BoNT/D (pink). Regions showing conformational differences from the H_C of BoNT/A and BoNT/B, including the conserved GBS, are shown as blue. From Strotmeier et al. (2010) (copyright clearance: order license ID 1382475-1).

BoNT/D utilises two ganglioside binding sites and also uses protein receptors to enter neuronal cells, however the conserved GBS with the SxWY motif is not present in BoNT/D. The crystal structure of the H_C domain of BoNT/D is shown in Figure 1.10 (Strotmeier et al., 2010), with regions showing conformational differences from the BoNT/A and BoNT/B HC domains are shown in blue, most notably from the lack of the conserved GBS from BoNT/A and BoNT/B. There is one glycerol molecule found in the conserved GBS pocket from H_C/A-GT1b and BoNT/B-siallylactose structures. Although a similar glycerol molecule was also observed in the H_C of BoNT/D, it is not involved in ganglioside binding. Instead, a ganglioside binding pocket is formed by AAs D1233-Y1235 and V1251-N1253 in Hc-D, which corresponds to a homologous position of the conserved GBS, but with a different AA configuration (Strotmeier et al., 2010, Rummel, 2017). The Hc-D also contains a sialic acid binding site, at R1239, which constitutes a second, main binding pocket for gangliosides (Strotmeier et al., 2010). R1239 in the Sia-1 site binds to GD2 strongly and less preferentially to GT1b and GD1b (Rummel, 2017). In BoNT/D, all SV2 isoforms are utilized, with the affinity order of SV2B, SV2C, and SV2A. However, SV2 binding appears to be different from BoNT/A because mutations of any three glycosylation sites in

SV2A did not change BoNT/D entry and SV2-L4 on its own could not mediate BoNT/D entry (Peng et al., 2011, Rummel, 2017, Dong et al., 2019).

1.1.3.5 Botulinum neurotoxin DC

Genetic sequences of BoNT/C and BoNT/D serotypes revealed that they have two naturally occurring mosaic variants called BoNT/CD and BoNT/DC that both cause veterinary botulism. BoNT/D and BoNT/C with their two variants pose a threat to wildlife and livestock. Recently, BoNT/DC caused a serious animal botulism outbreak in Italian cattle with a high level of mortality (Mariano et al., 2019). As a way to identify mosaic variants, the first letter represents catalytic activity while the second letter represents receptor binding activity (Hansbauer et al., 2016). The LC and H_N domains of BoNT/C and BoNT/CD are 92% homologous, while the H_C domains are less similar at 40%. Similar to this, the LC and HN domains of BoNT/D and BoNT/DC share a high degree of identity at 94%. However, a lower level of preservation is observed in the H_C domains at 37%. However, the H_C domains of BoNT/D and BoNT/CD are highly conserved (91%) whereas the H_C domains of BoNT/C and BoNT/DC are relatively poorly conserved (74%).

The crystal structure of the H_C domain of BoNT/DC is compared with the H_C domains of BoNT/C and BoNT/D (Figure 1.11 A). The rmsd value for the H_C-DC and the H_C-D calculated as 2.5 Å while it is calculated for the H_C-DC and the H_C-C as 0.5 Å (Kroken et al., 2011a). As a result, the crystal structure was found to be similar between the H_C-DC and the H_C-C, as expected. Higher rmsd values for the H_C-DC and the H_C-D could be explained by different angles of rotation between N-terminal jelly-roll domain and C-terminal β-trefoil domain. The three H_C domains differ primarily in their C-terminal subdomain and the loops of their β-trefoil domains, including their GBS pockets. This explains the different ganglioside preferences of the three toxin serotypes.

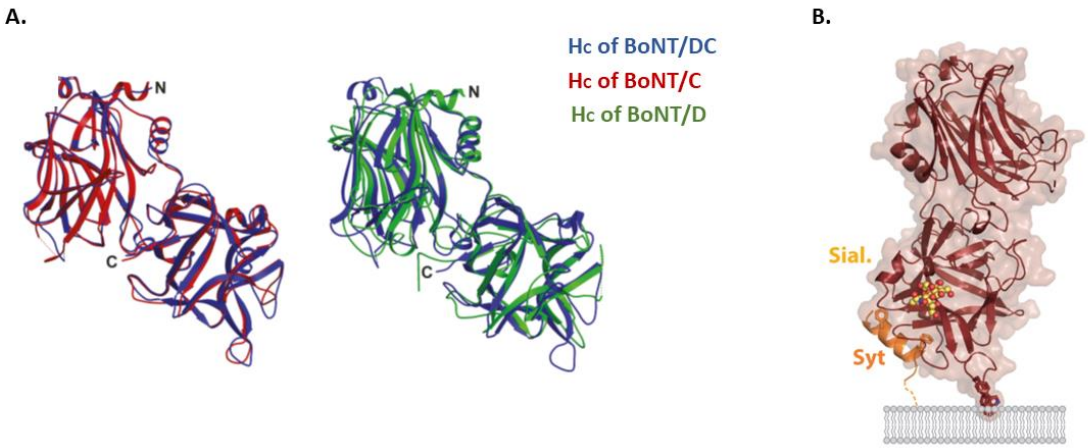

Figure 1.12 Crystal structure of BoNT/DC and its interaction with receptors.

A) *Crystallographic overlay of the H_C-DC domain with the H_C-C domain and the H_C-D domain is shown. Calculated rmsd value is 0.5 Å for the H_C-C (red) and the H_C-DC (blue), and it is 2.5 Å for the H_C-D (green) and the H_C-DC (blue). From Kroken et al. (2011a) (copyright clearance: order license ID 1382460-1).* ***B)*** *the H_C-DC (red) binds to Syt (orange) and sialic acid (dots). Hydrophobic loops involving lipid interaction are illustrated as sticks. From Dong et al. (2019) (copyright clearance: order license ID 1382211-1).*

BoNT/DC binds to the sialic acid moiety as well as protein receptors to enter neuronal cells (Figure 1.11 B). Although the conserved GBS is missing from H_C-DC it has a different configuration of AAs, containing Y1243 and L1270 residues, within the homologous position. It also contains a YWF-loop in the sialic acid binding site (Rummel, 2017). According to mutational analysis, Y1243 and L1270 residues as well as the YWF-loop play an active role in the binding of H_C-DC to liposomes with GM1. The YWF-loop is the main attachment to gangliosides, binding to GM1a and GD1a with a high affinity but less so to GD1b and GT1b. As BoNT/DC binds only to the sialic acid moiety without interacting with the carbohydrate backbone, it can employ a wide range of sialic acid-containing molecules as receptors (Zhang et al., 2017, Dong et al., 2019). In addition, it can enter cells without complex gangliosides.

As protein receptors, BoNT/DC uses mainly SYTII and to a lesser degree SYTI (Rummel, 2017), but both bind to the H_C-DC similarly. The SYTI (37-48) and SYTII (43-54) constitute an amphipathic helix binding into the hydrophobic pocket at the C-terminus of the H_C (Dong et al., 2019). Due to the mutation, human SYTII, like BoNT/B, is less sensitive to BoNT/DC. The H_C-DC possesses very low sequence identity (~33%) with the H_C-B. The surface area in the H_C-DC is also very different from the homologous Syt-II site in the H_C/B (Rummel, 2017, Dong et al., 2019). As a result, the SYT binding site of BoNT/DC differs from BoNT/B by being perpendicular to the binding site of BoNT/B.

1.1.3.6 TeNT

TeNT displays 65% sequence homology and 35% identity with BoNT serotypes (Lacy and Stevens, 1999). The crystal structure of full length TeNT (the closed conformation) was calculated at 2.3 Å (Zhang et al., 2021). TeNT shows a different domain organization compared to BoNT serotypes. The H_C is located on the same side as the LC by making a 90° shift and half-turn twist (Masuyer et al., 2018, Dong et al., 2019) (Figure 1.12 A). Thus, all three domains interact with each other, in contrast to the linear arrangement of BoNT/A and BoNT/B. However, TeNT undergoes a conformational change under different pH conditions (Masuyer et al., 2018). At neutral pH, it has an extended conformation, which is similar to the linear structures of BoNT/A and BoNT/B. During retrograde transport, the organelles do not contain vacuolar (H+) adenosine triphosphatase (vATPase), so TeNT has the extended conformation until transcytosis. Upon transcytosis to inhibitory neurons, TeNT forms a closed conformation due to the acidic pH of synaptic vesicles. As *Clostridium tetani* expresses and releases TeNT as a solitary protein, this pH-mediated domain rearrangement allows TeNT to adapt itself to several environmental conditions through intoxication. This is not the case for BoNTs because they are naturally produced with several non-toxic neurotoxin associated proteins (NAPs) that protect BoNTs from an acidic environment and destruction (Lam and Jin, 2015).

Unlike BoNTs, TeNT has two di-sulphide bonds. In addition to the di-sulphide bond between the LC and H_N (C430-C454), which is conserved among all CNTs, TeNT contains an additional one. The second disulphide bond between C869 and C1093, which interconnects the H_N and the H_{CN} domains, is a unique structure of TeNT (Zhang et al., 2021). However, it is still unclear what the function of this TeNT-specific di-sulphide bridge is in the process of toxication.

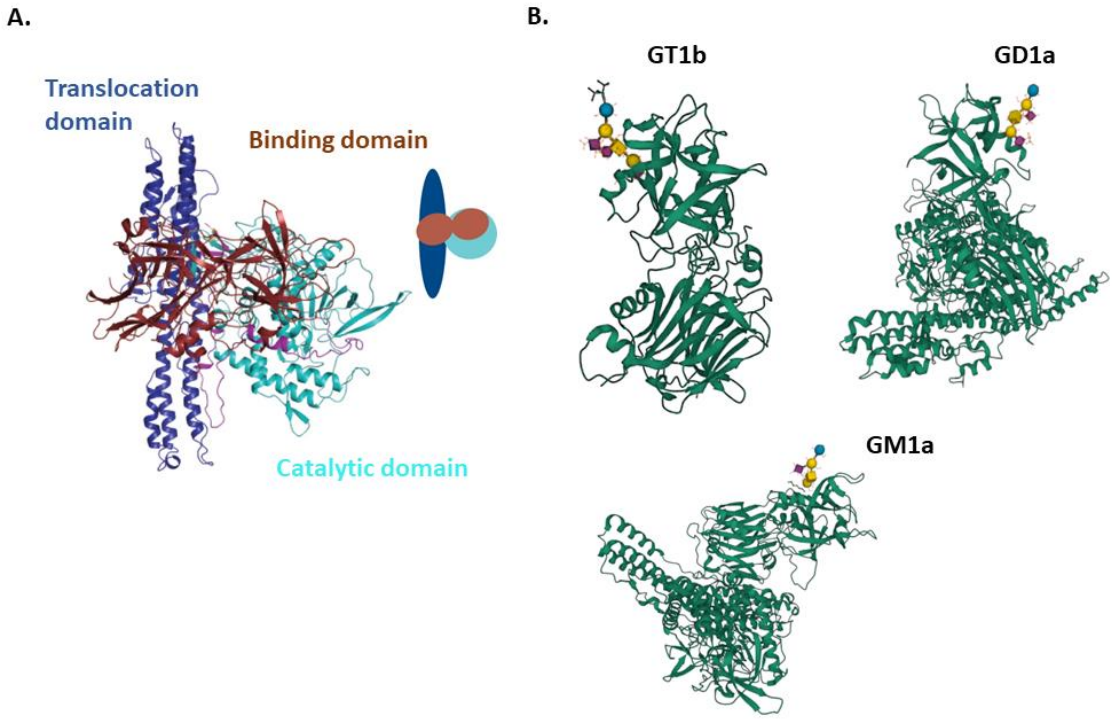

Figure 1.13 Structure of TeNT and its interaction with receptors based on crystallographic analysis.

A) *TeNT with its three functional domains, the translocation domain (blue) with belt in purple, the catalytic domain (cyan), and binding domain (red), is shown. Both the binding domain and the catalytic domain are present on the same side of the translocation domain, and all three domains interact (closed conformation). From Dong et al. (2019) (copyright clearance: order license ID 1382211-1).* ***B)*** *Crystal structure of TeNT and its interaction with different gangliosides, GT1b, GD1a, GM1a. From PDB: 1FV2 (GT1b), 5N0B (GD1a), 5N0C (GM1a).*

TeNT contains two GBS, which are a lactose binding site with a deep cleft, and a sialic acid binding site with a shallow groove (Fotinou et al., 2001). The lactose binding site is the conserved GBS with SXWY motif, which binds to GM1a and GD1a with a higher affinity and weaker affinity to GT1b and GD1b (Rummel, 2017, Masuyer et al., 2018). Figure 1.12 B shows the interactions of gangliosides GT1b, GD1a, and GM1a with lactose binding sites on HC-TeNT (Masuyer et al., 2018). The sialic acid binding site, with the key residue R1226, binds most preferentially to b-series gangliosides, GT1b and GD1b. The same site also binds to GM1a and GD1a but with less affinity. Mutational analyses revealed that the sialic acid binding site is most essential for entry of TeNT as a mutation in R1226 reduced TeNT activity 70 fold (Rummel, 2017). There are two significant sites on GT1b, Gal4-GalNAc3 for the lactose binding site and Sia-6 Sia-7 groups for the sialic acid binding site, which are required for GT1b-TeNT recognition (Fotinou et al., 2001). A receptor protein for TeNT has not yet been confirmed. However, SV2A and SV2B were suggested as protein receptors for TeNT present only in central neurons (Rummel, 2017). Moreover, TeNT might interact with nidogen 1 and nidogen 2 to enter cells. They are glycoprotein structures that have key roles in the stabilisation of the basement membrane at the end

of embryonic development (Zhou et al., 2022). Further clarification is needed regarding TeNT and its protein receptor.

1.2 Uses of botulinum neurotoxins

In 1973, BoNT was first described by a German physician and poet, Justinus Kerner (Patil et al., 2016). After conducting many animal experiments with BoNT, Kerner suggested that the toxin could be used for therapeutic purposes as it can prevent both hypersecretion and abnormal movements. Despite the fact that BoNT is a deadly toxin, safe doses have been used for therapeutic and cosmetic purposes for many years. Multiple conditions associated with involuntary muscle spasms and contractions can be treated with BoNT due to its reversible muscle paralysis effect. BoNT was used as a therapeutic for the first time by Dr. Alan Scott to treat strabismus (crossed eyes), in monkeys and humans (Lew, 2002). BoNT/A and BoNT/B serotypes are clinically used to treat several conditions as shown in Figure 1.13. BoNT/A, commercially known as BOTOX, was licensed by the FDA for the treatment of strabismus, blepharospasm (involuntary spasm of eyelid muscles), hemifacial spasm (face nerve-supplied muscles contract intermittently) in 1989. Since then it has also been approved for the use of cervical dystonia (abnormal and involuntarily contractions of neck and shoulder muscles), glabellar wrinkles, axillary hyperhidrosis (excessive sweating) and for cosmetic use (Chen, 2012). Although BoNT has been investigated for various pain conditions for many years, it has only been approved by the FDA for use in chronic migraine. BoNT/B, also known as MyoBloc, has been approved to treat cervical dystonia but the duration of its effect is a little shorter than BoNT/A.

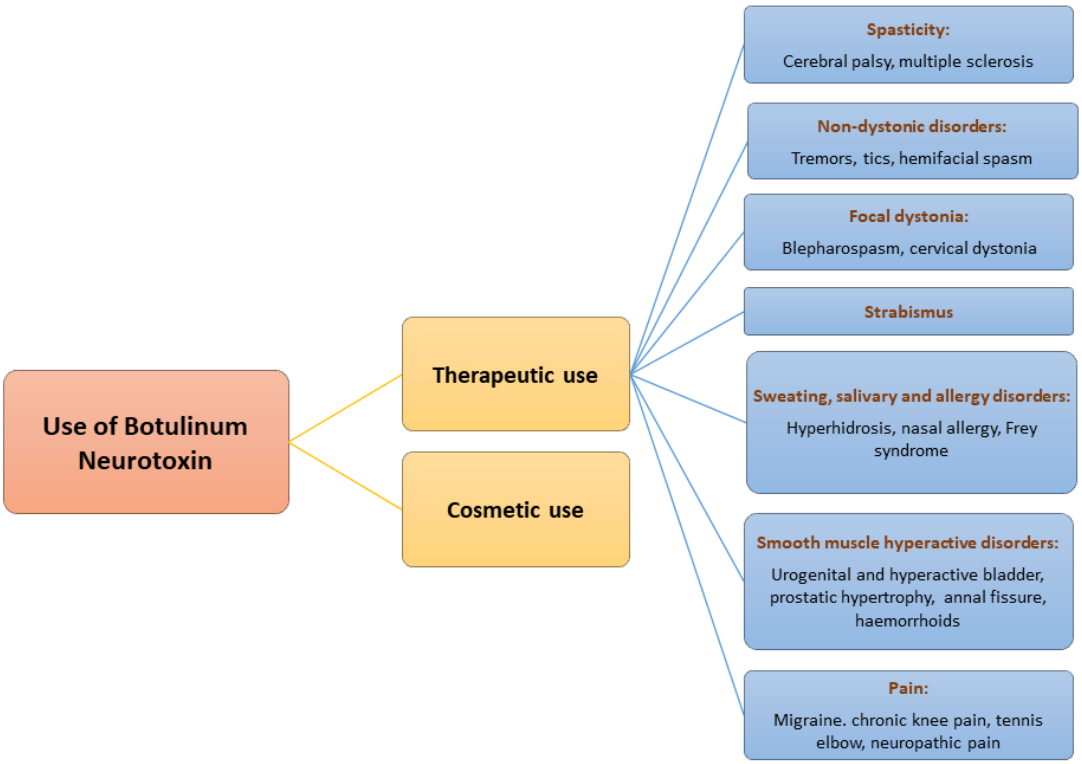

Figure 1.14 Therapeutic and cosmetic use of BoNTs.

BoNT/A and BoNT/B serotypes have been used for different conditions for many years.

Although BoNT shows high efficacy, a long-lasting effect, and a high safety profile, its use has some limitations. BoNT may cause the patient to develop neutralizing antibodies against the corresponding toxin, which can decrease its effectiveness or cause the patient to become unresponsive to the toxin (Chen, 2012). Compared with BoNT/B, fewer patients develop an immune response to BoNT/A. This might be due to the use of smaller doses of BoNT/A compared to BoNT/B. Furthermore, disorders such as cervical dystonia and spastic paralysis, which require high doses and repeated administrations of the toxin, are more likely to cause immuno-resistance. Therefore, reducing the dosage used might prevent the development of an immune response. In addition, other serotypes would be suitable candidates for use when patients are no longer responsive to BoNT/A and BoNT/B. BoNT/F and BoNT/C were used for patients who developed immuno-resistance to BoNT/A used for the treatment of focal dystonia and both serotypes demonstrated clinical efficacy but with shorter durations (Eleopra et al., 2006). However, BoNT/C has a longer duration effect than BoNT/F, so BoNT/C is an efficient alternative to treat focal dystonia. Other serotypes should also be tested for several medical conditions.

1.2.1 Re-engineering botulinum neurotoxins

The unique structure of BoNT allows for convenient re-engineering of the toxin to produce novel therapeutic properties, which could be used to treat several different disorders. Besides therapeutic uses of native BoNT serotypes, there have been many studies to generate novel derivatives of BoNT for treatment of several conditions. Re-engineering of BoNT is generally performed by either replacing the receptor binding domain with a modified peptide or retargeting the catalytic domain to various targets (Chen, 2012). Different cell types including non-neuronal cells and non-cholinergic neurons are targeted through altering the receptor binding domain with a different protein-targeting domain.

A mutated BoNT/E catalytic domain is able to cleave Synaptosomal-associated protein 23 (SNAP23), a non-neuronal isoform of SNAP25, which is involved with regulating the process of several secretion events in non-neuronal systems (Chen, 2012, Tian et al., 2022). This re-engineered BoNT/E LC could be used to treat hypersecretion disorders by targeting non-neuronal cells. The binding domain of BoNT/A has been conjugated with nerve growth factor (NGF) and epidermal growth factor (EGF) to retarget BoNT to non-cholinergic neurons and epithelial cells, respectively (Kostrzewa et al., 2015). In a similar manner, BoNT/D binding domain has been linked with the growth-hormone releasing hormone domain (GHRH) to interact with GHRH receptors on somatotrophic cells (Kostrzewa et al., 2015). It is therefore possible to target different types of cells with modified BoNTs in order to inhibit both neurotransmitter release and secretion of any cells. With these modifications, the therapeutic use of BoNT can be considerably improved and promoted.

In another study, it was shown that BoNT/D could be used as a transport vehicle, by delivering enzymatically active molecules into the cytosol of neurons (Bade et al., 2004). The fusion of the cargo protein to BoNT/D did not change its binding affinity to neuronal cells. Moreover, it was possible to evaluate the efficacy of delivery by measuring the intrinsic enzyme activity of the toxins. The catalytic domain of BoNT/A was also attached to the full-length BoNT/D and delivered to the cytosol of neuronal cells, whereupon cleaved SNAP25 was successfully detected. As the binding domain is the strongest immunogenic part of the toxin, this outcome would be advantageous for patients who develop an immune response to BoNT/A and BoNT/B.

Furthermore, BoNT molecules are re-engineered by combining domains from different serotypes. This results in the generation of novel recombinant molecules with properties that differ from their native serotypes. Several BoNT chimeric molecules with two binding domains were engineered by using the 'stapling' system (Leese et al, 2020). In this study, the stapling system used the SNARE complex to combine LC-H_N of BoNT/A with H_C domains of TeNT, BoNT/D, and their duplicated forms that

generated BiTox-D, BiTox-DD, BiTox-T, and BiTox-TT recombinant molecules. With direct integration of an additional H_C domain of BoNT/C, BoNT/C-C was also generated. As a result, duplicated forms of BiTox molecules and BoNT/C-C enhanced toxin delivery into neurons, increasing catalytic activity. Enhanced BoNT therapeutics can demonstrate faster therapeutic effects at lower doses. This makes them a feasible option for treating diseases that require high doses of toxin, which commonly induce an immune response in most patients. With the use of the same stapling system, the LC-H_N of BoNT/A is reassembled with the H_C domain of BoNT/A, forming BiTox-A and its double-binding version, BiTox-AA (Andreou et al., 2021). It was found that BiTox-AA cleaves the target protein, SNAP25, at the same rate as BoNT/A. However, BiTox-AA showed 100 times lower muscle paralysing activity compared to BoNT/A, which could be advantageous for migraine treatment. The activity of re-engineered BiTox molecules were tested in differentiated NanoLuc SiMa cell line (see Appendix 1).

1.3 Testing potency of clostridial neurotoxins

As BoNT is very poisonous, very small amounts of the toxin can lead to the rare but deadly disease botulism. Botulism is commonly caused by contaminated food or drugs that contain *C. botulinum* spores or preformed toxin (Stern et al., 2018). The disorder is characterized by progressive muscle paralysis, and if it reaches the respiratory muscles, it can lead to respiratory failure and death. Furthermore, due to its potency, it could be used as a biological weapon. BoNT must therefore be tested for in a highly sensitive manner. On the other hand, safe doses of the toxin have been used for the treatment of several disorders since 1989 (Chen, 2012). Expanding the use of BoNT as both a cosmetic and therapeutic product has also increased the need for sensitive BoNT testing. At present, the mouse bioassay (MBA) is the gold standard test for BoNT detection. It is also essential to detect residual TeNT in generated TeNT vaccines, which is tested on animals, commonly on guinea pigs (Greenberg et al., 1943). Animal testing is not a suitable test for both ethical and practical reasons. Therefore, there have been many attempts to develop a replacement assay with 3Rs principles (refine, reduce, and replace animal use in research) for testing of CNTs (Liebsch et al., 2011). The table 1.2 summarises the several methods for the test of CNTs.

Testing Clostridial Neurotoxins			
Assay		**Advantages**	**Limitations**
The mouse bioassay		Highly sensitive	Sacrificing animals, expensive, laborious, time-consuming
Ex vivo assays		Highly sensitive, less severe and shorter	Sacrificing animals
In vitro assays	**Immunoassays**	Fast, simple, reproducible	Expensive (requires high quality antibodies), false positive results
	Nucleic acid based assays	Rapid detection in any type of samples	Could not measure the toxin
	Catalytic activity assays	Specifically detect enzymatically active toxins	Measures only LC activity
	BINACLE assays	Sensitive	Could not reflect all intoxication steps
	Cell based assays	Could reflect all intoxication steps	Depending on cell types

Table 1.2 Summary of detection methods for CNTs.

1.3.1 Mouse bioassay

In the 1920s, the MBA was proposed for the testing of toxins and has been used as the most reliable method for testing BoNT ever since. The test involves injection of diluted particle-free toxin samples into mice intraperitoneally. Afterwards, the mice are examined for characteristic botulism symptoms such as ruffled fur, shortness of breath, weakness of limbs, and finally total paralysis and death due to respiratory failure. The duration of an assay is at least four days (Stern et al., 2018). The LD50 (the dosage at which 50% of mice are expected to die) is determined by the number of mice that died in each dilution group at the end of the test. About 90% of mice in the highest concentration group and 10% of mice in the lowest concentration group are expected to die as a result of the assay (Taylor et al., 2019). Next, toxin neutralization is conducted using specific antiserum in order to determine the serotype (Stern et al., 2018). Although the MBA has been a gold standard assay by detecting BoNT/A sensitively as low as 0.02 ng and 0.03 ng, it has several disadvantages such as being time-consuming, slow, expensive, and requiring exceptionally qualified laboratories and staff (Scarlatos et al., 2005). Moreover, many animals have to be sacrificed for only one test, with an estimate of at least 100 mice per MBA (Taylor et al., 2019). Their method of dying is extremely cruel, as they are suffocated to death. Approximately 150,000 mice were used to test pharmaceutical BoNTs in only Germany in 2014 and around 400,000 mice annually have been used across Europe to test BoNT batches (Stern et al., 2018,

Taylor et al., 2019). In a similar manner, guinea pigs are injected with concentrated TeNT toxoid and monitored for tetanus symptoms to confirm the complete elimination of toxin and irreversibility of toxoid. Even though the gold standard test for TeNT is the guinea pig assay, which detects TeNT as low as 0.1 ng/ml, this test has similar limitations to the MBA (Behrensdorf-Nicol et al., 2013). Therefore, a rapid, sensitive, and convenient replacement assay with 3Rs is an urgent need for testing CNTs.

1.3.2 Alternative assays for the mouse bioassay

In order to test CNTs, many alternative tests have been developed based on the 3Rs principles. Refinement assays could be established by using lower species, reducing the duration of the test, and performing non-lethal endpoints (Adler et al., 2010). Additionally, the number of animals in the MBA could be reduced if companies improved their dosing ranges, such as Allergan, which requires fewer doses and therefore fewer animals.

Ex vivo methods are available for BoNT testing, including the mouse hemidiaphragm assay and the intercostal neuromuscular junction assay. The mouse hemidiaphragm assay utilises isolated mouse nerve muscle after mice are humanely sacrificed in order to test BoNTs (Adler et al., 2010, Nepal and Jeong, 2020). BoNT/A, BoNT/B, and BoNT/E serotypes were measured sensitively in this method, with excellent comparability to the MBA. The intercostal neuromuscular junction assay employs stimulated rat intercostal muscles or rodent diaphragm and detects BoNT/A and BoNT/B with sensitivity as high as the MBA. In this method, the endpoint is less severe, and paralysis is observed for a shorter period of time than in the MBA. However, although ex vivo methods allow sensitive detection of the toxin, they are still required the use of high number of animals.

A variety of in vitro methods are available for BoNT detection, including immunoassays, nucleic acid-based assays, catalytic activity assays, and cell-based assays. Immunoassays are advantageous as they are capable of detecting BoNTs in a fast, simple, and reproducible way. Moreover, they do not require skilled personnel and equipment, unlike MBA. Immunoassays rely on the association between an antigen and an antibody, and they use a wide range of methods such as enzyme-linked immunosorbent assay (ELISA), electrochemiluminescence (ECL), flow cytometry, and lateral flow (Scarlatos et al., 2005, Nepal and Jeong, 2020). As immunoassays employ polyclonal, monoclonal, and recombinant antibodies, the sensitivity of the assay is mainly based on the production of highly efficient antibodies (Scarlatos et al., 2005). Therefore, a major limitation of immunoassays is the need for high-quality antibodies, which are expensive and challenging to produce. Moreover, as immunoassays might detect active and inactive toxins together, false positive results are observed

quite commonly (Pellett, 2013). Immunoassays can be used both quantitatively and qualitatively to detect BoNTs, but they are limited in assessing their biological potency.

Nucleic acid-based methods employ the polymerase chain reaction (PCR) to determine the existence of the toxin in food, clinical, environmental samples, and pharmaceutical products (Nepal and Jeong, 2020). This method eliminates the incubation of BoNT in culture, which enables more rapid detection of the neurotoxin. PCR assays, however, do not measure the toxin. Instead, they detect the organism carrying the BoNT gene in the tested samples (Scarlatos et al., 2005). Therefore, an additional assay is required to quantify the amount of toxin in the samples. Also, this method requires more skilled personnel and a longer amount of time for analysis than other in vitro methods.

Catalytic activity assays utilise the endopeptidase activity of BoNTs. The assays are based on the detection of specific targets, such as SNAP25 or VAMP2, which are cleaved by BoNTs and generally employ ELISA. Cleaved substrates are detected by specific antibodies, which allow the detection of exclusively enzymatically active BoNTs (Scarlatos et al., 2005, Adler et al., 2010). Despite this, the assay measures only LC activity and cannot assess the functions of other main domains. Therefore, BINACLE (binding and cleavage) assays have been developed which are dependent on functional BoNT activity for both binding to specific receptor molecules and cleavage of substrates. With BINACLE assays, active BoNT/B is sensitively measured with a limit of detection below 0.1 mouse LD50/ml (Wild et al., 2016). Similarly, BoNT/A is also sensitively detected with a detection limit of less than 0.5 mouse LD50/ml (Behrensdorf-Nicol et al., 2018). Although BINACLE is a very sensitive assay, it is still unable to reflect the function of the translocation domain in BoNTs. Therefore, it cannot be used instead of the MBA. As cell-based assays include all steps of intoxication, they are viable candidates for replacement assays for the MBA.

1.3.2.1 Cell-based assays

A variety of cell types have been employed to develop cell-based assays for CNT detection (Table 1.3). Primary neurons from rodents or chickens are tested for BoNT detection and found to be highly sensitive to detecting BoNTs (Stahl et al., 2007, Whitemarsh et al., 2013). Although they are highly sensitive to BoNTs and relatively cheap to use, they have limitations that make them impractical to use in cell-based assays (Kiris et al., 2014). Animals are still required to be sacrificed to obtain neurons. It is difficult to get a sufficient number of cells each time and preparation needs skilled personnel. Moreover, as primary cells do not form a homogenous neuronal population, variation in the results is expected from test to test (Pellett, 2013). As stem cell technology has advanced, CNT-based assay platforms have opened up new opportunities. Mouse embryonic stem cell (ESC)- derived neurons and

motor neurons, human ESC-derived neurons and human induced pluripotent stem cells (hiPSC)-derived neurons have been investigated thoroughly and found to be quite sensitive to BoNT detection (Whitemarsh et al., 2012b, Pellett et al., 2017, Jenkinson et al., 2017). However, a major disadvantage of stem cell-based assays is that differentiation of the cells into neurons requires weeks or even months, which makes them unsuitable for fast cell-based assays (Pellett et al., 2019). It would be more appealing if their maturation time was shortened. To illustrate, Pellet et al. (2017) used hiPSC-derived neurons, which were matured for 18 days, and sensitively detected BoNT/A. In contrast, the other commercial hiPSCs were matured into sensory neurons within only 8 days, and BoNT/A was detected in a sensitive manner (see Appendix 2). HiPSC-derived neurons are more advantageous than mouse-ESC-derived neurons in terms of being reproducible and easy to culture. However, hiPSC-derived neurons are more expensive.

Cell types	Sensitivity (BoNT/A)	Advantages	Disadvantages
Primary neurons	~0.3-1 U	Highly sensitive, cheap	2-3 weeks maturation time, difficult to culture, not homogenous, sacrificing animals
Mouse ESC-derived neurons	~0.8-1 U	Highly sensitive, cheap	~2 weeks maturation time, difficult to culture, less reproducibility
hiPSC-derived neurons	~0.3 U	Highly sensitive, easy to culture, reproducible	Expensive, long maturation time
Immortalised cell lines	>2.5 U	Reproducible, easy to culture, 1-day- 2 weeks cell differentiation, cheap, easy to manipulate	Less sensitive

Table 1.3 Properties of different cell types used in cell-based assays for detecting CNTs.

Immortalised cells are another cell type commonly employed for CNT detection and a variety of cell lines, such as human SiMa neuroblastomas, P19 embryonal carcinoma cells and NG108-15 cells, have been tested for this purpose (Tsukamoto et al., 2012, Whitemarsh et al., 2012a, Rust et al., 2017). Immortalized cells are very practical for several reasons. They are simple to culture, consist of homogeneous populations, and can be generated in a considerable amount, making them more advantageous than primary neurons (Kiris et al., 2014, Pellett et al., 2019). Their differentiation usually takes a shorter time and involves fewer steps compared to stem cell-derived neurons. Furthermore, they are renewable and inexpensive. Although they have several strengths, they are less sensitive than

primary and stem-cell-derived neurons. However, they are easy to manipulate, so their sensitivity could be enhanced by several methods such as transduction of desired receptor and target proteins, addition of GT1b gangliosides, and chemical simulation of KCl or $CaCl_2$ (Pellett, 2013, Kiris et al., 2014). All these properties make immortalised cells more suitable candidates for cell-based assays. Human neuroblastoma cells, SiMa and SH-SY5Y, were extensively studied for BoNT detection and SiMa cells in particular demonstrated quite high sensitivity for BoNT/A and BoNT/B, and were approved by food and drug administration (FDA) for BoNT/A detection (Purkiss et al., 2001, Fernandez-Salas et al., 2012, Rust et al., 2017). In this thesis, SiMa cells were examined for sensitivity to other BoNT serotypes and TeNT. Moreover, I investigated another human neuroblastoma cell line, LAN-5, to develop cell-based assays for detection of CNTs.

1.4 Aims of thesis

This introduction has focused on four main themes: Clostridial neurotoxins, their mechanism of action and biochemical properties, their medical and therapeutic use, and their detection methods. This thesis aims to develop cell-based replacement assays by using human neuroblastoma cell lines for sensitive detection of Clostridial neurotoxins. A novel human neuroblastoma cell line, LAN-5, has been introduced and established for CNTs detection. SiMa and LAN-5 cell lines were then compared their ability to detect the activity of BoNT/A, BoNT/B, BoNT/C, BoNT/D, BoNT/DC, and TeNT. Further, neuroblastoma cells and HeLa cells were examined to determine if they possess the receptors required for CNT entry, and the effect adding exogenous receptors on the cell sensitivity to BoNT was determined. Finally, a one-step ELISA assay was adapted for BoNT/A and BoNT/C detection, which provides more convenient and faster detection. As a result, it is hoped that novel findings in these areas will be made as well as limitations explained. The goal of this project is to contribute to the development of cell-based assays for CNTs that can be used for a broader range of scientific research.

2 Chapter 2: Materials and Methods

2.1 Materials

2.1.1 Reagents

Reagent	Supplier/ Product code
Benzonase nuclease	Sigma-Aldrich/ E1014-25KU
Bovine Serum Albumin (BSA)	Sigma Life Science/ A2153-100G
Bromophenol Blue	BDH Chemicals / 200152E
Dimethyl sulfoxide (DMSO)	Santa Cruz/ SC-358801
Ethylenediaminetetraacetic acid (EDTA) 0.5 M (pH 8.0)	Invitrogen/ 15575-038
Ethanol	Fisher Chemical/ E/0665DF/17
Fish skin gelatin	Sigma Life Science/ G7765
Glycerol	Fisher Chemical/ G/0650/17
HEPES 1M (pH 7.3)	Fisher Bioreagents/ BP299-500
Hydrochloric acid (HCl) 12M 37 %	Thermo Fischer Scientific/ 124635001
Magnesium Chloride ($MgCl_2$)	Acros Organics/ 223210010
Laminin (1 mg/mL)	Sigma/ L2020
MES running buffer (20X)	Invitrogen/ NP0002
Methanol	Fisher Chemical/ M/4045/17
NaCl	BDH Chemicals/ 27808.297
Skimmed milk powder	Millipore Sigma/ 70166-500G
Opti-MEM (Reduced Serum Media) (1X)	Gibco Life Technologies/ 31985-062
Paraformaldehyde (PFA) 16 % w/v	Alfa Aesar/ 43368
Phosphate Buffered Saline (PBS) (10X) pH 7.4	Fisher Bioreagents/ BP399-4
Phosphate Buffered Saline (PBS) (1X) pH 7.4	Gibco Life Technologies/ 10010-015
Protease inhibitor, EDTA-Free	SigmaFast™/ S8830
Sodium Dodecyl Sulphate (SDS)	Fisher Chemical/ S/S200/53
Transfer Buffer (10X)/ Tris-glycine Buffer	Geneflow/ EC-880
0.5 M Tris-HCl pH 6.8 (Stacking gel buffer)	Bio-Rad/ 1610799
Triton-X-100 (Electrophoresis)	Fisher Bioreagents/ BP151-500
Tween-20	Fisher Bioreagents/ BP337-500

Table 2.1 Details of reagents used.

2.1.2 Solutions and buffers

Blocking Solution for ICC: Mixed 4 mL Fish skin gelatin (2 %, v/v), 4g BSA (2 %, w/v), and 0.2 mL Tween-20 (0.1 %, v/v) in 200 mL 1X PBS, aliquoted in 10 mL portions and stored at -20 °C.

Blocking solution for WB: 5 mL skimmed milk powder (10 %, w/v) made up to 50 mL with 1 % PBS-Tween, mixed for 10 min in the rotator and centrifuged at 7197 relative centrifugal force (RCF) for 5 min. Stored at +4 °C for up to 1 week.

Blocking solution for ELISA: 1 g BSA (1%, w/v) in 100 mL 1X PBS, aliquoted in 1 mL portions and stored at -20 °C.

Buffer A- (prepared by Dr Charlotte Leese): Mixed 10 mL 1 M HEPES pH 7.3 (20 mM) and 10 mL 5 M NaCl (100 mM) in 500 mL dH_2O.

BSA-Opti-MEM: 0.05 g BSA (0.5 %, w/v), in 10 mL Opti-MEM, kept in aliquots at -20 °C.

Cell extract solution (for ELISA): Dissolved 1 tablet of protease inhibitor and 125 µL Triton-X 100 (0.5 %, v/v) in 50 mL 1X PBS, stored in aliquots at -20 °C.

Laminin: 1 mL Laminin (1 mg/mL) in 4 mL sterile 1X PBS, stored in aliquots at -20 °C. It was diluted again in 1:20 with 1X PBS when it was used for coating (Final concentration was 10 µg/mL in the well).

Membrane Transfer Buffer: Mixed 200 mL Methanol (20 %, v/v), 700 mL cold dH_2O, 100 mL 10X Tris-glycine (10 %, v/v) in given order.

MES Running Buffer: Mixed 50 mL 20X MES running buffer (5 %, v/v) with 950 mL cold dH_2O.

Permeabilization solution for ICC, 0.1 % Triton X-100 (v/v): 50 µL Triton X-100 in 50 mL 1X PBS, kept at room temperature (22 °C).

Wash buffer for ELISA: 100 µL Tween (0.05 %, v/v) in 200 mL 1X PBS, kept at room temperature.

1 % PBS-Tween (v/v): Mixed 500 mL 10X PBS, 4.5 L dH_2O and 5 mL Tween (0.1 %, v/v).

70 % Ethanol (v/v): Mixed 1400 mL Ethanol and 600 mL dH_2O.

4X Sample Lysis Buffer (Westerns): Mixed 4 g SDS (8 %, w/v), 25 mL 0.5 M Tris-HCl pH 6.8 (0.25 M), 0.8 mL 0.5 M EDTA (8 mM), 10 mL 100 % Glycerol (20 %, v/v), 1 tip Bromophenol Blue, add dH_2O up to 50 mL, kept in 1 mL aliquots at -20 °C.

1X Phosphate Buffered saline (PBS): 100 mL 10X PBS in 900 mL dH_2O.

10 % SDS (w/v): 50 g SDS (sodium dodecyl sulphate) in 500 mL dH_2O, stored at room temperature.

10 % SDS (w/v) -0.25 M HCl solution: 250 mL 10 % w/v SDS + 12.5 mL of 5 M HCl, stored at room temperature.

1M $MgCl_2$: 9.5 g $MgCl_2$ mixed with 100 mL dH_2O very slowly in a glass bottle.

2.1.3 Toxins

Native clostridial neurotoxins used to treat cells are listed in the Table 2.2. Toxicity was determined by suppliers as $2.7x10^8$ LD_{50}/mg for BoNT/A, $1.25x10^8$ LD_{50}/mg for BoNT/B, and 2.6 10^7 LD_{50}/mg for BoNT/DC.

Toxins	Source	Supplier	Reference
BoNT/A	Bacterial fermentation	Metabiologics	Lot#A042519-01
BoNT/B	Bacterial fermentation	Merz	Lot#90171002
BoNT/C	Bacterial fermentation	Gifted from Thomas Binz[1]	
BoNT/D	Bacterial fermentation	Gifted from Thomas Binz[1]	
BoNT/DC	Bacterial fermentation	Metabiologics	Lot#D112117-01
TeNT	Bacterial fermentation	List Labs	Lot#19050A2

Table 2.2 Details of toxins and reengineered BiTox molecules used.

[1] Hannover Medical School, Institute of Cell Biochemistry, Hannover, Germany

2.1.4 Cell lines

All cell lines used for experiments are listed below.

Cell line	Species	Disease derived from	Cell type	Supplier	Reference
HeLa	Human	Cervical cancer	Epithelial	Gift from Andrew Peden[2]	RRID:CVCL_0030
HEK293	Human		Embryonic Kidney	Davletov Lab	RRID:CVCL_0045
LAN-5	Human	Neuroblastoma	Neuroblast	DSMZ, ACC 673	RRID:CVCL_0389
SiMa	Human	Neuroblastoma	Neuroblast	DSMZ	RRID:CVCL_1695

Table 2.3 Details of cell lines used.

[2] University of Sheffield, School of Biosciences, Sheffield, United Kingdom

2.1.5 Antibodies

Primary and secondary antibodies used in western blot (WB), immunocytochemistry (ICC), and ELISA are listed below. For SNAP25 detection, in-house SNAP25 antibodies were used mostly during this

project and cleavage products recognised by the antibody was schematically demonstrated in Figure 2.1 below.

Primary Antibody	Target	Species	Dilutions	Supplier
Intact SNAP25	SNAP25	Rabbit polyclonal	1:3000 (WB); 1:500 (ICC); 1:10 (ELISA)	In-house
BoNT/A cleaved SNAP25	BoNT/A; BoNT/C cleaved SNAP25	Rabbit polyclonal	1:2000 (WB); 1:5000 (ICC); 1:50 (ELISA)	In-house
Syntaxin 1	Uncleaved Syntaxin 1	Rabbit polyclonal	1:2000 (WB)	In-house
2F7-1	BoNT/B; TeNT cleaved cytosolic VAMP2	Rabbit monoclonal	1:2000 (WB)	Genscript (Custom made)
131G9-1	BoNT/B; TeNT cleaved cytosolic VAMP2	Rabbit monoclonal	10 µg/mL (ELISA)	Genscript (Custom made)
5593 BoNT/C cleaved SNAP25	BoNT/C cleaved SNAP25	Mouse monoclonal	1:2000 (WB); 1:10 (ELISA)	Robert Koch Institute
D27 cleaved vesicular VAMP2	BoNT/D; BoNT/DC cleaved vesicular VAMP2	Mouse monoclonal	1:2000 (WB); 1:500 (ICC)	Robert Koch Institute
BoNT/D cleaved cytosolic VAMP2	BoNT/D; BoNT/DC cleaved cytosolic VAMP2	Rabbit polyclonal	1:2000 (WB)	Davids Biotechnology (Custom made)
Beta actin AC-15		Mouse monoclonal	1:1500 (WB)	Sigma-Aldrich-A1978
Beta-III tubulin		Mouse monoclonal	1:1000 (ICC)	R&D systems-MAB1195
SV2-pan	SV2-A; SV2-B; SV2-C	Mouse monoclonal	2 µg/mL (WB); 5 µg/mL (ICC)	DSHB-AB_2315387
Synaptotagmin I	Synaptotagmin I cytoplasmic tail	Mouse monoclonal	1:1000 (WB); 1:100 (ICC)	Synaptic Systems-105011
Synaptotagmin II	Synaptotagmin II luminal domain	Rabbit polyclonal	1:1000 (WB); 1:100 (ICC)	Synaptic Systems-105222
GD2		Mouse monoclonal	1:200 (ICC)	Abcam-68456
GD1a		Mouse monoclonal	5 µg/mL (ICC)	DSHB-AB_2619567
GT1b-2b		Mouse monoclonal	5 µg/mL (ICC)	DSHB-AB_2619575

VAMP2		Rabbit monoclonal	1:10.000 (WB)	Abcam-1818169
VAMP2		Rabbit	1:200 (ICC)	Gift from Liz Seward[3]
HA tag		Rabbit	1:400 (ICC)	Gift from Andrew Peden[2]

Table 2.4 Details of primary antibodies used.

[2] University of Sheffield, School of Biosciences, Sheffield, United Kingdom

[3] University of Sheffield, School of Biosciences, Sheffield, United Kingdom

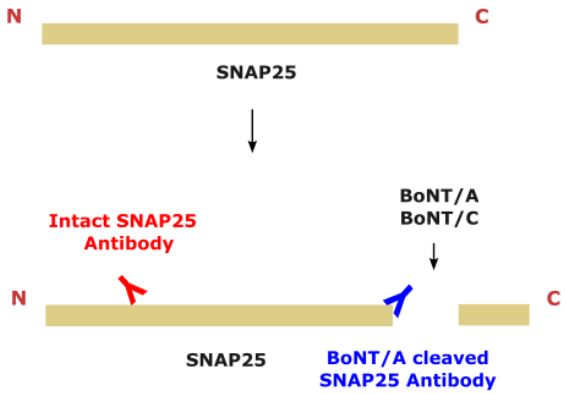

Figure 2.1 Schematic representation of cleaved and uncleaved SNAP25 detection by in-house SNAP25 antibodies.

Intact SNAP25 antibody recognises part of SNAP25 independently of SNAP25 cleavage. Both uncleaved and cleaved SNAP25 can be detected separately due to the slight difference between molecular size of uncleaved (25kDa) and cleaved SNAP25 (24kDa). BoNT/A cleaved SNAP25 antibody recognises the N terminal fragment of SNAP25 after cleavage. Figure was created by using Inkscape.

Secondary Antibody	Dilutions	Supplier
Sheep anti-mouse HRP tag linked	1:24000 (WB)	Amersham/ NA931
Donkey anti-rabbit HRP tag	1:24000 (WB)	Amersham/ NA934D
Goat anti-mouse (Alexa Fluor 594 tag)	1:2000 (ICC)	Life Technologies/ A11005
Goat anti-rabbit (Alexa Fluor 594 tag)	1:2000 (ICC)	Life Technologies/ A11012
Goat anti-mouse (Alexa Fluor 488 tag)	1:2000 (ICC)	Life Technologies/ A11029

Table 2.5 Details of secondary antibodies used.

2.2 Cell culture

2.2.1 Cell line cultures

All cell lines were cultured at 37 °C and 5 % CO_2 in an incubator (Panasonic, MCO-170AIC-PE) with humidity. SiMa and LAN-5 human neuroblastoma cell lines were cultured in RPMI 1640 (1X) + Glutamax (Gibco Life Technologies, 61870-010) with 10 % foetal bovine serum (FBS) (Gibco Life Technologies, 10082-147). HeLa cells were cultured in Dulbecco's modified Eagle medium (DMEM) (1X) + Glutamax (Gibco Life Technologies, 10564-011) with 10 % FBS. The cell lines were passaged when they reach 70-80 % confluency. The growth media was replaced when it turned yellow because of acidity.

All cell lines were passaged with 0.25 % trypsin-EDTA (Gibco Life Technologies, 25200-056). After trypsinization, collected cells were centrifuged (VWR Compact Star CS 4) at 857 RCF for 5 min and the pellet resuspended with the media for cell counting. For viable cell count, the cells were diluted in 1:1 in trypan blue dye (Sigma Life Science, T8154-100ML) and counted in the automated cell counter (Bio-Rad, TC20^{TM}) using dual-chamber cell counting slides (Bio-Rad, 1450011). The machine gave the results of the total cell concentration (cells/ml), alive cell concentration (cells/ml), and % viability of the cells.

The neuroblastoma cell lines were killed when they reached the passage number of 30, and the fresh cells with lower passage number were defrosted. The cells were first expanded at T25 flask (Sarstedt, 83.3910.002) and followingly transferred to T75 flask (Sarstedt, 83.3911.002).

2.2.2 Cell seeding

Unless otherwise indicated, SiMa and LAN-5 neuroblastoma cell lines were seeded at $2x10^4$ cells per well in 96-well plates (Greiner bio-one, 655090), $1x10^5$ cells (differentiated) and $8x10^4$ cells (undifferentiated) per well in 48-well plates (Thermo Fisher Scientific, 150687), and $5x10^5$ cells per well in 24 well plates (Corning Costar, 3526). HeLa cell line was seeded at $6x10^3$ or $12x10^3$ cells per well in 96-well plates, $3x10^4$ cells per well in 48-well plates, and $1x10^5$ cells per well in 6 well plates (Corning Costar, 3506).

Cells were seeded into 96-well plates had a volume of 200 µL, 48-well plates had a volume of 600 µL, 24-well plates had a volume of 1 mL, 6-well plates had a volume of 2 mL cell media.

After seeding, neuroblastoma cell lines were kept at room temperature for 15 minutes and shook gently to allow to cells to settle before putting 37 °C incubator. This step helps ensure an equal distribution of the cells in the bottom of the well (Lundholt et al., 2003).

2.2.3 Neuroblastoma cell line differentiation

For laminin coating, the plate wells were incubated with 10 µg/mL laminin in sterilised 1X PBS for at least 2 hrs at 37 °C. 50 µL, 150 µL, and 300 µL of laminin were used for 96-well, 48-well, and 24-well plates respectively. The wells were washed twice with 1X PBS (the last wash was done immediately before seeding cells in order to make sure wells did not dry out). After cell counting, the required number of cells were mixed in differentiation media. Differentiation media was made up with 4 % B27 (50X) (Gibco Life Technologies, 17504-044), 1 % 1M HEPES, 1 % penicillin-streptomycin (Gibco Life Technologies, 15140-122) in Neurobasal medium (1X) (Gibco Life Technologies, 21103-049). 10 µM all-trans-retinoic acid (Sigma, R2625) was added immediately before mixing with the cells. The seeded cells were incubated for 3 days to allow differentiation. The brightfield images below show the appearance of the cells at different time points (Figure 2.2). The images were recorded using a live cell movie analyser (JuLI^{TM} Br & FL station, NanoEnTek).

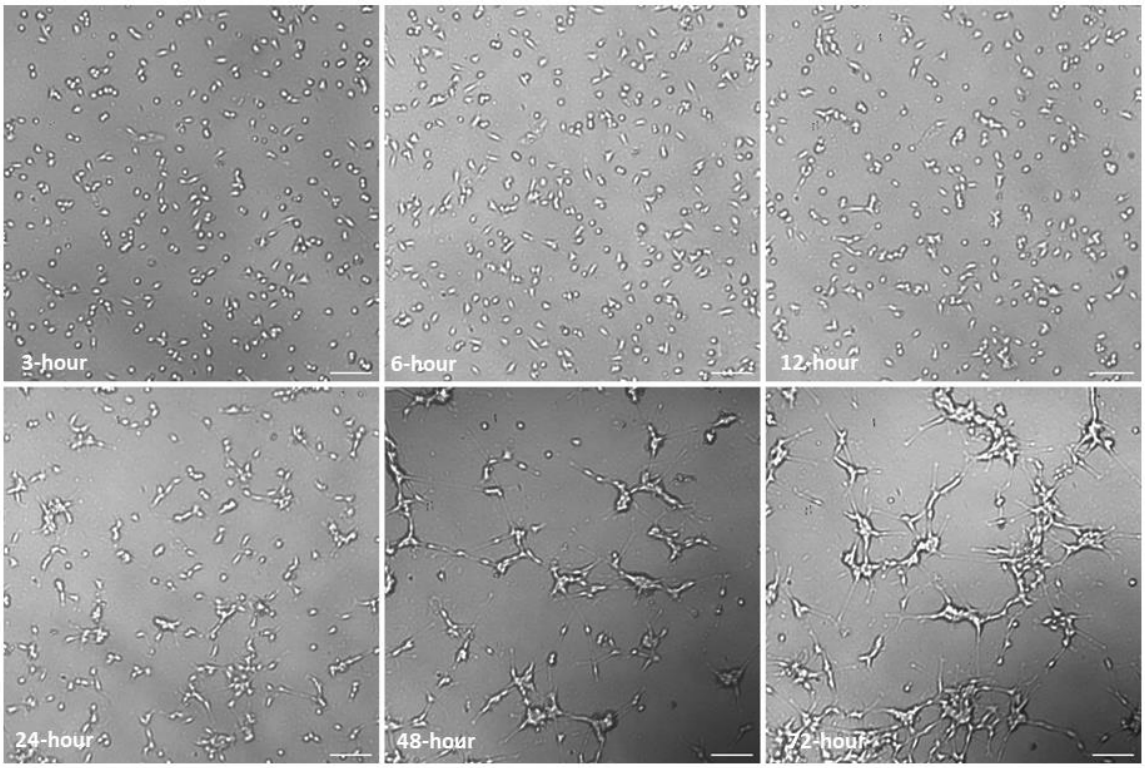

Figure 2.2 The differentiation of LAN-5 neuroblastoma cell lines for 3 days.

The LAN-5 neuroblastomas were seeded on laminin coated 96 well plates in differentiated media. The cells were incubated for 3 days at 37 °C, 5 % CO_2. The brightfield channel of the JuLi live cell movie analyser took the images every 15 minutes for 3 days. The images were the same area on the well at given time points. All scale bars are 100 µm.

2.2.4 Cell treatment

Undifferentiated neuroblastoma cells and HeLa cells were treated with the toxins 1-day after seeding, while differentiated neuroblastoma cells were treated 3-days after seeding. Native toxins were initially diluted in reduced serum media OPTI-MEM including 1 % penicillin-streptomycin. However, in this condition, some of the toxin was lost during titration. Therefore, to prevent this loss, samples were diluted in Opti-MEM mixed with 0.5 % bovine serum albumin (BSA) (Figure 2.3). If GT1b (Ganglioside GT1b trisodium salt from bovine brain, Enzo Life Sciences, ALX-302-011-M005) was added, 50 µg/mL (unless indicated) of GT1b was mixed with the toxins. For dilutions of the reengineered BiTox molecules, proteins were diluted in fresh differentiation media to 2x desired final concentration. Then 2/3 of the cell media volume was removed replaced with 1/3 volume of the fresh media mixed with toxin, to replenish the cell media and dilute the toxin to the desired final concentration. Unless stated, cells were treated with samples for 3 days. The schematic demonstration of an example of cell differentiation and treatment, and subsequent collection of cells to be used for either western blot or ELISA (Figure 2.4)

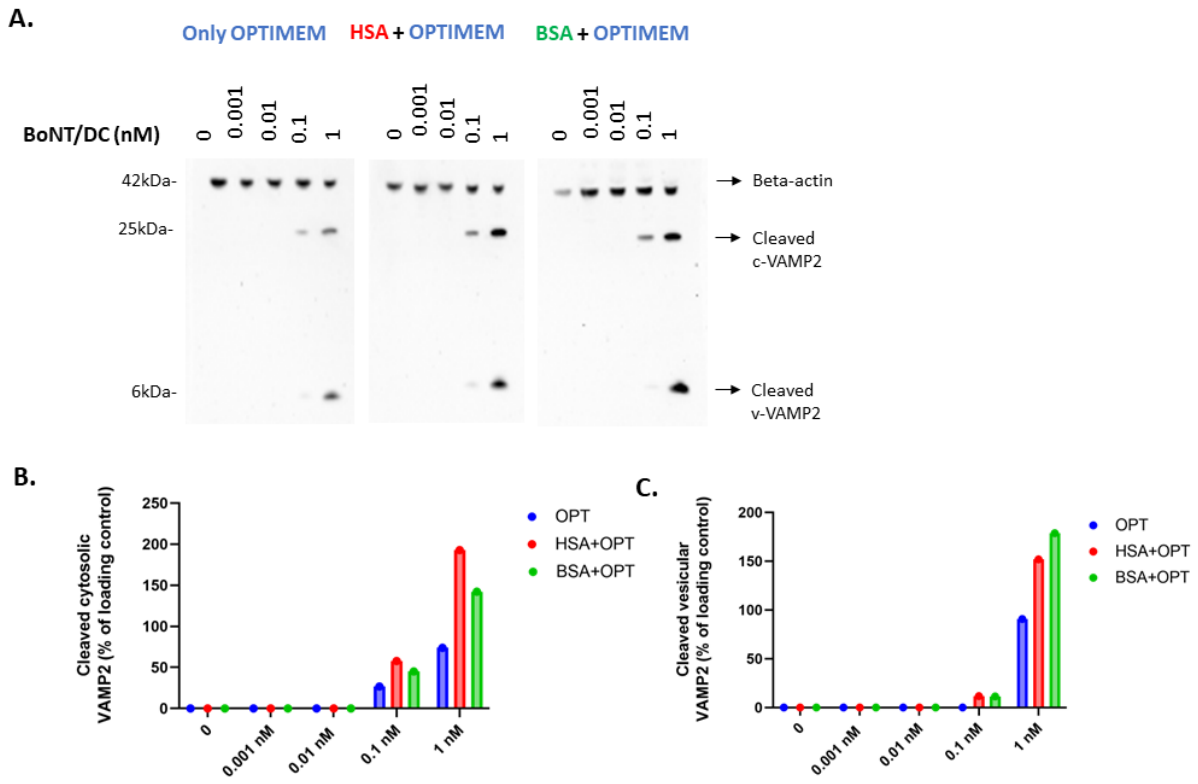

Figure 2.3 Either BSA or HSA addition to Opti-MEM prevent toxin loss during titration.

A) *Western blot results show the proportion of cellular cleaved VAMP2 in differentiated GFP-VAMP2 LAN-5 neuroblastoma cells following application of BoNT/DC.* ***B-C)*** *The graphs above showing the quantification of immunosignals for cleaved cytosolic VAMP2 and for cleaved vesicular VAMP2 between different conditions. Toxins were applied to the cells by 1:10 dilution. Cells were treated with the diluting agents which are only Opti-MEM, Opti-MEM with 0.5 % HSA, and Opti-MEM with 0.5 % BSA, respectively. Mouse monoclonal Ab (D27) was added in 1:2000 dilution to see BoNT/DC cleaved vesicular VAMP2; D cleaved VAMP2 cytosolic rabbit polyclonal Ab was used in 1:2000 dilution to see BoNT/DC cleaved cytosolic VAMP. Mouse beta-actin Ab was added in 1:1200 dilution as a loading control. Images were taken from ChemiDoc XRS.*

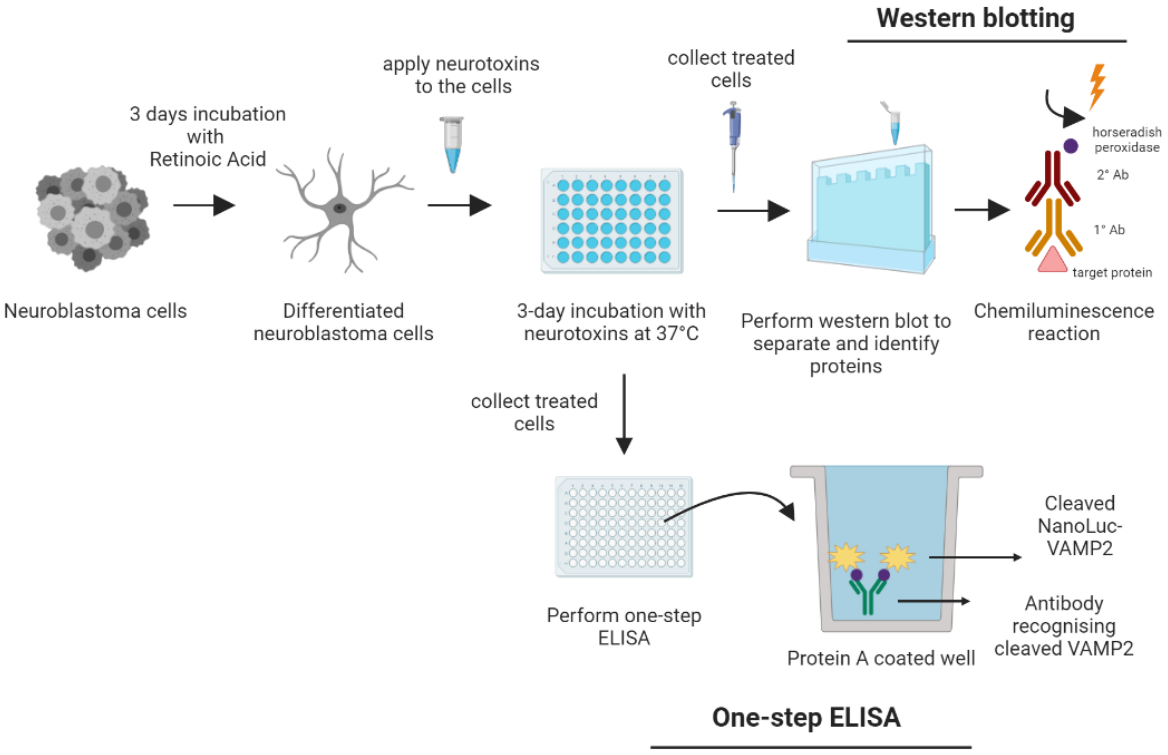

Figure 2.4 Schematic example of cell differentiation, treatment, and collection for the western blot or ELISA method.

Figure was created by using BioRender.

2.2.5 Lentiviral cell line transduction

Several target proteins and receptor proteins were inserted via viral plasmid to cell lines to enhance our cell-based assay. NanoLuc VAMP2 SiMa and GFP VAMP2 LAN-5 cell lines were generated by Dr. Ciara Doran. NanoLuc VAMP2 LAN-5, SYTII- NanoLuc VAMP2 LAN-5, NanoLuc VAMP2 HeLa, and SYTII-NanoLuc VAMP2 HeLa cell lines were generated by Dr. Ceyda Caliskan. NanoLuc SNAP25 LAN-5 and SNAP25 NanoLuc LAN-5 cell lines were generated by myself, and the procedure is explained below. It has two main steps as transfection of HEK cell (lentivirus production) and lentiviral transduction.

2.2.6 Transfection of HEK cells

On day-1 HEK cell lines were cultured in RPMI 1640 + Glutamax with 10 % foetal bovine serum (FBS). They were passaged at least two times after defrosting to make them more suitable for transfection. The number of $3x10^6$ HEK cells were seeded in 10 mL media at in a 10 cm dish (Nunclon Delta surface treated for Tissue Culture, Thermo Fisher) and incubated overnight. The dish was shaken gently to ensure an even distribution of cells, which is important for the cells to take in DNA efficiently.

On day-2, the media was then aspirated, and 6.5 mL antibiotic-free fresh media was added to cells 1 hr before transfection. Transfection solutions (each 400 µL) were prepared (Table 2.6) half an hour before transfection. After incubation of each tube individually for 5 minutes, tubes were mixed with each other and incubated further for 20 minutes. The mixture was added onto cells by dropwise and incubated at 37 °C, 5% CO_2 overnight.

DNA mixture (Tube 1)	Polyethyleneimine (PEI) (Tube 2)
Opti-MEM	Opti-MEM
5 µg DNA plasmid (N-SNAP25 (1.5 µg/µL); SNAP25-N (1.5 µg/µL)), pMMLV (Vector Builder)	33 µg PEI (1 µg/mL) (Polysciences, 23966)
5 µg Gag-pol virus (2 µg/µL), pUMVC (plasmid) (Addgene, 8449)	
1 µg vesicular stomatitis virus G (VSV-G) (240 ng/µL), pMD2.G (Addgene, 12259)	

Table 2.6 Details of reagents used for cell transfection.

The following day (day-3), the media on the HEK cells was replaced with fresh antibiotic-free media. Native LAN-5 cells were seeded at $7.5x10^5$ cells per well in 2 mL of media at 6-well plate. On day-4, HeLa cells were seeded at 1 $x10^5$ cells per well as a positive control for transduction because they can take DNA inside very efficiently (Ning and Tang, 2012). As the HeLa cell line is one of the most contagious cell lines, LAN-5 and HeLa cells were seeded in separate 6-well plates to prevent cross contamination (Capes-Davis et al., 2010).

2.2.6.1 Lentiviral transduction of LAN-5 and HeLa cells

On day-5, the viral supernatant of the HEK cells was collected by a syringe and filtered using 0.45 µm filter. The media of seeded HeLa and LAN-5 cells was replaced with the filtered supernatant viral media. The cells were centrifuged at 2000 RCF for 1 hour at room temperature. Then these cells were incubated at 37 °C overnight.

The following day (day-6), the viral supernatant was replaced with fresh growth media. The cells were left at the incubator for 2-3 days to start expressing the transgene. When the cells reached confluency, they were expanded to T25 flask and maintained in growth media including 1 µg/mL puromycin (1 mg/mL, Sigma, P8833) to begin selecting transduced cells. Because the transduced plasmid has puromycin resistant gene, transduced cells were always maintained with the puromycin added growth media.

2.2.7 Cell line defrosting and freezing

For thawing, cells were removed from liquid nitrogen and incubated for 2 minutes in a 37 °C water bath. After the cells were thawed, they were diluted to 5 mL with pre-warmed growth media. The cells were centrifuged at 857 RCF for 5 minutes. The media was removed, and the cells were resuspended in fresh growth media. The cells were placed in a culture flask and incubated at 37 °C. They were passaged at least twice ensure they had recovered from freeze-thaw before they were used in any experiments.

To freeze cells, confluent cells in a T75 flask were trypsinized and cell counting was performed in order to calculate how many vials containing $1.5x10^6$ cells each could be prepared. The amount of freezing media (10 % DMSO in cold FBS) needed to allow 1 mL per vial was then calculated and prepared. After calculation of total amount of cells and media needed, the necessary number of cells were centrifuged at 3000 RCF for 5 minutes and re-suspended in the cold freezing media. 1 mL of mixed solution (each containing $1.5x10^6$ cells) were placed in 1.8 mL cryo-tube vials (Thermo Fisher Scientific, 377267). The cryo-tubes were put in a freezing container (Nalgene) and frozen at 80 °C for overnight. Afterwards, they were stored long-term in liquid nitrogen.

2.3 Western blotting

2.3.1 Cell harvesting and lysis

To lyse cells, 1X western lysis buffer was prepared by mixing 300 µL 4X western lysis buffer with 900 µl dH_2O, 26 µL 1M $MgCl_2$ and 2.6 µL ≥250 units/µl benzonase nuclease (added immediately before use). Media of the cells seeded in a 48-well plate (Section 2.2.4) was removed and replaced with 45 µL of 1X western lysis buffer. The 48-well plate was then shaken at 650 rpm on a plate shaker (Grant-bio, PMS-1000i) for 10 minutes, and each sample placed into a 0.5 mL tube. Samples were boiled at 100 °C for 3 minutes, then centrifuged at 15,700 RCF for 1 minute. (The boiling step was skipped for the lysates prepared for SV2, SYTI or SYTII detection). An additional benzonase digestion step was then performed to remove excessive DNA in the samples. A second benzonase solution was prepared by mixing 4 µL dH_2O, 0.9 µL 1M $MgCl_2$, and 0.1 µL benzonase nuclease per sample and 5 µL was added to each sample tube. The tubes were then shaken at 650 rpm on a micro shaker (CAMLAB) for 20 minutes. After boiling the samples again at 100 °C for 3 minutes (unless samples were being prepared for SV2, SYTI or SYTII detection), they were centrifuged at 15,700 RCF for 1 minute. The samples were then used immediately for western blot or stored at -20 °C until use.

2.3.2 Lysate protein quantification

The detergent compatible (DC) assay (Bio-Rad) was used to measure protein concentration in the lysates according to manufacturer's instructions. The DC assay is a modified version of the Lowry assay and relies on the reaction of protein with a Folin reagent and alkaline copper solution. The reduction of Folin reagent causes colour and spectral change which is measured by absorbance (Berges et al., 1993). BSA was used as a standard protein and diluted in concentrations from 2.0 mg/mL to 0.2 mg/mL. Reagent A' was prepared by diluting Reagent S (surfactant solution) 1:50 in Reagent A (alkaline copper tartrate solution). After putting 5 µL of standards and samples into a 96-well plate (Corning Incorporated Costar, 3595), 25 µL of Reagent A' was added to them. Followingly, 200 µL of Reagent B (Folin) was added to each wells and the plate was shaken at 650 rpm on shaker for 5 minutes. After the plate was incubated at room temperature for 15 minutes, the absorbance at 750 nm was read using a microplate reader (Bio-Rad, iMark^{TM}). The concentrations of lysates were calculated by the standard curve. A result of one experiment set was given as an example (Figure 2.5).

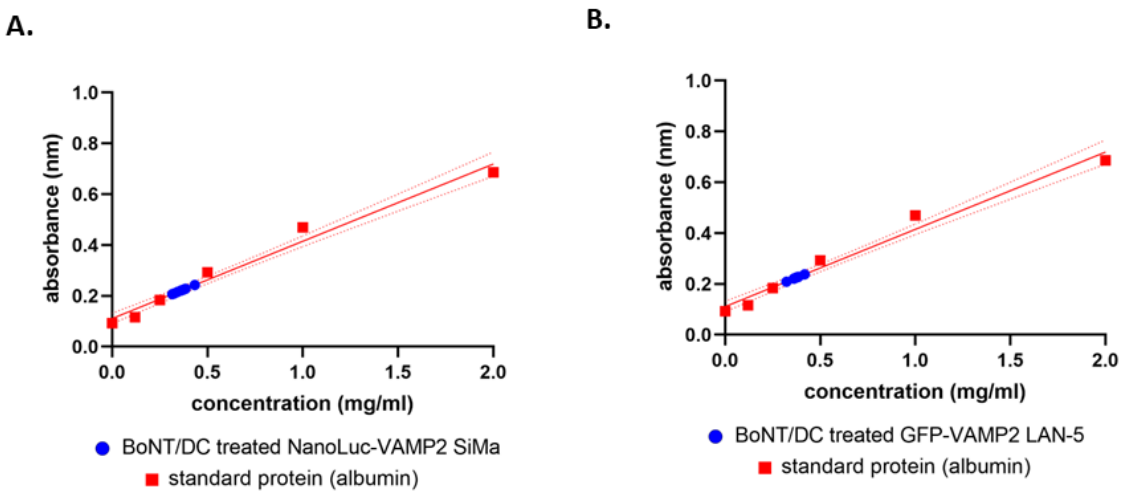

Figure 2.5 Standard curves of DC protein assay for SiMa and LAN-5 cell lysates from one experimental set.

A) *The standard curve showing BoNT/DC treated differentiated NanoLuc-VAMP2 SiMa cell lysates.* ***B)*** *The standard curve showing BoNT/DC treated differentiated GFP-VAMP2 LAN-5 cell lysates. BoNT/DC was applied to the cells by 1:10 dilution. Bovine serum albumin protein was used as a standard protein. Albumin was diluted from 2 mg/mL to 0.2 mg/mL. Absorbance of the samples and protein standards were read at 750 nm wavelength in microplate reader.*

2.3.3 SDS-PAGE

If samples had been stored at -20 °C, they were first boiled at 100 °C for 3 minutes, vortexed and centrifuged if they were frozen before use in sodium dodecyl sulphate polyacrylamide gel electrophoresis (SDS-PAGE).

The wells of a pre-cast gel (NuPage 12 % Bis-Tris Gel, Invitrogen, 1.0 mm x 15 wells) were washed 2-3 times with dH_2O to remove the sucrose storage solution, then the pre-cast gel was placed in a mini gel tank (Invitrogen) which was filled with cold (+4 °C) 1X MES running buffer. Between 1 µg and 3 µg protein of the samples were loaded onto the gel with a maximum volume of 6 µL, unless indicated. (7-10 µg of protein loaded for SYTI, SYTII and SV2). The different loading concentrations of the protein were shown to detect changes in protein amounts between different samples (Figure 2.6). One well of the gel was loaded with 10 µL of 1:5 diluted protein ladder (Bio-Rad Precision Plus Protein Dual colour protein standard) in 1X western lysis buffer to identify the molecular size of the protein bands. For detection of most proteins, the gel was run at constant voltage 180 mV for 60 minutes, until the bromophenol blue reached the bottom. For detecting cleaved and uncleaved SNAP25, which are very close to each other in terms of molecular weight, the gel was run at 180 mV for 120 minutes in a bucket of ice, then run at room temperature for a further 40 minutes, in order to prevent the gel from overheating during the longer running time needed to separate them.

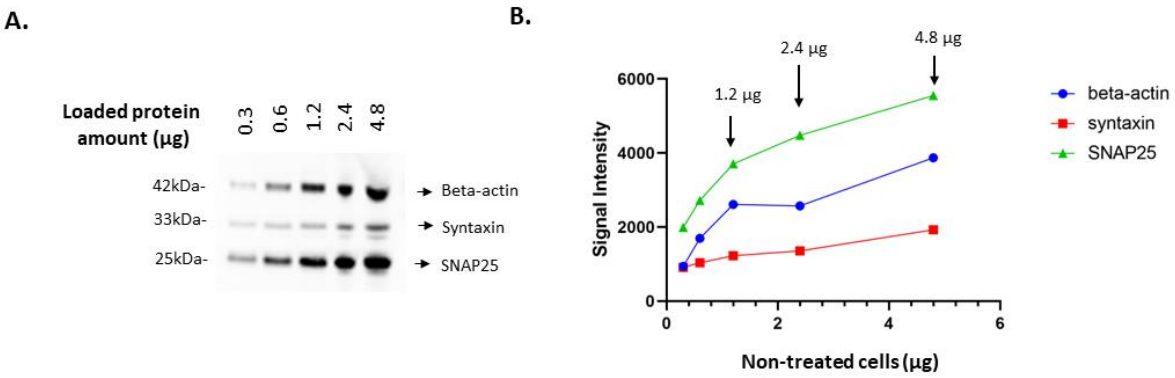

Figure 2.6 The detection of the maximum protein loading.

A) *An immunoblot image showing the increasing concentrations of LAN-5 cell lysates.* ***B)*** *The graph giving the signal intensity of each band according to the protein amounts. SNAP25 antibody was added in 1:3000 dilution to detect uncleaved SNAP25. Syntaxin antibody was added in 1:2000 dilution. Mouse beta-actin Ab was added in 1:1200 dilution. Images were taken from ChemiDoc XRS.*

2.3.4 Western blotting

After the SDS-PAGE had run, the gel was removed from the pre-cast casing and a transfer cassette was set up for western blotting. PVDF transfer membrane (Immobilon-P, Millipore) was activated by soaking in methanol. A sponge, 1 Whatman paper (GE Healthcare), the gel (flipped), pre-activated membrane, 1 Whatman paper, and a second sponge were soaked in membrane transfer buffer and layered on the black side of transfer cassette in the given order. After the cassette was closed, it was placed in transfer tank (Mini Protean Tetra System, Bio-Rad) filled with cold (+4 °C) membrane transfer buffer. Protein transfer was run at constant current of 250 mA for 60 minutes. If the protein ladder had transferred onto the membrane after this time, the transfer was considered successful.

The membrane was incubated with blocking solution at 25 rpm on a rocker (Stuart TM Gyratory rocker SSL3) for 30 minutes at room temperature. Primary antibodies were added in given dilutions at Table 2.4 and rocked overnight in a +4 °C cold room. The following day, the membrane was washed three times with 1X PBS-Tween for 5 minutes on the rocker. The membrane was then incubated with the secondary antibody in given dilutions at Table 2.5 on the rocker for 30 minutes at room temperature. After the membrane was washed another two times with 1X PBS-Tween for 5 minutes on the rocker, SuperSignal West Dura extended duration substrate (Thermo Scientific) was prepared by mixing stable peroxide and luminol/enhancer reagents in 1:1 (total volume of 750 µL per membrane). SuperSignal West solution was added on the membrane evenly which was placed on visualisation tray. Images were taken by ChemiDoc XRS (Bio-Rad) for band quantification.

2.3.5 Western blot band quantification and analyses

Images of blot were quantified by using a band analyses software (Quantity One, version 4.5.1, Bio-Rad). A densitometric measurement of a band was received by a chemi hi sensitivity detection starting from an exposure time of 200 seconds. After the detection was completed, the software created a report which gave a value for the relative band intensities. The percentages of SNAP25 or VAMP2 cleavage were calculated using these values. The % SNAP25 cleavage was calculated by dividing the value of cleaved SNAP25 band by the total value of cleaved and uncleaved SNAP25 bands (Figure 2.7). The % VAMP2 cleavage was calculated by dividing the value of cleaved VAMP2 band by the value of the loading control band (Figure 2.8). Total SNAP25 or beta actin was used as a loading control.

A.

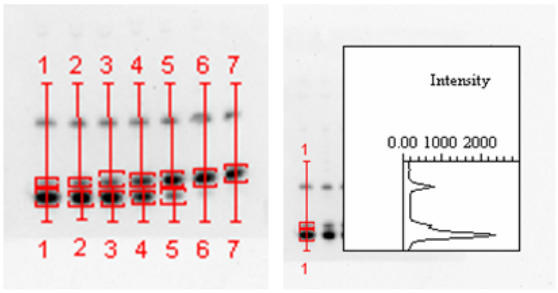

B.

Lane	Band 1 Int. x mm (uncleaved SNAP25)	Band 2 Int. x mm (cleaved SNAP25)	total SNAP25	Band 2 %
1	742.688	3687.925	4430.613	83.23735
2	1113.938	3380.363	4494.301	75.21443
3	1674.588	3210.75	4885.338	65.72217
4	2369.662	2249.8	4619.462	48.70264
5	2958.288	1249.613	4207.901	29.69683
6	3045.613	0	3045.613	0
7	2669.013	0	2669.013	0

Figure 2.7 Demonstration of band analysis of % cleaved SNAP25 for Western blot.

A) *Images showing the band detection on the software.* ***B)*** *Quantification of band intensities and following calculation of % SNAP25 cleaved band based on total SNAP25 band intensity.*

A.

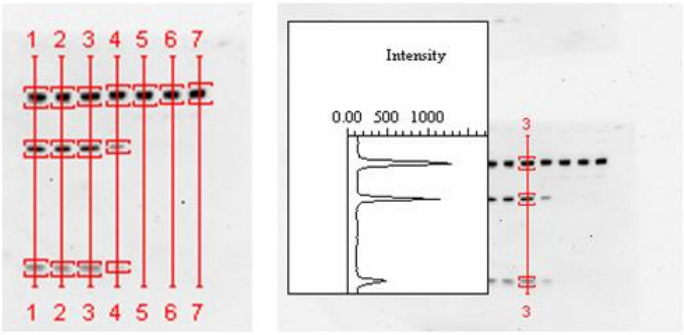

B.

Lane	Band 1 Int. x mm (beta actin)	Band 2 Int. x mm (cleaved c-VAMP2)	Band 3 Int. x mm (cleaved v-VAMP2)	Band 2 %	Band 3 %
1	1780.613	1220.413	711.038	68.53892	39.9322
2	1637.35	1209.688	637.75	73.88084	38.95013
3	1798.588	1221.025	722.275	67.88798	40.15789
4	1669.125	467.6	309.613	28.01468	18.54942
5	1675.125	0	0	0	0
6	1580.313	0	0	0	0
7	1796.338	0	0	0	0

Figure 2.8 Demonstration of band analysis of % cleaved VAMP2 for Western blot.

A) *Images showing the band detection on the software.* ***B)*** *Quantification of band intensities and following calculation of % VAMP2 cleaved band based on band intensity of loading control.*

2.4 ELISA

2.4.1 Cell harvesting and lysis

Media of the treated cells in a 48-well plate (Section 2.2.4) was aspirated and replaced with 40 µL per well of freshly defrosted cell extract buffer (CES), on ice. The plate, still kept on ice, was then shaken at 650 rpm on a shaker for 15 minutes. Each sample was collected into pre-chilled 1.5 mL tubes and kept on ice. The tubes were then centrifuged in a pre-cooled centrifuge (+4 °C) at 20,800 RCF for 15 minutes. The supernatant was then transferred to new pre-chilled 1.5 mL tubes. Collected samples could then be used for ELISA directly or kept at -20 °C until use.

2.4.2 ELISA

Protein A coated plate (Pierce Protein A coated white 96-well plate, Thermo Scientific, ref 15154) was taken from +4 °C and kept at room temperature for half an hour before it covered with the relevant rabbit primary antibodies at the dilutions given in Table 2.4. As the Protein A coated plate was sensitive to light, all incubation steps were performed with the plate covered by a light guard. One Protein A coated plate was used at most 2 times and stored at +4 °C between uses. For the BoNT/C cleaved SNAP25 mouse monoclonal Ab, a Protein G coated plate (Pierce Protein G coated white 96-well plate, Thermo Scientific, ref 15156) was used instead.

The antibody covered Protein A coated plate was rocked overnight in a +4 °C cold room. The following day, after aspiration of the antibody, the plate was washed three times with 100 µL per well of ELISA wash buffer for 5 minutes at 25 rpm on a rocker (Stuart TM Gyratory rocker SSL3). The antibody coated plate was incubated with 100 µL per well of freshly defrosted ELISA blocking solution on the rocker for 1 hr at room temperature. The plate was again washed three times with ELISA wash buffer for 5 minutes on the rocker after the blocking step. In the meantime, 30 µL of the samples were diluted with 40 µL 1X PBS, and 50 µL of the last solution was added into the plate. Approximately between 6 µg and 10 µg protein of the samples were used. The plate was incubated on the rocker for 90 minutes at room temperature. After the samples were aspirated, the plate was washed three times with 100 µL per well of ELISA wash buffer for 5 minutes on the rocker. To measure luminescence, Nano Glo Luciferase assay (Promega, N1130) was prepared by adding 4 % Nano Glo Luciferase assay substrate to the Nano Glo Luciferase assay buffer, keeping the mixture in the dark due to light sensitivity. The luciferase solution was added to the wells 50 µL per well and incubated for 5 minutes at room temperature on the lab bench. The luminescence of the samples was read using a fluorescence plate

reader (Fluoroskan Ascent FL, Thermo Labsystems). Ascent software was used for luminometric measurement by choosing NanoLuc option with 200 msec integration time at 1200 PMT Voltage.

2.5 Microscopy

An inverted epifluorescence microscope (DMIRB, Leica) and a confocal microscope (Nikon A1 TIRF) were used during the project. All brightfield images and images 20x magnification were taken using the Leica microscope and Leica Application Suite X software, The images at 40x magnification were taken on the Nikon A1 TIRF microscope. Image J was used to organise and visualise the images.

2.5.1 Immunocytochemistry

Cells were seeded on a µClear 96-well plate (Greiner bio-one, 655090) as described in section 2.2.2, unless indicated. After cell growth and differentiation, cells were washed with 150 µL of cold 1X PBS for 5 minutes on ice. The cells were then fixed for 15 minutes at room temperature with 16 % PFA diluted to 4 % in the well. After the cells were washed two times with 1X PBS for 5 minutes, they were permeabilised with 150 µL of PBS-0.1 % Triton X-100 for 15 minutes at room temperature. For the staining of GD2, GT1b, GD1a gangliosides, permeabilization step was skipped according to antibody brand instructions. After washing the cells two times with 1X PBS for 5 minutes, they were saturated with blocking solution for 1 hour at room temperature. The cells were incubated with relevant primary antibodies at the dilutions given in Table 2.4 for overnight at cold room. The following day, the cells were washed two times with 1X PBS for 5 minutes, they were then incubated with secondary antibody at the dilutions given in Table 2.4 alongside a 1:1000 dilution of DAPI (Sigma-Aldrich) for 45 minutes at room temperature under a light guard. After washing the plate three times 1X PBS wash for 5 minutes, it was imaged using either the confocal or florescence microscope. The cells were subsequently post-fixed with 1 % PFA for 10 minutes to preserve them for future use. After a final wash with 1X PBS for 5 minutes, the plate was filled with 1X PBS (to avoid cells drying out) and wrapped in foil at +4 °C for 2-3 weeks.

2.6 Statistics

N refers to the number of repeat experiments which were performed independently, n refers to the numbers of repeats within the experiments. All error bars demonstrated in this project represent the mean ± Standard Error of Mean (S.E.M.) for experiments that had 3 or more repeats. Individual values were shown on the graphs for experiments that had 2 replicas or for values that represented experimental errors. Statistical analyses were performed using GraphPad Prism 9.4.1. For dose-

response stimulation analyses, graphs were curve fitted by non-linear regression followed by log(agonist) vs. response (three parameters). Where half maximal effective concentrations (EC50) were given from the data, the goodness of fit the data (R^2) and 95% confidence interval (CI) of the quoted values were provided together. To determine statistical significance, data with one independent variable was analysed by ordinary one-way Analysis of Variance (ANOVA) followed by Tukey's multiple comparison test. Data was analysed by two-way ANOVA followed by either Sidak's or Tukey's multiple comparison tests to assess two independent variables. When there were two data sets, an unpaired two-tailed t-test were performed to determine whether the null hypothesis was correct. Statistical significance was considered as P-value <0.05. P-value of 0.05 means that there is no statistical significance between different experimental conditions with 5% of possibility, NS= P> 0.05 (NS=not significant). Other significance values are displayed as follows: *= P<0.05; **= P<0.01; ***= P<0.001; ****= P<0.0001.

The statistical test used to analyse data, statistical significance level and the number of repeats are stated in the relevant figure legend.

2.7 Safety

Good laboratory practices were performed during the project. Lab coat and gloves were always worn when handling the toxin. Pipette tips used when diluting the native clostridial toxins were deactivated by 0.5 % SDS-HCL mixture. The viral media for transfection/transduction were disinfected with Virkon. Used PFA was kept in a separate bottle as a waste and collected by the health and safety staff regularly.

3 Chapter 3: The establishment of neuroblastoma cell lines for testing the potency of clostridial neurotoxins

3.1 Introduction

Clostridial neurotoxins (CNTs), consisting of botulinum neurotoxins (BoNTs) and tetanus neurotoxin (TeNT), are highly poisonous proteins and small quantities can cause the deadly diseases botulism and tetanus (Turton et al., 2002). During a botulinum infection, the peripheral cholinergic terminals are blocked from releasing acetylcholine, resulting in flaccid paralysis. TeNT, however, inhibits neurotransmitter release at inhibitory interneurons in the spinal cord, leading to spastic paralysis. Despite their opposite clinical symptoms, both neurotoxins cause neuronal cell intoxication in the same manner (Pellizzari et al., 1999).

Sensitive detection of CNTs is essential for several reasons. Regarding BoNTs, there are two main reasons for requiring a sensitive test of BoNT activity. Firstly, safe doses of BoNT/A and BoNT/B serotypes are commonly used for therapeutical and cosmetic reasons (Rossetto et al., 2013a, Pirazzini et al., 2017). Therefore, BoNT therapeutics need to be approved by a potency test before application. Secondly, any environmental sample or food can be contaminated with botulinum serotypes and there is a possibility that CNTs can be used as a bioweapon due to its severity (Rossetto, 2012). Thus, diagnosis of botulism in any suspicious incident is crucial. In relation to TeNT, it is inactivated by formaldehyde treatment and converted into a TeNT toxoid, which becomes an effective vaccine for tetanus (Rossetto et al., 2013b). Generated TeNT vaccines therefore have to be subjected to a safety test checking for absence of any residual neurotoxin.

Currently, both BoNTs and TeNT are tested on animals. TeNT is mostly tested on guinea pigs (Behrensdorf-Nicol et al., 2013); while the mouse bioassay, Mouse LD_{50} (mLD_{50}) is a gold standard assay for detection of BoNTs (Fernandez-Salas et al., 2012). In the mLD50 procedure, intraperitoneal injection of diluted particle-free samples to mice causes blocking of the respiratory muscles and death of the mice. Even though, mLD_{50} is highly sensitive, it has many drawbacks for both technical and ethical reasons. The mLD_{50} is time-consuming, expensive, requires highly trained staff and a well-equipped animal facility. Moreover, it is very difficult to standardise this assay because the results can vary according to the species and age of the mice (Stern et al., 2018). Following detection of the neurotoxin, antitoxin was used to neutralize the toxicity for identification of BoNT serotype. However, despite the high sensitivity of the assay, it is not very effective for determining toxin type (Curran et

al., 2009). Last but not least, a high number of mice is required for one test and approximately 400,000 animals per year were killed across Europe (Taylor et al., 2019), in a way that is cruel and painful. Therefore, developing a sensitive replacement method using the 3Rs principles (replace, reduce, refine the use of animal in the research) is crucial to test toxins in a shorter time and more practical way.

Cell-based assays are a good alternative to replace the mLD_{50} assay because they enable the detection of neurotoxin with a complete mode of action including binding and translocation of neurotoxin into cells and subsequent cleavage of the substrate cleavage (Stern et al., 2018). A variety of cell types from different sources has been tested for detection of BoNTs. Neuroblastoma cells are a cancerous cell of the sympathetic nervous system that cause solid tumours in children (Brodeur, 2003). However, they have been used to test BoNTs for a long time. Fernandez-Salas et al. (2012) developed a sensitive replacement cell-based assay using the SiMa human neuroblastoma cell line for the detection of BoNT/A. This Allergan-funded research established a sandwich ELISA test which has similar sensitivity to the mLD_{50} assay. Based on a sensitive SiMa cell line, this cell-based assay was approved by the FDA as a first alternative assay for the mLD50 assay and is currently used for testing BoNT/A samples (Stern et al., 2018).

Followingly, Rust et al. (2017) developed a one-step ELISA test, using the SiMa human neuroblastoma cell line, for BoNT/B detection. In this research, several neuroblastoma cell lines, SiMa, SH-SY5Y, IMR-32, and N2A, were investigated for BoNT/B sensitivity. The expression of VAMP2, which is substrate of BoNT/B, synaptotagmin I protein, and GT1b gangliosides, which are essential for BoNT/B entry inside cells, were explored in these cells. It was found that only N2A expressed the VAMP2 among other cell lines, but it did not express GT1b gangliosides required for BoNT/B entry. SiMa cells expressed GT1b and synaptotagmin I but did not express VAMP2. Therefore, SiMa cell line was re-engineered by inserting NanoLuc luciferase-tagged VAMP2 to the cells. The insertion of exogenous VAMP2 with NanoLuc provided other benefits for BoNT/B detection. Firstly, endogenous VAMP2 is degraded quickly when it is cleaved by CNTs in the cytosol (Pellizzari et al., 1998). However, when exogenous VAMP2 is introduced to cells as a NanoLuc-tagged construct, it remains stable after VAMP2 is cleaved and prevents degradation. Secondly, cleaved VAMP2 could be measured by a one-step ELISA test based on luminescent read out, which is more convenient and efficient method than immunoblotting. Moreover, immunoblotting is not a suitable method for high-throughput screening and quality control approval due to the intrinsic variability (Fernandez-Salas et al., 2012).

Here, SiMa neuroblastoma cell lines were further explored for other BoNT serotypes and TeNT. Subsequently, I introduced another neuroblastoma cell line, LAN-5. This is a novel candidate cell line

for the development of a replacement cell-based assay to test CNTs potency. LAN-5 cell line was derived from the bone marrow metastatic site of a 5-month-old boy with neuroblastoma, a tumour of the peripheral nervous system (Reynolds et al., 1988). As a result of its capability to differentiate and proliferate, LAN-5 neuroblastoma makes an effective in vitro model for a wide variety of studies (Shastry et al., 2001).The enhancement of neuroblastoma cell differentiation and apoptosis are potentially effective treatment strategies for neuroblastoma (Ponzoni et al., 1992, Borriello et al., 2000, Shastry et al., 2001). For this purpose, LAN-5 neuroblastoma was utilised as an experimental model in several studies. For example, RA was included in clinical trials after intensive studies with LAN-5 (Shastry et al., 2001). The differentiation mechanisms and differentiation pathways of LAN-5 neuroblastomas have been extensively studied, and numerous biological factors, such as IFN-7, TNF, MYCN, p27Kip1, PKC, have been identified to be significant to LAN-5 neuroblastomas in the differentiation process (Ponzoni et al., 1992, Ponzoni et al., 1993, Borriello et al., 2000, Guglielmi et al., 2014). Moreover, the differentiation factors of LAN-5 neuroblastomas were also investigated for nerve tissue development (Passalacqua et al., 1998). Additionally, neuroblastomas are excellent in vitro models for neurotoxicity studies. In one study, Businaro et al. (2006) used LAN-5 neuroblastoma cells as an in vitro model to investigate AB-amyloid mediated neurotoxicity for Alzheimer's disease research.

In this study, the LAN-5 neuroblastoma cell line has been tested for the sensitivity of TeNT and several BoNT serotypes, including BoNT/A, BoNT/B, BoNT/C, BoNT/D, and BoNT/DC. Last, the maximum detection limits of SiMa and LAN-5 neuroblastoma cell lines were summarized and compared in order to determine which has the most effective sensitivity.

3.2 Results

3.2.1 A one-step ELISA detects BoNT/B in differentiated SiMa human neuroblastoma cells

BoNT/B is the second most common serotype of BoNT after BoNT/A, which has been used as biological medicine for many years. Myobloc® and Neurobloc® are pharmaceutical BoNT/B products licensed for treatment of neuromuscular spasms. Therefore, development of a sensitive and practical replacement assay for the detection of BoNT/B is essential. In recent years, Rust et al. (2017) developed the sensitive replacement assay as discussed above, and here I validated his research. Before the validation, sensitivity of the SiMa cell line for BoNT/B detection was enhanced by puromycin treatment, as the NanoLuc VAMP2 construct (Figure 3.1 B) that was transduced into the SiMa cell line has a puromycin resistance gene. Upon puromycin treatment, SiMa cells carrying NanoLuc VAMP2 construct were selected, whereas SiMa cells with no construct were killed. The more NanoLuc VAMP2 SiMa cells selected, the higher the BoNT/B sensitivity. SiMa cells were differentiated before they were treated with toxins because they become a neuron like cell after differentiation. Figure 3.1 A shows the morphology of native undifferentiated SiMa cells in growth media, and how they developed neurites and became neuron like cells after a 3-day retinoic acid (RA) treatment in differentiation media.

The BoNT/B cleavage site on the NanoLuc VAMP2 construct is shown on the schematic in Figure 3.1 B. Immunoblot results show cleaved NanoLuc VAMP2 was successfully detected in differentiated NanoLuc VAMP2 SiMa cells after treatment with diluted concentrations of BoNT/B (Figure 3.1 C). A very faint band of cleaved VAMP2 was observed at the lowest concentration of 0.1 nM BoNT/B. Followingly, diluted concentrations of BoNT/B were tested with the one-step ELISA test developed by Rust et al. (2017). The premise of the one-step ELISA is shown in Figure 3.1 D. The assay is based on the luminescence reaction of cleaved NanoLuc VAMP2, which is captured by a specific cleaved-end VAMP2 antibody immobilized on a Protein A coated plate. According to one-step ELISA result, the sensitivity significantly increased compared to previous research (Rust et al., 2017) as the luminescence level of cleaved VAMP2 was considerably higher even at lowest detectable concentration of 0.01 nM (Figure 3.1 E). They detected BoNT/B activity at the lowest concentration of 0.1 nM with a luminescence level lower than 200. However, BoNT/B activity was detected as low as 0.01 nM with a luminescence level of about 600 in this study. Additionally, luminescence levels were significantly higher (saturated) than non-treated samples at the concentrations of 10 nM, 5 nM, 1 nM, and 0.1 nM, while Rust et al. (2017) measured a luminescence level of approximately 600 at 30 nM,

which was the highest concentration they tested. One step ELISA test allowed the detection of BoNT/B significantly.

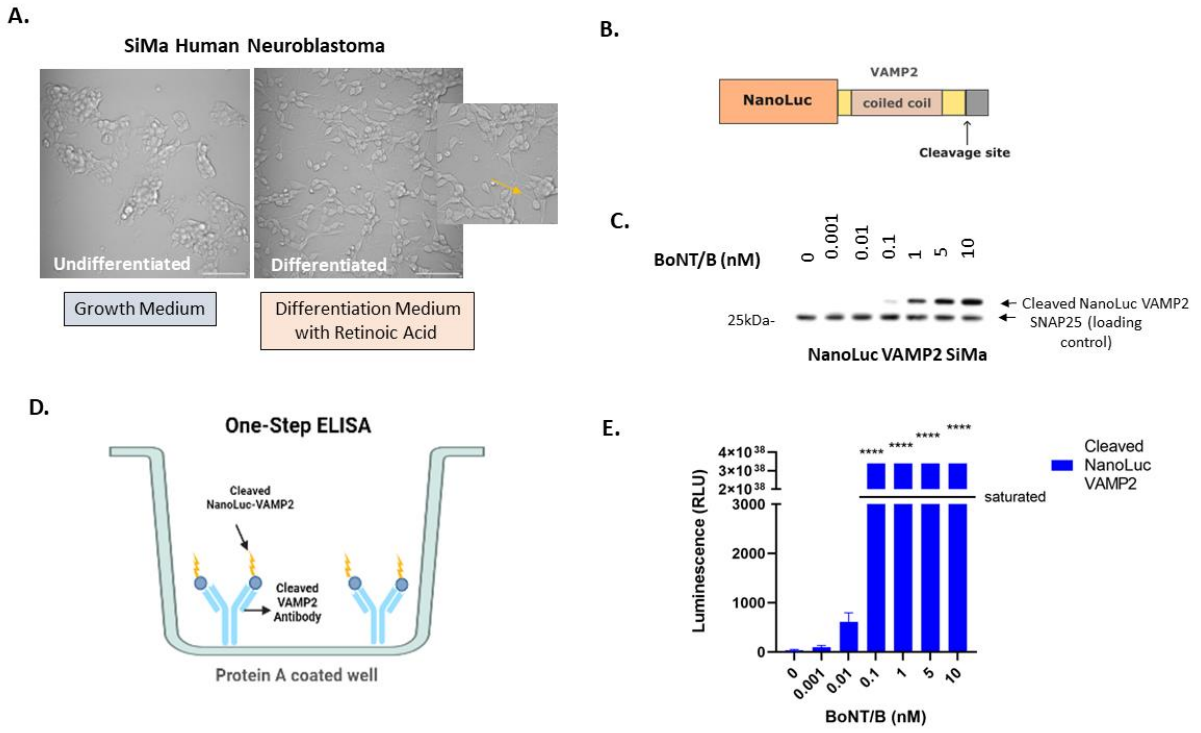

Figure 3.1 NanoLuc VAMP2 SiMa cell line is sensitive to detect BoNT/B activity.

A) *Brightfield images showing native SiMa neuroblastoma cells become neuron-like cells after a 3-day retinoic acid treatment. (x40 objective, all scale bars 100 µm)* ***B)*** *Schematic representation of the NanoLuc VAMP2 construct transduced to native SiMa neuroblastoma cells.* ***C)*** *Western blot results show the proportion of cleaved cytosolic NanoLuc VAMP2 following application of BoNT/B. Rabbit monoclonal Ab (2F7-1) was added in 1:2000 dilution for cleaved cytosolic VAMP2 detection. SNAP25 antibody was added in 1:3000 dilution as a control antibody to detect uncleaved SNAP25.* ***D)*** *Schematic representation of the one-step ELISA method. Protein A coated plate wells were incubated overnight, with antibodies which capture cleaved NanoLuc VAMP constructs. Differentiated cells were treated with toxins for 3 days and lysates were collected for one-step ELISA method detection.* ***E)*** *Bar chart showing the luminescence levels received from one step ELISA results (N=3, ± SEM). Multiple comparisons were examined by an ordinary one-way ANOVA followed by Tukey's test. Significances refer to comparisons between different toxin concentrations and untreated control and alpha P values of <0.05 were considered statistically significant. ****= P<0.0001. Schematics were created by using Inkscape and BioRender.*

3.2.2 SiMa human neuroblastoma cells are also sensitive to other clostridial neurotoxins

Following the sensitive detection of BoNT/B, SiMa cell lines were tested for the activity of other CNTs through immunoblotting. The immunoblots are shown in appendix 3. It was found that NanoLuc VAMP2 SiMa neuroblastoma cell line shows significant sensitivity for most of the neurotoxins. Toxin activity was detected quite sensitively for BoNT/A, BoNT/C and BoNT/DC, whereas it was less sensitive for BoNT/D and TeNT as summarised in Table 3.1. In spite of the fact that the SiMa human neuroblastoma cell line is highly sensitive to most CNTs, it has several limitations that make it difficult to use in the development of cell-based assays in my research. The following section introduces LAN-5 human neuroblastoma, a novel cell line.

3.2.3 LAN-5 human neuroblastoma is a new sensitive cell line for BoNT/B detection

As previously mentioned, the SiMa cell line is disadvantageous for both practical reasons and patent issues. During the use of SiMa cells for testing of CNTs I found some difficulties in handling SiMa cells, as they tend to aggregate with and often become clumped together, which causes a serious problem in terms of differentiation. If the cells are not seeded as separate individuals and are instead seeded as clumps of cells, the differentiation does not properly occur, and the subsequent sensitivity of the cells is significantly affected. There are also patent issues with the SiMa cells that could cause issues with attempts to move the cell assay forward into wide-scale use. As mentioned before, the first FDA approved replacement assay for BoNT/A test was developed and patented by Allergan (Fernandez-Salas et al., 2012), which might limit the use of the SiMa cell line for similar aims. Because of this an alternative cell line, human LAN-5 neuroblastoma which was obtained from a 5-month-old boy's bone marrow metastatic tissue (Reynolds et al., 1988), was investigated for testing of CNTs.

As a first step, the differentiation ability of LAN-5 cells was tested by seeding them in differentiation medium with retinoic acid in the same manner as SiMa cells and observing their morphology through microscopy. Brightfield images of the cells show that LAN-5 cells have the ability to perfectly differentiate due to the presence of neurites (Figure 3.2 A). Moreover, undifferentiated LAN-5 cells, cultured in growth media, had also looked like neuron cells which was quite similar to a differentiated form, in contrast to undifferentiated SiMa cells.

Following this, the NanoLuc VAMP2 construct, schematically shown in Figure 3.2 B, was transduced into a LAN-5 cell line. After NanoLuc VAMP2 LAN-5 cells were generated, they were tested for BoNT/B activity. In order to establish an optimum protocol, the time course of BoNT/B activity was tested with

both the immunoblotting and ELISA methods, to determine an ideal treatment time to achieve the most efficient results in shortest time possible. Due to the fact that NanoLuc VAMP2 SiMa cells were treated with BoNT/B for 3 days, a 3-day duration was chosen as the maximum treatment time. In the immunoblot analysis of cells treated with of 1 nM BoNT/B, cleaved NanoLuc VAMP2 bands could be detected after a single treatment day (Figure 3.2 C). However, the cleaved amount of NanoLuc VAMP2 was greater for 2-day than for 1-day treatment and best result was received after a 3-day treatment (Figure 3.2 D). Similar to immunoblot results, one step ELISA results demonstrated that cleaved NanoLuc VAMP2 was detected at all treatment days at a concentration of 1 nM BoNT/B (Figure 3.2 E). Furthermore, the luminescence level was saturated for 3-day treatment of BoNT/B, and it was significantly higher than other treatment days.

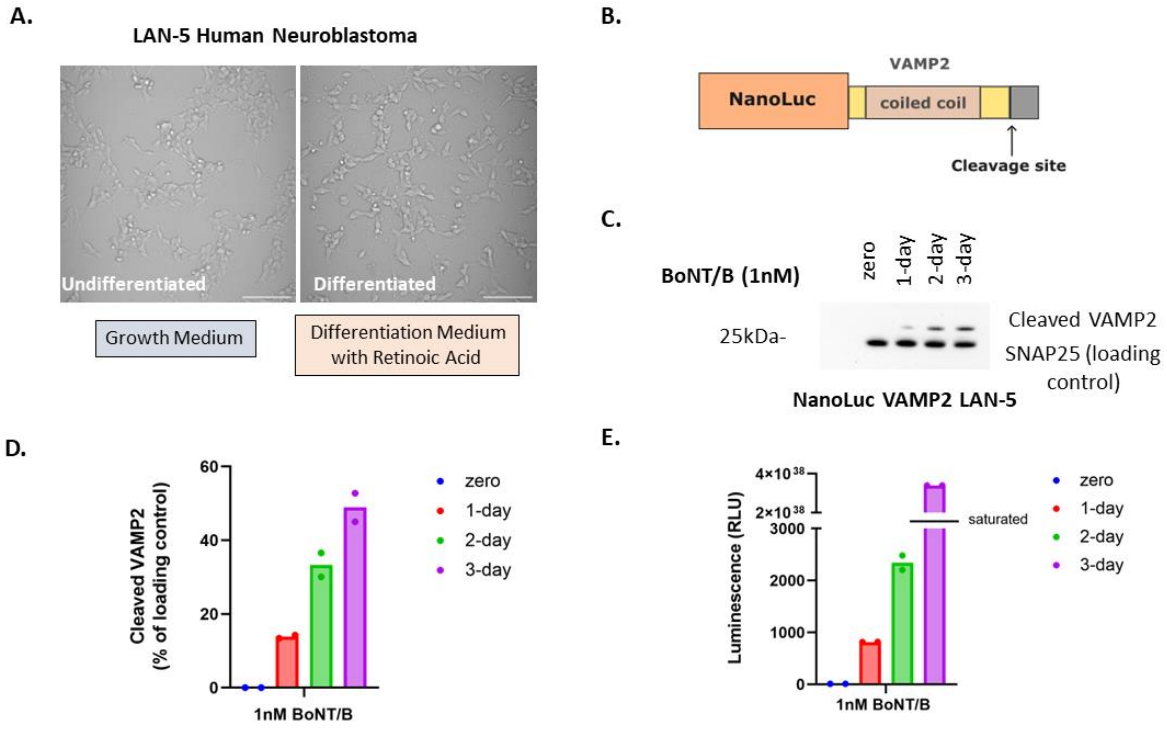

Figure 3.2 Another human neuroblastoma cell line, NanoLuc VAMP2 LAN-5, was established to test BoNT/B.

A) *Brightfield images showing that native LAN-5 neuroblastoma cells become neuron-like cells after a 3-day retinoic acid treatment. (x40 objective, all scale bars 100 µm)* ***B)*** *Schematic representation of NanoLuc-VAMP2 construct transduced to native LAN-5 neuroblastoma cells.* ***C)*** *Immunoblot image showing the proportion of cleaved VAMP2 in NanoLuc-VAMP2 LAN-5 cell line treated with 1nM BoNT/B for 1-day, 2-day, and 3-day. Images were taken from ChemiDoc XRS.* ***D)*** *Graph showing the quantification of cleaved VAMP2 immunosignals according to different days (n=2, ± experimental errors).* ***E)*** *Graph showing the detection of NanoLuc-VAMP2 with one-step ELISA assay after treatment with 1 nM BoNT/B for varying numbers of days (n=2, ± experimental errors). Schematic was created by using Inkscape.*

Overall, LAN-5 human neuroblastoma cells were easier to culture and handle than SiMa cells. These cells were not clumpy and resembled neurons in their undifferentiated form. The toxin activity of BoNT/B was detected in LAN-5 cells, and a 3-day treatment was found to be the optimum duration to deliver a high signal for both ELISA and immunoblotting.

3.2.4 Validation of BoNT/B sensitivity using a GFP VAMP2 LAN-5 cell line

Following the establishment of the LAN-5 neuroblastoma cell line for one-step ELISA testing of BoNT/B, the sensitivity of the cell line was tested for other CNTs. Since ELISA-compatible cleaved-end antibodies were unavailable for most of the BoNT serotypes, the sensitivity of the cells to CNTs was assessed through immunoblotting. Upon native VAMP2 being cleaved by CNTs, the N-terminal VAMP2 (cytosolic VAMP2) product was released to cytosol from vesicles and degraded by an intracellular clearance mechanism (Pellizzari et al., 1998, Foran et al., 2003). By immunoblotting, cleaved GFP VAMP2 product was found to be completely stable in neuroblastomas (Rust et al., 2017). However, even though cleaved NanoLuc VAMP2 was detected in neuroblastomas by immunoblotting, the NanoLuc construct seemed only to protect VAMP2 degradation to a limited extent and a small portion of NanoLuc carrying VAMP2 was possibly degraded. The situation is further confirmed with the results presented in Table 3.1 of this study. Because of this, the sensitivity of LAN-5 cells to CNTs was evaluated using GFP VAMP2 LAN-5 cells rather than NanoLuc VAMP2 LAN-5 cells.

As mentioned before, the second most common BoNT serotype used as a medicine is BoNT/B, and the development of sensitive replacement assays is of vital importance. Thus, LAN-5 cells were further validated for BoNT/B sensitivity on GFP VAMP2 LAN-5 cells in order to verify that LAN-5 is an appropriate cell line for BoNT/B detection. The GFP VAMP2 construct, schematically shown in Figure 3.3 A, was inserted into LAN-5 cells. According to Figure 3.3 B, two cleaved VAMP2 fragments were formed after the neurotoxin cleaved VAMP2, the cytosolic cleaved VAMP2 (N-terminal fragment) and vesicular cleaved VAMP2 (C-terminal fragment). This provides two different means of detecting VAMP2 cleavage by BoNT/B, TeNT, BoNT/D, and BoNT/DC. Moreover, having a sensitive antibody for each fragment allows further confirmation of the assay. Since antibodies to cleaved vesicular VAMP2 have not been developed, BoNT/B activity has only been assessed on cleaved cytosolic VAMP2. Diluted concentrations of BoNT/B were applied to differentiated GFP VAMP2 LAN-5 cells. Based on immunoblot results (Figure 3.3 C), distinct bands of cleaved cytosolic VAMP2 were observed at concentrations of 10 nM, 5 nM, and 1 nM. The presence of a faint band was observed at a concentration of 0.1 nM. From the graph, it can be seen that the amount of cleaved VAMP2 was greater at the 10 nM and 5 nM concentrations, and that it decreased considerably between the 1 nM

and 0.1 nM concentrations (Figure 3.3 D). According to dose response curve, estimated EC50 value was calculated as 0.76 nM with 0.9578 R^2 and 0.3775 to 1.472 95%CI.

Overall, GFP VAMP2 LAN-5 is a viable cell model for assessing the activity of CNTs through immunoblotting, and BoNT/B activity was validated successfully in GFP VAMP2 LAN-5 cells with detection level as low as 0.1 nM.

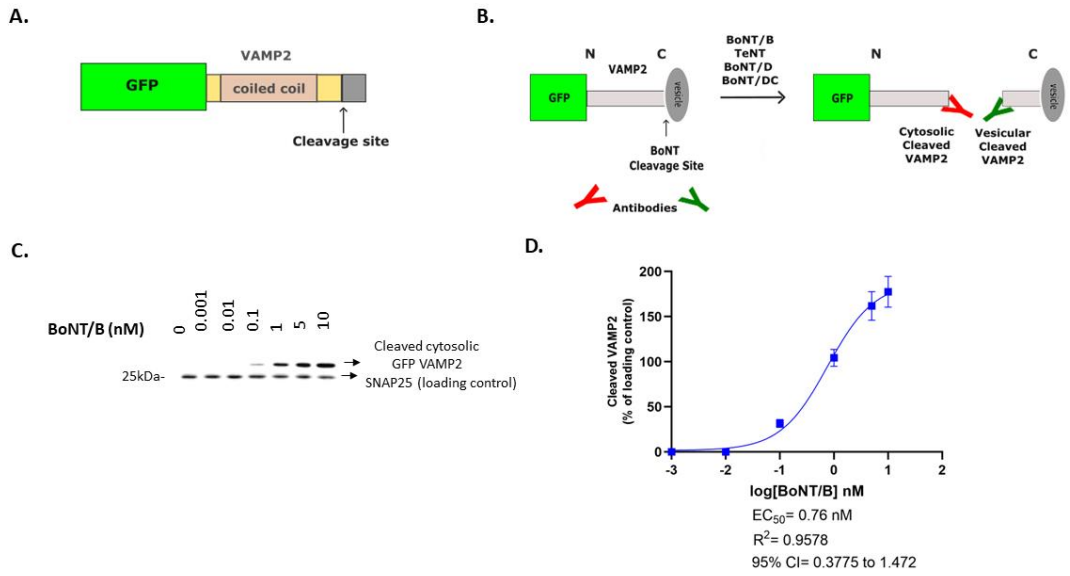

Figure 3.3 BoNT/B activity was sensitively detected in differentiated GFP VAMP2 LAN-5 cell line.

A) *Schematic representation of GFP-VAMP2 construct transduced to native LAN-5 neuroblastoma cells.* ***B)*** *Schematic representation showing the detection of cleaved cytosolic and vesicular VAMP2 following BoNT/B, TeNT, BoNT/D and BoNT/DC cleavage of GFP VAMP2.* ***C)*** *Western blot result showing the proportion of cleaved cytosolic GFP VAMP2 in differentiated GFP VAMP2 LAN-5 neuroblastomas following 3-day treatment with 1:10 titrated BoNT/B. Cells were treated with the diluting agent (Opti-MEM, reduced serum media) as a no treatment control. Rabbit monoclonal Ab (2F7-1) was added in 1:2000 dilution for cleaved cytosolic VAMP2 detection. SNAP25 antibody was added in 1:3000 dilution as a control antibody to detect uncleaved SNAP25. Images were taken from ChemiDoc XRS.* ***D)*** *Graph showing the quantification of cleaved cytosolic VAMP2 immunosignals (N=3, ± S.E.M.). Schematics were created by using Inkscape.*

3.2.5 GFP-VAMP2 LAN-5 cell line can detect the activity of TeNT through immunoblotting.

As described previously, TeNT is a CNT that inhibits neurotransmitter release at inhibitory interneurons in the spinal cord, which leading to spastic paralysis called tetanus. BoNT/B and TeNT cleave VAMP2 at the same peptide bond which is Gln76-Phe77. However, they produce the opposite symptoms of botulism and tetanus due to their blockage of neurotransmitters at different points in the nervous system. It is likely that TeNT and BoNTs arrive at different destinations as a result of their specific receptors which direct them to different intracellular paths (Pellizzari et al., 1999).

A tetanus vaccine was developed following the identification of TeNT, and most developed countries are now immunized against the disease (Dong et al., 2019). However, there is still a need to establish an effective vaccination schedule for developing countries. Although TeNT is a highly poisonous substance, it can be inactivated by formaldehyde to create a TeNT toxoid, which is a very effective and safe vaccine against tetanus (Rossetto et al., 2013b). As a major product of the pharmaceutical industry, tetanus toxoid must be tested for toxicity in order to ensure that residual toxins are not present. It is therefore crucial to have a detection method that is both sensitive and practical.

Here, in order to develop cell-based replacement assay, LAN-5 human neuroblastoma cell line was assessed for TeNT sensitivity. Various concentrations of TeNT were tested in differentiated GFP-VAMP2 LAN-5 cells by immunoblotting. Because TeNT cleaves VAMP2 at the same location as BoNT/B, the same antibody was used to detect the cytosolic cleaved VAMP2. Immunoblot results showed substantial cleaved VAMP2 bands were observed down to a concentration of 1 nM TeNT, showing the sensitivity of LAN-5 cells is high (Figure 3.4 A). According to the graph, considerable amounts of cleaved VAMP2 were detected at the concentrations of 10 nM and 5 nM and estimated EC50 value was calculated as 3.03 nM with 0.9837 R^2 and 1.947 to 5.025 95%CI (Figure 3.4 B).

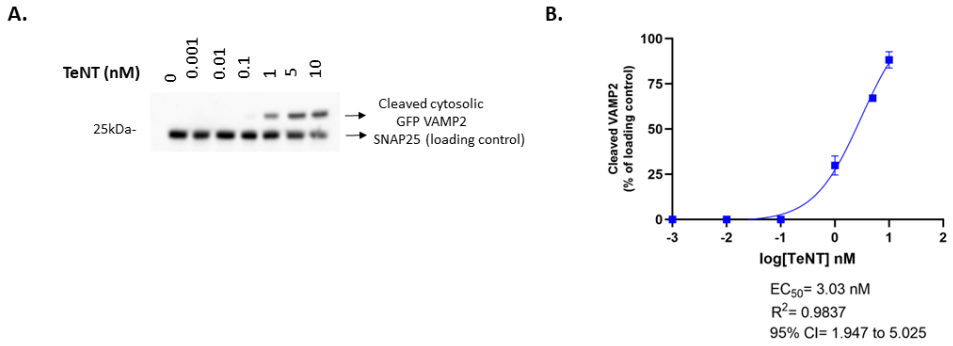

Figure 3.4 TeNT activity was detected in differentiated GFP VAMP2 LAN-5 cell line.

A) *Western blot showing the proportion of cleaved cytosolic GFP VAMP2 in differentiated GFP VAMP2 LAN-5 neuroblastomas following 3-day treatment with 1:10 titrated TeNT. Cells were treated with the diluting agent (Opti-MEM, reduced serum media) as a no treatment control. Rabbit monoclonal Ab (2F7-1) was added in 1:2000 dilution for cleaved cytosolic VAMP2 detection. SNAP25 antibody was added in 1:3000 dilution as a control antibody to detect uncleaved SNAP25. Images were taken from ChemiDoc XRS.* ***B)*** *Graph showing the quantification of cleaved cytosolic VAMP2 immunosignals (N=3, ± S.E.M.).*

3.2.6 GFP-VAMP2 LAN-5 cell line is slightly sensitive BoNT/D based on immunoblotting result.

BoNT/A and BoNT/B serotypes cause human botulism, whereas BoNT/D and BoNT/C serotypes cause botulism mainly in animals such as birds, bovines, and horses (Stahl et al., 2009, Hedeland et al., 2011). The outbreak of animal botulism poses a significant risk to both the environment and the economy. Thus, any suspicions of botulism at a farm or natural animal habitat must be confirmed in order to prevent further spread. Vaccination is the only effective way of preventing botulism in animals. Currently, commercially available vaccines are made using formalin inactivation of BoNT/C and BoNT/D serotypes (Stahl et al., 2009).

In rare cases, BoNT/D can also cause human botulism. (Demarchi et al., 1958). Pellett et al. (2015) showed that cultured human neurons are susceptible to BoNT/D and concluded that sufficient amounts of BoNT/D can cause human botulism. Furthermore, BoNT/D was found as an alternative treatment option for patients who develop neutralizing antibodies and have become non-responsive to BoNT/A and BoNT/B (Kutschenko et al., 2019). Sensitivity detection assays for the BoNT/D serotype are therefore needed in order to confirm botulism in humans and animals, as well as ensure the safety of toxoid vaccines and therapeutics.

Here, LAN-5 cells were evaluated for BoNT/D activity. VAMP2 is a target protein for BoNT/D (Gardner and Barbieri, 2018) and as mentioned earlier, once VAMP2 is cleaved, cleaved vesicular VAMP2 (v-VAMP2) and cleaved cytosolic VAMP2 (c-VAMP2) are generated (Figure 3.3 B). As we have access to specific antibodies for both cleaved-ends of the fragments, BoNT/D toxicity was assessed with respect to both cleaved cytosolic and vesicular VAMP2, providing further confirmation of sensitivity. However, immunoblot showed that BoNT/D cleaved cytosolic VAMP2 was detected only at 10 nM and 5 nM concentrations, whereas cleaved vesicular VAMP2 was detected at the lowest concentration of 0.01 nM (Figure 3.5 A). Detection of c-VAMP2 may be less accurate due to the antibody. Immunosignal quantification of c-VAMP2 was similar at the concentrations of 5 nM and 10 nM shown in Figure 3.5 B. Moreover, similar amounts of cleaved v-VAMP2 were detected at the concentration of 5 nM and 10 nM (Figure 3.5 C). The cleaved v-VAMP2 amount decreased sharply at 1 nM, and as the amount of cleaved v-VAMP2 was too low to detect at concentrations of 0.1 nM and 0.01 nM, they could not be displayed in the graph. The estimated EC50 value for v-VAMP2 was calculated as 3.99 nM with 0.6551 R^2 and 0.4868 to? 95%CI.

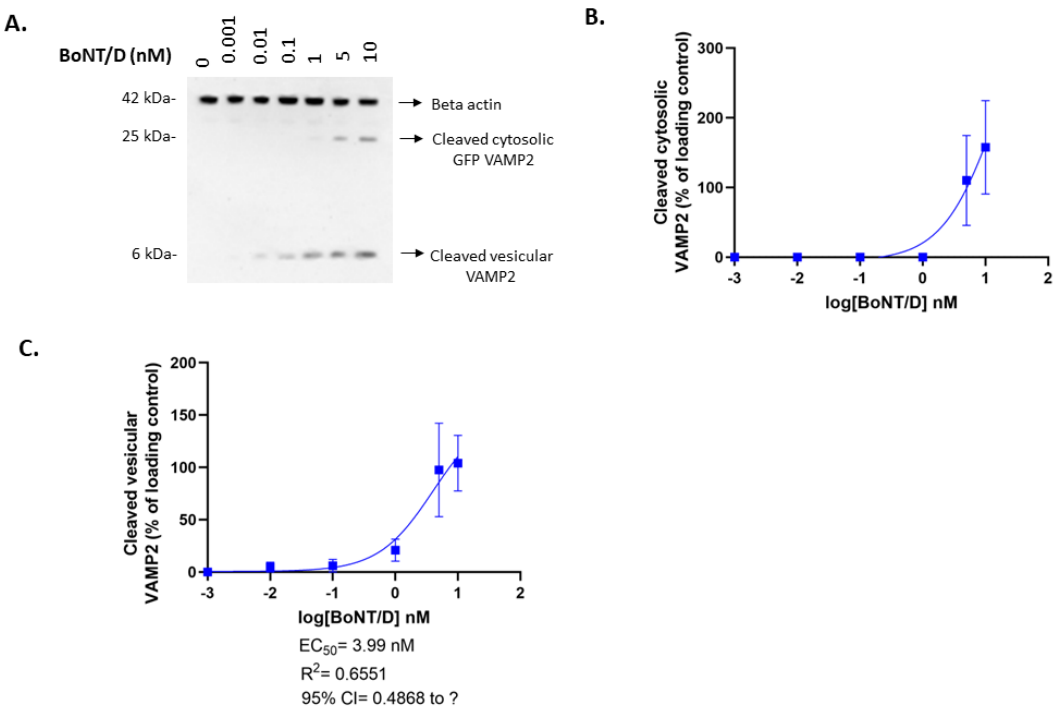

Figure 3.5 BoNT/D activity was detected in GFP VAMP2 LAN-5 cell line.

A) *Western blot showing the proportion of cleaved cytosolic and vesicular GFP VAMP2 in differentiated GFP VAMP2 LAN-5 neuroblastomas following 3-day treatment with 1:10 titrated BoNT/D. Cells were treated with the diluting agent (Opti-MEM, reduced serum media) as a no treatment control. Mouse monoclonal Ab (D27) was added in 1:2000 dilution for vesicular VAMP2 cleavage detection; D cleaved VAMP2 cytosolic rabbit polyclonal Ab was used in 1:2000 dilution for cytosolic VAMP2 cleavage detection. Mouse beta-actin Ab was added in 1:1200 dilution as a loading control. Images were taken from ChemiDoc XRS.* ***B)*** *Graph showing the quantification of cleaved cytosolic VAMP2 immunosignals (N=3, ± S.E.M.).* ***C)*** *Graph showing the quantification of cleaved vesicular VAMP2 immunosignals (N=3, ± S.E.M.).*

3.2.7 GFP-VAMP2 LAN-5 cell line is sensitive to BoNT/DC based on immunoblotting.

Sequence analysis of BoNT/C and BoNT/D has revealed that some strains produce chimeric structures called BoNT/DC and BoNT/CD mosaic toxins (Nakamura et al., 2013). BoNT/DC causes botulism in cattle and a devastating outbreak with a high fatality rate has recently been reported in a dairy herd in Italy (Mariano et al., 2019). A timely and effective diagnosis of neurotoxins in animals is essential in such circumstances. In addition to causing bovine botulism, BoNT/DC has also been found to be highly toxic to mice, which poses a threat to the spread of the disease (Nakamura et al., 2012). Thus, development of a sensitive and serotype-specific replacement detection method is essential.

In order to develop such a replacement assay, the sensitivity for BoNT/DC of the GFP VAMP2 LAN-5 cell line was assessed activity through immunoblotting. The BoNT/DC mosaic consists of the light chain and translocation domain of BoNT/D and binding domain of BoNT/C (Mariano et al., 2019). In short, BoNT/DC cleaves VAMP2 at the same point as BoNT/D. Therefore, BoNT/DC sensitivity of GFP VAMP2 LAN-5 cell line were assessed by visualising both the cleaved vesicular and cytosolic VAMP2 using the same antibodies as BoNT/D. Immunoblot imaging showed that great amount of cleaved c-VAMP2 and v-VAMP2 bands were observed at the concentrations of 10 nM, 5 nM, 1 nM, and 0.1 nM (Figure 3.6 A). Very faint bands of cleaved c-VAMP2 and v-VAMP2 were seen at a concentration of 0.01 nM. According to the band analysis, cleavage of c-VAMP2 and v-VAMP2 at increasing concentrations of the toxin showed similar trends, but the amount of cleaved c-VAMP2 was slightly higher than cleaved v-VAMP2 at the same concentrations (Figure 3.6 B-C). As seen in Figure 3.6 B, the cleaved amount of c-VAMP2 was almost similar for the concentration of 10 nM, 5 nM, and 1 nM. Following this, it decreased slowly at 0.1 nM and dropped to its lowest level at 0.01 nM. Similarly, the cleaved amounts of v-VAMP2 were found to be very close at higher concentrations, 10 nM, 5 nM, and 1 nM. Afterward, it decreased considerably at concentrations of 0.1 nM and 0.01 nM (Figure 3.6 C). According to the dose response curves, the EC50 value of c-VAMP2 was estimated as 0.05 nM with 0.4825 R^2 and 0.0006195 to 2.736 95%CI, whereas it was estimated as 0.098 nM for v-VAMP2 with 0.8185 R^2 and 0.02362 to 0.4251 95%CI.

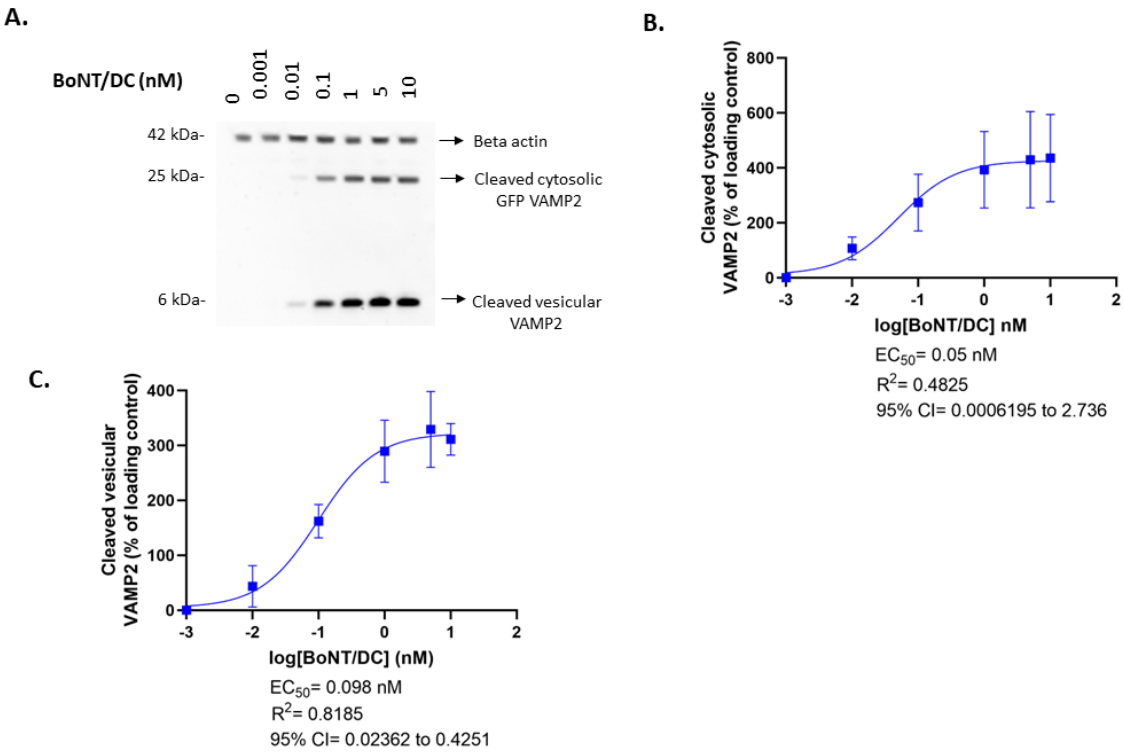

Figure 3.6 BoNT/DC activity was sensitively detected in GFP VAMP2 LAN-5 cell line.

A) *Western blot showing the proportion of cleaved cytosolic and vesicular GFP VAMP2 in differentiated GFP VAMP2 LAN-5 neuroblastomas following 3-day treatment with 1:10 titrated BoNT/DC. Cells were treated with the diluting agent (Opti-MEM, reduced serum media) as a no treatment control. Mouse monoclonal Ab (D27) was added in 1:2000 dilution for vesicular VAMP2 cleavage detection; D cleaved VAMP2 cytosolic rabbit polyclonal Ab was used in 1:2000 dilution for cytosolic VAMP2 cleavage detection. Mouse beta-actin Ab was added in 1:1200 dilution as a loading control. Images were taken from ChemiDoc XRS.* ***B)*** *Graph showing the quantification of cleaved cytosolic VAMP2 immunosignals (N=3, ± S.E.M.).* ***C)*** *Graph showing the quantification of cleaved vesicular VAMP2 immunosignals (N=3, ± S.E.M.).*

3.2.8 GFP-VAMP2 LAN-5 cell line is sensitive to detect the activity of BoNT/A based on immunoblotting result.

As previously mentioned, BoNT/A is the most common serotype used for both neurological treatments and cosmetic reasons. Clinical use of BoNT/A began in the early 1980s and is currently used for the treatment of migraine, muscle spasm, hyperhidrosis, cerebral palsy, and pain (Sesardic et al., 2003). It is therefore highly desirable to develop a sensitive replacement assay for BoNT/A serotypes.

The FDA-approved assay developed by Allergan detects BoNT/A sensitively using the SiMa neuroblastoma cell line (Fernandez-Salas et al., 2012). In this case, I tested BoNT/A in another neuroblastoma cell line, LAN-5, to determine if it is more sensitive to BoNT/A than SiMa. To do this, diluted concentrations of BoNT/A were applied to differentiated GFP VAMP2 LAN-5 cells for 3 days. Following this, lysates were collected for immunoblotting. SNAP25 is the target protein for BoNT/A (Gardner and Barbieri, 2018) and recognising intact SNAP25 antibody was used to detect cleaved SNAP25. The recognising intact SNAP25 antibody detects the portion of SNAP25 before the cleavage site, allowing the detection of both cleaved and non-cleaved forms of SNAP25. Cleaved and uncleaved SNAP25 were detected separately due to the slight difference in their molecular size. Uncleaved SNAP25 fragment was 25kDa, whereas cleaved SNAP25 was 24 kDa (Figure 3.7 A). Because molecular sizes are very close, the proteins were run on the SDS-PAGE gel for longer than normal.

Based on the immunoblot image, SNAP25 was cleaved 100 % at the concentration of 10 nM BoNT/A, as no uncleaved SNAP25 band is observed. Again, most of the SNAP25 was cleaved at the concentrations of 5 nM, 1 nM, and 0.1 nM. At a concentration of 0.01 nM, similar amounts of both cleaved and uncleaved bands were observed. A concentration of 0.001 nM resulted in a very weak cleaved band and a significant uncleaved band (Figure 3.7 B)., As can be seen from the graph, the percentage of cleaved SNAP25 was 100% at a 10 nM concentration, and it was in the range of 80-90 % at concentrations of 5 nM, 1 nM, and 0.1 nM of BoNT/A. Afterward, it dropped slightly at a concentration of 0.01 nM and decreased to the lowest level of detection at a concentration of 0.001 nM (Figure 3.7 C). In accordance with the dose-response curve, an EC50 was indicated as 0.0085 nM with 0.8205 R^2 and 0.001712 to 0.04833 95%CI.

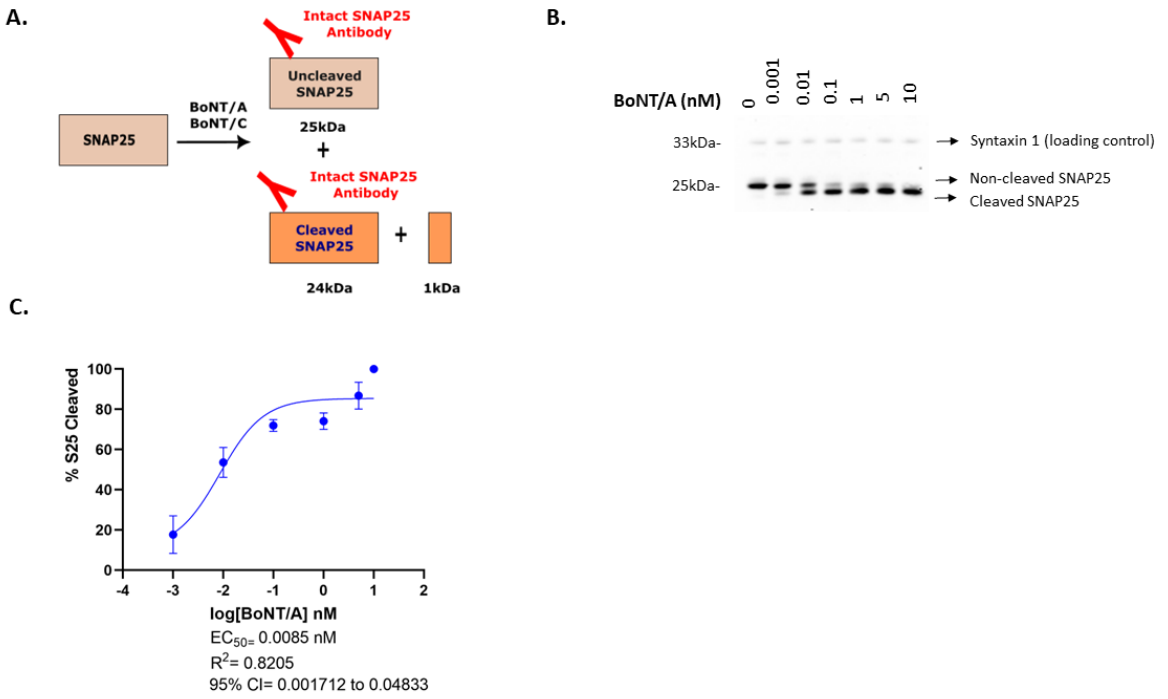

Figure 3.7 BoNT/A activity was sensitively detected in differentiated GFP-VAMP2 LAN-5 cell line.

A) *Schematic representation of the action of intact SNAP25 antibody, allowing the detection of both cleaved and uncleaved SNAP25 following BoNT/A and BoNT/C treatment.* ***B)*** *Western blot showing the proportion of cellular cleaved SNAP25 in differentiated GFP VAMP2 LAN-5 neuroblastomas following 3-day treatment with 1:10 titrated BoNT/A. Cells were treated with the diluting agent (Opti-MEM, reduced serum media) as a no treatment control. SNAP25 antibody was added in 1:3000 dilution. Syntaxin antibody was added in 1:2000 dilution as a control antibody. Image was taken from ChemiDoc XRS. C) Graph showing the quantification of cleaved SNAP25 immunosignals expressed as a percentage of total SNAP25 (N=3, ± S.E.M.). Schematic was created by using Inkscape.*

3.2.9 GFP-VAMP2 LAN-5 cell line is sensitive to BoNT/C based on immunoblotting.

BoNT/C serotype causes botulism in animals but it is also potentially dangerous for humans (Moura et al., 2011). A sensitive assay specific for BoNT/C detection is therefore required for both diagnosis of botulism and validation of toxoid vaccines. Although there have been some efforts to develop a replacement assay, the mouse bioassay is currently the valid test for BoNT/C detection.

Therefore, I tested the sensitivity to BoNT/C of the LAN-5 neuroblastoma cell line to determine if it could be a candidate for a cell-based assay. For this purpose, differentiated GFP VAMP2 LAN-5 cells were treated with diluted concentrations of BoNT/C for 3 days and immunoblotting was performed. SNAP25 and Syntaxin 1 are substrates of BoNT/C (Gardner and Barbieri, 2018). In this study, only

SNAP25 cleavage was evaluated to assess BoNT/C activity. In order to detect cleaved SNAP25, the same antibody, recognising intact SNAP25, was used as BoNT/A (Figure 3.6 A).

It can be seen from the immunoblot that most of SNAP25 has been cleaved and only a small amount of uncleaved SNAP25 remained at concentrations of 5 and 10 nM (Figure 3.8 A). At 1nM concentration, the amount of cleaved SNAP25 band was still significantly higher than uncleaved band, whereas there were similar amounts of cleaved and uncleaved SNAP25 at 0.1 nM. A very faint cleaved SNAP25 band was observed at the concentration of 0.01 nM. Based on the graph, approximately 80-70% of SNAP25 was cleaved and the cleaved amounts were very similar at concentrations of 10 nM, 5 nM, and 1 nM (Figure 3.8 B). At a concentration of 0.1 nM, the amount of cleaved SNAP25 decreased gradually, and reached its lowest level at a concentration of 0.01 nM. According to dose response curve, the EC50 value for BoNT/C is 0.031 nM with 0.9473 R^2 and 0.01267 to 0.07590 95%CI.

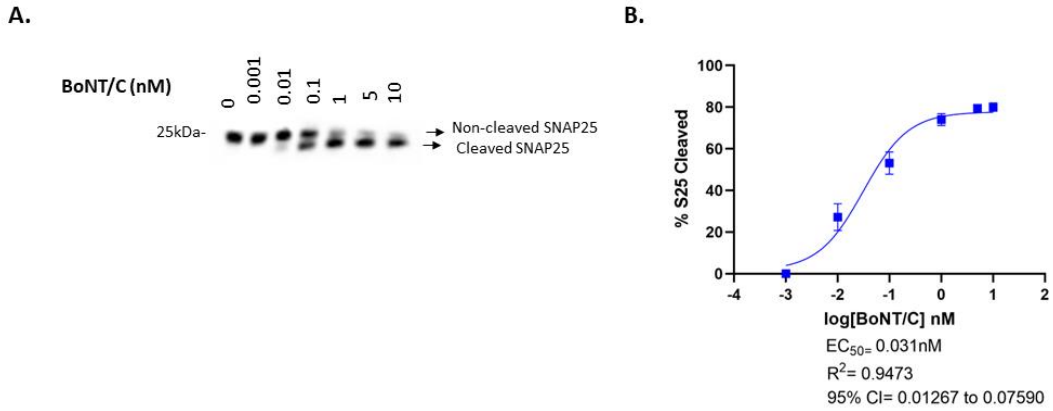

Figure 3.8 BoNT/C activity was sensitively detected in differentiated GFP VAMP2 LAN-5 cell line.

A) *Western blot showing the proportion of cleaved cellular SNAP25 in differentiated GFP VAMP2 LAN-5 neuroblastomas following 3-day treatment with 1:10 titrated BoNT/C. Cells were treated with the diluting agent (Opti-MEM, reduced serum media) as a no treatment control. SNAP25 antibody was added in 1:3000 dilution to detect both cleaved and uncleaved SNAP25. Syntaxin antibody was added in 1:2000 dilution as a control antibody. Images were taken from ChemiDoc XRS.* ***B)*** *Graph showing the quantification of cleaved SNAP25 immunosignals expressed as a percentage of total SNAP25 (N=3, ± S.E.M.).*

3.2.10 Human SiMa and LAN-5 neuroblastoma cells are both sensitive to clostridial neurotoxins and good alternatives for cell-based assays

During this project, two neuroblastoma cell lines were re-engineered through transduction of different constructs. As the cells lack target protein VAMP2, either NanoLuc VAMP2 or GFP VAMP2 were inserted to cells in order to use them for BoNT/B, TeNT, BoNT/D and BoNT/DC activity. NanoLuc VAMP2 was used for one step ELISA, whereas GFP VAMP2 was mostly used for validation of cell lines through immunoblotting. SYTII is a receptor protein specifically for BoNT/B and BoNT/DC (Schenke et al., 2020), which was transduced into our VAMP2 inserted cells in order to determine how it affects the sensitivity to BoNT/B and BoNT/DC. Later, NanoLuc SNAP25 and SNAP25 NanoLuc constructs were transduced into cells to develop a one-step ELISA for BoNT/A and BoNT/C toxins. CNTs were tested on these cell lines (see Table 3.1). Some cell lines were tested for all CNTS, while other cell lines were tested for only relevant toxins. EC50 values and the lowest detectable concentrations of CNTs are given in Table 3.1.

Looking at the results of BoNT/A, all cell lines yielded similar results. However, GFP VAMP2 LAN-5 gave slightly better results than the others, as BoNT/A it had both the lowest detectable concentration (0.001 nM) and the lowest EC50 value (0.008 nM with 0.8205 R^2 and 0.0017 to 0.048 95%CI) in the GFP VAMP2 LAN-5 cell line.

For BoNT/B, the highest level of sensitivity was observed in NanoLuc VAMP2 LAN-5 transduced with Synaptotagmin II receptor, the specific receptor protein for BoNT/B entry. BoNT/B was detected at the lowest concentration of 0.01 nM and 0.08 nM of EC50 value with 0.8931 R^2 and 0.02837 to 0.2750 95%CI in this SYTII-NanoLuc VAMP2 LAN-5 cell line.

Regarding BoNT/C, GFP VAMP2 LAN-5 was slightly more sensitive, while the other cell lines yielded almost the same results. The lowest BoNT/C concentration detected in GFP VAMP2 LAN-5 cells was 0.01 nM, in contrast to the 0.1 nM that was detected in others. EC50 values were very close to each other, but the lowest value belonged to GFP VAMP2 LAN-5 cells with 0.031 nM concentration with 0.9473 R^2 and 0.012 to 0.075 95%CI.

For BoNT/D, cleaved c-VAMP2 could only be detected at 10 nM and 5 nM in NanoLuc VAMP2 SiMa and GFP VAMP2 LAN-5 cell lines respectively. However, cleaved v-VAMP2 was detected at the lowest concentration of 0.01 nM in both cell lines. No cleavage was observed in the NanoLuc VAMP2 LAN-5 cell line. Whereas for BoNT/DC, NanoLuc VAMP2 LAN-5 and NanoLuc VAMP2 SiMa cell lines yielded very similar results and the lowest concentration of BoNT/DC was detected at 0.1 nM for both cleaved c-VAMP2 and v-VAMP2. The lowest detection of c-VAMP2 was dropped to 0.01 nM concentration in

GFP VAMP2 LAN-5 and in SYTII-NanoLuc VAMP2 LAN-5 cells, which made them more sensitive than other cell lines. Moreover, estimated EC50 values of c-VAMP2 were yielded as 0.05 nM in both cell lines. It was generated with 0.4825 R^2 and 0.0006 to 2.73 95%CI in GFP VAMP2 LAN-5 while it was yielded with 0.8396 R^2 and 0.015 to 0.177 95%CI in SYTII-NanoLuc VAMP2 LAN-5 cells. However, cleaved v-VAMP2 was detected at the lowest concentration of 0.01 nM in GFP VAMP2 LAN-5 cells, while it was detected at the lowest concentration of 0.1 nM in SYTII-NanoLuc VAMP2 LAN-5 cell line.

Lastly, for TeNT, all re-engineered LAN-5 cell lines detected TeNT activity at the lowest concentration of 1 nM and yielded very similar EC50 values, around 3 nM. The EC50 values were generated with 0.8401 R^2 and 0.7220 to 75.10 95%CI in NanoLuc VAMP2 LAN-5 cell line, with 0.9837 R^2 and 1.947 to 5.025 95%CI in GFP-VAMP2 LAN-5, and with 0.8704 R^2 and 0.9235 to 33.85 95%CI in SYTII-NanoLuc VAMP2 LAN-5. However, the NanoLuc VAMP2 SiMa cell line detected the lowest concentration of TeNT at 5 nM.

It is interesting to observe that the sensitivity of the same cell line changed slightly depending on the construct. For example, GFP VAMP2 LAN-5 gave more sensitive results for BoNT/B and BoNT/DC than NanoLuc VAMP2 LAN-5. Moreover, BoNT/D toxin activity was not detected in NanoLuc VAMP2 LAN-5, whereas it was slightly observed in GFP VAMP2 LAN-5. This phenomenon may be explained by the possibility that the NanoLuc construct only partially prevents VAMP2 degradation, while at the same time some VAMP2 is degraded. As a result, the stability of constructs might be different from each other. However, I also found that GFP VAMP2 LAN-5 and NanoLuc VAMP2 LAN-5 generated better results for BoNT/A than NanoLuc SNAP25 LAN-5, which indicates that VAMP2 degradation is not an issue here. This difference might be based on other reasons. Transduction efficiency could be less in the case of NanoLuc SNAP25 and SNAP25 NanoLuc transductions. Another reason could be the state of the cell line before transduction of NanoLuc SNAP25 and SNAP25 NanoLuc. For example, transduced cells might be less healthy because of their higher passage number than others.

Neuroblastoma cell line	Clostridium Neurotoxins													
	BoNT/A		BoNT/B		BoNT/C		BoNT/D		BoNT/DC		TeNT	
	Detectable lowest concentration (nM)	EC50 (nM), R2, 95%CI	Detectable lowest concentration (nM)	EC50 (nM), R2, 95%CI	Detectable lowest concentration (nM)	EC50 (nM), R2, 95%CI	Detectable lowest concentration (nM)	EC50 (nM), R2, 95%CI	Detectable lowest concentration (nM)	EC50 (nM), R2, 95%CI	Detectable lowest concentration (nM)	EC50 (nM), R2, 95%CI
NanoLuc VAMP2 SiMa	0.01 nM	0.01 nM, 0.8175, 0.0024 to 0.7788	0.1 nM	0.70 nM, 0.9584, 0.3524 to 1.374	0.1 nM	0.06 nM, 0.9860, 0.05092 to 0.09331	c-VAMP: 10 nM v-VAMP: 0.01 nM	c-VAMP: >10 nM v-VAMP: 0.08 nM, 0.7967, 0.016 to 1.59	c-VAMP: 0.1 nM v-VAMP: 0.1 nM	c-VAMP: 0.1nM, 0.45, 0.0035 to ? v-VAMP: 0.1 nM, 0.79, 0.027 to 0.713	5 nM	>10 nM
NanoLuc VAMP2 LAN-5	0.001 nM	0.06 nM, 0.8818, 0.01207 to 0.2594	1 nM	1.4 nM, 0.9628, 0.8266 to 2.708	0.1 nM	0.05 nM, 0.9676, 0.03507 to 0.08932	—	—	c-VAMP: 0.1 nM v-VAMP: 0.1 nM	c-VAMP: 0.25 nM, 0.5357, 0.011 to 1139 v-VAMP: 0.07 nM, 0.6765, 0.01 to 0.758	1 nM	3.19 nM, 0.8401, 0.7220 to 75.10
GFP VAMP2 LAN-5	0.001 nM	0.008 nM, 0.8205, 0.0017 to 0.048	0.1 nM	0.76 nM, 0.9578, 0.3775 to 1.472	0.01 nM	0.031 nM, 0.9473, 0.012 to 0.075	c-VAMP: 5 nM v-VAMP: 0.01 nM	c-VAMP: >10 nM v-VAMP: 3.99 nM, 0.6551, 0.4868 to ?	c-VAMP: 0.01 nM v-VAMP: 0.01 nM	c-VAMP: 0.05 nM, 0.4825, 0.0006 to 2.73 v-VAMP: 0.09 nM, 0.81, 0.023 to 0.42	1 nM	3.03 nM, 0.9837, 1.947 to 5.025
SYT1I-NanoLuc VAMP2 LAN-5			0.01 nM	0.08 nM, 0.8931, 0.02837 to 0.2750					c-VAMP: 0.01 nM v-VAMP: 0.1 nM	c-VAMP: 0.05 nM, 0.8396, 0.015 to 0.177 v-VAMP: 0.06 nM, 0.7806, 0.016 to 0.26	1 nM	3.42 nM, 0.8704, 0.9235 to 33.85
NanoLuc SNAP25 LAN-5	0.01 nM	0.01 nM, 0.8823, 0.03297 to 0.04303	0.1 nM	0.08 nM, 0.9430, 0.04335 to 0.1752								
SNAP25 NanoLuc LAN-5	0.01 nM		0.1 nM									

— : No result □ : Not tested

Table 3.1 Table demonstrating the sensitivity of each cell line for tested CNTs.

Detectable lowest concentration of toxins and EC50 values were given for different neuroblastoma cell lines.

As can be seen from Table 3.1, SiMa and LAN-5 neuroblastoma cell lines are both sensitive to CNTs, but at different levels. In order to compare the sensitivity of SiMa and LAN-5 neuroblastoma cells, the cell lines must carry the same constructs. In the light of this information, NanoLuc VAMP2 SiMa and NanoLuc VAMP2 LAN-5 cell lines were compared for each toxin. As EC50 values could not always be estimated accurately, the lowest detection thresholds were taken into consideration more heavily in order to determine which cell line was the most sensitive. BoNT/A was detected at the lowest concentration of 0.001 nM BoNT/A in NanoLuc VAMP2 LAN-5 cells, while it was observed at lowest concentration of 0.01 nM in NanoLuc VAMP2 SiMa. This suggests that LAN-5 cells are more sensitive than SiMa cells for BoNT/A. Similarly, TeNT was detected more sensitively in NanoLuc VAMP2 LAN-5 cells at the lowest concentration of 1 nM TeNT, compared to NanoLuc VAMP2 SiMa where the lowest concentration that cleavage was seen at was 5 nM.

On the other hand, the limit of detection for BoNT/B in NanoLuc VAMP2 SiMa was 0.1 nM, whereas it was 1 nM in NanoLuc VAMP2 LAN-5, which made SiMa cells more sensitive. And BoNT/D cleaved c-VAMP2 and v-VAMP2 were detected at the lowest concentrations of 10 nM and 0.01 nM respectively in NanoLuc VAMP2 SiMa cells, while no cleavage was observed in NanoLuc VAMP2 LAN-5 cells. SiMa cells therefore might be more sensitive than LAN-5 cells for these toxins. As regard to BoNT/C and BoNT/DC, they were detected in both cell lines with similar sensitivity at the threshold of detection of 0.1 nM. It showed SiMa and LAN-5 have similar sensitivity for BoNT/C and BoNT/DC.

The following Table 3.2 gives minimum detectable concentration of each CNTs in these neuroblastoma cell lines. Apparently, BoNT/A was the most sensitively detected serotype in neuroblastoma cell lines compared to other CNTs. It was detected at the lowest concentration of 0.001 nM, which is less than other toxins. Neuroblastoma cell lines showed also significant sensitivity for BoNT/B, BoNT/C, and BoNT/DC. Their toxin activities were detected at the lowest concentrations of 0.01 nM. Neuroblastoma cells showed a modest sensitivity for TeNT detection; it was detected at the lowest concentration of 1 nM. In terms of BoNT/D sensitivity, v-VAMP2 was detected at a 0.01 nM, whereas c-VAMP2 was detected at the lowest concentration of 5 nM, which contradicts the results. Without BoNT/B, the lowest concentration of each CNT was detected in GFP VAMP2 cell line.

Clostridium Neurotoxin	Detectable lowest concentration (nM)	Detected Neuroblastoma cell line
BoNT/A	0.001 nM	GFP VAMP2 LAN-5; NanoLuc VAMP2 LAN-5
BoNT/B	0.01 nM	SYTII-NanoLuc VAMP2 LAN-5
BoNT/C	0.01 nM	GFP VAMP2 LAN-5
BoNT/D	0.01 nM	GFP VAMP2 LAN-5; NanoLuc VAMP2 SiMa
BoNT/DC	0.01 nM	GFP VAMP2 LAN-5; SYTII-NanoLuc VAMP2 LAN-5
TeNT	1 nM	GFP VAMP2 LAN-5; NanoLuc VAMP2 LAN-5 SYTII-NanoLuc VAMP2 LAN-5

Table 3.2 Table summarising detectable lowest concentration of CNTs in neuroblastoma cell line.

3.3 Discussion

Animal testing is currently the gold standard assay for CNTs. However, it has severe limitations such as being time consuming, expensive, and most importantly requires the sacrifice of a large number of animals. Therefore, development of a sensitive replacement assay for each serotype of BoNT and TeNT detection is essential. Although some assays have been developed for this purpose, they are not sufficiently sensitive or are not practical to use wide-scale. The mouse hemidiaphragm assay was developed as an ex vivo replacement method (Rasetti-Escargueil et al., 2009). However, this assay still required the use of animals. Several in vitro replacement assays have been established as immunological detection methods and endopeptidase assays. Some of these assays are sensitive but have serious limitations. For example, immunological detection-based assays might detect both active and inactive toxin; and endopeptidase assays measure only the proteolytic activity of LC (Pellett, 2013). However, an ideal replacement assay must detect all of the functional steps of the neurotoxin: receptor binding, translocation, and catalytic activity. Since in vitro cell-based assays detect all steps, they are more advantageous than other in vitro assays.

This chapter has identified a new cell line in terms of CNT testing, LAN-5 human neuroblastoma, which would be a good candidate to develop a novel replacement cell-based assay. In addition to LAN-5, a prior cell line studied in our lab, SiMa human neuroblastoma, has been investigated as a potential candidate for several different CNTs. Even though SiMa cells were found to be sensitive to other BoNT serotypes and TeNT, LAN-5 cells were more advantageous overall. The advantages of the LAN-5 cell line is that there are no patent issues, and the cells are easier to culture. Therefore, it is a prominent candidate for development of cell-based replacement assays. The following section will discuss LAN-5 cells as well as SiMa cells, along with a one-step ELISA assay for CNTs detection and compare it with other methods currently available.

As previously described, the one-step ELISA had previously been established in our lab for BoNT/B detection using NanoLuc VAMP2 SiMa cells (Rust et al., 2017), after another study developed a cell-based assay using SiMa cells for BoNT/A detection (Fernandez-Salas et al., 2012). This sensitive sandwich ELISA based assay was approved by the FDA for testing BoNT/A commercial products. This study also revealed that SiMa outperformed other candidate neuronal cell lines, PC12, Neuro-2a, and LA1-55n, in terms of BoNT/A sensitivity. In other research, a cell-based assay was developed using a SiMa cell line stably expressing HPOMC1-26-Gluc (Pathe-Neuschafer-Rube et al., 2015, Pathe-Neuschafer-Rube et al., 2018). Their assay was based on the inhibition of reagent-stimulated neurosecretory vesicle release, which can be used to represent neurotransmitter release, by BoNTs.

BoNT/A was detected as low as 1 pM in their assay, which is the same as in LAN-5 cells. Although this assay might be advantageous in terms of offering a route to test each serotype, the endpoint of the assay is not ideal as it does not directly detect neurotoxin activity unlike a one-step ELISA.

In addition to SiMa neuroblastoma, the SH-SY5Y human neuroblastoma cell line was also found to be sensitive for BoNTs detection (Purkiss et al., 2001). They detected BoNT/A, BoNT/B, BoNT/C and BoNT/D with the IC50 values of 5.56 ± 2.37 nM, 41.65 ± 18.82 nM, 0.54 ± 0.11 nM and, 2.56 ± 0.54 nM, respectively. However, the EC50 values for these toxins in SiMa and LAN-5 cells were all lower than this, with the exception of BoNT/D (Table 3.1). Therefore, their sensitivity was poor and it seems that the lowest detectable concentrations of BoNTs were much higher in SH-SY5Y cells compared to SiMa and LAN-5 neuroblastomas. This may be due to the use of undifferentiated SH-SY5Y cells. On the contrary, Rassetti-Escargueil et al. (2011) used differentiated SH-SY5Y neuroblastoma cells, which resulted in enhanced sensitivity. However, SH-SY5Y neuroblastomas were still not advantageous because the differentiation process took 18 days and required many laborious steps (Shipley et al., 2016), whereas SiMa and LAN-5 can be differentiated in 3 days using a simple method.

Another cell line, P19 embryonal carcinoma cells, was found to be sensitive to BoNT/C and BoNT/DC serotypes (Tsukamoto et al., 2012). However, P19 cells need to be differentiated to neuronal cells with RA for 4 days, and subsequently seeded for a further 4 days before toxin treatment. Therefore, SiMa and LAN-5 neuroblastomas have an advantage in terms of differentiation time. Furthermore, my findings showed that the activity of BoNT/DC was detected more sensitively in a LAN-5 cell line than P19. The lowest detectable concentration was found approximately 0.06 nM in P19 cells, whereas it was found 0.01 nM in LAN-5 cells. In regard to BoNT/C sensitivity, P19 and LAN-5 cells showed similar sensitivity; the limit of detection was around 0.01 nM in both cell lines. However, P19 cells were treated with toxins for only 18 hours whereas LAN-5 cells were treated for 72 hours. There is a possibility that P19 sensitivity may improve after 72 hours of treatment with the toxin. Therefore, P19 and LAN-5 cell lines would need to be exposed to toxins for the same duration to reach a precise conclusion.

NG108-15, a mouse neuroblastoma/rat glioma hybrid cell line, was found to be sensitive to BoNT/A after differentiation with purmorphamine and RA (Whitemarsh et al., 2012a). As undifferentiated NG108-15 cells were relatively insensitive to BoNTs, the cells must be differentiated at least for 5 days to induce motor neuron differentiation. Furthermore, they were exposed to the toxin for 48 hours to achieve effective results. According to these findings, the NG108-15 and LAN-5 assays require similar time periods. However, NG108-15 is a more sensitive cell line than LAN-5 and SiMa. BoNT/A was

detected in differentiated NG108-15 with an EC50 value of 16 U, whereas it was detected in LAN-5 cell line with EC50 value of 194.4 U.

Besides continuous cell lines, primary neurons have been used to develop replacement cell-based assays for CNTs detection. Primary rat spinal cords (RSC) and primary mouse spinal cords (MSC) were extensively tested and found to be sensitive to CNTs activity (Whitemarsh et al., 2013). The sensitivity of primary RSC cells was quite high; BoNT/A and BoNT/B were detected at the lowest detection level of 0.033 pM and 5.5 pM, respectively (Pellett et al., 2007). Despite their high sensitivity, one main limitation was that they needed to be matured for at least 18 days before they could be used. In another study, 4 different primary neurons, DRG, sympathetic ganglia, ventral spinal cord and forebrain, were collected from 6-9 day old chick embryos and tested for BoNT/A detection (Stahl et al., 2007). According to their cellular assay, after 3 hours treatment with BoNT/A, individual primary neurons from different regions cleaved approximately 50% of SNAP25 at 1 nM concentration. The sensitivity was lower in comparison to primary neurons from rats and mice, but it might increase with a longer treatment duration. However, a major disadvantage was that chicken embryos need to be incubated for 6-11 days before isolation of primary neurons. In another study, BoNT/D sensitivity was evaluated in primary RSC, MSC and mouse cortical neurons (Pellett et al., 2015). Interestingly, no cleavage was detected in RSC and MSC cells even at a higher concentration of 16,000 U, whereas BoNT/D was detected sensitively in mouse cortical neurons with an EC50 value of 7 U. Overall, despite their high sensitivity, primary neurons have some limitations that make them impractical for cell-based assay. It is still necessary to use animals, and skilled personnel to prepare the cells. The cells are difficult to obtain from animals and their maturation time is quite long. Additionally, their reproducibility is very low due to their biological variability (Adler et al., 2010). Therefore, SiMa and LAN-5 neuroblastoma cell lines are more preferable for cell-based assays. They are easier to culture and can be used in a shorter period of time, which makes them more advantageous than primary neurons.

Advances in stem cell technology has opened a new cell platform for CNTs detection. Human induced pluripotent stem cell (hiPSCs) derived neurons and embryonic stem cell (ES) derived neurons were extensively tested for BoNTs activity. For the first time, Pellet et al. (2011) used mouse ES-derived neurons to detect BoNTs. According to their results, BoNT/A was detected at the lowest concentration of 0.104 pM after treatment with BoNT/A for 24 hr. In another study, BoNT/A was detected with enhanced sensitivity in murine ES-derived neurons. Cleaved SNAP25 was detected at the lowest concentration of 0.067 pM after 24 hr exposure to the toxin (McNutt et al., 2011). Additionally, another study found mouse ES-derived neurons had cleaved SNAP25 at as little as 10 pM BoNT/A after 3 hr exposure (Kiris et al., 2011). Recently, Jenkinson et al. (2017) cultured mouse ES-derived neurons

on multi-electrode arrays and measured inhibition of synaptic transmission after BoNT/A exposure. Synaptic transmission was reduced significantly at the concentration of 1.67 pM following 24 hr treatment with toxin. The loss of synaptic activity in mouse ES-derived neurons after 20 hours of BoNT/A treatment has been observed even at concentrations as low as 0.01 pM and 0.005 pM in similar studies (Hubbard et al., 2015, Beske et al., 2016).

The results of these studies demonstrate that ER-derived neurons are highly sensitive to BoNT/A, with the lowest detection limit varying between 0.067 pM and 10 pM even after short exposure periods to toxins. In addition to BoNT/A, BoNT/B was also detected sensitively in mouse ES-derived neurons with a EC50 value of 20 pM (Beske et al., 2016). However, a major limitation is that the cells were maintained for 9-10 days or even 21 days before being exposed to toxins. Even though differentiated LAN-5 cells were less sensitive, with the lowest detection level of 1 pM for BoNT/A, they are more advantageous in terms of cell culture protocol and time.

There are also several studies about the use of hiPSCs-derived neurons for BoNT detection. The hiPSCs-derived neurons were characterised, and it was found that they produced essential target and receptor proteins specific for BoNTs. It was subsequently shown that BoNT/A, BoNT/B, BoNT/C and BoNT/E were sensitively detected in hiPSCs-derived neurons (Whitemarsh et al., 2012b). In this study, hiPSCs-derived neurons detected BoNTs with equal or even greater sensitivity than RSC neurons. BoNT/D activity was also assessed in hiPSCs derived neurons and was found that the cells were moderately sensitive to BoNT/D with a EC50 value of 50 U (Pellett et al., 2015). Furthermore, Pellet et al. (2017) developed a sensitive cell-based assay using hiPSCs-derived neurons based on ELISA for BoNT/A detection. The ELISA assay detected BoNT/A with an EC50 value of 0.3 U/well. In another study, hiPSCs-derived motor neurons were found to be more sensitive to BoNT/A than SiMa cells (Schenke et al., 2020). The hiPSCs-derived motor neurons detected BoNT/A with IC50 of concentration of 0.046 pM, while SiMa cells detected with IC50 value of 13.31 pM. Despite the fact that hiPSCs-derived neurons are highly sensitive to BoNTs, these cells have limitations for use in a replacement assay. They must be differentiated for 5 days, then matured for 18 days prior to use in a toxin assay. Furthermore, their differentiation protocol consists of a number of steps. In contrast, LAN-5 and SiMa neuroblastoma cells were easily differentiated and are then ready to be treated with toxin after just 3 days. Due to the importance of fast detection of CNTs, SiMa and LAN-5 cells are more suitable candidates for developing a cell-based assay than hiPSCs-derived neurons.

It is clear that the majority of the research discussed above is focused on developing a cell-based assay for BoNTs, especially for BoNT/A and BoNT/B. However, it is also essential to generate a cell-based assay for TeNT detection. Currently, TeNT toxoids are tested on guinea pigs and there have been some

studies into development of a replacement assay. A test of TeNT activity on cells was conducted some years ago. Pelizzari et al. (1998) detected TeNT activity on hippocampal cells in a semi quantitative way. They developed an antibody against the 1-33 fragment of VAMP2 and stained untreated and TeNT treated hippocampal neurons. When VAMP2 was cleaved by TeNT, cleaved N-fragment VAMP2 (1-76 fragment) was degraded in the cytosol. Consequently, immunofluorescence staining in TeNT-treated neurons disappeared, which is the endpoint of their assay. However, quantitative measurement is essential in order to replace animal testing. In another cell-based study, TeNT activity was detected in mouse ES-derived neurons by inhibition of synaptic transmission and VAMP2 cleavage (Beske et al., 2016). TeNT was detected with an IC50 value of 1.14 pM for the synaptic transmission inhibition assay, and with an EC50 value of 6.80 pM for VAMP2 cleavage. In spite of the high sensitivity of mouse ES-derived neurons, the cells matured 24-30 days after seeding, a significant limitation.

There have also been some in vitro assays for TeNT detection. One study combined an endopeptidase assay with GT1b ganglioside binding for TeNT detection (Behrensdorf-Nicol et al., 2010). In spite of the fact that the detection limit of the assay was similar to animal tests, it did not measure all steps of intoxication, as this assay did not assess endocytosis of the toxin. Another in vitro assay is called BINACLE (Binding and cleavage) which is capable of measuring active TeNT in the samples based on its binding capacity and proteolytic activity (Behrensdorf-Nicol et al., 2013). An ideal replacement assay should include all steps of intoxication. However, the BINACLE test does not cover the detection of neurotoxin translocation. Furthermore, the sensitivity of the test is lower than that of the animal assay. One-step ELISA enables the measurement of all stages of intoxication, which is more advantageous than the BINACLE and endopeptidase tests. In light of this information, it would appear that the human neuroblastoma cell line LAN-5 would be an appropriate candidate for a replacement assay for the detection of TeNT.

In order to establish a sensitive cell-based assay, the most significant component is undoubtedly a sensitive cell line. In addition to being sensitive, a candidate cell should be easier to handle and culture and be ready for the assay in a short time. LAN-5 neuroblastoma cell line is sensitive to each CNTs to different extents. Also, their preparation is effortless and shorter compared to primary and stem cell derived neurons. With all these properties, LAN-5 cell line is a promising candidate for a replacement assay. Even though the current sensitivity is not ideal for some serotypes, cell line sensitivity could be improved by exogenous addition of gangliosides and transduction of receptor proteins targeted by those serotypes.

Another important factor for a sensitive replacement assay is the development of an antibody that is capable of detecting cleaved products. We have sensitive and specific rabbit monoclonal antibody for

the detection of BoNT/B and TeNT cleaved products. There is, however, a requirement to develop monoclonal antibodies for BoNT/A, BoNT/C, BoNT/D, and BoNT/DC. With a production of mouse or rabbit monoclonal antibodies specific for each serotype, a one-step ELISA test would be available for other toxins.

Another key factor for a replacement assay is improving practical and reliable quantitative methods. Western blot is a useful technique for validation of cell lines or antibodies; however, it is a semi-quantitative method. Moreover, it has many steps and only allows a limited number of samples to be tested at once. One-step ELISA is a more practical and shorter method. It is appropriate for high content screening and QC validations. However, one limitation of our current ELISA assay is that there is no normalization process. It gives only the results for cleaved products, which is an endpoint of the assay. A suitable normalisation method is one of the future aims of this project.

Overall, LAN-5 neuroblastoma cell line is a promising candidate for cell-based assays. As a future direction, the sensitivity of this cell line will be enhanced by insertion of receptor proteins. Additionally, one-step ELISA is a prominent model for cellular assay. For future studies, monoclonal antibodies will be produced in order to use with the ELISA assay for each CNT. Moreover, an easy and practical normalisation method will be developed and combined with the one-step ELISA.

4 Chapter 4: Investigating neuroblastoma and HeLa cells for clostridial neurotoxin sensitivity

4.1 Introduction

The mechanism by which BoNT and TeNT enter and intoxicate cells is well established. The intoxication mechanism of CNTs has multiple steps. First, the neurotoxin binds to gangliosides and receptor proteins which are specific for each CNT. Second, the neurotoxin is internalised into the cells by endocytosis. The light chain of the neurotoxin is then translocated from the membrane of endosome to the cell cytosol. Finally, the released light chain cleaves the target SNARE protein in the cytosol (Binz and Rummel, 2009, Pirazzini et al., 2016). Understanding the mechanism of intoxication, especially the way the toxins enter cells, led to improvements in the methods for testing CNTs.

The uptake of neurotoxin into cells depends on two sequential receptor routes. They first bind to gangliosides, which are abundant on the surface of neuronal cell membranes. The interaction between gangliosides and the neurotoxins is considered to be low affinity (Binz and Rummel, 2009). They subsequently bind to receptor proteins to enter neuronal cells. It is suggested that the neurotoxins still bind to gangliosides when they interact with the receptor proteins. The simultaneous binding of gangliosides and protein receptors to neurotoxins may result in high levels of affinity and may be essential for the subsequent endocytosis mechanism of the neurotoxins. As this receptor binding process involves both gangliosides and receptor proteins, it is known as the dual-receptor concept. As such, this dual-receptor binding mechanism may be responsible for the exceptional binding affinity and selective nature of CNTs (Brunger et al., 2008).

The specific receptor proteins and gangliosides required for internalisation of each BoNT serotype are clearly identified (Connan and Popoff, 2017, Schenke et al., 2020). Each BoNT serotype utilises specific gangliosides and receptor proteins with different levels of affinity. Although TeNT uses two ganglioside sites to enter neuronal cells, it is still not known which receptor proteins it uses (Brunger et al., 2008, Zuverink and Barbieri, 2018). It is crucial to characterise cell lines in terms of relevant receptors and target proteins or gangliosides of the CNTs. This would enable a comprehensive understanding of the sensitivity of cell line. The information would also allow researchers to determine if some of these proteins and gangliosides are not expressed in sufficient amounts, and potentially enhance the sensitivity of the cells by introducing extra proteins and gangliosides.

This chapter identifies a range of factors in relation to cell sensitivity for CNTs. SiMa and LAN-5 cells are characterised for expression of gangliosides, receptors, and target proteins. First, testing of undifferentiated LAN-5 cells for CNTs and their comparison with differentiated LAN-5 cells is reported. Then the effects of exogenous addition of GT1b gangliosides for CNTs activity in LAN-5 cells is shown, followed by the effect of SYTII protein on the sensitivity of BoNT/B, BoNT/DC, and TeNT. Finally, further knowledge about SYTII, GT1b relations to BoNT/B is provided, based on testing BoNT/B with a non-neuronal cell line, HeLa. These studies were conducted in order to understand why cells show sensitisation to neurotoxins. This has provided an important understanding about the relationship between neuroblastoma cells and CNTs, promoting improvement in the conditions of the cells and enabling more sensitive and faster assays.

4.2 Results

4.2.1 Undifferentiated native LAN-5 and SiMa show neuronal properties

Beta tubulin III is a specific marker for neuronal differentiation (Jirasek et al., 2002). Here, both SiMa and LAN-5 were characterised for beta tubulin III in order to confirm their neuronal origins. According to immunofluorescence images, both undifferentiated and differentiated SiMa and LAN-5 cell lines were extensively stained with beta tubulin III (Figure 4.1). These results indicated that both undifferentiated and differentiated forms of SiMa and LAN-5 human neuroblastoma cells had neuronal origins. Additionally, the undifferentiated form of LAN-5 also had neuronal processes, similar to differentiated cells, whereas undifferentiated SiMa cells appeared totally different from differentiated forms. Therefore, LAN-5 cells might be easier to differentiate than SiMa cells.

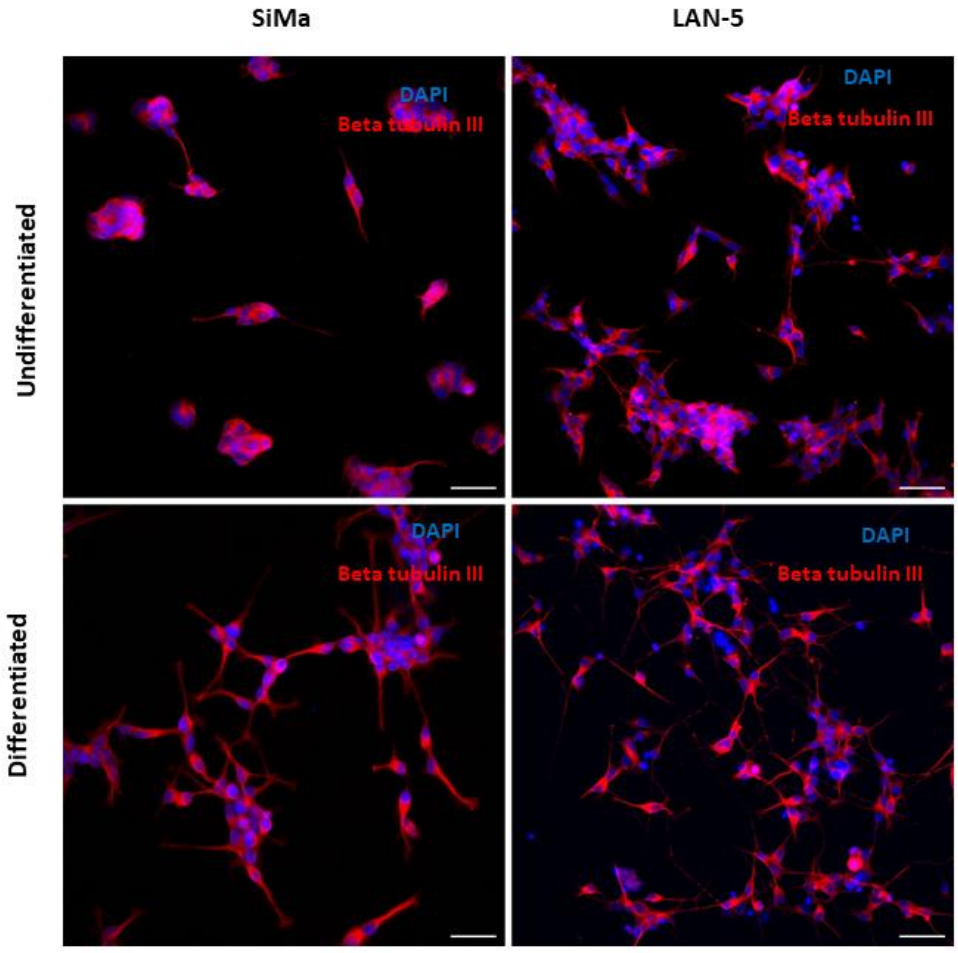

Figure 4.1 SiMa and LAN-5 have neuronal properties even they are undifferentiated.

Immunofluorescence images showing the expression of beta tubulin III (stained in red), which is neuronal marker. Undifferentiated cells were incubated with growth media for 3 days. Differentiated cells were incubated with differentiation media for 3 days. Mouse beta tubulin III Ab is used at 1:1000 dilution. DAPI is used at 1:1000 dilution to see nucleus (stained in blue). Images were taken with epifluorescence microscope at 20x objective. All scale bars are 50 µm. No primary antibody controls were included.

4.2.2 Undifferentiated and differentiated native LAN-5 and SiMa cells express gangliosides that help the entry of clostridial neurotoxins

Gangliosides, which belongs to glycosphingolipids, are found extensively in extracellular plasma membranes as well as intracellular organelles (Zuverink and Barbieri, 2018). Although they occur in all tissues of vertebrates, they are primarily expressed on the surface of neuronal cells. They include one or more sialic acid molecules attached to the sugar chain. Gangliosides with one sialic acid are called 'a series' and two sialic acids are called 'b series' (Popoff, 2018). Specifically, GT1b and GD1a are

responsible for myelin formation, enhancing axon stability and neurite inhibition (Zuverink and Barbieri, 2018). They also play a role in cell-to-cell communication, adhesion, and signal transduction on the cell membrane (Yu et al., 2011). Moreover, they are critical receptors for entry of CNTs to the neuronal cells. Each CNT uses different gangliosides with varying affinity depending on the toxin type. Here, some specific gangliosides to CNTs, GD1a, GT1b, and GD2, were characterised on undifferentiated and differentiated forms of SiMa and LAN-5 cells.

GD1a exhibits strong affinity for BoNT/A, BoNT/B, BoNT/C, and BoNT/DC neurotoxins, while it is not an active receptor for BoNT/D and TeNT (Binz and Rummel, 2009, Connan and Popoff, 2017, Schenke et al., 2020). Immunofluorescence images showed that GD1a was extensively stained on the neuronal processes of differentiated SiMa and LAN-5 cells, and the staining was observed in the form of spots (Figure 4.2 A). The processes of undifferentiated LAN-5 cells were also stained with GD1a successfully. As undifferentiated SiMa did not develop neuronal process, the small amount of GD1a present was stained on the soma.

GT1b is a common ganglioside showing high affinity for all BoNT serotypes and TeNT (Connan and Popoff, 2017, Schenke et al., 2020). Similar to GD1a, GT1b was expressed mainly as dots on neuronal processes. A great amount of GT1b expression was observed in both differentiated cells, and undifferentiated LAN-5 cells (Figure 4.2 B). A slight amount of GT1b was observed in the soma membrane of undifferentiated SiMa cells.

Uniquely, GD2 is only a receptor for BoNT/D (Popoff, 2018, Schenke et al., 2020). Moreover, GD2 binds to the receptor binding domain of BoNT/D with more affinity than GT1b and GD1b (Kroken et al., 2011b). Immunofluorescence images showed that GD2 was extensively expressed on neuronal processes as well as on the soma in differentiated SiMa and LAN-5 cell lines (Figure 4.2 C). It was stained mostly on the soma membrane in undifferentiated SiMa and LAN-5 cells.

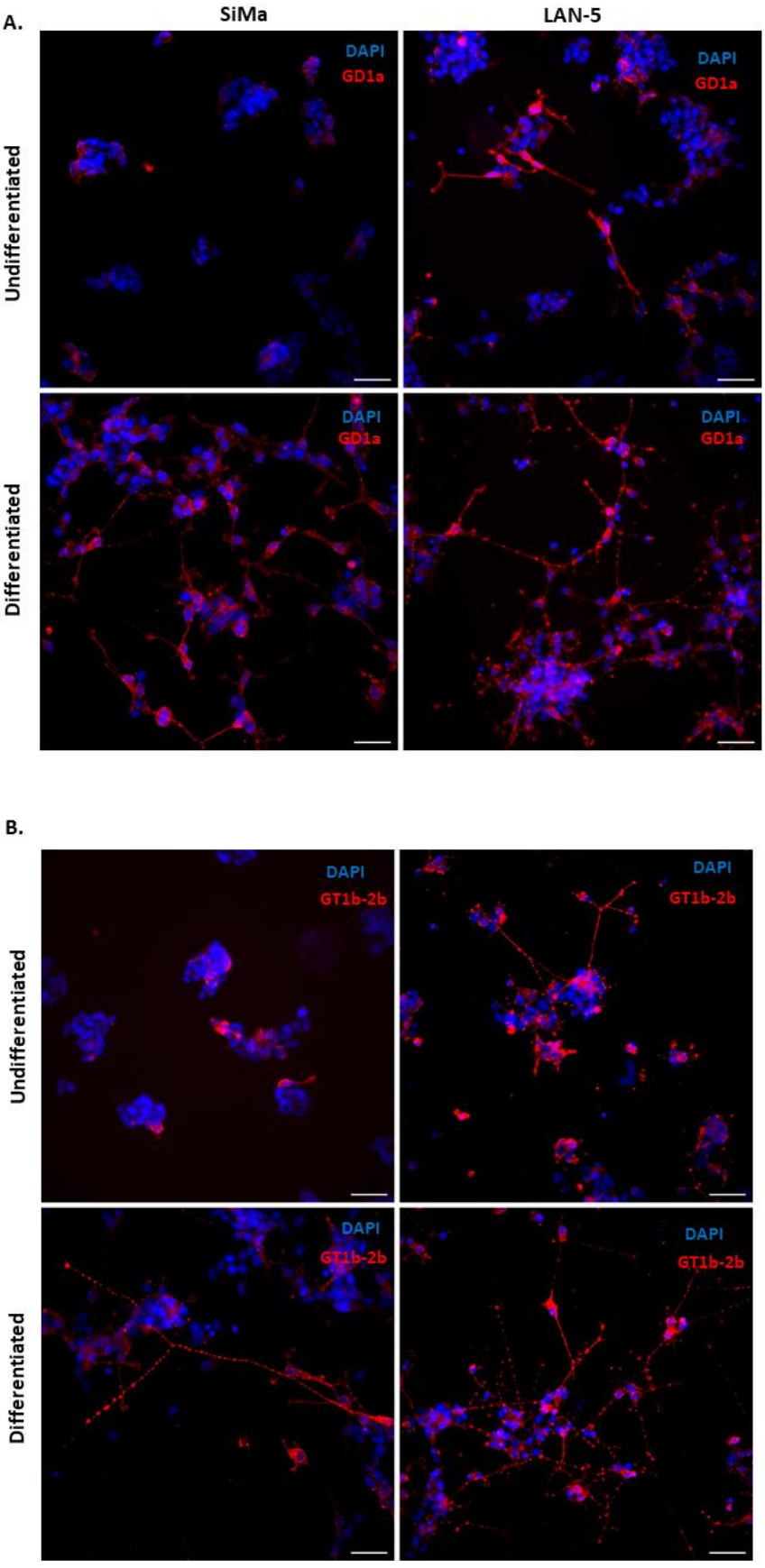
A.
SiMa
LAN-5
Undifferentiated
Differentiated
DAPI
GD1a
B.
GT1b-2b

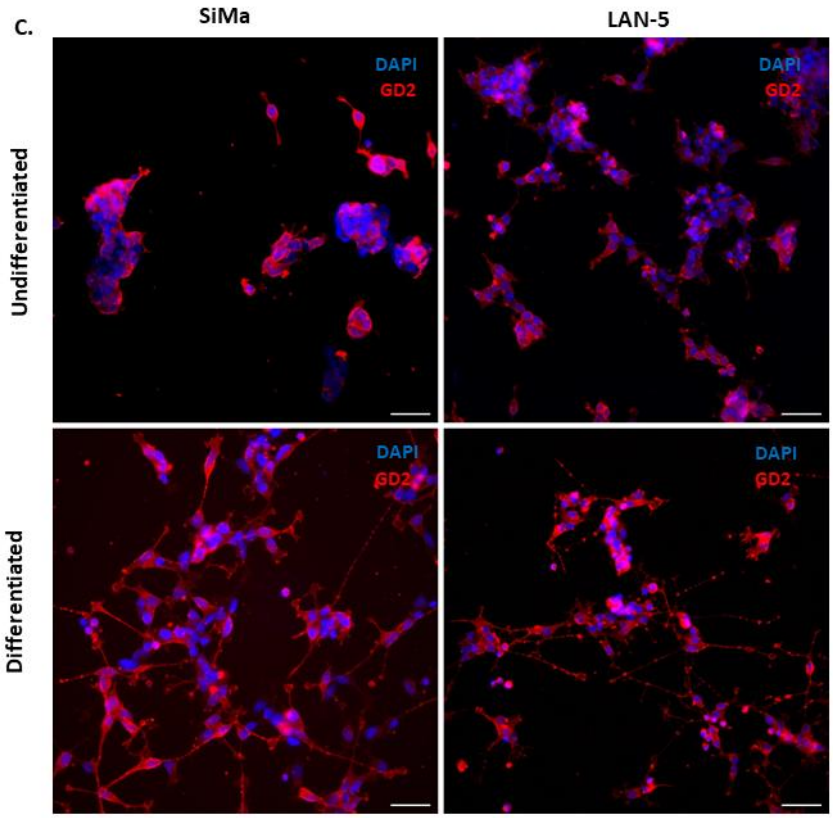

Figure 4.2 SiMa and LAN-5 could express gangliosides for entry of CNTs.

A) *Immunofluorescence images showing the expression of GD1a (stained in red). Mouse GD1a Ab is used 5 µg/mL as a concentration without permeabilization of the cells.* ***B)*** *Immunofluorescence images showing the expression of GT1b-2b (stained in red). Mouse GT1b-2b Ab is used 5 µg/mL as a concentration without permeabilization of the cells.* ***C)*** *Immunofluorescence images showing the expression of GD2 (stained in red). Mouse GD2 Ab is used at 1:200 dilution without permeabilization of the cells. Undifferentiated cells were incubated with growth media for 3 days. Differentiated cells were incubated with differentiated media for 3 days. DAPI is used at 1:1000 dilution to see nucleus (stained in blue). Images were taken with epifluorescence microscope at 20x objective. All scale bars are 50 µm. No primary antibody controls were included.*

4.2.3 Undifferentiated and differentiated native LAN-5 and SiMa cells express target and receptor proteins of clostridial neurotoxins

In addition to gangliosides, BoNTs use receptor proteins to be endocytosed into the cells (Brunger et al., 2008) Therefore, SiMa and LAN-5 cell lines were characterised for the expression of SYTI, SYTII, and SV2 receptor proteins. In contrast to BoNTs, the receptor protein of TeNT has not been identified yet (Rummel et al., 2003).

SYTI is one of the specific receptor proteins of BoNT/B and BoNT/DC serotypes (Schenke et al., 2020). Immunofluorescence results showed SYTI was expressed extensively on neuronal processes in both

differentiated cells (Figure 4.3 A). SYTI expression was also observed on the membranes of the soma of undifferentiated cells. According to immunoblot results, SYTI expression was nearly the same between undifferentiated and differentiated SiMa cells (Figure 4.3 B). The expression level of SYTI was reduced in undifferentiated LAN-5 cells compared to differentiated LAN-5 cells.

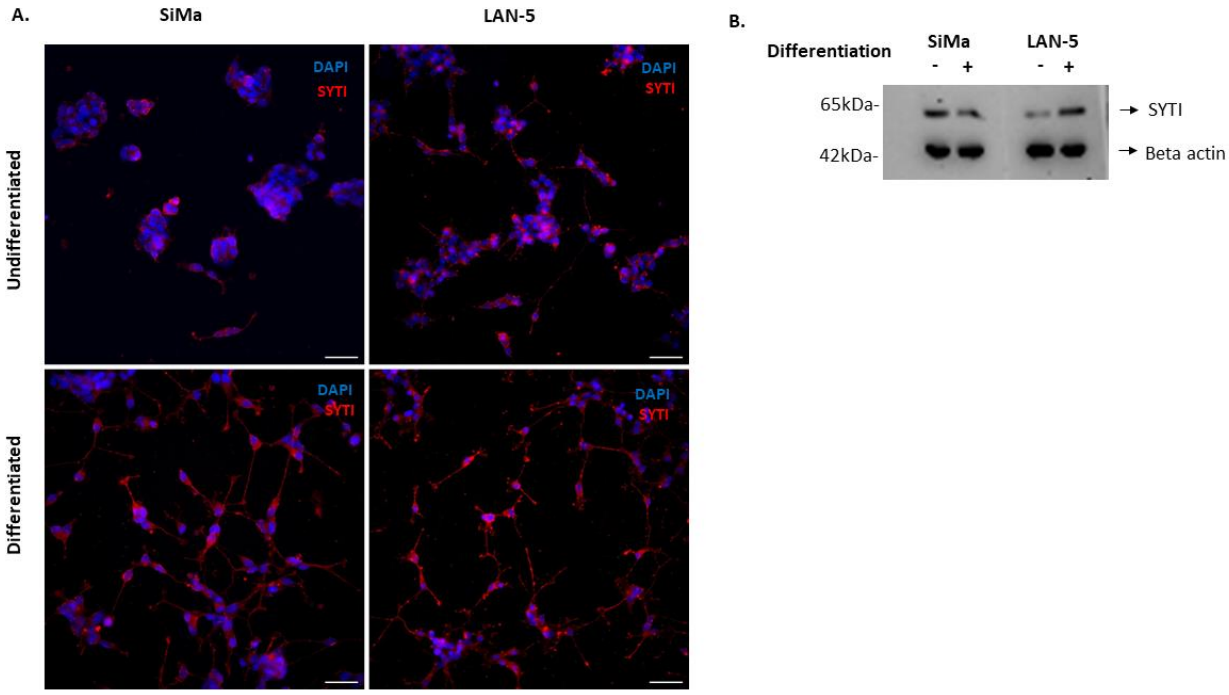

Figure 4.3 SiMa and LAN-5 could express SYTI receptor protein for entry of CNTs.

A) *Immunofluorescence images showing the expression of SYTI (stained in red). Mouse SYTI Ab is used at 1:100 dilution. DAPI is used at 1:1000 dilution to see nucleus (stained in blue). Images were taken with epifluorescence microscope at 20x objective. All scale bars are 50 µm.* ***B)*** *Representative immunoblot showing the proportion of cellular SYTI expression in undifferentiated and differentiated SiMa and LAN-5 neuroblastoma cells. Mouse SYTI Ab is used at 1:1000 dilution. Mouse beta-actin Ab was added at 1:1200 dilution as a loading control. Images were taken from ChemiDoc XRS. Undifferentiated cells were incubated with growth media for 3 days. Differentiated cells were incubated with differentiated media for 3 days. No primary antibody controls were included.*

SYTII is another receptor protein required for BoNT/B and BoNT/DC entry (Schenke et al., 2020). Immunofluorescence images showed that SYTII was expressed on membranes of the soma and on the processes (Figure 4.4 A). SYTII was successfully stained on the processes of differentiated SiMa and LAN-5 cells. Moreover, it was extensively stained on the surface of undifferentiated cells. Immunoblot results of both SiMa and LAN-5 cells showed that the expression level of SYTII protein increased slightly after differentiation (Figure 4.4 B).

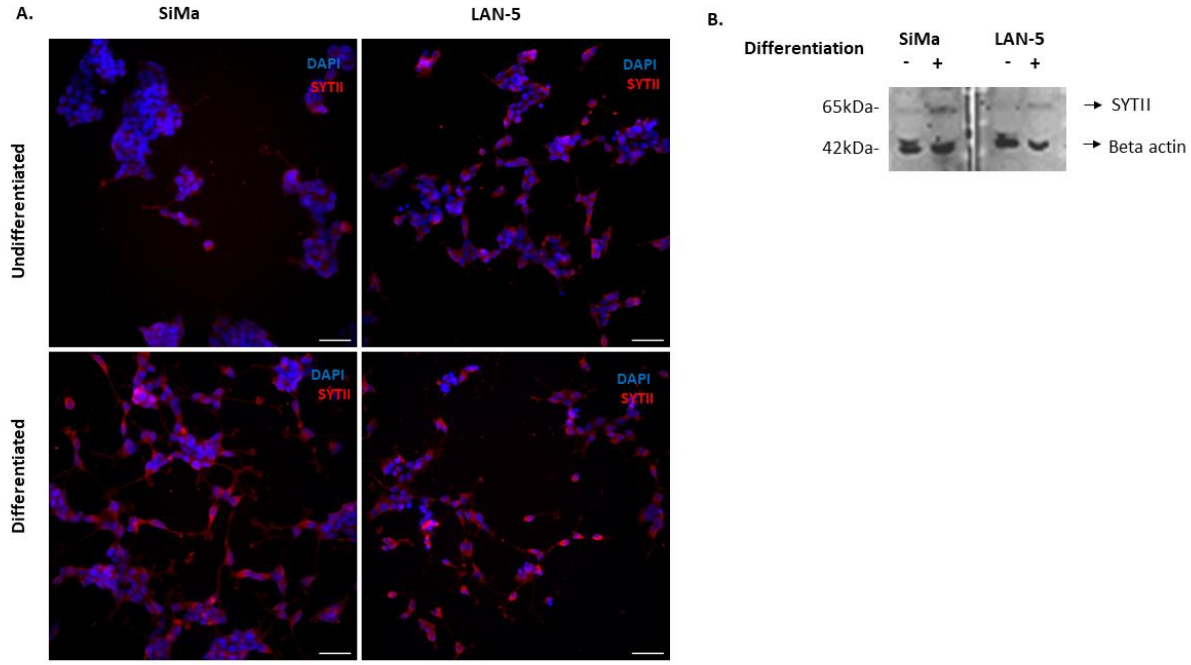

Figure 4.4 SiMa and LAN-5 could express SYTII receptor protein for entry of CNTs.

A) *Immunofluorescence images showing the expression of SYTII (stained in red). Rabbit SYTII Ab is used at 1:100 dilution. DAPI is used at 1:1000 dilution to see nucleus (stained in blue). Images were taken with epifluorescence microscope at 20x objective. All scale bars are 50 µm.* ***B)*** *Representative immunoblots showing the proportion of cellular SYTII expression in undifferentiated and differentiated SiMa and LAN-5 neuroblastoma cells. Rabbit SYTII Ab is used at 1:1000 dilution. Mouse beta-actin Ab was added at 1:1200 dilution as a loading control. Images were taken from ChemiDoc XRS. Undifferentiated cells were incubated with growth media for 3 days. Differentiated cells were incubated with differentiated media for 3 days. No primary antibody controls were included.*

SV2, consists of SV2A, SV2B, SV2C isoforms, and they are receptor proteins for BoNT/A and BoNT/D entry into neuronal cells (Connan and Popoff, 2017). Here, SV2-pan antibody, which recognises SV2A, SV2B, SV2C isoforms, was used. Immunofluorescence images showed that SV2 isoforms were successfully stained on the processes of differentiated SiMa and LAN-5 cells (Figure 4.5 A). SV2 was also stained in undifferentiated cells, primarily on the soma membrane. However, immunoblot showed that the expression of SV2 was less in undifferentiated cells than differentiated cells for both SiMa and LAN-5 (Figure 4.5 B).

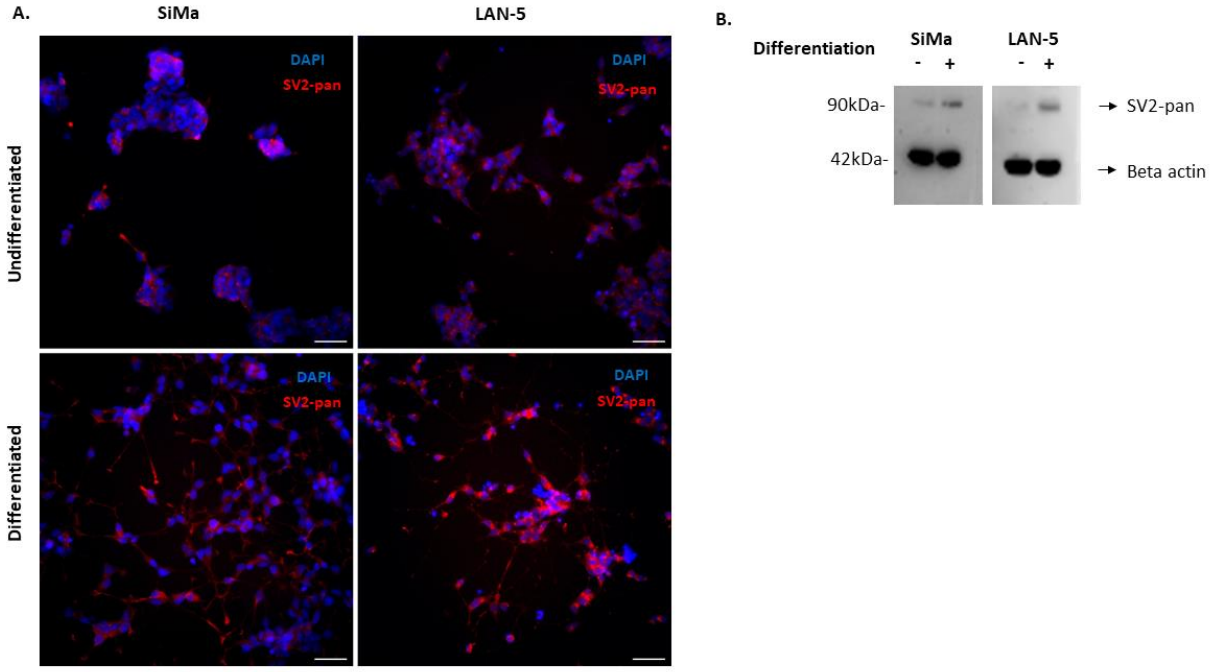

Figure 4.5 SiMa and LAN-5 could express SV2 receptor proteins required for CNTs entry.

A) *Immunofluorescence images showing the expression of SV2-pan (stained in red). Mouse SV2-pan (detects A, B, C isoforms) Ab is used at 5 µg/mL. DAPI is used at 1:1000 dilution to see nucleus (stained in blue). Images were taken with epifluorescence microscope at 20x objective. All scale bars are 50 µm.* ***B)*** *Representative immunoblots showing the proportion of cellular SV2 expression in undifferentiated and differentiated SiMa and LAN-5 neuroblastoma cells. Mouse SV2-pan Ab is used at 2 µg/mL. Mouse beta-actin Ab was added at 1:1200 dilution as a loading control. Images were taken from ChemiDoc XRS. Undifferentiated cells were incubated with growth media for 3 days. Differentiated cells were incubated with differentiated media for 3 days. No primary antibody controls were included.*

In addition to these receptor proteins, the target protein of BoNT/A and BoNT/C, SNAP25, was characterised in the cells (Schenke et al., 2020). According to immunofluorescence images, SNAP25 expression was observed on the soma of neurons as well as on neuronal processes (Figure 4.6 A). It can be seen from the images that SNAP25 had similar staining in undifferentiated and differentiated cells. Immunoblot results also confirmed that SNAP25 expression levels were similar between undifferentiated and differentiated cells for both SiMa and LAN-5 cell lines (Figure 4.6 B-C).

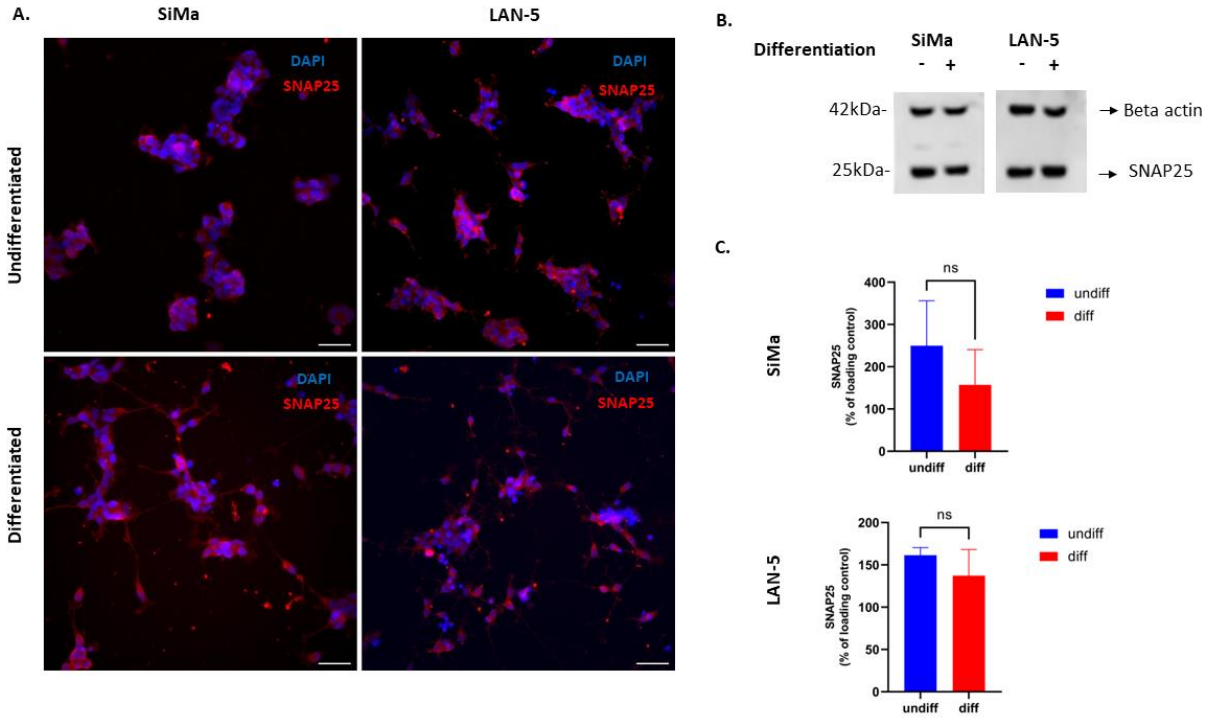

Figure 4.6 SiMa and LAN-5 could express a target protein of BoNT/A and BoNT/C, SNAP25.

A) *Immunofluorescence images showing the expression of SNAP25 (stained in red). Rabbit SNAP25 Ab (in house) is used at 1:500 dilution. DAPI is used at 1:1000 dilution to see nucleus (stained in blue). Images were taken with epifluorescence microscope at 20x objective. All scale bars are 50 µm.* ***B)*** *Representative immunoblots showing the proportion of cellular SNAP25 expression in undifferentiated and differentiated SiMa and LAN-5 neuroblastoma cells. Rabbit SNAP25 Ab (in house) is used at 1:3000 dilution. Mouse beta-actin Ab was added at 1:1200 dilution as a loading control. Images were taken from ChemiDoc XRS. Undifferentiated cells were incubated with growth media for 3 days. Differentiated cells were incubated with differentiated media for 3 days.* ***C)*** *Graphs showing the quantification of immunosignals from undifferentiated and differentiated cells for native SiMa and native LAN-5 cell line (N=3, ±SEM). Comparisons were examined by an unpaired two-tailed t-test. Alpha P values of <0.05 were considered statistically significant. No primary antibody controls were included.*

Another target protein of CNTs, VAMP2, was extensively discussed for SiMa and LAN-5 neuroblastoma cells in Chapter 3. SiMa neuroblastoma did not express endogenous VAMP2 which was previously shown by Rust et al. (2017). Therefore, I looked at the endogenous VAMP2 expression only for the native LAN-5 cell line. It was shown that LAN-5 cells expressed endogenous VAMP2 and the expression level increased slightly after the differentiation (Figure 4.7). However, the expression of endogenous VAMP2 is not significant for our assay because it is degraded when it is cleaved by the toxin (Pellizzari et al., 1998).

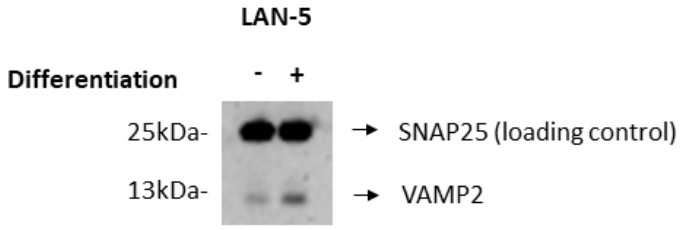

Figure 4.7 LAN-5 could express endogenous VAMP2, a target protein of BoNT/B, BoNT/D, BoNT/DC, and TeNT.

A) *Immunoblot image showing the proportion of endogenous VAMP2 expression in undifferentiated and differentiated LAN-5 neuroblastoma cells. Rabbit VAMP2 was added at 1:10.000 dilution. Rabbit SNAP25 Ab (in house) was added at 1:3000 dilution as a control antibody to detect uncleaved SNAP25. Images were taken from ChemiDoc XRS. Undifferentiated cells were incubated with growth media for 3 days. Differentiated cells were incubated with differentiated media for 3 days.*

Similarly, another target protein of BoNT/C, syntaxin, is degraded when it is cleaved. Although BoNT/C detection was quantified based on cleaved SNAP25, syntaxin degradation by toxin was also showed in parallel. It was confirmed by immunoblots that syntaxin was expressed both in undifferentiated and differentiated cells for both SiMa and LAN-5 (Figure 4.8).

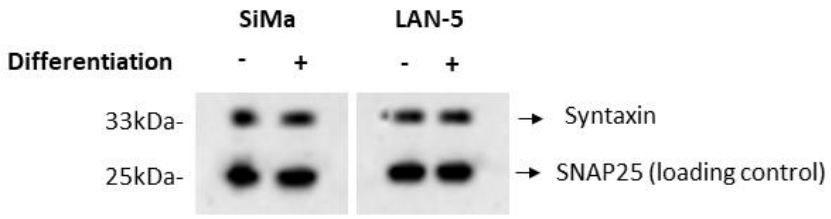

Figure 4.8 SiMa and LAN-5 could express a target protein of BoNT/C, syntaxin.

Immunoblot image showing the proportion of cellular syntaxin expression in undifferentiated and differentiated SiMa and LAN-5 neuroblastoma cell lines. Rabbit anti-syntaxin (in house) was added at 1:2000 dilution. Rabbit SNAP25 Ab (in house) was added at 1:3000 dilution as a control antibody to detect uncleaved SNAP25. Images were taken from ChemiDoc XRS. Undifferentiated cells were incubated with growth media for 3 days. Differentiated cells were incubated with differentiated media for 3 days.

4.2.4 Undifferentiated LAN-5 cells are sensitive to clostridial neurotoxins but differentiation increases the sensitivity

In this study, neuroblastomas were tested for CNT activity after they were differentiated unless otherwise stated. However, it would be useful if undifferentiated neuroblastomas showed similar sensitivity to toxins as differentiated neuroblastomas, as the assay duration could be reduced by eliminating 3 days of differentiation. Furthermore, since preparation steps for differentiation are omitted, a more practical test would be available. Here, therefore, the activity of CNTs was compared between differentiated and undifferentiated LAN-5 neuroblastomas. Undifferentiated LAN-5 neuroblastomas developed neurites and appeared differentiated, as shown in the immunofluorescence images above. Moreover, undifferentiated LAN-5 cells expressed target and receptor proteins, and gangliosides. Therefore, LAN-5 neuroblastoma cells were chosen to test sensitivity of undifferentiated cells.

Looking at the results of BoNT/A and BoNT/C, significant amount of SNAP25 were cleaved in both undifferentiated and differentiated cells (Figure 4.9 A-B). The difference in toxin potency between differentiated and undifferentiated cells increased significantly at lower BoNT/A and BoNT/C concentrations (Figure 4.9 C-D). Undifferentiated and differentiated cells produced almost the same amount of cleaved SNAP25 at 10 nM concentration of BoNT/A. However, the amount of cleaved SNAP25 decreased significantly in undifferentiated cells at 1 nM and 0.1 nM concentrations of BoNT/A (Figure 4.9 C). Similarly, SNAP25 cleavage declined significantly when BoNT/C concentration was lowered, especially at the concentration of 0.1 nM (Figure 4.9 D).

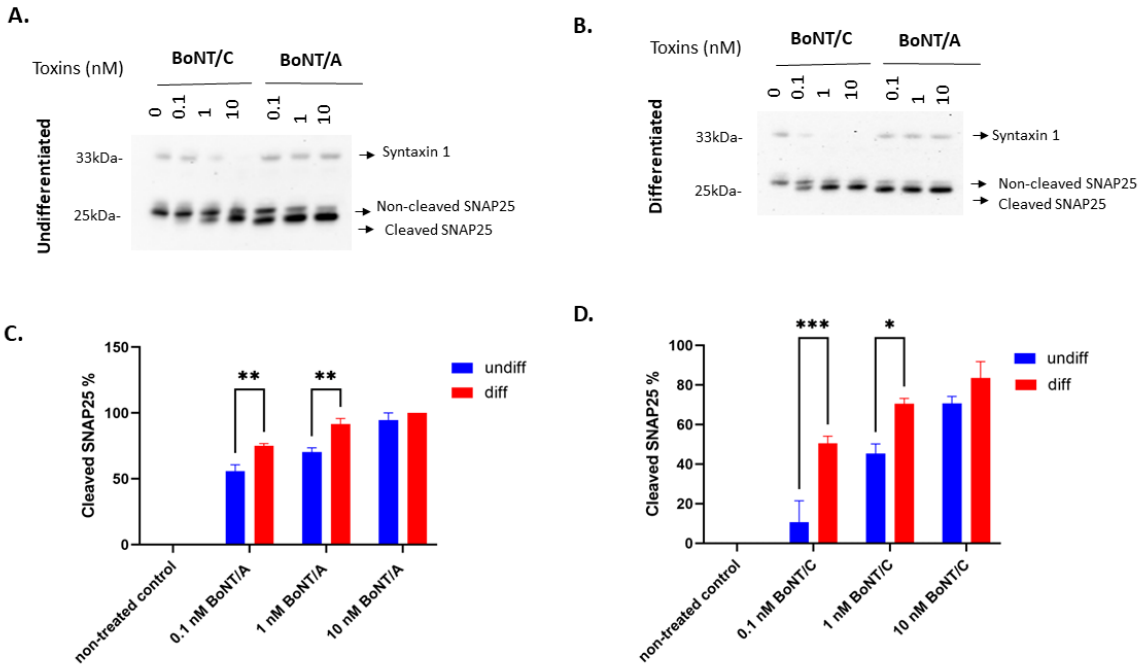

Figure 4.9 BoNT/A and BoNT/C activities are detectable in undifferentiated GFP VAMP2-LAN-5 cell line.

A-B) *Representative immunoblots showing the proportion of cellular cleaved SNAP25 in undifferentiated (A) and differentiated (B) GFP-VAMP2 LAN-5 neuroblastoma cells following application of BoNT/A and BoNT/C. Toxins were titrated at 1:10 serial dilution and treated with cells for 3 days. Cells were treated with the diluting agent (Opti-MEM with 0.5% BSA) as a no treatment control. SNAP25 antibody was added at 1:3000 dilution to detect both cleaved and uncleaved SNAP25. Syntaxin antibody was used at 1:2000 dilution as a control. Images were taken from ChemiDoc XRS.* ***C)*** *Graphs showing the quantification of immunosignals from undifferentiated and differentiated cells following BoNT/A treatment (N=3, ±SEM).* ***D)*** *Graph showing the quantification of immunosignals from undifferentiated and differentiated cells following BoNT/C treatment (N=3, ±SEM). Multiple comparisons were examined by a two-way ANOVA analysis followed by Sidak's test. Alpha P values of <0.05 were considered statistically significant. *=P<0.05; **=P<0.01; ***=P<0.001.*

In regard to BoNT/B and TeNT, cleaved VAMP2 was detected in undifferentiated cells only at higher concentrations (Figure 4.10 A), whereas it was observed in differentiated cells at lower concentrations (Figure 4.10 B). Cleaved VAMP2 was only detected in undifferentiated cells at 1 nM and 10 nM of BoNT/B, but it was also detected at 0.1 nM when cells were differentiated (Figure 4.10 C). The difference in cleaved VAMP2 amounts was not significant between undifferentiated and differentiated cells. For TeNT, cleaved VAMP2 was detected only at 10 nM concentration in undifferentiated cells; and amount of cleaved VAMP2 was considerably higher in differentiated cells than undifferentiated cells at this concentration (Figure 4.10 D). A faint band of VAMP2 cleavage was observed at the concentration of 1 nM in differentiated cells, while it was not observed in undifferentiated cells.

Looking at the results of BoNT/D, no cleavage was observed when the cells were undifferentiated (Figure 4.10 A). However, the amount of cleaved VAMP2 was also considerably less in differentiated cells (Figure 4.10 B). The difference in toxin activity was significant between undifferentiated and differentiated cells at 10 nM concentration for both cleaved c-VAMP2 and v-VAMP2 (Figure 4.10 E-F). In relation to BoNT/DC, a great amount of cleaved c-VAMP2 and v-VAMP2 was detected in both undifferentiated and differentiated cells at the concentrations of 1 nM and 10 nM (Figure 4.10 A). The amounts of cleaved c-VAMP2 at concentrations of 10 nM and 1 nM, and the amounts of cleaved v-VAMP2 at concentrations of 10 nM were almost same in undifferentiated and differentiated cells. The amounts of cleaved c-VAMP2 and v-VAMP2 slightly declined at a concentration of 0.1 nM when cells were undifferentiated (Figure 4.10 G-H).

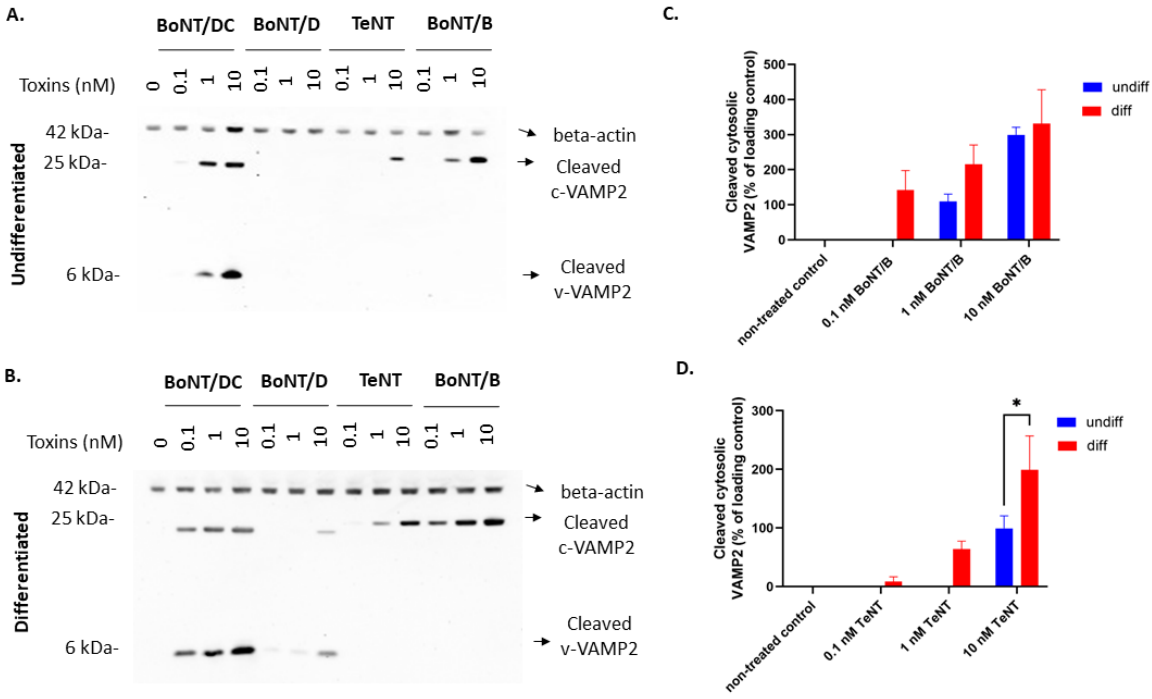

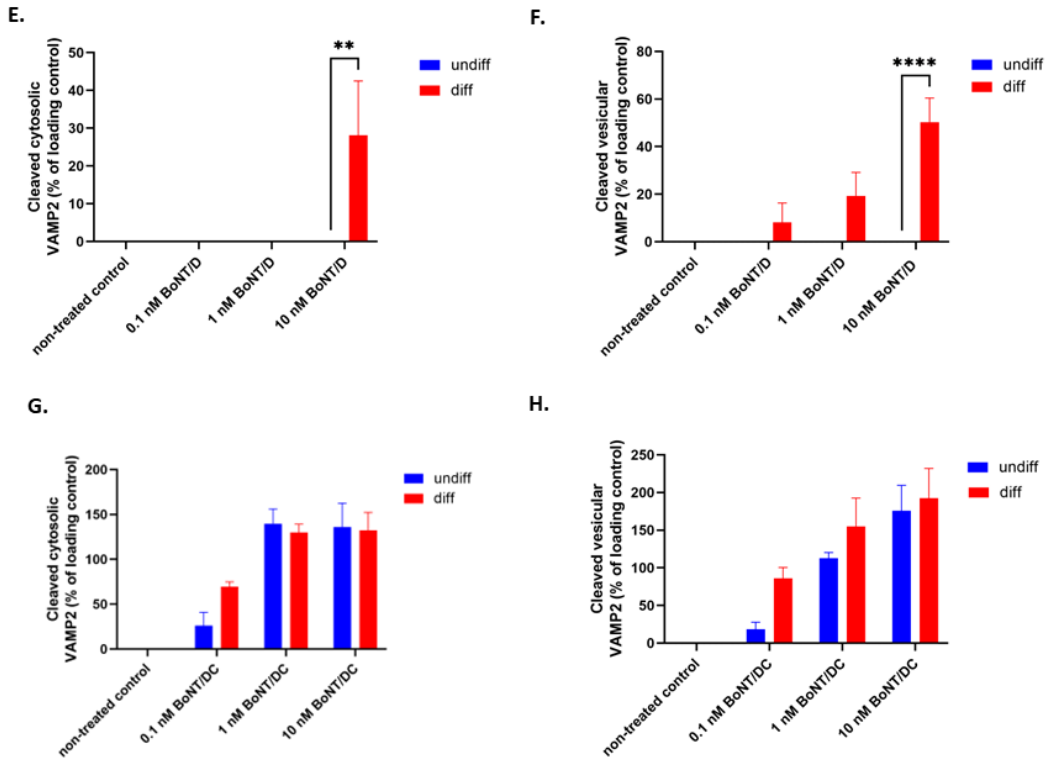

Figure 4.10 BoNT/B, TeNT and BoNT/DC activities are detectable in undifferentiated GFP VAMP2-LAN-5 cell line, but BoNT/D is not detectable.

A-B) *Representative immunoblots showing the proportion of cleaved cytosolic and vesicular VAMP2 in undifferentiated (A) and differentiated (B) GFP-VAMP2 LAN-5 neuroblastoma cells following application of BoNT/B, TeNT, BoNT/D, and BoNT/DC. Toxins were titrated at 1:10 serial dilutions and treated with cells for 3 days. Cells were treated with the diluting agent (Opti-MEM with 0.5% BSA) as a no treatment control. Rabbit monoclonal Ab (2F7-1) was added at 1:2000 dilution to see BoNT/B and TeNT cleaved cytosolic VAMP2. Mouse monoclonal Ab (D27) was added at 1:2000 dilution to see BoNT/D and BoNT/DC cleaved vesicular VAMP2; D cleaved VAMP cytosolic rabbit polyclonal Ab was used at 1:2000 dilution to see BoNT/D and BoNT/DC cleaved cytosolic VAMP2. Mouse beta-actin Ab was added at 1:1200 dilution as a loading control. Images were taken from ChemiDoc XRS.* ***C)*** *Graphs showing the quantification of immunosignals from differentiated and undifferentiated cells following BoNT/B treatment (N=3, ±SEM).* ***D)*** *Graphs showing the quantification of immunosignals from undifferentiated and differentiated cells following TeNT treatment (N=3, ±SEM).* ***E-F)*** *Graphs showing the quantification of immunosignals for cytosolic (E) and vesicular (F) VAMP2 cleavage from undifferentiated and differentiated cells following BoNT/D treatment (N=3, ±SEM).* ***G-H)*** *Graphs showing the quantification of immunosignals for cytosolic (G) and vesicular (H) VAMP2 cleavage between differentiated and undifferentiated cells following BoNT/DC treatment (N=3, ±SEM). Multiple comparisons were examined by a two-way ANOVA analysis followed by Sidak's test. Alpha P values of <0.05 were considered statistically significant. *=P<0.05; **=P<0.01; ***=P<0.001.*

Overall, the activity of most BoNT serotypes and TeNT was detectable in undifferentiated LAN-5 neuroblastomas. The amount of cleaved target proteins was very close between undifferentiated and differentiated cells at higher concentrations of toxins. The difference in toxin activity between undifferentiated and differentiated cells increased slightly at lower concentrations of toxins.

4.2.5 Exogenous GT1b addition significantly increases the sensitivity of LAN-5 neuroblastoma cells to BoNT/A

GT1b is a common ganglioside used by all CNTs with varying affinities to enter cells (Connan and Popoff, 2017, Schenke et al., 2020). It was previously shown that GT1b was expressed in both SiMa and LAN-5 neuroblastoma cells. Moreover, a number of studies have demonstrated that the exogenous addition of GT1b during cell differentiation enhances the sensitivity of N2a, SK-N-SH, SiMa and NG108-15 cells to BoNT/A (Yowler et al., 2002, Whitemarsh et al., 2012a, Fernandez-Salas et al., 2012). Cells were pre-treated with 25 µg/ml and 50 µg/ml GT1b prior to toxin treatment in these studies. As part of this study, GT1b was incubated with toxins to determine whether toxin uptake in cells could be enhanced and increase the sensitivity. Additionally, each CNT binds to GT1b with a different affinity. It was therefore examined how the exogenous addition of 50 µg/ml GT1b affected the uptake of each toxin and subsequently the sensitivity of cells. As ganglioside expression is expected to be changed with differentiation, the effect of exogenous GT1b addition on the sensitivity of CNTs was investigated for both undifferentiated and differentiated LAN-5 cells.

GT1b is the strongest affinity ganglioside receptor for BoNT/A (Rummel, 2017). According to immunoblot results, exogenous addition of GT1b had an enhanced impact on toxin uptake and subsequently the sensitivity of both undifferentiated and differentiated cells (Figure 4.11 A-B). In undifferentiated cells without GT1b addition, the amount of cleaved SNAP25 was about 50% at the concentration of 1 nM and 0.1 nM; however, after GT1b addition, it increased significantly, reaching almost 100% (Figure 4.11 A-C). Similarly, in differentiated cells, the amount of cleaved SNAP25 increased slightly at 1 nM concentration, and significantly at 0.1 nM concentration, reaching 100% cleavage after GT1b addition (Figure 4.11 B-D).

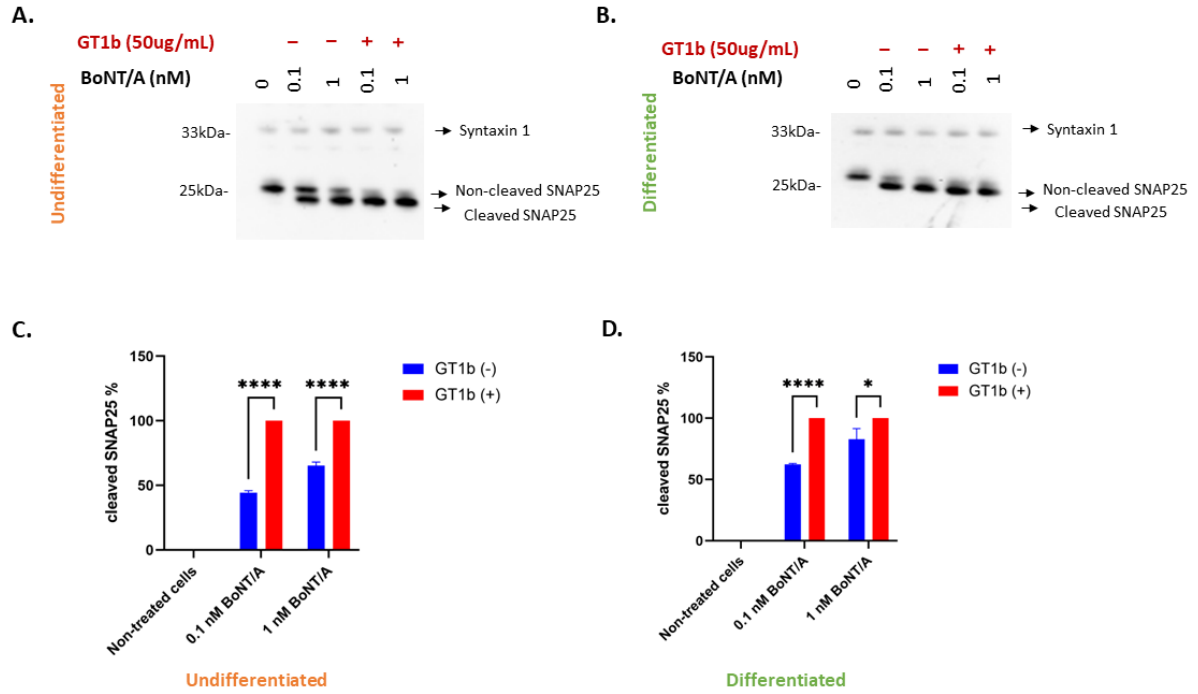

Figure 4.11 Exogenous GT1b addition enhanced the sensitivity in both undifferentiated and differentiated LAN-5 neuroblastomas for BoNT/A.

A-B) *Representative immunoblots showing the proportion of cellular cleaved SNAP25 in undifferentiated (A) and differentiated (B) GFP-VAMP2 LAN-5 neuroblastoma cells following application of BoNT/A either with GT1b or without GT1b. The concentrations of 1nM and 0.1nM BoNT/A were applied to undifferentiated and differentiated cells either with (+; 50 µg/mL) or without (-) GT1b gangliosides for 3 days. SNAP25 antibody was added at 1:3000 dilution to detect both cleaved and uncleaved SNAP25. Syntaxin antibody was used at 1:2000 dilution as a control. Images were taken from ChemiDoc XRS.* ***C)*** *Graph showing the quantification of immunosignals following BoNT/A treatment of undifferentiated cells with and without added GT1b (N=3, ±SEM).* ***D)*** *Graph showing the quantification of immunosignals following BoNT/A treatment of differentiated cells with and without added GT1b (N=3, ±SEM). Multiple comparisons were examined by a two-way ANOVA analysis followed by Sidak's test. Alpha P values of <0.05 were considered statistically significant. *=P<0.05; **=P<0.01; ***=P<0.001.*

4.2.6 Exogenous GT1b addition does not affect the sensitivity for BoNT/D, BoNT/DC or TeNT

GT1b and GD1b are other key gangliosides for BoNT/D after GD2 (Rummel, 2017). However, exogenous addition of GT1b did not affect the sensitivity of cells for BoNT/D. No cleavage was observed in undifferentiated cells (Figure 4.12 A). Immunoblot images showed that a very faint amount of cleaved v-VAMP2 was observed in differentiated cells but did not increase after GT1b

addition (Figure 4.12 B). The graph also showed that the amount of cleaved v-VAMP2 remained the same after GT1b addition (Figure 4.12 C). Additionally, cleaved c-VAMP2 was not detected in any conditions.

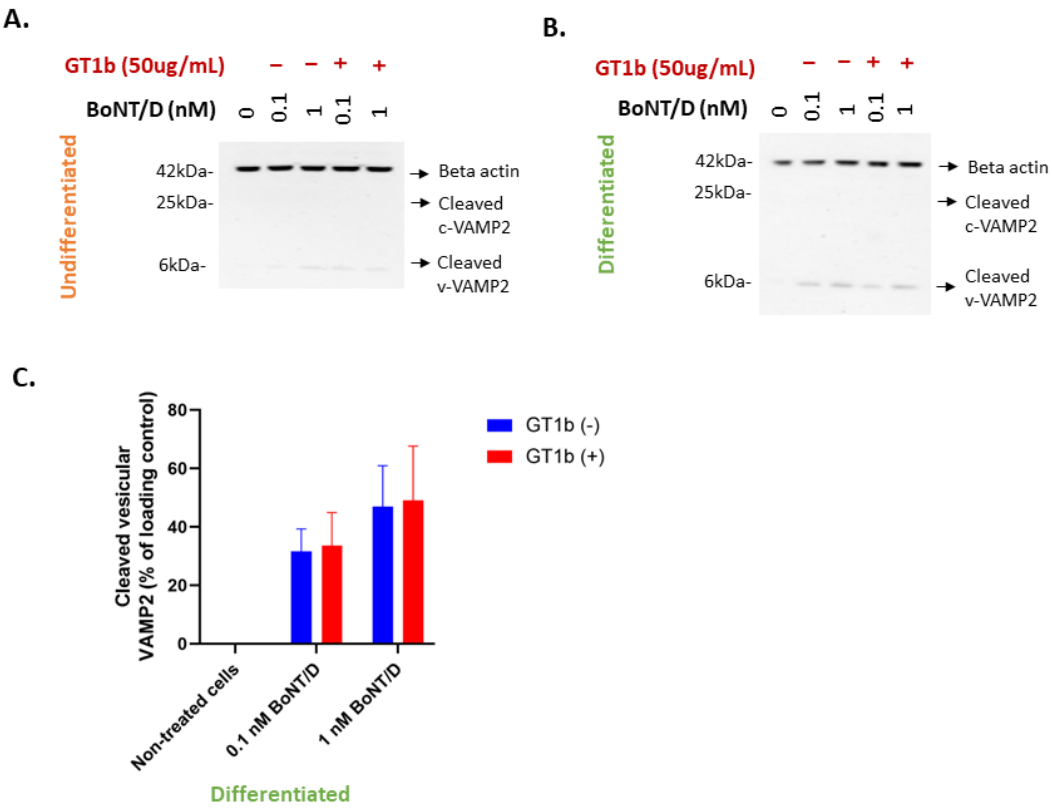

Figure 4.12 Exogenous GT1b addition did not have sufficient effect on the sensitivity for BoNT/D.

A-B) *Representative immunoblots showing the proportion of cleaved cytosolic VAMP2 in undifferentiated (A) and differentiated (B) GFP-VAMP2 LAN-5 neuroblastoma cells following application of BoNT/D either with or without GT1b. The concentrations of 1nM and 0.1nM BoNT/D were applied to undifferentiated and differentiated cells either with (+; 50 µg/mL) or without (-) GT1b gangliosides for 3 days. Mouse monoclonal Ab (Robert Koch D27) was added at 1:2000 dilution to see BoNT/D cleaved vesicular VAMP2; rabbit polyclonal D cleaved VAMP cytosolic Ab was used at 1:2000 dilution to see BoNT/D cleaved cytosolic VAMP2. Mouse monoclonal beta-actin Ab was added at 1:1200 dilution as a loading control. Images were taken from ChemiDoc XRS.* ***C)*** *Graph showing the quantification of immunosignals following BoNT/D treatment of differentiated cells with and without added GT1b (N=3, ±SEM). Multiple comparisons were examined by a two-way ANOVA analysis followed by Sidak's test. Alpha P values of <0.05 were considered statistically significant.*

In terms of BoNT/DC, the most significant ganglioside receptors are GM1a and GD1a, while GD1b and GT1b are less selective. That was also confirmed by our results for GT1b. Exogenous addition of GT1b had no impact on the sensitivity of cells to BoNT/DC activity. It was seen from immunoblots that the cleaved c-VAMP2 and v-VAMP2 bands observed were almost same after GT1b addition (Figure 4.13 A-B). According to graphs, the cleaved amounts of c-VAMP2 and v-VAMP2 were almost equal at given concentrations after GT1b addition (Figure 4.13 C-F).

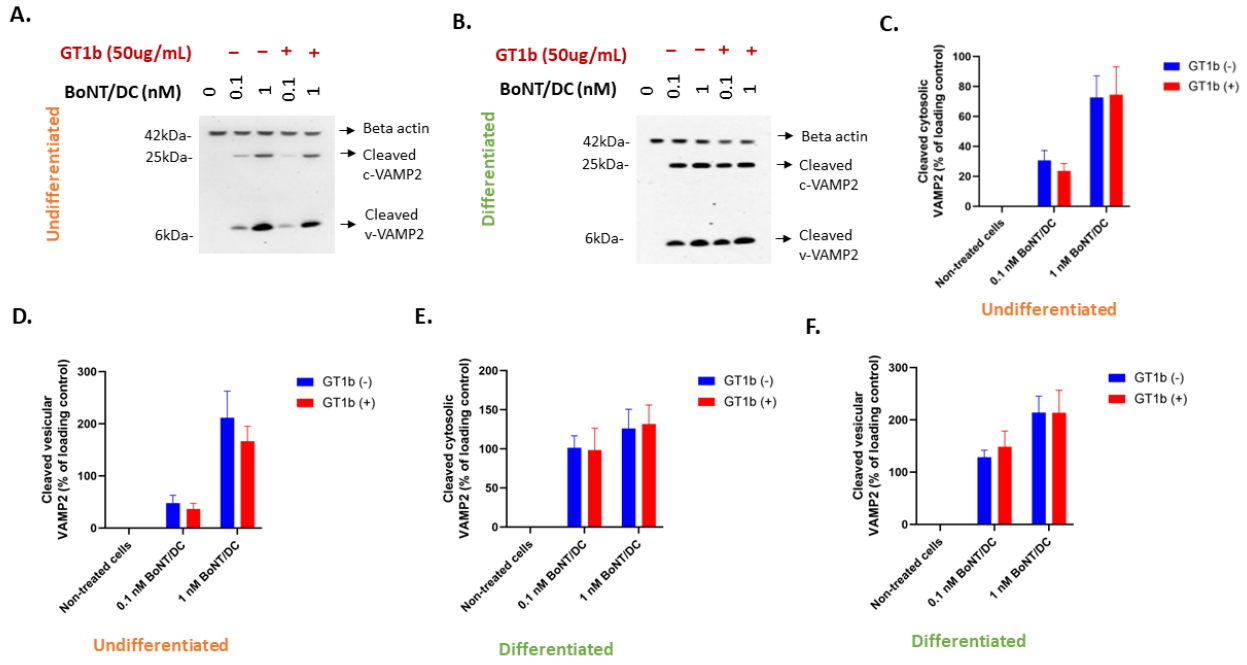

Figure 4.13 Exogenous GT1b addition did not affect the sensitivity for BoNT/DC.

A-B) *Representative immunoblots showing the proportion of cleaved cytosolic and vesicular VAMP2 in undifferentiated (A) and differentiated (B) GFP-VAMP2 LAN-5 neuroblastoma cells following application of BoNT/DC either with GT1b or without GT1b. The concentrations of 1nM and 0.1nM BoNT/DC were applied to undifferentiated and differentiated cells either with (+; 50 µg/mL) or without (-) GT1b gangliosides for 3 days. Mouse monoclonal Ab (Robert Koch D27) was added at 1:2000 dilution to see BoNT/D cleaved vesicular VAMP2; rabbit polyclonal D cleaved VAMP cytosolic Ab was used at 1:2000 dilution to see BoNT/D cleaved cytosolic VAMP2. Mouse monoclonal beta-actin Ab was added at 1:1200 dilution as a loading control. Images were taken from ChemiDoc XRS.* ***C-D)*** Graphs *showing the quantification of immunosignals following BoNT/DC treatment of undifferentiated cells with and without added GT1b (N=3, ±SEM).* ***E-F)*** Graphs *showing the quantification of immunosignals following BoNT/DC treatment of differentiated cells with and without added GT1b (N=3, ±SEM). Multiple comparisons were examined by a two-way ANOVA analysis followed by Sidak's test. Alpha P values of <0.05 were considered statistically significant.*

GT1b is one of the ganglioside receptors of TeNT. The sialic acid site of TeNT interacts preferentially with GT1b, whereas the conserved ganglioside binding site of TeNT preferentially binds to GM1a (Rummel, 2017). According to our results, exogenous addition of GT1b did not change the sensitivity of cells for TeNT activity. Immunoblot images showed that cleaved VAMP2 bands remained the same after GT1b addition (Figure 4.14 A-B). As can be seen from the graphs, the amount of cleaved VAMP2 was not significantly affected by GT1b addition at given concentrations (Figure 4.14 C-D).

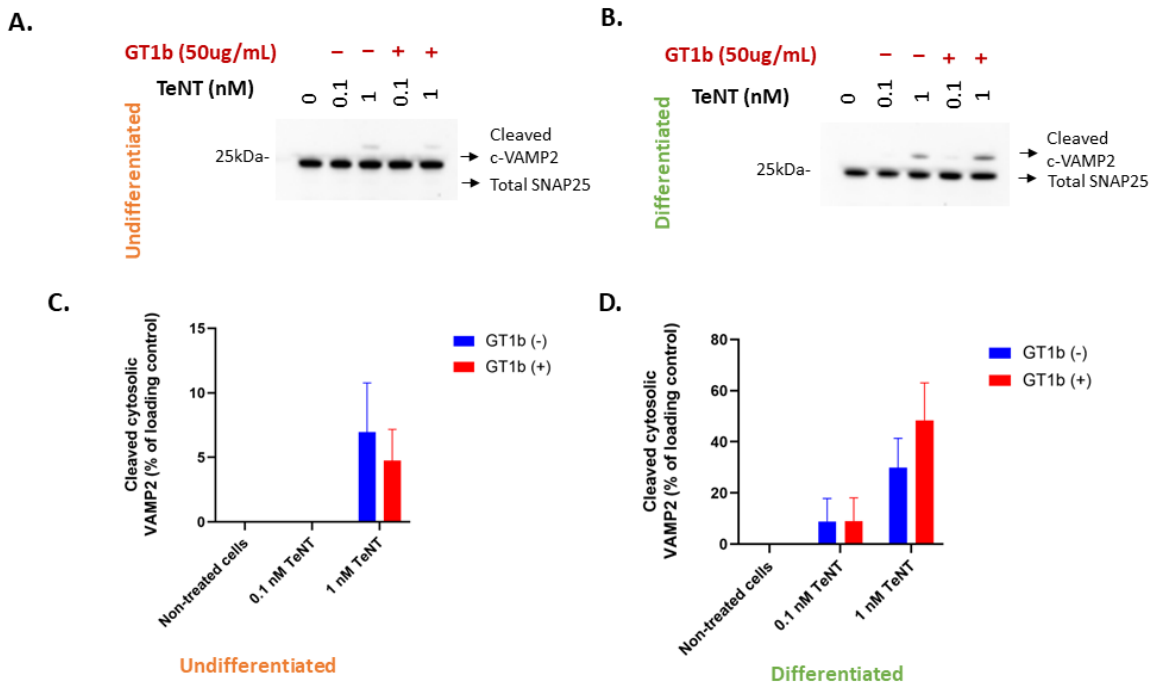

Figure 4.14 Exogenous GT1b addition did not affect the sensitivity for TeNT.

A-B) *Representative immunoblots showing the proportion of cleaved cytosolic VAMP2 in undifferentiated (A) and differentiated (B) GFP-VAMP2 LAN-5 neuroblastoma cells following application of TeNT either with or without GT1b. The concentrations of 1 nM and 0.1 nM TeNT were applied to undifferentiated and differentiated cells either with (+; 50 µg/mL) or without (-) GT1b gangliosides for 3 days. Rabbit monoclonal Ab (Genscript 2F7-1) was added at 1:2000 dilution to detect cleaved cytosolic VAMP2. Intact SNAP25 antibody was added at 1:3000 dilution as a control antibody to detect non-cleaved SNAP25. Images were taken from ChemiDoc XRS.* ***C)*** *Graph showing the quantification of immunosignals with or without GT1b added to undifferentiated cells following TeNT treatment (N=3, ±SEM).* ***D)*** *Graph showing the quantification of immunosignals with or without GT1b added to differentiated cells following TeNT treatment (N=3, ±SEM). Multiple comparisons were examined by a two-way ANOVA analysis followed by Sidak's test. Alpha P values of <0.05 were considered statistically significant.*

4.2.7 Exogenous GT1b addition has variable effects for BoNT/B and BoNT/C

BoNT/B shows a strong binding preference for GT1b (Rummel, 2017). Exogenous addition of GT1b increased BoNT/B activity significantly in undifferentiated cells. After GT1b addition, the cleaved VAMP2 band was observed more strongly at 1 nM concentration in undifferentiated cells. Moreover, no cleavage was observed at 0.1 nM concentration, while a faint VAMP2 band was detected with GT1b addition (Figure 4.15 A). The graph also shows that the amount of cleaved VAMP2 was enhanced significantly after GT1b addition at the concentrations of 1 nM and 0.1 nM in undifferentiated cells (Figure 4.15 C). However, the amount of cleaved VAMP2 increased very slightly in differentiated cells at the given concentrations after GT1b was added (Figure 4.15 B-D).

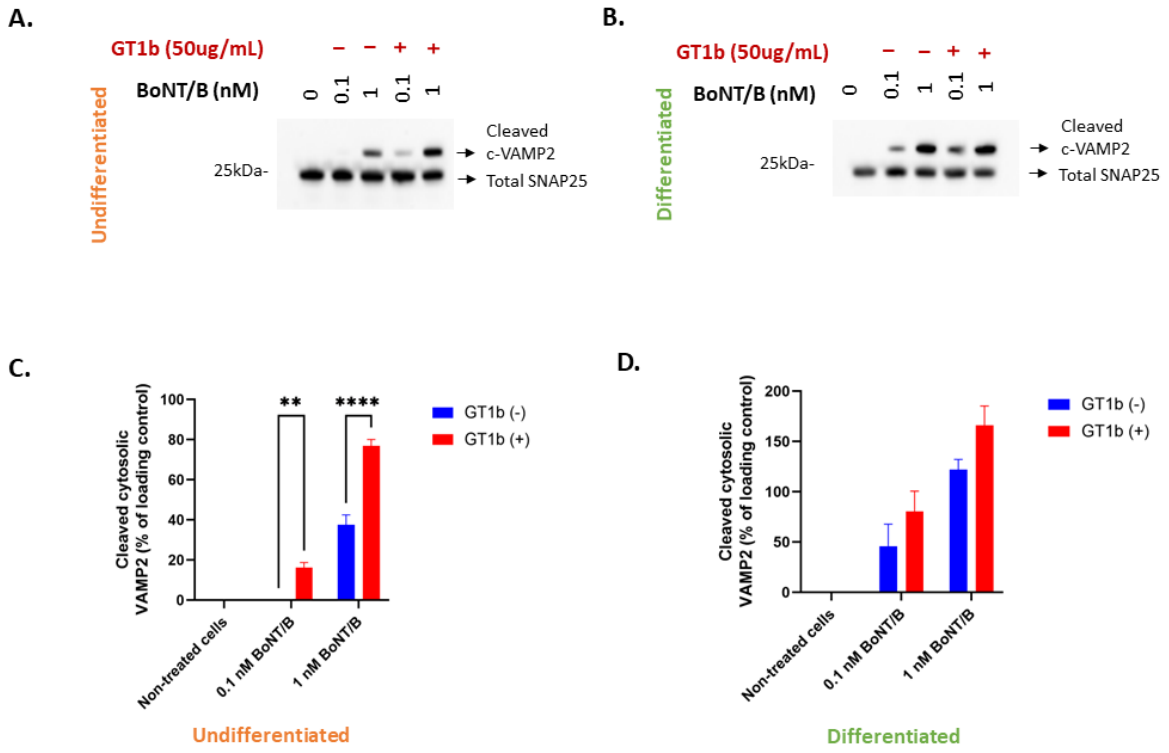

Figure 4.15 Exogenous GT1b addition significantly enhanced the sensitivity of undifferentiated cells to BoNT/B.

A-B) *Representative immunoblots showing the proportion of cleaved cytosolic VAMP2 in undifferentiated (A) and differentiated (B) GFP-VAMP2 LAN-5 neuroblastoma cells following application of BoNT/B either with or without GT1b. The concentrations of 1 nM and 0.1 nM BoNT/B were applied to undifferentiated and differentiated cells either with (+; 50 µg/mL) or without (-) GT1b gangliosides for 3 days. Rabbit monoclonal Ab (Genscript 2F7-1) was added at 1:2000 dilution to detect cleaved cytosolic VAMP2. Intact SNAP25 antibody was added at 1:3000 dilution as a control antibody to detect non-cleaved SNAP25. Images were taken from ChemiDoc XRS.* ***C)*** *Graph showing the quantification of immunosignals following BoNT/B treatment of undifferentiated cells with and without added GT1b (N=3, ±SEM).* ***D)*** *Graph showing the quantification of immunosignals following BoNT/B treatment of differentiated cells with and without added GT1b (N=3, ±SEM). Multiple comparisons were examined by a two-way ANOVA analysis followed by Sidak's test. Alpha P values of <0.05 were considered statistically significant. **=P<0.01; ****=P < 0.0001.*

BoNT/C preferentially binds GD1b and has a weaker affinity for GT1b (Rummel, 2017). Exogenous addition of GT1b increased the sensitivity of differentiated cells significantly but did not affect the sensitivity of undifferentiated cells to BoNT/C activity. The immunoblot image demonstrated cleaved SNAP25 bands remained unchanged in undifferentiated cells after GT1b addition (Figure 4.16 A). The graph also confirmed that the level of cleaved SNAP25 was almost the same either with or without GT1b at 1nM (Figure 4.16 C). However, uncleaved SNAP25 bands started to disappear more in differentiated cells after GT1b addition (Figure 4.16 B). The level of cleaved SNAP25 was enhanced in

differentiated cells at 0.1 nM and 1 nM concentrations by GT1b addition. Specifically, it significantly increased the amount of cleaved SNAP25 from 50% to almost 100% at 1 nM concentration (Figure 4.16 D).

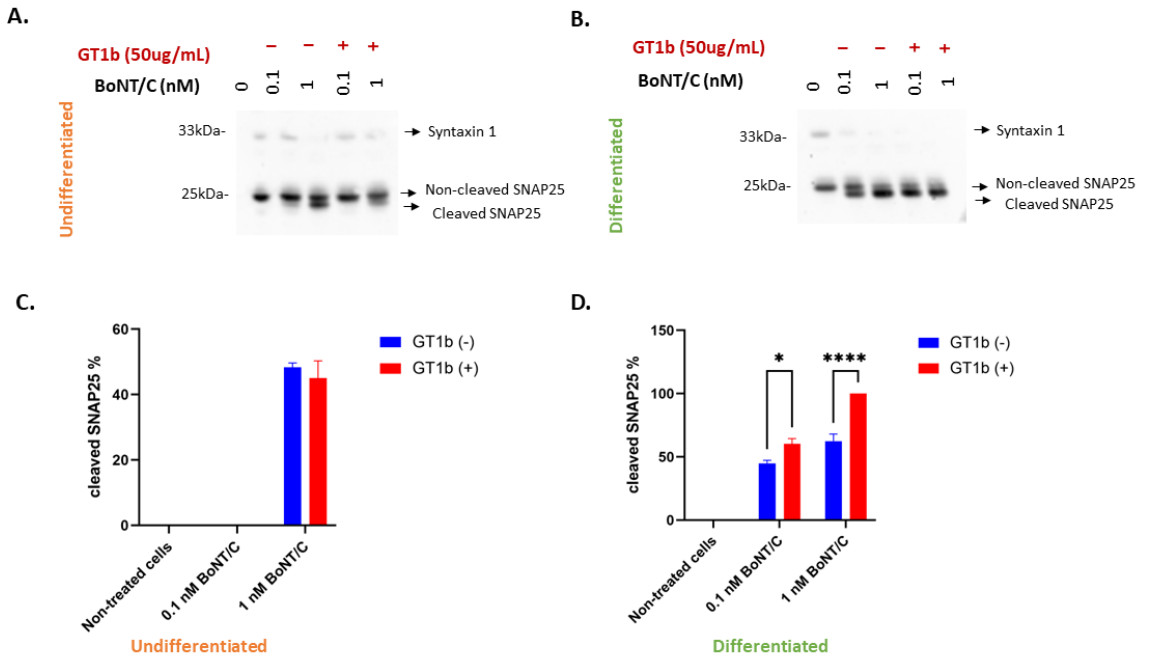

Figure 4.16 Exogenous GT1b addition enhanced the sensitivity of differentiated LAN-5 cells to BoNT/C.

A-B) *Representative immunoblots showing the proportion of cellular cleaved SNAP25 in undifferentiated (A) and differentiated (B) GFP-VAMP2 LAN-5 neuroblastoma cells following application of BoNT/C either with or without GT1b. The concentrations of 1 nM and 0.1 nM BoNT/C were applied to undifferentiated and differentiated cells either with (+; 50 µg/mL) or without (-) GT1b gangliosides for 3 days. SNAP25 antibody was added at 1:3000 dilution to detect both cleaved and uncleaved SNAP25. Syntaxin antibody was used at 1:2000 dilution as a control. Images were taken from ChemiDoc XRS.* ***C)*** *Graph showing the quantification of immunosignals following BoNT/C treatment of undifferentiated cells with and without added GT1b (N=3, ±SEM).* ***D)*** *Graph showing the quantification of immunosignals following BoNT/C treatment of differentiated cells with and without added GT1b (N=3, ±SEM). Multiple comparisons were examined by a two-way ANOVA analysis followed by Sidak's test. Alpha P values of <0.05 were considered statistically significant. *=P<0.05; ****=P < 0.0001.*

4.2.8 SYTII transduction to NanoLuc VAMP2 LAN-5 cell line significantly enhanced the BoNT/B sensitivity

SYTII is one of the receptor proteins of BoNT/B (Rummel, 2017). Even though human neuroblastoma SiMa and LAN-5 cells expressed SYTII, administration of more SYTII could enhance the sensitivity of cells to BoNT/B because the single mutation in the human SYTII decreases the affinity to BoNT/B (Strotmeier et al., 2012). Therefore, murine SYTII was exogenously introduced into NanoLuc VAMP2 LAN-5 cells, and SYTII-NanoLuc VAMP2 LAN-5 cells were generated (Figure 4.17 A). It was then evaluated whether the toxin activity of BoNT/B increases after SYTII transduction in cells. It can be clearly seen from immunoblot images that no cleavage was observed at 1 nM and 0.1 nM in NanoLuc VAMP2 LAN-5 cells (Figure 4.17 B), while cleaved VAMP2 bands were detected at these concentrations after SYTII transduction to cells (Figure 4.17 C). According to the quantification of the immunoblot, the level of cleaved VAMP2 was very close for both cell lines at the concentration of 10 nM and 5 nM (Figure 4.17 D). However, the amount of cleaved VAMP2 increased significantly in SYTII-NanoLuc VAMP2 LAN-5 cells at the concentrations of 1 nM and 0.1 nM. Moreover, the EC50 value decreased from 1.4 nM (0.9628 R^2, 0.8266 to 2.708 95%CI) to 0.08 nM (0.8931 R^2, 0.02837 to 0.2750 95%CI) after SYTII transduction, showing the sensitivity of the cells was significantly enhanced. The sensitivity of cell lines was also compared by the one-step ELISA method. The ELISA results were consistent with the immunoblot results. The signal of cleaved VAMP2 was saturated for both cell lines at the concentrations of 10 nM and 5 nM (Figure 4.17 E). Similar to immunoblot results, the cleaved VAMP2 signal was strongly enhanced at concentrations of 1 nM and 0.1 nM after cells were transduced with SYTII.

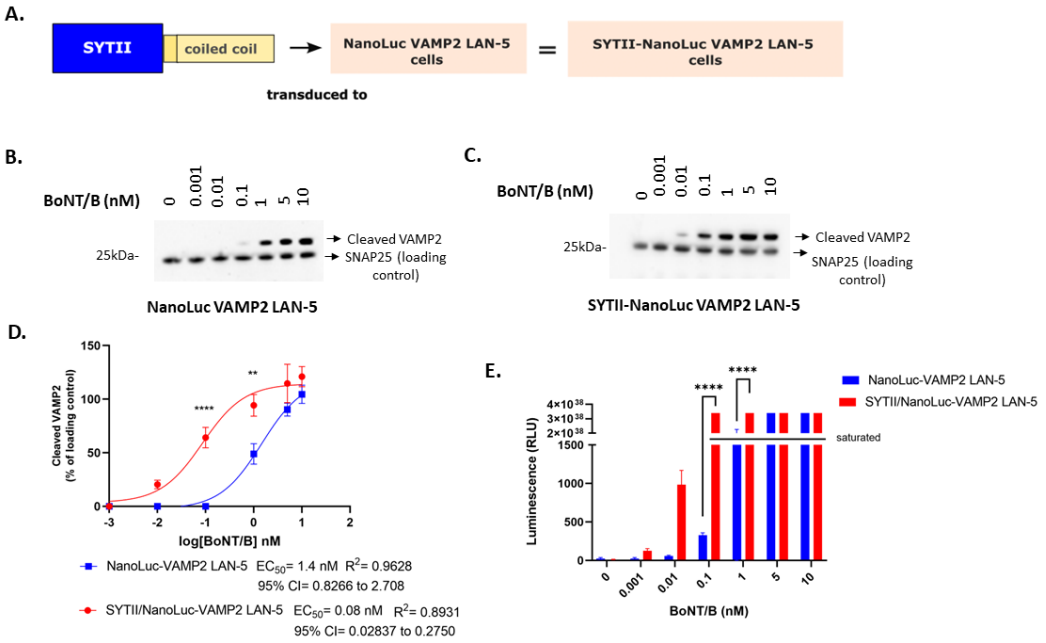

Figure 4.17 SYTII transduction to NanoLuc VAMP2 LAN-5 cells increased the BoNT/B sensitivity.

A) *Schematic showing the SYTII construct transduced to NanoLuc VAMP2 LAN-5 cell line.* ***B)*** *Representative immunoblots showing the proportion of cleaved cytosolic VAMP2 in differentiated NanoLuc VAMP2 LAN-5 cells following application of BoNT/B.* ***C)*** *Representative immunoblots showing the proportion of cleaved cytosolic VAMP2 in differentiated SYTII-NanoLuc VAMP2 LAN-5 cells following application of BoNT/B. The cells were treated with 1:10 titrated BoNT/B for 3 days. Rabbit monoclonal Ab (Genscript 2F7-1) was added at 1:2000 dilution to detect cleaved cytosolic VAMP2. Intact SNAP25 antibody was added at 1:3000 dilution as a control antibody to detect non-cleaved SNAP25. Images were taken from ChemiDoc XRS.* ***D)*** *Graph showing the quantification of immunosignals for the two cell lines (N=3, ±SEM).* ***E)*** *Bar chart comparing the luminescence levels between two cell lines received from one step ELISA results (N=3, ± SEM). Multiple comparisons were examined by a two-way ANOVA analysis followed by Sidak's test. Alpha P values of <0.05 were considered statistically significant. **=P<0.01; ****=P < 0.0001. Schematic was created by using Inkscape.*

4.2.9 SYTII transduction to NanoLuc VAMP2 LAN-5 cell line slightly affected the BoNT/DC sensitivity

SYTII is also a receptor protein of BoNT/DC (Rummel, 2017). Therefore, the effect of SYTII transduction on BoNT/DC activity was also examined. According to immunoblot results, cleaved c-VAMP2 and v-VAMP2 bands did not clearly changed between NanoLuc VAMP2 LAN-5 cells (Figure 4.18 A) and SYTII-NanoLuc VAMP2 LAN-5 cells (Figure 4.18 B). SYTII transduction did not significantly affect the sensitivity to BoNT/DC. The graph showed that the amount of cleaved c-VAMP2 was slightly higher in NanoLuc VAMP2 LAN-5 cells at concentrations of 10 nM, 5 nM, and 1 nM (Figure 4.18 C). Although no significant difference was observed between the cell lines in terms of cleaved amount of c-VAMP2,

the EC50 value decreased from 0.25 nM (0.5357 R^2, 0.011 to 11.39 95%CI) to 0.054 nM (0.8396 R^2, 0.015 to 0.177 95%CI) after SYTII transduction to the cells. In relation to v-VAMP2, there was an almost identical trend in VAMP2 cleavage between cell lines (Figure 4.18 D). Additionally, the EC50 values also remained almost the same for NanoLuc VAMP2 LAN-5 with 0.07 nM (0.6765 R^2, 0.01 to 0.758 95%CI) and SYTII-NanoLuc VAMP2 LAN-5 with 0.065 nM (0.7806 R^2, 0.016 to 0.26 95%CI).

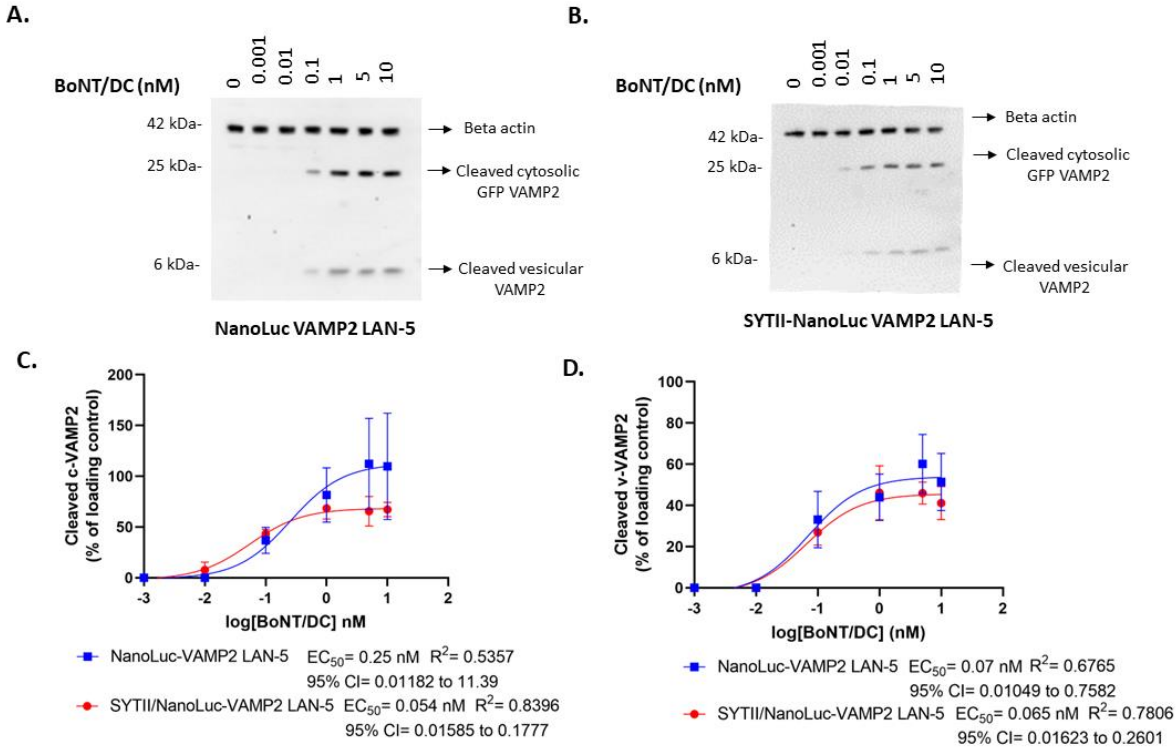

Figure 4.18 SYTII transduction to NanoLuc VAMP2 LAN-5 cells slightly changed the BoNT/DC sensitivity.

A) *Representative immunoblots showing the proportion of cleaved cytosolic and vesicular VAMP2 in NanoLuc VAMP2 LAN-5 cells following application of BoNT/DC.* ***B)*** *Representative immunoblots showing the proportion of cleaved cytosolic and vesicular VAMP2 in SYTII-NanoLuc VAMP2 LAN-5 cells following application of BoNT/DC. The cells were treated with 1:10 titrated BoNT/B for 3 days. Mouse monoclonal Ab (Robert Koch D27) was added at 1:2000 dilution to see BoNT/D cleaved vesicular VAMP2; rabbit polyclonal D cleaved VAMP cytosolic Ab was used at 1:2000 dilution to see BoNT/D cleaved cytosolic VAMP2. Mouse monoclonal beta-actin Ab was added at 1:1200 dilution as a loading control. Images were taken from ChemiDoc XRS.* ***C)*** *Graph showing the quantification of immunosignals for cleaved cytosolic VAMP2 from two cell lines (N=3, ±SEM).* ***D)*** *Graph showing the quantification of immunosignals for cleaved vesicular VAMP2 from two cell lines (N=3, ±SEM). Multiple comparisons were examined by a two-way ANOVA analysis followed by Sidak's test. Alpha P values of <0.05 were considered statistically significant.*

4.2.10 SYTII transduction to NanoLuc VAMP2 LAN-5 cell line had no effect on the TeNT sensitivity

TeNT has two ganglioside binding sites to enter neuronal cells (Rummel et al., 2003) However, the receptor protein for TeNT has not yet been identified (Brunger et al., 2008). The discovery of specific receptor proteins is crucial to the development of a sensitive cell-based assay. Upon discovering a specific receptor for TeNT, the receptor could be transduced into cells to enhance their sensitivity and toxin sensitivity. Therefore, the effect of SYTII on TeNT activity was investigated in order to determine whether it is a receptor protein for TeNT. According to immunoblot images, cleaved VAMP2 bands remained at similar levels following SYTII transduction, as cleaved VAMP2 bands were observed only at 1 nM, 5 nM, and 10 nM concentrations in both cell lines (Figure 4.19 A-B). The graph also confirmed that the amount of cleaved VAMP2 was almost the same between NanoLuc VAMP2 LAN-5 and SYTII-NanoLuc VAMP2 cell lines (Figure 4.19 C). Moreover, the EC50 values were very close with 3.19 nM for NanoLuc VAMP2 LAN-5 cells (0.8401 R^2, 0.7220 to 75.10 95%CI) and with 3.42 nM for SYTII-NanoLuc VAMP2 LAN-5 cells (0.8704 R^2, 0.9235 to 33.85 95%CI). ELISA results were consistent with immunoblot results and confirmed that the sensitivity did not change after SYTII transduction. According to the graph, the luminescence levels were saturated for both cell lines at concentrations of 10 nM and 5 nM, and they were at the same levels at concentrations of 1 nM and 0.1 nM (Figure 4.19 D). The results suggested SYTII is not a specific receptor for TeNT entry.

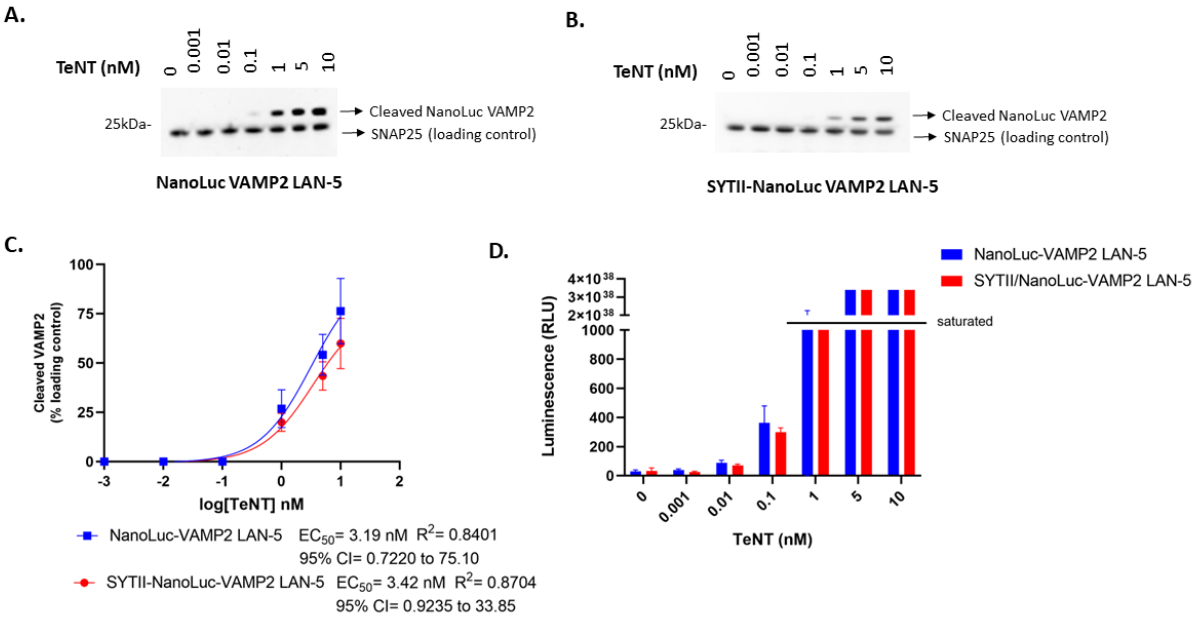

Figure 4.19 SYTII transduction to NanoLuc VAMP2 LAN-5 cells did not affect the TeNT sensitivity.

A) *Representative immunoblots showing the proportion of cleaved cytosolic VAMP2 in differentiated NanoLuc VAMP2 LAN-5 cells following application of TeNT.* ***B)*** *Representative immunoblots showing the proportion of cleaved cytosolic VAMP2 in differentiated SYTII-NanoLuc VAMP2 LAN-5 cells following application of TeNT. The cells were treated with 1:10 titrated BoNT/B for 3 days. Rabbit monoclonal Ab (Genscript 2F7-1) was added at 1:2000 dilution to detect cleaved cytosolic VAMP2. Intact SNAP25 antibody was added at 1:3000 dilution as a control antibody to detect non-cleaved SNAP25. Images were taken from ChemiDoc XRS.* ***C)*** *Graph showing the quantification of immunosignals from two cell lines (N=3, ±SEM).* ***E)*** *Bar chart comparing the luminescence levels between two cell lines received from one step ELISA results (N=3, ± SEM). Multiple comparisons were examined by a two-way ANOVA analysis followed by Sidak's test. Alpha P values of <0.05 were considered statistically significant.*

4.2.11 SYTII receptor protein is essential for BoNT/B detection shown in HeLa cells

It was shown in Section 4.2.7 that the exogenous introduction of SYTII and GT1b significantly increased the sensitivity of LAN-5 cells to BoNT/B. Here, I tested a non-neuronal cell line, HeLa cells, to acknowledge the importance of SYTII and GT1b gangliosides for BoNT/B sensitivity. Brightfield image of HeLa cells showed that they do not have any neuronal properties (Figure 4.20 A). They also do not express GT1b and SYTII essential for BoNT entry (Figure 4.20 B-C). Therefore, HeLa cells were modified to become sensitive for BoNT/B. Native HeLa cells were transduced with NanoLuc-VAMP2, to produce NanoLuc VAMP2 HeLa cells. As the NanoLuc VAMP2 plasmid has GFP, immunofluorescence microscopy was used to determine that the cells were expressing NanoLuc VAMP2 as expected (Figure

4.20 D). NanoLuc VAMP2 HeLa cells were then transduced with SYTII, and SYTII-NanoLuc VAMP2 HeLa cell line was generated. SYTII antibody staining was then used to confirm that it was expressed in the resulting SYTII-NanoLuc VAMP2 HeLa cell line, as shown in red in Figure 4.20 E.

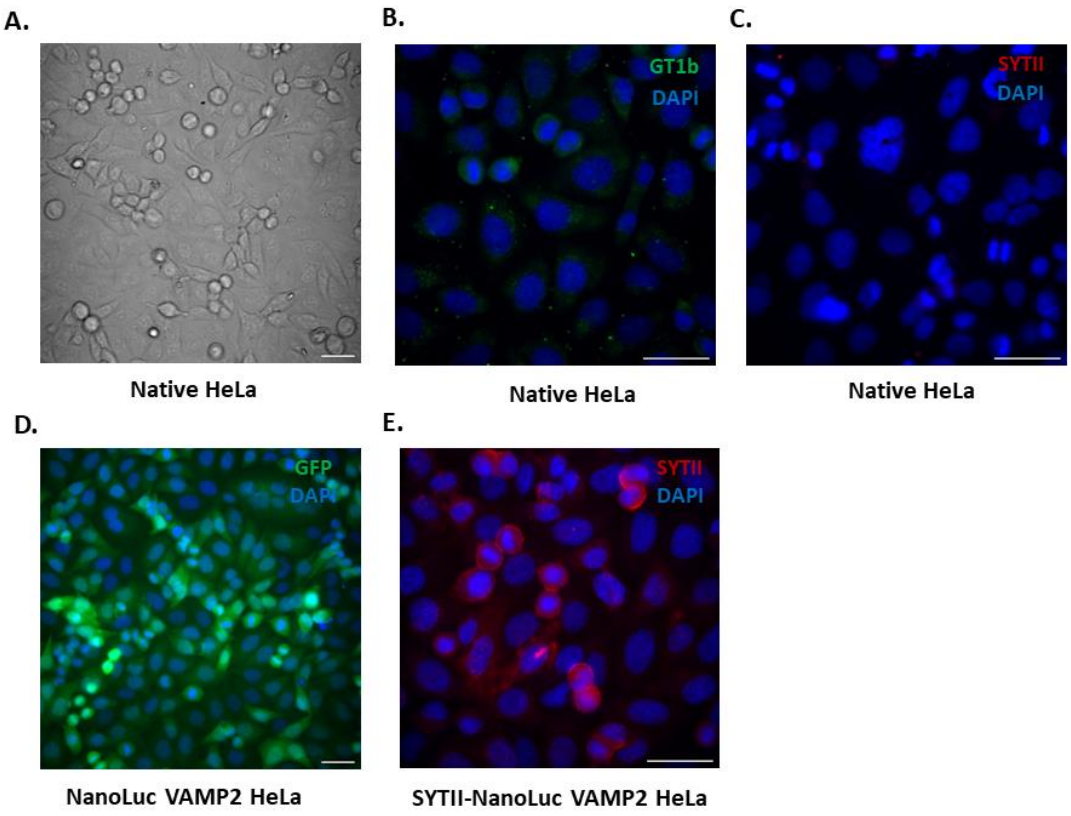

Figure 4.20 HeLa cells were characterized and re-engineered for BoNT/B detection.

A) *A brightfield image of native HeLa cells showing that they do not have neuronal morphology (20x objective).* ***B)*** *Immunofluorescence image for the staining of GT1b-2b gangliosides in native HeLa cells (40x objective). Mouse GT1b-2b Ab is used 5 µg/mL as a concentration without permeabilization of the cells.* ***C)*** *Immunofluorescence image for the staining of SYTII protein in native HeLa cells (40x objective). Rabbit SYTII Ab is used at 1:100 dilution.* ***D)*** *Immunofluorescence image of GFP expression in re-engineered NanoLuc VAMP2 HeLa cells (20x objective).* ***E)*** *Immunofluorescence image of SYTII expression (stained in red) in SYTII-NanoLuc VAMP2 HeLa cell lines (40x objective). Images were taken with epifluorescence microscope. All scale bars are 50 µm.*

After cells were re-engineered, the BoNT/B activity was tested in the cells either with or without exogenous addition of 50 µg/mL GT1b. Immunoblot images showed no cleavage in NanoLuc VAMP2 HeLa cells at any conditions, whereas a very faint cleaved VAMP2 band was observed in SYTII-NanoLuc VAMP2 HeLa cells after treatment of 1 nM BoNT/B (Figure 4.21 A). However, the cleaved VAMP2 band became stronger after exogenous addition of GT1b. The graph also showed that the amount of

cleaved VAMP2 increased significantly following GT1b addition in SYTII-NanoLuc VAMP2 LAN-5 cells at 1 nM BoNT/B (Figure 4.21 B). These results indicate that GT1b is required for a large amount of cleavage at a concentration of 1 nM BoNT/B even in the presence of SYTII. Based on these results, the sensitivity of NanoLuc VAMP2 HeLa cells was tested with increasing concentrations of GT1b addition. GT1b was added to the cells with 1 nM BoNT/B at ranging concentrations from 50 µg/mL to 200 µg/mL. Immunoblot result showed that no VAMP2 cleavage was observed (Figure 4.21 C), indicating that the SYTII receptor is essential for BoNT/B entry regardless of GT1b concentration.

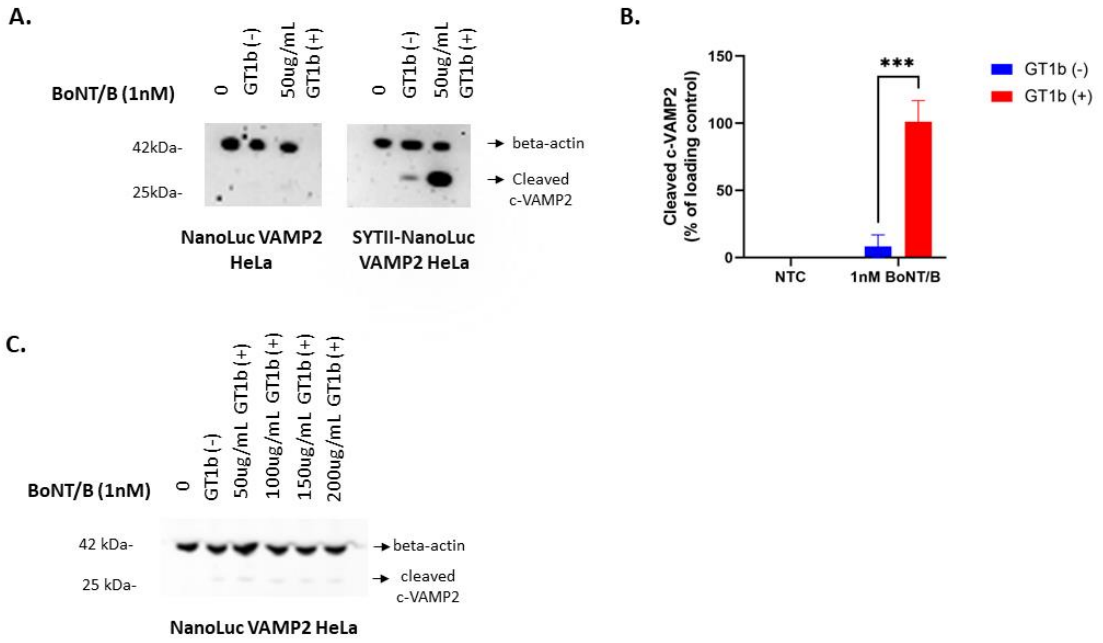

Figure 4.21 SYTII receptor protein is essential with GT1b for lower concentration of BoNT/B detection.

A) *Representative immunoblots showing the proportion of cleaved cytosolic VAMP2 in NanoLuc VAMP2 HeLa and SYTII-NanoLuc VAMP2 HeLa cells following application of 1 nM BoNT/B either with or without 50 µg/mL GT1b for 3 days. Rabbit monoclonal Ab (Genscript 2F7-1) was added at 1:2000 dilution to detect cleaved cytosolic VAMP2. Mouse monoclonal beta-actin Ab was added at 1:1200 dilution as a loading control. Images were taken from ChemiDoc XRS.* ***B)*** *Bar chart showing the quantification of immunosignals from SYTII-NanoLuc VAMP2 HeLa cells with and without GT1b (N=3, ±SEM). Multiple comparisons were examined by a two-way ANOVA analysis followed by Sidak's test. Alpha P values of <0.05 were considered statistically significant. ***=P<0.001.* ***C)*** *Representative immunoblots showing the proportion of cleaved cytosolic VAMP2 in NanoLuc VAMP2 HeLa following application of 1nM BoNT/B with increasing GT1b concentrations for 3 days.*

In the next step, the results of serial dilution of BoNT/B revealed that cleaved VAMP2 bands were observed in SYTII-NanoLuc VAMP2 HeLa cells at 5 nM and 10 nM concentrations without GT1b addition (Figure 4.22 A). The amount of cleaved VAMP2 was enhanced with increasing concentrations of BoNT/B from 1 nM to 10 nM (Figure 4.22 B), and the EC50 value was observed as 2.9 nM with 0.9563 R^2 and 1.126 to? 95%CI. The ELISA allowed more sensitive detection of BoNT/B compared to immunoblot. According to the ELISA results, the signal of cleaved VAMP2 significantly increased at concentrations of 10 nM, 5 nM and 1 nM compared to the control group (Figure 4.22 C). Moreover, the luminescence level of cleaved VAMP2 was saturated at concentrations of 5 nM and 10 nM, which was the same as the results from neuroblastoma cells. However, no cleavage of VAMP2 was observed in the NanoLuc VAMP2 HeLa cell line, even at higher concentrations of BoNT/B (Figure 4.22 D). These results suggested that GT1b is not required but SYTII is essential in order to detect BoNT/B activity at greater concentrations than 1 nM.

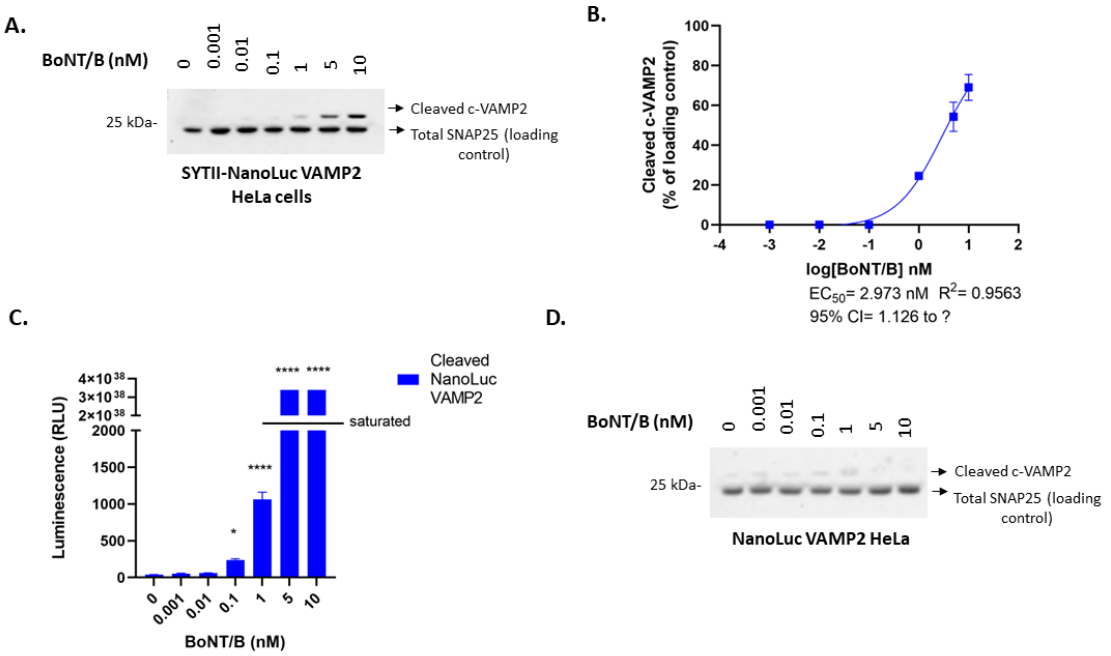

Figure 4.22 SYTII receptor protein is essential but not GT1b for higher concentrations of BoNT/B detection.

A) *A representative immunoblot image showing the proportion of cleaved VAMP2 in SYTII-NanoLuc VAMP2 HeLa cells following application of BoNT/B. The cells were treated with 1:10 titrated BoNT/B for 3 days. Rabbit monoclonal Ab (Genscript 2F7-1) was added at 1:2000 dilution to detect cleaved cytosolic VAMP2. Intact SNAP25 antibody was added at 1:3000 dilution as a control antibody to detect non-cleaved SNAP25. Images were taken from ChemiDoc XRS.* ***B)*** *Graph showing the quantification of cleaved VAMP2 immunosignals in SYTII-NanoLuc VAMP2 HeLa cells (N=3, ±SEM).* ***C)*** *Bar chart showing the luminescence levels for cleaved VAMP2 in SYTII-NanoLuc VAMP2 HeLa cells by one step ELISA (N=3, ±SEM). Multiple comparisons were examined by an ordinary one-way ANOVA followed by Tukey's test. Alpha P values of <0.05 were considered statistically significant. Significances were represented for the comparison of different concentrations with the untreated control. *= P<0.05; ****= P<0.0001.* ***D)*** *A representative immunoblot image for cleaved VAMP2 in NanoLuc VAMP2 HeLa cells following application of BoNT/B.*

4.3 Discussion

In this chapter, a range of conditions were examined for CNT sensitivity. LAN-5 and SiMa cells were examined for their expression of relevant proteins and gangliosides that are required for CNT activity. This provided further insight into cells in relation to CNT sensitivity. The sensitivity of undifferentiated LAN-5 cells to CNTs was assessed. The effect of additional administration of receptors, GT1b and SYTII, was investigated for the sensitivity. A non-neuronal cell line, HeLa, was re-engineered and tested for BoNT/B activity.

4.3.1 SiMa and LAN-5 neuroblastomas cell lines expressed relevant proteins and gangliosides necessary for clostridial neurotoxins activity

Understanding of the intoxication process at a cellular level has allowed development of many in vitro methods for testing of the toxins. Moreover, the identification of specific receptor proteins and gangliosides for most of the CNTs led to significant improvements in the sensitivity of the assays. Besides understanding the mechanism of the toxin, characterisation of cells for relevant proteins and gangliosides is the next step in order to establish a sensitive assay. Within this chapter, SiMa and LAN-5 cell lines were thus characterised in terms of receptor and target proteins, and gangliosides.

It has been shown that if CNTs are introduced into non-neuronal cells intracellularly, they still show their activity, preventing exocytosis (Humeau et al., 2000). The CNTs, however, acquire a neuronal cell to interact with and to be internalized. SiMa and LAN-5 cell lines extensively expressed beta-tubulin III, a neuronal cell marker (Jirasek et al., 2002). This confirms their neuronal origin and makes them appropriate candidates for CNT detection. Some other cell lines such as P19 cells were not stained by neuronal markers when they were undifferentiated, whereas differentiated cells were stained with them (Tsukamoto et al., 2012). However, it was shown that undifferentiated SiMa and LAN-5 cells were also successfully stained with neuronal marker, giving them an advantage over other cells.

Neuronal cells express gangliosides and receptor proteins required for entry of CNTs. GT1b is the most common ganglioside receptor for all CNTs, and GD1a is preferentially used by BoNT/A, BoNT/B, BoNT/C, and BoNT/DC serotypes to enter neuronal cells (Schenke et al., 2020, Connan and Popoff, 2017). The abundant expression of GD1a, and GT1b explains the sensitivity of cells to these toxins. Due to the expression of both GD1a and GT1b in SiMa and LAN-5 cells, they are more advantageous than other neuroblastomas such as SH-SY5Y, Neuro 2a and SK-N-SH neuroblastomas. The reason for this is that they express both GD1a and GT1b simultaneously, whereas SH-SY5Y, Neuro 2a and SK-N-SH neuroblastomas express only GD1a and not GT1b (Purkiss et al., 2001, Yowler et al., 2002).

Additionally, another ganglioside, GD2, suggested as a ganglioside for BoNT/D, is also extensively expressed on SiMa and LAN-5 cells. However, the use of gangliosides for BoNT/D to enter neuronal cells is controversial. On the one hand, it was suggested that BoNT/D enters cells in a ganglioside dependant manner and that GD2 is the preferred receptor for BoNT/D entry (Kroken et al., 2011b). On the other hand, it has been suggested that BoNT/D binds to phosphatidylethanolamine, in a hydrocarbon tail-dependent manner (Tsukamoto et al., 2005). According to our results, although GD2 was abundantly expressed in SiMa and LAN-5, the observed activity of BoNT/D was quite low in these cells. There might be several reasons for that. First, it might be due to the low expression of receptor

protein in the cells. Second, binding to phosphatidylethanolamine could be essential for BoNT/D entry and phosphatidylethanolamine expression might be lower or lacking in the cells. In order to determine the reason, the expression of phosphatidylethanolamine must be examined in future work.

In addition to gangliosides, receptor proteins are required for toxins to enter cells. SYTI and SYTII are specific receptor proteins for BoNT/B and BoNT/DC, whereas SV2 isoforms are used by BoNT/A and BoNT/D to enter the cells (Schenke et al., 2020). The expression of good amounts of SYTI and SYTII in the LAN-5 and SiMa cells explains their great sensitivity to BoNT/B and BoNT/DC. As SV2 was also successfully expressed on the cells, significant BoNT/A activity can be detected. However, although SV2 is also receptor protein for BoNT/D, the activity of BoNT/D was hardly detectable in these cells. This could be because the preferred isoform of SV2 for BoNT/D, SV2/B, may have lower expression than SV2C, the specific isoform targeted by BoNT/A. This cannot be determined from my results, since I used SV2-pan, which recognizes all SV2 isoforms but does not specifically differentiate between them. In order to understand this fully, specific antibodies for each isoforms should be used to individually characterise SV2A, SV2B and SV2C. Moreover, the binding process of BoNT/D to SV2 is different from BoNT/A (Peng et al., 2011). It was shown that BoNT/A directly binds to SV2-L4, which is a luminal domain of SV2 protein. However, BoNT/D binds to SV2 via recycling of synaptic vesicles which is mediated by SV2C expressed on the surface of plasma membrane. SV2C, located on the plasma membrane, is reconstituted into a binding site for BoNT/D. Therefore, the expression level and location of isoforms on the cells might create different sensitivities for BoNT/A and BoNT/D.

Additionally, SNAP25, as a target protein of BoNT/A and BoNT/C, was expressed in both cells, explaining how BoNT/A and BoNT/C are detectable without introduction of any protein. Moreover, the expression level of SNAP25 between undifferentiated and differentiated cells was almost same, making the cells more advantageous in terms of using them without the extra differentiation step.

Looking at the results for undifferentiated and differentiated cells, differentiated SiMa and LAN-5 cells generated similar level of gangliosides approximately, but undifferentiated LAN-5 was more advantageous than undifferentiated SiMa in terms of expression of overall gangliosides. This appears to be because gangliosides were mostly expressed on neuronal processes, which undifferentiated LAN-5 cells still have. However, both SiMa and LAN-5 are good candidates for cell-based assays as they expressed essential proteins and gangliosides for CNT activity.

4.3.2 The activity of clostridial neurotoxins is detectable in undifferentiated LAN-5 cells but the sensitivity increases upon differentiation

In this chapter, it was demonstrated that undifferentiated LAN-5 cells were sensitive to CNTs, yet the sensitivity was significantly enhanced by differentiation. One the one hand, if the toxins are less active in differentiated cells, such as with BoNT/D and TeNT, then there was either less detection or no detection at all in undifferentiated cells, even at higher concentrations. On the other hand, the undifferentiated cells showed a remarkable sensitivity with the toxins that had already shown high levels of activity in differentiated cells. This phenomenon could be seen in the results of BoNT/A, BoNT/B, BoNT/C, and BoNT/DC serotypes, which are already found to be very sensitive to differentiated LAN-5 cells. For these serotypes, the amount of cleaved target protein was observed to be almost the same between undifferentiated and differentiated cells at higher concentrations, whereas level of cleaved proteins was slightly less in undifferentiated cells than in differentiated cells at lower concentrations.

The detection of BoNT/A, BoNT/B, BoNT/C, and BoNT/DC in undifferentiated cells makes the LAN-5 cells very advantageous for cell-based assays compared to other cells. For example, undifferentiated NG108-15 cells were relatively not sensitive for BoNT detection (Whitemarsh et al., 2012a). They must be differentiated at least for 5 days to become sensitive to BoNT/A. Another neuroblastoma cell line, SH-SY5Y, was also tested in their undifferentiated state for BoNT detection (Purkiss et al., 2001). However, undifferentiated LAN-5 cells are significantly more sensitive than undifferentiated SH-SY5Y cells for BoNT/A and BoNT/B. A very small amount of cleaved SNAP25 was detected in undifferentiated SH-SY5Y cells at the concentration of 10 nM BoNT/A, whereas SNAP25 cleaved almost 100% at 10 nM in undifferentiated LAN-5 cells. BoNT/B was detected at the lowest concentration of 30 nM in undifferentiated SH-SY5Y cells, whereas it was detectable at the lowest concentration of 0.1 nM in undifferentiated LAN-5 cells.

Sensitive undifferentiated LAN-5 cells would be useful for several conditions. They could be used in situations where sensitive detection is not required. For example, BoNT/A, BoNT/B, BoNT/C, and BoNT/DC showed almost the same level of sensitivity in undifferentiated and differentiated cells at 10 nM concentration. That means the differentiation process could be eliminated when these toxins need to be detected at a higher concentration than 10 nM. This enables a range of benefits for cell-based assays. By eliminating differentiation processes such as coating the plates with laminin and preparing differentiation media by adding some reagents, a more cost-effective assay can be conducted. For undifferentiated cells, seeded cells were incubated for 2 days before testing. However, this period can be further reduced by optimizing cell number and media amount, which would provide a shorter

assay. I also came across differentiation difficulties with neuroblastoma cells during my project. Since they are vulnerable to any conditions, they sometimes fail to differentiate properly. Use of undifferentiated cells would prevent the possibility of improper differentiation, and make the assay simpler to use overall.

The sensitivity of undifferentiated LAN-5 cells and the sensitivity difference between undifferentiated and differentiated cells could be explained by several factors. As I have demonstrated, undifferentiated LAN-5 express substantial amounts of gangliosides and proteins for CNTs detection, which explains their high level of sensitivity. However, they are still slightly less sensitive to CNTs compared to differentiated cells, especially at lower concentrations. This might be a result of the lower expression of some target proteins, such as SV2, in undifferentiated cells compared to differentiated cells. While some of the gangliosides and proteins are expressed at similar levels regardless of differentiation, others are expressed at lower levels in undifferentiated cells. Also, even though the expression levels of proteins and gangliosides on the cells are similar, the expression area of these proteins and gangliosides on the cells might be different between undifferentiated and differentiated cells. Gangliosides and receptor proteins were expressed on the soma membrane as well as neuronal processes in both undifferentiated and differentiated cells. However, toxins may prefer to bind to neuronal processes to enter cells, and as differentiated LAN-5 cells have more neuronal processes, this might explain the higher sensitivity in them.

4.3.3 The effect of exogenous addition of GT1b on sensitivity is distinct for different types of clostridial neurotoxins

The effect of exogenous GT1b addition to LAN-5 cells was investigated in order to see if it increased sensitivity, even though the cells already expressed GT1b. The results showed that additional GT1b has variable effects on the sensitivity of each CNT. This can be explained because GT1b has varying binding affinity for each CNT, even though it is a common receptor ganglioside for all CNTs (Connan and Popoff, 2017, Schenke et al., 2020). BoNT/A activity was enhanced significantly in LAN-5 cells by exogenous addition of GT1b, consistent with research showing that BoNT/A binds most preferentially to GT1b rather than other gangliosides. For example, GT1b addition significantly increased BoNT/A activity compared to GD1a and GM1 addition when they were added to ganglioside depleted Neuro 2a and SK-N-SH neuroblastomas (Yowler et al., 2002). Previous studies also showed that GT1b addition significantly increase the sensitivity to BoNT/A in NG108-15 and SiMa cells (Whitemarsh et al., 2012a, Fernandez-Salas et al., 2012)

GT1b addition resulted in variable results for BoNT/B and BoNT/C, resulting in a partial increase in LAN-5 sensitivity to them. After GT1b addition, BoNT/B activity increased slightly in differentiated cells, whereas it increased significantly in undifferentiated cells. BoNT/B has stronger binding to GT1b than to other gangliosides (Schenke et al., 2020), which explains the improvement of undifferentiated sensitivity. However, GT1b alone might not be enough to increase BoNT/B sensitivity in differentiated cells. In addition to GT1b, additional SYTI and SYTII receptor proteins may be required to maximize BoNT/B sensitivity. In relation to BoNT/C, the sensitivity was unaffected by GT1b addition in undifferentiated cells. This may be a result of the fact that GT1b is the second preferential ganglioside for BoNT/C. The strongest ganglioside receptor for BoNT/C, GD1b, might be essential for entry. In contrast, additional GT1b enhanced the sensitivity to BoNT/C in differentiated LAN-5 cells, which has also been observed in PC12 cells (Nakamura et al., 2012). In other words, the addition of GT1b could increase the sensitivity to BoNT/C, but other factors might also be involved. One possible implication is that GD1b expression might be high enough for the entry in LAN-5 differentiated cells. BoNT/C uses two ganglioside binding site to enter the cells and a receptor protein has not been identified yet (Strotmeier et al., 2011). Thus, sufficient expression of two gangliosides, GD1b and GT1b together, could be crucial for entry of BoNT/C. There is also possibility that while GD1b is mostly used to internalise BoNT/C, additional GT1b might help to ease the entry of toxin.

In contrast to the other toxins tested, BoNT/D, BoNT/DC and TeNT activities did not change at all with the addition of GT1b. As previously explained, the way BoNT/D enters cells is controversial in terms of using gangliosides. Based on one side, it attaches to phosphatidylethanolamine rather than gangliosides to enter cells (Tsukamoto et al., 2005); however, another side indicates that it adheres to gangliosides, mainly GD2 and weakly to GT1b and GD1b (Kroken et al., 2011b). Moreover, BoNT/D has two ganglioside binding sites, including a sialic acid binding site and a conserved ganglioside binding site. The sialic acid binding site of BoNT/D is similar to the sialic acid binding site of TeNT (Strotmeier et al., 2010). However, the conserved ganglioside binding site has an equivalent position as in other toxins but with a completely different conformation, explaining the low affinity of BoNT/D for gangliosides (Connan and Popoff, 2017). Additionally, this provides an explanation for the fact that exogenous GT1b addition did not affect BoNT/D sensitivity.

With regards to BoNT/DC, the unchanged results with GT1b addition are not surprising since GT1b is the least effective ganglioside receptor for BoNT/DC. It preferentially binds GM1, less strongly GD1a and weakly GD1b (Karalewitz et al., 2010, Kroken et al., 2011a). Therefore, exogenous GM1 addition might increase the sensitivity for BoNT/DC instead of GT1b. This was actually shown in a previous study where exogenous addition of GM1a increased the activity of BoNT/DC in PC12 cells, whereas GT1b addition did not affect the activity in PC12 cells, as now observed in LAN-5 cells (Nakamura et

al., 2012). Initially, I suspected that the result would be different in LAN-5 cells, but once again, the lack of GT1b effect on BoNT/DC activity was confirmed. Regarding TeNT, it also has two ganglioside binding sites, like BoNT/C and BoNT/D. One is a sialic acid binding site and the other is a lactose binding site, which is similar to the conserved ganglioside binding site in BoNT serotypes. Even though the sialic acid binding site was found to be more essential than lactose binding site, both binding sites are required for TeNT entry (Rummel, 2017). Each binding site preferentially binds to different gangliosides. However, GT1b can bind to both binding sites, so two GT1b can attach to TeNT simultaneously (Rummel et al., 2003, Chen et al., 2009). Although GT1b has a high affinity for TeNT, additional GT1b did not affect the activity of TeNT in LAN-5 cells. In contrast, the exogenous addition of GT1b enhanced TeNT activity in PC12 cells (Chen et al., 2009). The reason might be that expression levels of other gangliosides in relation to TeNT entry might be different for each cell line. In addition to GT1b, other gangliosides, GM1a, GD1a, GD1b, GQ1b, and GD3, are involved in the entry of TeNT. It was found that PC12 cells expressed GD1b, GT1b, GQ1b and GM1a but did not express GD1a. As these gangliosides also contribute to entry, one or some of them might not be sufficiently expressed in LAN-5 cells. The lactose binding site, for example, preferentially binds GM1a and weakly binds GT1b (Rummel, 2017). If GM1a expression is insufficient in LAN-5 cells, higher GT1b may not affect entry. As the expression pattern of GM1a, GQ1b, and GD1b gangliosides has not been identified in LAN-5 cells, it is not possible to make a conclusion.

In spite of the fact that CNTs have a similar entry mechanism, the mode of ganglioside binding to toxins varies slightly from one to another. The reason for this might be that some CNTs have common ganglioside binding sites that are mostly conserved, whereas some toxins contain ganglioside binding sites that have unique AA configurations or positions. For example, the two ganglioside binding sites of BoNT/C have neither AA configuration nor positions in common with other binding pockets of CNTs (Rummel, 2017). It is also suggested that ganglioside binding could change the interactions between toxins and receptor proteins (Stenmark et al., 2008). Therefore, it cannot be excluded that other molecules, such as proteins or phospholipids, may have an impact on GT1b binding and toxin entry (Tsukamoto et al., 2012). These are other reasons for different responses of each serotypes to GT1b addition. Although GT1b is an affinity receptor for the toxin, its relationships with other gangliosides and receptors affect overall toxin entry and activity.

4.3.4 SYTII transduction increases the sensitivity of BoNT/B significantly but only affects BoNT/DC sensitivity slightly

Even though SYTII is already expressed in LAN-5 cells, the administration of more SYTII by transduction increased BoNT/B sensitivity significantly. The enhanced sensitivity could easily be explained by the fact that SYTI and SYTII are both receptor proteins for BoNT/B (Nishiki et al., 1996, Dong et al., 2003). SYTII binds to BoNT/B more strongly than SYTI because SYTI binds to BoNT/B only in the presence of gangliosides. However, although the interaction of SYTII with gangliosides forms a high binding affinity for BoNT/B, SYTII can still attach to BoNT/B without any gangliosides (Dong et al., 2003). This explains why additional SYTII alone increased sensitivity significantly in LAN-5 cells independent of other factors such as gangliosides.

Although SYTI and SYTII are also receptors for BoNT/DC (Berntsson et al., 2013b), the addition of SYTII only slightly altered BoNT/DC activity, rather than enhancing it as significantly as BoNT/B. One reason might be that BoNT/B and BoNT/DC show varying binding affinity to SYTII. A receptor-toxin pull down assay showed that the receptor binding domain of BoNT/DC pulled down less SYTI and SYTII than the receptor binding domain of BoNT/B, indicating that BoNT/B has a higher binding affinity to SYTI and SYTII than BoNT/DC (Peng et al., 2012). Another reason might be that SYTII binds differently to BoNT/B and BoNT/DC due to structural differences in their binding sites. Although BoNT/B and BoNT/DC recognise the same binding site on SYTII, residues 40-61, the BoNT/DC binding interface is distinct to that of BoNT/B (Peng et al., 2012). This is because a hydrophobic groove in the receptor binding domain of the toxins that attaches to SYTII is conserved in BoNT/B, while it is not conserved in BoNT/DC (Chai et al., 2006, Peng et al., 2012). Therefore, it was suggested that BoNT/DC uses a novel SYTII binding site which is distinct from the existing SYTII binding site in BoNT/B (Peng et al., 2012). This was confirmed by the following study that the SYTII binding site in BoNT/DC is adherent but it is oriented with a 90° rotation to the one in BoNT/B (Berntsson et al., 2013b).

Additionally, BoNT/DC and BoNT/B exhibit different patterns of interaction between gangliosides and SYTII binding sites. It was suggested that, unlike other serotypes, BoNT/DC possibly has three independent binding sites: SYT binding site, ganglioside binding site and ganglioside binding loop/Sia-1 site, making BoNT/DC entry unique from others. Moreover, the SYTII binding site is independent of the ganglioside binding sites in BoNT/DC (Berntsson et al., 2013b). However, although SYTII could bind all gangliosides without any selectivity, BoNT/B reacts with GT1b and GD1a in pre-treated SYTII (Nishiki et al., 1996). That means BoNT/B preferentially binds to the complex of SYTII associated with GT1b and GD1a. Although a recent study showed that the binding affinity of SYTII has not been affected by the presence of GD1a (Berntsson et al., 2013a), GT1b interaction with SYTII enhances BoNT/B binding.

The difference in the relationship between SYTII binding site and gangliosides may also explain why SYTII enhanced BoNT/B sensitivity more than BoNT/DC. These results suggested SYTII is a more critical receptor protein for BoNT/B than BoNT/DC.

4.3.5 SYTII is not a receptor protein for TeNT entry

TeNT uses two ganglioside binding sites in order to enter neuronal cells and a protein receptor for entry has not been fully identified (Brunger et al., 2008). When the toxin binds to gangliosides, unknown additional molecules propel it inside endocytosis vesicles (Rossetto et al., 2013b). Although several proteins on the cell surface were proposed for TeNT binding, their involvement was not necessary for intoxication (Zuverink and Barbieri, 2018) or the mechanism was not clarified. A glycosylated GPI-anchored protein, abundant in lipid rafts in the plasma membrane, interacted with TeNT as a supplementary cell surface (Herreros et al., 2001, Munro et al., 2001) and a lack of GPI-anchored proteins decreased TeNT toxicity (Munro et al., 2001). The idea was that after gangliosides attracted TeNT, and subsequently occupied two ganglioside binding sites, the presence of GPI-anchored glycoprotein would facilitate the displacement of the bound ganglioside in sialic acid binding site. The exchange would be triggered by a high affinity of TeNT for carbohydrates found in glycoproteins (Rummel et al., 2003). Additionally, TeNT interacts with the ECM proteins nidogen-1 and nidogen-2, and the depletion of nidogens prevents TeNT binding to the neuronal cell surface (Bercsenyi et al., 2014).

It was also suggested that SV2A and SV2B protein receptors might facilitate TeNT entry (Yeh et al., 2010), but this remained hypothetical because TeNT and the receptor binding domain of TeNT use differential ways to enter cells (Blum et al., 2014). TeNT interacted with neurons independent of SVs, whereas the receptor binding domain of TeNT enters cells either independent of SVs or with SVs but without direct interaction of SV2 (Blum et al., 2012, Blum et al., 2014). Therefore, the use of SV2A and SV2B as receptor proteins requires further investigation. Moreover, this chapter identified that SYTII transduction to the cells had no effect on the activity of TeNT, suggesting SYTII is not a receptor protein for TeNT entry. The use of receptor proteins for TeNT is not fully understood and needs to be clarified. Even though TeNT interacts with some cell surface proteins, this might only serve to ease entry of TeNT and the necessity of a protein receptor for TeNT remains unclear. Therefore, there are two possibilities: an essential receptor protein and trafficking that TeNT utilises to enter cells has not been identified yet or TeNT enters cells independent of a receptor protein.

4.3.6 SYTII is essential for BoNT/B entry shown in re-engineered non-neuronal cells

The relationship between CNTs and their receptors can be better understood through the study of non-neuronal cells. HeLa cells were re-engineered with transduction of VAMP2 and SYTII exclusively for BoNT/B activity. According to the results, BoNT/B activity was successfully detected in SYTII-NanoLuc VAMP2 HeLa cells without GT1b gangliosides at concentrations of 10 nM and 5 nM. The reason might be that SYTII is a more efficient receptor than SYTI for BoNT/B, and BoNT/B binds to SYTII without gangliosides in contrast to SYTI (Dong et al., 2003). My results in non-neuronal cells support their findings. However, there is an inconsistency with the results that exogenous GT1b addition was required for BoNT/B to be detected significantly in SYTII-NanoLuc VAMP2 HeLa cells at 1 nM concentration. If the quantity of gangliosides is significantly higher than the toxin, the toxin would bind first to gangliosides and then to protein receptors. However, if the toxin concentration is higher and the gangliosides are either lacking or absent, the toxin could directly bind to a receptor protein and enter cells, explaining these findings (Montecucco, 1986). NanoLuc VAMP2 HeLa cells, however, showed no activity at increasing GT1b concentrations or at high BoNT/B concentrations. This indicates that GT1b facilitates entry, but not enough to account for its own absence, showing SYTII is the essential receptor for BoNT/B entry.

This study provided a better understanding of the relationship between BoNT/B activity and its receptors, SYTII and GT1b. Moreover, it generated a novel cell line to test BoNT/B, even though it was not as sensitive as neuroblastomas. However, the use of SYTII-NanoLuc VAMP2 HeLa for BoNT/B detection could be more advantageous in certain situations. It allows faster detection than neuroblastomas because there is no need to differentiate them for 3 days. Skipping the differentiation step also provides a more cost-effective assay. If concentrated samples of BoNT/B were detected, SYTII-NanoLuc VAMP2 HeLa cells could be used as they might enable the detection of BoNT/B in a more practical and faster way.

Additionally, the activity of BoNT/D, BoNT/DC and TeNT was also tested in the re-engineered HeLa cells (Appendix 4). In regard to TeNT, no activity was observed in either NanoLuc VAMP2 HeLa or SYTII-NanoLuc VAMP2 HeLa with or without GT1b addition. Chen et al. (2009) showed that the receptor binding domain of TeNT could bind to the HeLa cell membrane only after incubation with either GT1b or GM1a/GD3. The receptor binding domain of TeNT attached but remained on the periphery of the cells. Therefore, GT1b could enable binding of TeNT to the cell membrane but might not be sufficient alone for toxin entry. This could explain why no cleavage was seen in re-engineered HeLa cells after TeNT exposure. In relation to BoNT/D, no activity was observed in re-engineered HeLa cells. However,

BoNT/DC activity was detected significantly in both NanoLuc VAMP2 HeLa and SYTII-NanoLuc VAMP2 HeLa cells with or without GT1b addition, showing that SYTII is not an essential receptor for BoNT/DC. This finding confirmed that BoNT/DC shows less binding affinity for SYTII (Peng et al., 2012). BoNT/DC could enter cells without complex gangliosides (Zhang et al., 2017), and HeLa cells are abundant in basic gangliosides, such as GM1a and GM3, but lack complex gangliosides. That explains why BoNT/DC activity was detected successfully in re-engineered HeLa cells irrespective of the addition of GT1b.

Overall, toxin-receptor binding is not the only indicator of toxin potency. There may be other factors involved, such as internalisation rate, suitability of the endosomal environment for translocation of light chain, substrate abundance, and speed of biosynthesis of substrate (Purkiss et al., 2001). Therefore, other factors should not be excluded when the toxin-receptor relationship is assessed by endpoint activity of the toxin, which is cleavage of the target proteins for CNTs.

5 Chapter 5: Developing one step ELISA to test BoNT/A and BoNT/C

5.1 Introduction

BoNTs cause flaccid muscle paralysis by preventing acetylcholine release at the neuromuscular junction (Sesardic et al., 2003). This muscle paralysing effect of the toxin has been officially used to treat several diseases such as strabismus, blepharospasm, and hemifacial spasms since 1989. The BoNT activity is fully reversible, and each serotype paralyses the muscle for different durations (Kukreja and Singh, 2015). However, the duration of paralysis caused by BoNT/A is longer than that of other serotypes, ranging from 4-6 months, which makes it an effective treatment in clinical settings (Foran et al., 2003). BoNT/A, also known as BOTOX® commercially, is the first FDA approved serotype for medical and cosmetic use (Chen, 2012, Kukreja and Singh, 2015). The high efficacy of BoNT/A leads to its application in a number of other medical conditions associated with abnormal muscle contractions including tremor, hyperhidrosis, spasticity, dystonia, and pain relief (Schantz and Johnson, 1992, Naumann and Jost, 2004, Chen, 2012). Extensive and efficient use of BoNT/A has resulted in the production of other licensed commercial brands of BoNT/A such as Dysport®, Xeomin®, and its use has been growing significantly (Cocco and Albanese, 2018). Therefore, it is more essential to develop a sensitive replacement assay for BoNT/A than for other serotypes. As explained in Chapter 3, several studies have been conducted to detect BoNT/A in a sensitive and practical manner through cell-based assays using a variety of cell lines, which have several advantages over other methods.

With the use of neuroblastoma cell lines, several cell-based assays were developed for BoNT/A detection. Some of these assays detect toxin activity by measuring the inhibition of neurotransmitter release (Purkiss et al., 2001, Pathe-Neuschafer-Rube et al., 2018). In contrast, other assays determine BoNT/A activity by detecting the cleavage of the target protein, such as the sandwich ELISA developed by Fernandez-Salas et. al (2012). Such a similar replacement assay, one-step ELISA, was also developed for BoNT/B detection by Rust et al. (2017). A re-engineered NanoLuc VAMP2 SiMa cell line was used to detect BoNT/B activity by luminescent reaction, which is a result of cleaving VAMP2. Based on previous research, this chapter describes the establishment of a novel one-step ELISA using re-engineering LAN-5 neuroblastoma cell line for BoNT/A detection. Additionally, as BoNT/C and BoNT/A have the same target protein, re-engineered LAN-5 cells and the one-step ELISA were also tested and partly confirmed for BoNT/C.

5.2 Results

5.2.1 Generation of new two LAN-5 cell lines for one step ELISA

The one-step ELISA assay has several specific requirements. As part of these requirements, the cell line must be sensitive to Clostridial neurotoxins and capable of expressing NanoLuc-tagged with a specific target protein. Although the LAN-5 cell line expresses SNAP25, NanoLuc tagged SNAP25 is required to obtain results for BoNT/A and BoNT/C based on one-step ELISA. In order to overcome this limitation, two novel LAN-5 cell lines were re-engineered by transduction to express SNAP25 with an N-terminal NanoLuc tag (NanoLuc SNAP25) or a C-terminal NanoLuc tag (SNAP25 NanoLuc). Cells were transduced with both an N- and C-terminal NanoLuc tag in order to ensure that cleaved SNAP25 with a NanoLuc tag could be detected following the cleavage process either in N-term or C-term cell lines, regardless of which cleaved-end of SNAP25 the antibody targeted.

Figure 5.1 shows re-engineering of LAN-5 cells transduced with N-term NanoLuc. The map of the N-term plasmid, having HA-tag, GFP and puromycin resistance genes, is shown in Figure 5.1 A. The plasmid has a GFP tag that enables the use of fluorescence microscopy to track transfected and transduced cells. The puromycin resistance gene allows for antibiotic selection of transduced cells. The HA-tag sequence is used to detect and confirm transduced cells. Figure 5.1 B illustrates the transfection and transduction steps. The transfer plasmid containing a gene of interest, envelope plasmid, and packaging plasmid were co-transfected into HEK cells (a cell line for the production of lentiviruses) to produce lentiviral particles (Elegheert et al., 2018). GFP expression was observed in immunofluorescence images, indicating that lentiviral particles were successfully generated in HEK cells. Both LAN-5 and HeLa cells were transduced using the produced lentiviral vectors and GFP expression was shown to be positive in both cell lines, indicating successful transduction. HeLa cells were transduced as a positive control because they have a high capacity for the uptake of DNA (Ning and Tang, 2012). In order to characterize the cells further, the generated NanoLuc SNAP25 LAN-5 cell line was extensively stained with HA-tag and GFP as shown in immunofluorescence images (Figure 5.1 C).

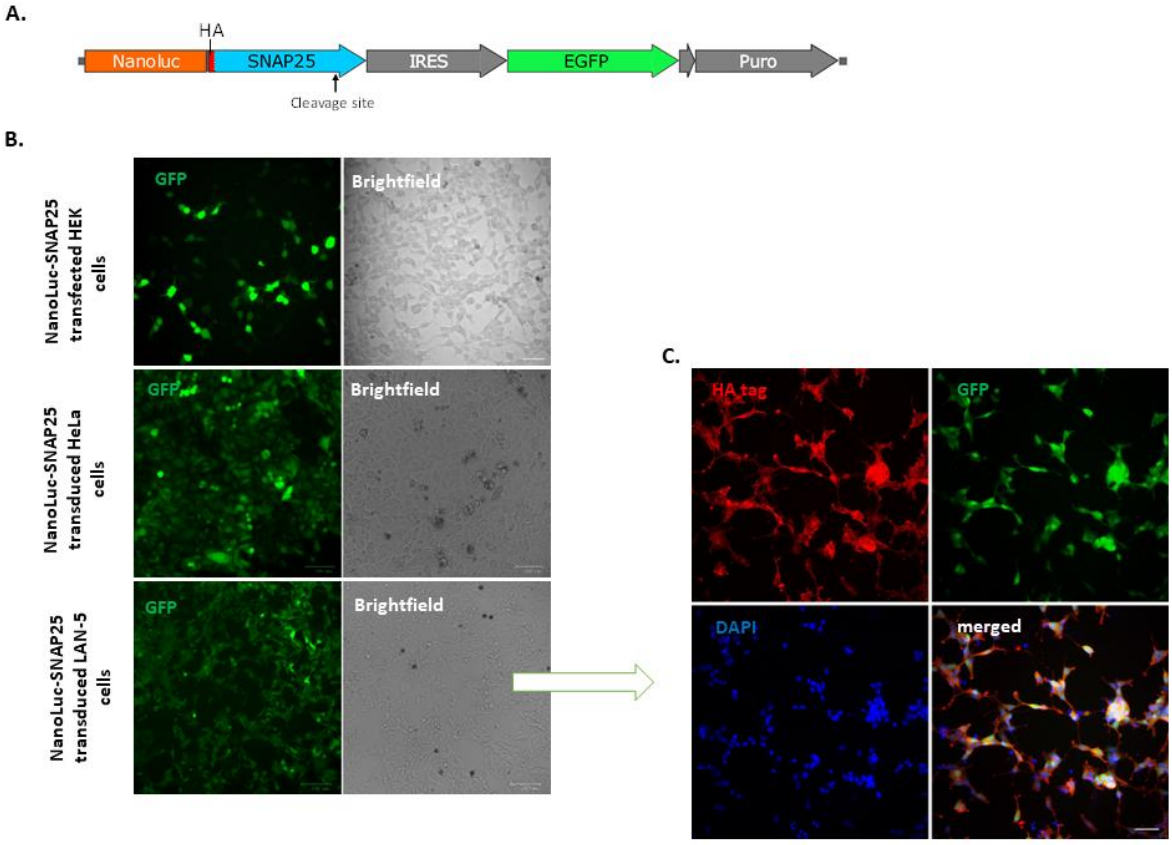

Figure 5.1 N-term NanoLuc SNAP25 LAN-5 cell line was generated and characterized.

A) *The map of NanoLuc SNAP25 plasmid transduced into native LAN-5 cells (the map is created by Dr Charlotte Leese using Snap Gene Viewer software). The plasmid has a GFP tag that allows tracking of transfected and transduced cells under a fluorescence microscope. Puromycin resistance gene allows for antibiotic selection of transduced cells. HA-tag sequence allows the detection and confirmation of transduced cells.* ***B)*** *Immunofluorescence and brightfield images showing NanoLuc SNAP25 transfection of HEK cells, followed by transduction of HeLa cells as a positive control, and transduction of native LAN-5 cells. GFP (coloured in green) indicated that the plasmid was expressed in the cells. Images were taken with epifluorescence microscope at 20x objective. All scale bars are 100 µm.* ***C)*** *Immunofluorescence images showing HA tag (coloured in red) and GFP (coloured in green) confirming the plasmid successfully expressed in the cells. Images were taken with epifluorescence microscope at 20x objective. All scale bars are 50 µm. Rabbit HA-tag antibody diluted in 1:400, DAPI (blue) is diluted at 1:1000.*

Similar to the N-term NanoLuc SNAP25 LAN-5 cell line, the C-term SNAP25 NanoLuc LAN-5 cell line was generated and characterised (Figure 5.2). Figure 5.2 A shows the map of the C-terminal plasmid, in which the NanoLuc construct is located at the C-terminal end of the SNAP25 part. Lentiviral production in HEK cells and viral transduction in HeLa and LAN-5 cells were successful as confirmed by GFP expression (Figure 5.2 B). It can be seen from immunofluorescence images that transduction efficiency in LAN-5 cells was low but improved after puromycin selection. It is evident that the LAN-5

cells were extensively stained with HA-tag and GFP after puromycin treatment (Figure 5.2 C). Overall, LAN-5 cells were successfully transduced with NanoLuc SNAP25 and SNAP25 LAN-5 plasmids; NanoLuc SNAP25 LAN-5 cell line and SNAP25 NanoLuc LAN-5 cell line were generated.

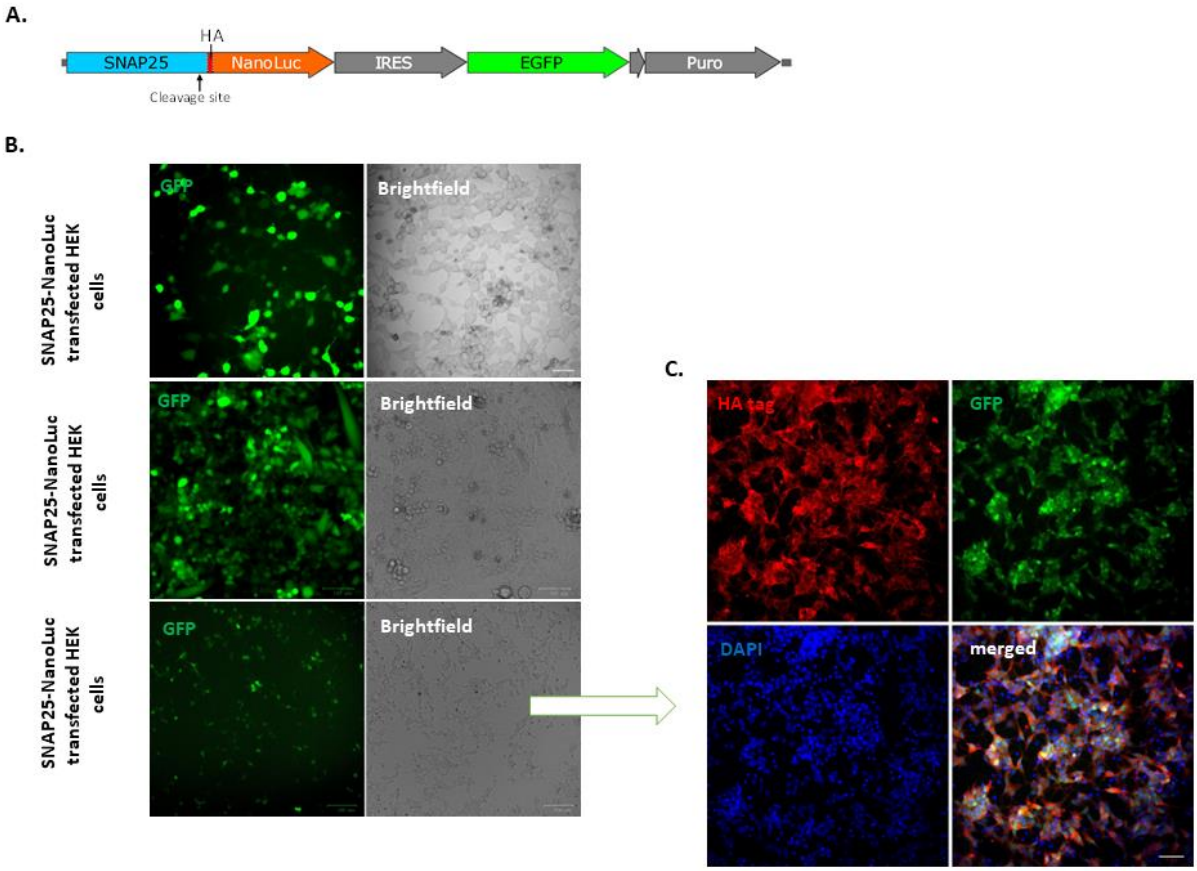

Figure 5.2 C-term SNAP25 NanoLuc LAN-5 cell line was generated and characterized.

A) *The map of SNAP25 NanoLuc plasmid transduced to native LAN-5 cells (the map is created by Dr Charlotte Leese using Snap Gene Viewer software). The plasmid has GFP tag that enables tracking of transfected and transduced cells under a fluorescence microscope. Puromycin resistance gene allows for antibiotic selection of transduced cells. HA-tag sequence also allows for the detection and confirmation of transduced cells.* ***B)*** *Immunofluorescence and brightfield images showing SNAP25 NanoLuc transfection of HEK cells, followed by transduction of HeLa cells as a control, and transduction of native LAN-5 cells. GFP (coloured in green) indicated that the plasmid is expressed in the cells. Images were taken with epifluorescence microscope at 20x objective. All scale bars are 100 µm.* ***C)*** *Immunofluorescence images showing HA tag (coloured in red) and GFP (coloured in green) confirming the plasmid was successfully expressed in the cells. Images were taken with epifluorescence microscope at 20x objective. All scale bars are 50 µm. Rabbit HA-tag antibody diluted in 1:400, DAPI (blue) is diluted at 1:1000.*

5.2.2 N-term NanoLuc SNAP25 LAN-5 is the functional cell line to detect cleaved NanoLuc SNAP25

After production of the cell lines, the cells were treated with BoNT/A and then tested for the detection of cleaved NanoLuc SNAP25. Two different rabbit polyclonal antibodies were tested to capture cleaved NanoLuc SNAP25 by immunoblotting. The intact SNAP25 antibody recognizes the portion of the protein before the cleavage site. Therefore, it can detect both uncleaved and cleaved SNAP25 as schematically shown in Figure 5.3 A. Immunoblot image shows that native SNAP25 and NanoLuc SNAP25 were successfully detected in N-term NanoLuc SNAP25 LAN-5 cells (Figure 5.2 B). Due to the small shift in molecular size of SNAP25 after cleavage, it was possible to detect uncleaved and cleaved native SNAP25 separately by running the gel longer than usual. However, uncleaved and cleaved NanoLuc SNAP25 cannot be distinguished and are found in the same protein band. In C-term SNAP25 NanoLuc LAN-5 cell line, native SNAP25 and NanoLuc SNAP25 were also detected by intact SNAP25 antibody (Figure 5.3 C). However, only uncleaved NanoLuc SNAP25 was detected in C-term cells. This is expected because the cleaved SNAP25 NanoLuc would lose the NanoLuc part so that it would remain the same size as the cleaved native SNAP25. The intensity of the uncleaved NanoLuc SNAP25 band decreased with increasing BoNT/A concentrations, showing in Figure 5.3 C.

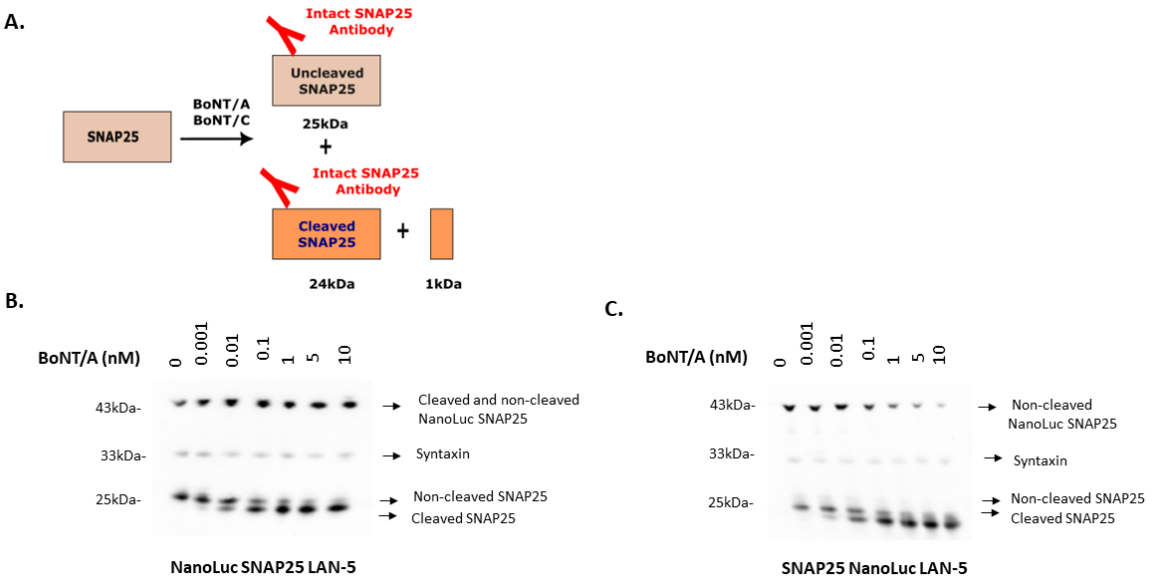

Figure 5.3 Native SNAP25 and NanoLuc SNAP25 were detectable by SNAP25 intact Ab.

A) *Schematic representation showing the antibody recognising intact SNAP25 (in house) functionality, which could detect both cleaved and uncleaved SNAP25 following treatment with BoNT/A or BoNT/C.* ***B)*** *Immunoblot image showing the cleaved and uncleaved native SNAP25 and NanoLuc SNAP25 in N-term NanoLuc SNAP25 LAN-5 cell line following treatment with BoNT/A.* ***C)*** *Immunoblot image showing the cleaved and uncleaved native SNAP25 and uncleaved NanoLuc SNAP25 in C-term SNAP25 NanoLuc LAN-5 cell line following treatment with BoNT/A. The differentiated cells were treated with 1:10 serial dilution of BoNT/A for 3 days. Cells were treated with the diluting agent (Opti-MEM, reduced serum media) as a no treatment control. SNAP25 intact antibody was added at 1:3000 dilution. Syntaxin antibody was added at 1:2000 dilution as a control antibody. Image was taken from ChemiDoc XRS. Schematic was created by using Inkscape.*

The cleaved NanoLuc SNAP25 was detectable in N-term LAN-5 cell line but was indistinguishable from uncleaved NanoLuc SNAP25. Therefore, the antibody recognising only cleaved SNAP25 was tested for capturing cleaved SNAP25 in the N-term NanoLuc SNAP25 LAN-5 cell line. Immunofluorescence images showed that cleaved SNAP25 was successfully stained in NanoLuc SNAP25 LAN-5 cells following treatment with 1 nM concentration of BoNT/A, while no staining was observed in untreated cells, demonstrating that the antibody detects only cleaved SNAP25 (Figure 5.4 A-B). Moreover, the cleaved SNAP25 was found to be stable on the plasma membrane, shown with a yellow arrow.

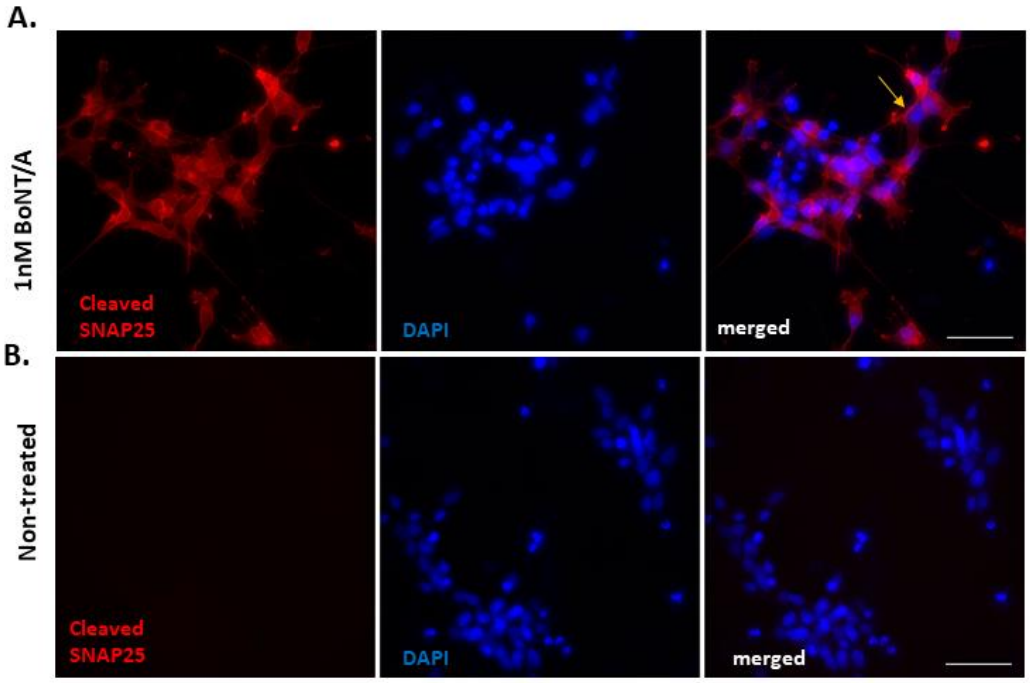

Figure 5.4 Only cleaved form of SNAP25 was detected by BoNT/A cleaved SNAP25 Ab.

A) *Immunofluorescence images of cleaved SNAP25 (coloured in red) on the plasma membrane (yellow arrow) in differentiated N-term NanoLuc SNAP25 LAN-5 cell line following treatment of 1nM BoNT/A.* ***B)*** *Immunofluorescence images showing no SNAP25 cleavage in non-treated cells. Rabbit BoNT/A-cleaved SNAP25 Ab used at 1:5000 dilution. The nucleus (coloured in blue) was stained with DAPI at 1:1000 dilution Images were taken at 40x immunofluorescence microscopy. All scale bars are 50 µm.*

BoNT/A cleaved SNAP25 antibody was used in both N-term and C-term LAN-5 cells to capture cleaved SNAP25. Figure 5.5 contains schematics showing how the antibody recognizes SNAP25 fragments after cleavage in both cell lines. As the antibody recognises the N-term SNAP25 fragment following cleavage of SNAP25, the cleaved NanoLuc SNAP25 was detected in N-term NanoLuc SNAP25 LAN-5 cells (Figure 5.5 A). In C-term SNAP25 NanoLuc LAN-5 cells, only cleaved SNAP25 was detected without the NanoLuc tag because the NanoLuc tag was associated with C-term SNAP25 fragment once SNAP25 was cleaved (Figure 5.5 B). Immunoblot analysis confirmed that cleaved NanoLuc SNAP25 was detected with a size of 43 kDa in N-term NanoLuc SNAP25 LAN-5 cell lines (Figure 5.5 C). However, only native cleaved SNAP25 with a size of 25 kDa was detected in C-term SNAP25 NanoLuc LAN-5 cells.

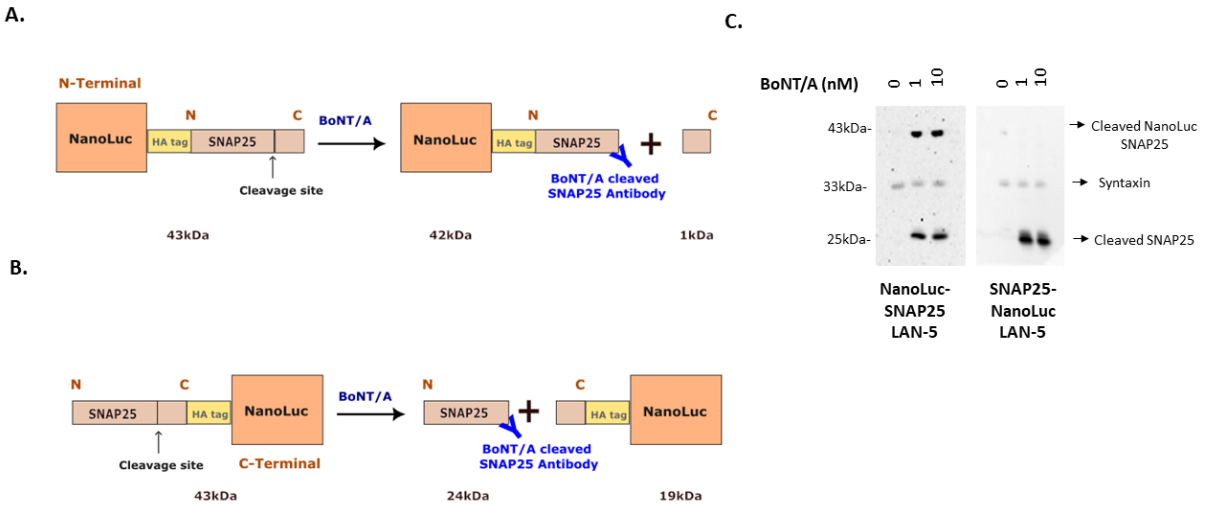

Figure 5.5 BoNT/A cleaved NanoLuc SNAP25 was successfully detected in NanoLuc SNAP25 LAN-5 cell line.

A) *Schematic showing the detection of cleaved NanoLuc SNAP25 following BoNT/A treatment of NanoLuc SNAP25 LAN-5 cell line.* ***B)*** *Schematic showing the detection of SNAP25, but not NanoLuc SNAP25, following treatment of BoNT/A on SNAP25 NanoLuc LAN-5 cell line.* ***C)*** *Immunoblot image showing the proportional cleavage of native SNAP25 in both cell lines and NanoLuc SNAP25 cleavage in NanoLuc SNAP25 LAN-5 cell line following BoNT/A treatment for 3-days. Cells were treated with the diluting agent (Opti-MEM, reduced serum media) as a no treatment control. BoNT/A cleaved SNAP25 Ab (in house) was used at 1:2000 dilution to see only SNAP25 cleavage. Syntaxin Ab was added at 1:2000 dilution as a loading control. Image was taken from ChemiDoc XRS. Schematics were created by using Inkscape.*

In conclusion, N-term NanoLuc SNAP25 LAN-5 is confirmed as a functional cell line in which BoNT/A cleaved NanoLuc SNAP25 can be detected.

5.2.3 Establishing a one-step ELISA for BoNT/A in the N-term NanoLuc SNAP25 LAN-5 cell line

In addition to a proper cell line, one-step ELISA requires a suitable antibody that recognises cleaved NanoLuc SNAP25 and can attach to a surface proteins immobilised into wells, as schematically shown in Figure 5.6 A. Protein A, which is one such surface protein, can be coupled with immunoglobulins and immobilized on a solid surface to detect antibodies (Hjelm et al., 1972). Moreover, Protein A shows strong affinity for rabbit immunoglobulins (Mota et al., 1983). As we have rabbit polyclonal antibodies, Protein A coated plates were used. A one-step ELISA was performed using the same two rabbit polyclonal antibodies in both N-term and C-term LAN-5 cells treated with 1 nM BoNT/A.

With the use of recognising intact SNAP25 Ab in the assay, a high level of signal was produced showing that the antibody bound both Protein A and the target protein (Figure 5.6 B). The signal was saturated

for treated and untreated N-term LAN-5 cells. Uncleaved NanoLuc SNAP25 was detected in untreated cells whereas both cleaved and uncleaved NanoLuc SNAP25 were detected in toxin treated N-term NanoLuc SNAP25 LAN-5 cells. In C-term SNAP25 NanoLuc LAN-5 cell line, the signal represents the amount of uncleaved NanoLuc SNAP25 was saturated in untreated cells. However, the signal level indicates the amount of uncleaved NanoLuc SNAP25 significantly decreased in toxin treated cells due to cleavage of target protein, as expected.

When the antibody recognising only cleaved SNAP25 was used in both N-term and C-term LAN-5 cells, no signal was seen in C-term SNAP25 NanoLuc LAN-5 cells, as expected due to the removal of the NanoLuc tag during the cleavage, whereas a high level of signal was detected for cleaved NanoLuc SNAP25 in BoNT/A treated N-term NanoLuc SNAP25 LAN-5 cells (Figure 5.6 C). Additionally, no signal was detected in untreated N-term LAN-5 cells, showing the antibody is capable of specifically recognizing cleaved NanoLuc SNAP25 in the one-step ELISA assay as well. With this, the one-step ELISA was established for BoNT/A detection with N-term NanoLuc SNAP25 LAN-5 cells and BoNT/A cleaved SNAP25 Ab.

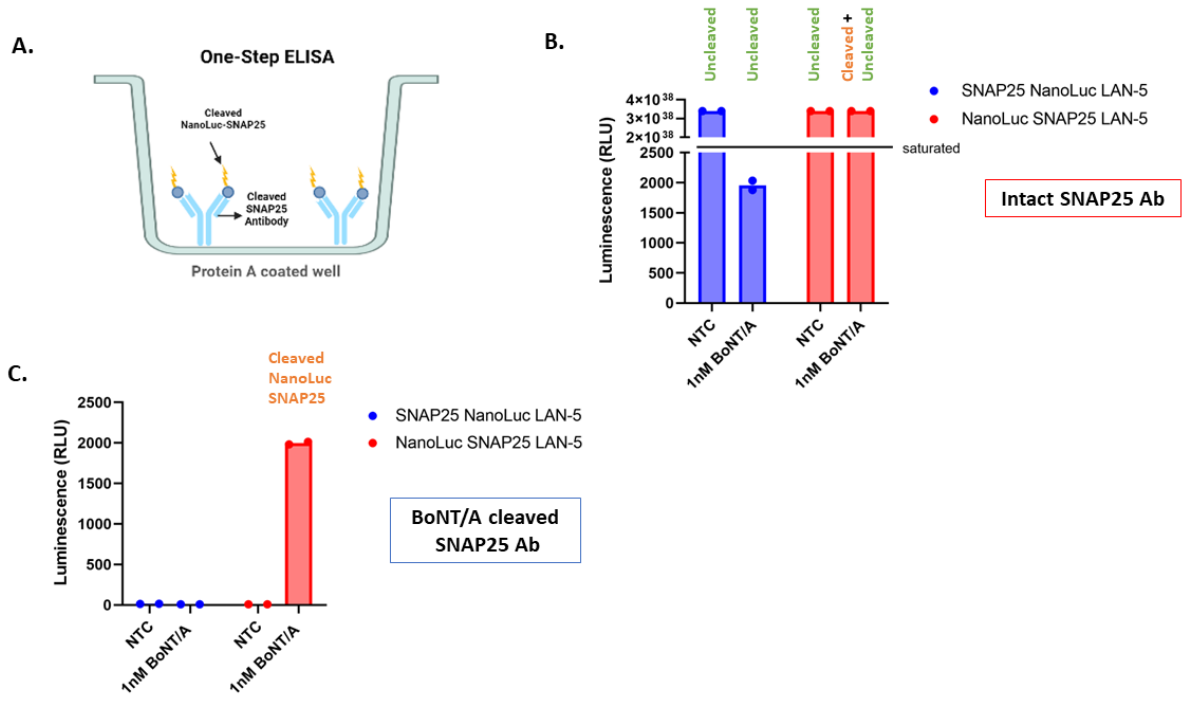

Figure 5.6 Cleaved NanoLuc SNAP25 was successfully detected in N-term NanoLuc SNAP25 LAN-5 cell line by one step ELISA.

A) *Schematic showing the detection of cleaved NanoLuc SNAP25 following BoNT/A treatment by one step ELISA.* ***B)*** *Bar chart showing NanoLuc SNAP25 detection using SNAP25 intact Ab in the one step ELISA (n=2, ±experimental errors).* ***C)*** *Bar chart showing cleaved NanoLuc SNAP25 detection in the N-term NanoLuc SNAP25 LAN-5 cell line using cleaved SNAP25 Ab in the one step ELISA following treatment with BoNT/A (n=2, ±experimental errors). Differentiated both cell lines were treated with 1 nM BoNT/A for 3 days. Cells were treated with the diluting agent (Opti-MEM, reduced serum media) as a no treatment control. Protein A plate was incubated with either SNAP25 intact Ab or cleaved SNAP25 antibody at 1:10 dilution overnight. Schematic was created by using BioRender.*

After establishment of a one-step ELISA for BoNT/A, the assay was optimized and the detection threshold was determined. BoNT/A cleaved SNAP25 Ab was diluted from 1/10 to 1/1500 and tested for 1 nM BoNT/A activity (Figure 5.7 A). Cleaved NanoLuc SNAP25 amount increased significantly from the dilution ratio of 1/1500 to 1/80 and reached the saturation point at 1/50 dilution ratio. As it increased very slowly from 1/50 to 1/10, 1/50 was chosen as a dilution ratio for the assay. Following this, serially titrated BoNT/A was detected in one-step ELISA in order to identify its level of sensitivity (Figure 5.7 B). A high level of signal was detected at concentrations of 10 nM, 5 nM, and 1 nM BoNT/A, and the difference was considerably significant compared to the control group. Although the signal decreased slightly at a lower concentration of 0.1 nM, the difference was still statistically significant

in comparison to the control group. BoNT/A was detected in the assay at a limit of detection as low as 0.01 nM concentration, showing it is a highly sensitive assay.

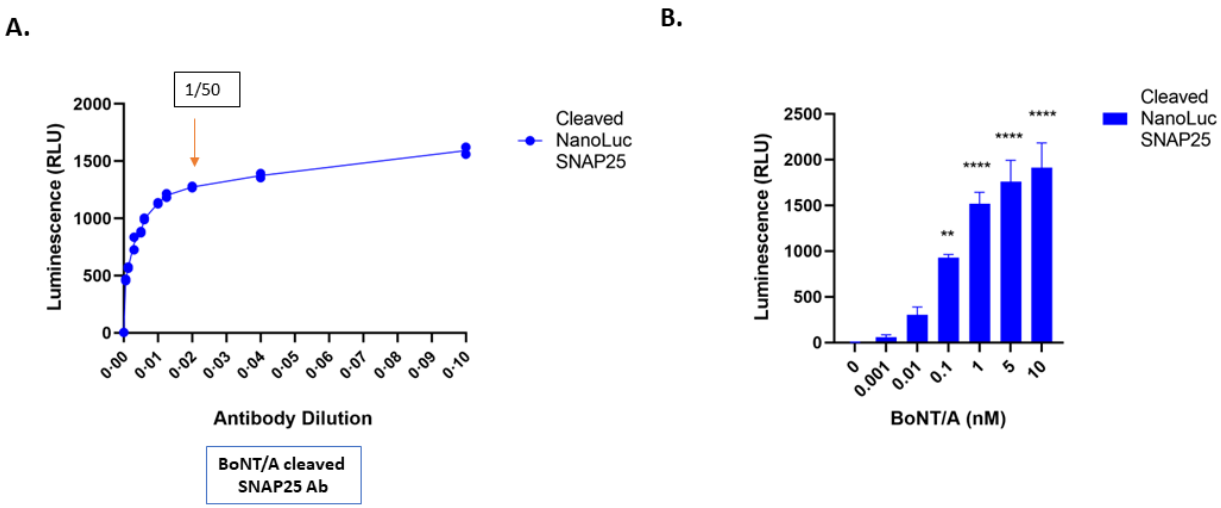

Figure 5.7 A newly developed one-step ELISA is sensitive to detecting low levels of BoNT/A.

A) *Graph showing cleaved NanoLuc SNAP25 levels with different dilution rates of cleaved SNAP25 antibody (n=2, ±experimental errors). Protein A plate was coated with cleaved SNAP25 Ab ranging from 1:10 to 1:1500 dilution ratios. Differentiated NanoLuc SNAP25 LAN-5 cell line was treated with 1nM concentration of BoNT/A.* ***B)*** *Bar chart showing cleaved NanoLuc SNAP25 detection in NanoLuc SNAP25 LAN-5 cell line following treatment with BoNT/A (N=3; ±SEM). Multiple comparison was examined by an ordinary one-way ANOVA followed by Tukey's test. Significances refer to comparisons between different toxin concentrations and untreated control and alpha P values of <0.05 were considered statistically significant. **= P<0.01; ****= P<0.0001. The differentiated cells were treated with 1:10 titrated BoNT/A for 3 days. Cells were treated with the diluting agent (Opti-MEM, reduced serum media) as a no treatment control. Protein A plate was coated with cleaved SNAP25 Ab at 1:50 dilution.*

5.2.4 Investigating the time course of BoNT/A activity by one step ELISA and immunoblotting

To optimize the assay further, time-course experiments were performed. Moreover, one-step ELISA and immunoblot methods were compared for time-dependent activity. NanoLuc SNAP25 LAN-5 cells were treated with 1 nM BoNT/A for 1-day, 2-day, and 3-day incubations. The immunoblot image showed that cleaved NanoLuc SNAP25 and native SNAP25 bands were nearly identical for each day of treatment (Figure 5.8 A). This was also confirmed by the graph showing the immunosignals for cleaved SNAP25, cleaved NanoLuc SNAP25, and total SNAP25 cleavage (Figure 5.8 B). According to the graph, the amount of cleaved NanoLuc SNAP25 was about the same for each day, whereas the amount of cleaved native SNAP25 increased slightly after the 3-day treatment. As a result, the total amount of

cleaved SNAP25 was slightly higher when the cells were treated with BoNT/A for 3 days. Time-course results of the one-step ELISA method were consistent with immunoblot results. The luminescence signal increased slightly with increasing time, but there was no significant difference between the days (Figure 5.8 C). As no significant difference was seen between days, longer treatment days were performed to determine whether the cleaved amount of protein increased further.

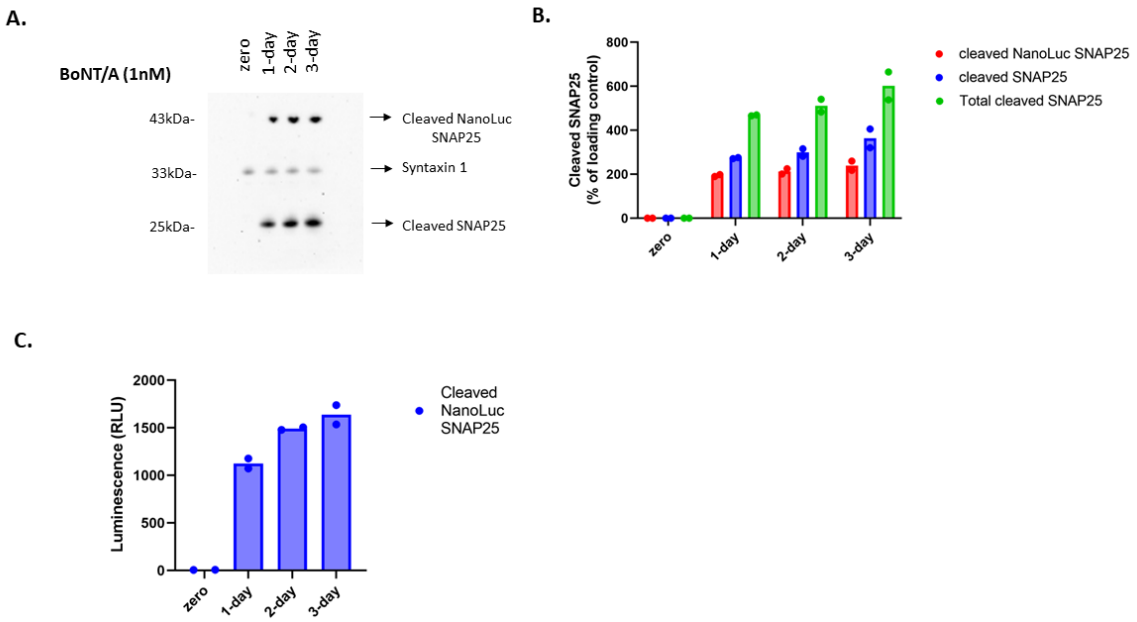

Figure 5.8 Cleaved SNAP25 detection was similar between 2-day treatment and 3-day treatment.

A) *Representative immunoblot showing the proportional cleavage of SNAP25 for different treatment times.* ***B)*** *Graph showing the quantification of immunosignals for cleaved SNAP25, NanoLuc SNAP25, and total cleaved SNAP25 (n=2, ±experimental errors). BoNT/A cleaved SNAP25 Ab was used at 1:2000 dilution to see SNAP25 cleavage. Syntaxin was used at 1:2000 dilution as a loading control.* ***C)*** *Bar chart showing cleaved NanoLuc SNAP25 levels detected by one step ELISA for different treatment times (n=2, ±experimental errors). Protein A was coated with BoNT/A cleaved SNAP25 Ab at 1:50 dilution. Differentiated NanoLuc SNAP25 LAN-5 cells were treated with the concentration of 1nM BoNT/A on the relevant treatment day.*

The cells were treated with BoNT/A for 1-day, 2-day, 3-day as well as for extended durations, 4-day, 5-day, and 6-day. The immunoblot image showed that cleaved bands were almost the same for all treatment days (Figure 5.9 A). It can also be seen from the graph that the amount of SNAP25 cleavage was approximately similar for each treatment day. As a result, a longer durations than 3 days had no effect on the cleavage rate (Figure 5.B). Similar results were obtained with the one-step ELISA method, where the luminescence signal remained unchanged for extended durations (Figure 5.9 C). The level of luminescence signal was almost the same for all treatment days, except the 1-day treatment. These results showed that BoNT/A activity saturated after 2 days of treatment. Therefore, the optimal

treatment period should be 2 or 3 days for BoNT/A detection in one-step ELISA and immunoblotting methods.

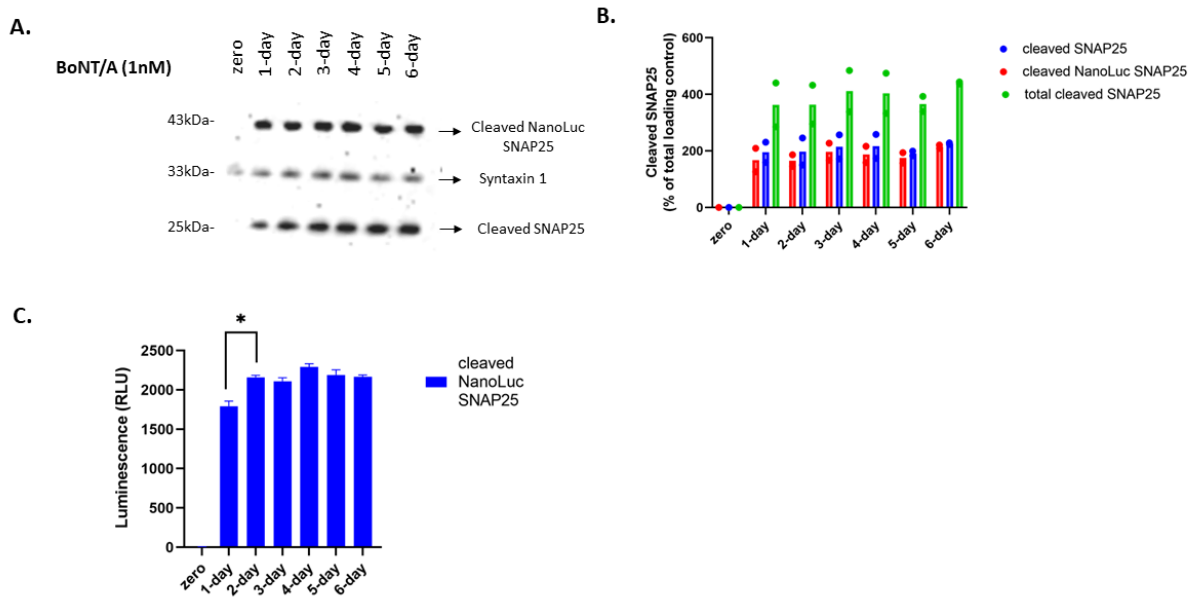

Figure 5.9 The level of cleaved SNAP25 detection did not increase with increasing treatment days.

A) *Representative immunoblot showing the proportional cleavage of SNAP25 from 1-day to 6-day of treatment.* ***B)*** *Graph showing the quantification of immunosignals for cleaved SNAP25, NanoLuc SNAP25, and total cleaved SNAP25 (n=2, ±experimental errors). BoNT/A cleaved SNAP25 Ab was used at 1:2000 dilution to see SNAP25 cleavage. Syntaxin was used at 1:2000 dilution as a loading control.* ***C)*** *Bar chart showing cleaved NanoLuc SNAP25 levels for different treatments days, determined by one step ELISA (n=4, ±SEM). Multiple comparisons were examined by an ordinary one-way ANOVA analysis followed by Tukey's test. Alpha P values of <0.05 were considered statistically significant. *=P<0.05. Protein A was coated with BoNT/A cleaved SNAP25 Ab at 1:50 dilution. Differentiated NanoLuc SNAP25 LAN-5 cells were treated with the concentration of 1 nM BoNT/A for each treatment day.*

5.2.5 BoNT/C cleaved NanoLuc SNAP25 was hardly detectable in one-step ELISA using the current antibodies

As BoNT/C has the same target protein as BoNT/A, the generated NanoLuc SNAP25 LAN-5 cells and one-step ELISA method were tested against BoNT/C activity. Both N-term and C-term LAN-5 cells were treated with BoNT/C, and NanoLuc SNAP25 capture was tested with the intact SNAP25 Ab. Immunoblot image showed that both cleaved and uncleaved NanoLuc SNAP25 were detected in the N-term NanoLuc SNAP25 LAN-5 cell line, but not distinguishable from one another (Figure 5.10 A). In the C-term SNAP25 NanoLuc LAN-5 cell line NanoLuc SNAP25 bands, corresponding to only uncleaved protein, were observed (Figure 5.10 B). Unlike BoNT/A, these uncleaved NanoLuc SNAP25 bands did

not disappear significantly at higher concentrations. This can be explained by the fact that BoNT/A activity is stronger than BoNT/C activity in LAN-5 cells. The one-step ELISA assay using the intact SNAP25 Ab detected NanoLuc SNAP25 in N-term and C-term LAN-5 cell lines, and the signal from both BoNT/C treated and control cells were saturated (Figure 5.10 C). Different from the result of BoNT/A, the signal, which represents uncleaved NanoLuc SNAP25, was saturated in BoNT/C treated C-term LAN-5 cells. This is likely to be because BoNT/C cleaved less NanoLuc SNAP25 than BoNT/A, so there was more uncleaved NanoLuc SNAP25 left after BoNT/C treatment. Overall, although its activity was less than BoNT/A, the re-engineered NanoLuc SNAP25 LAN-5 cells were still functional for BoNT/C based assays.

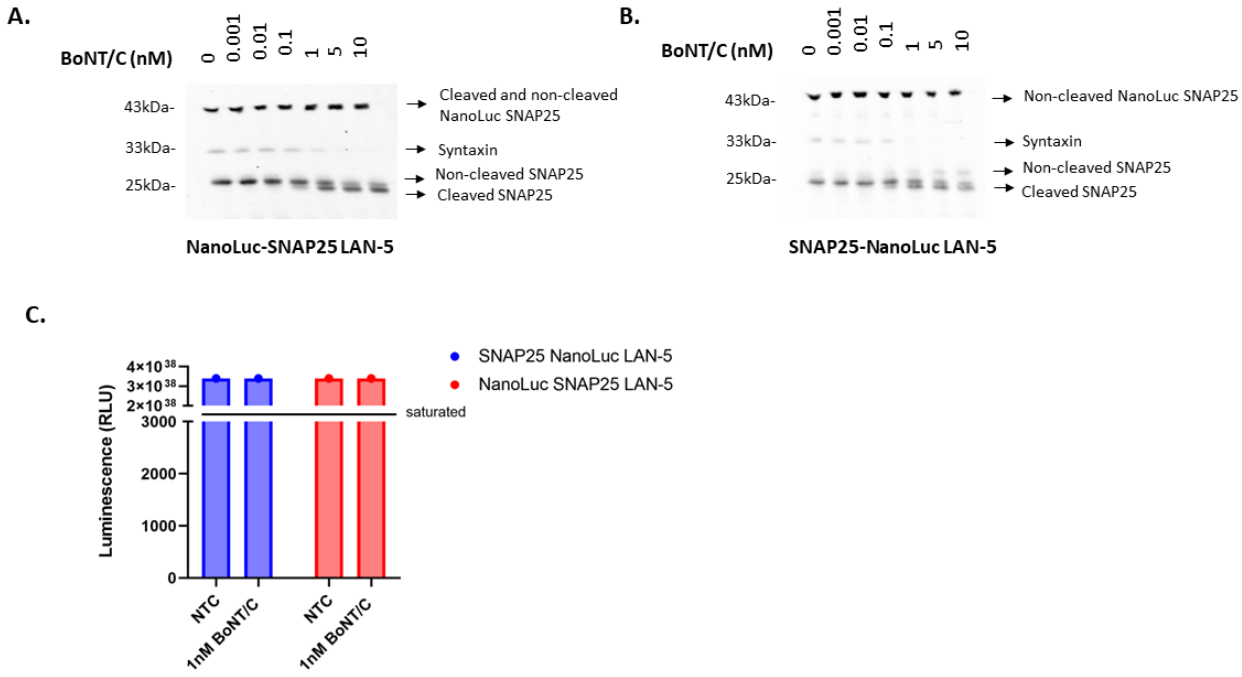

Figure 5.10 NanoLuc SNAP25 were detectable by both immunoblotting and one step ELISA.

A) *Immunoblot image showing the cleaved and uncleaved both native SNAP25 and NanoLuc SNAP25 in N-term NanoLuc SNAP25 LAN-5 cell line following treatment of BoNT/C.* ***B)*** *Immunoblot image showing the cleaved and uncleaved native SNAP25 and uncleaved NanoLuc SNAP25 in C-term SNAP25 NanoLuc LAN-5 cell line following treatment of BoNT/C. The differentiated cells were treated with 1:10 titrations of BoNT/C for 3 days. Cells were treated with the diluting agent (Opti-MEM, reduced serum media) as a no treatment control. SNAP25 intact antibody was added at 1:3000 dilution. Syntaxin antibody was added at 1:2000 dilution. Image was taken from ChemiDoc XRS.* ***C)*** *Bar chart showing NanoLuc SNAP25 detection using SNAP25 intact Ab by one step ELISA (n=2, ± experimental errors). Differentiated both cell lines were treated with 1 nM BoNT/A for 3 days. Cells were treated with the diluting agent (Opti-MEM, reduced serum media) as a no treatment control. Protein A plate was incubated with SNAP25 intact Ab at 1:10 dilution.*

N-term and C-term LAN-5 cells were tested with antibodies that capture only cleaved SNAP25 in order to detect BoNT/C cleaved NanoLuc SNAP25. BoNT/A cleaved SNAP25 Ab was tested for BoNT/C activity because the cleavage sites of BoNT/A and BoNT/C are very close. BoNT/A cleaves the peptide bond from 197 residues whereas BoNT/C cleaves the peptide bond from 198 residues on SNAP25 (Binz et al., 2010). Immunoblot image demonstrated that cleaved NanoLuc SNAP25 and cleaved native SNAP25 bands were observed in N-term NanoLuc SNAP25 LAN-5 cell line, showing BoNT/A cleaved SNAP25 Ab can recognise BoNT/C cleaved SNAP25 (Figure 5.11 A). As expected, only the cleaved native SNAP25 bands were detected in C-term SNAP25 NanoLuc LAN-5 cell line. However, the level of luminescence signal detected by one-step ELISA in N-term NanoLuc SNAP25 LAN-5 cell line treated with 1 nM BoNT/C was very low (Figure 5.11 B). Although there is a difference between the signals from treated and untreated cells in N-term LAN-5 cells, it is not statistically significant. BoNT/C activity was tested with different antibody dilution ratios ranging from 1/50 to 1/5. The level of luminescence signal did not change with the use of higher concentrations of the antibody. This shows that the BoNT/A cleaved SNAP25 Ab has limited specificity for BoNT/C cleaved SNAP25 (Figure 5.11 C).

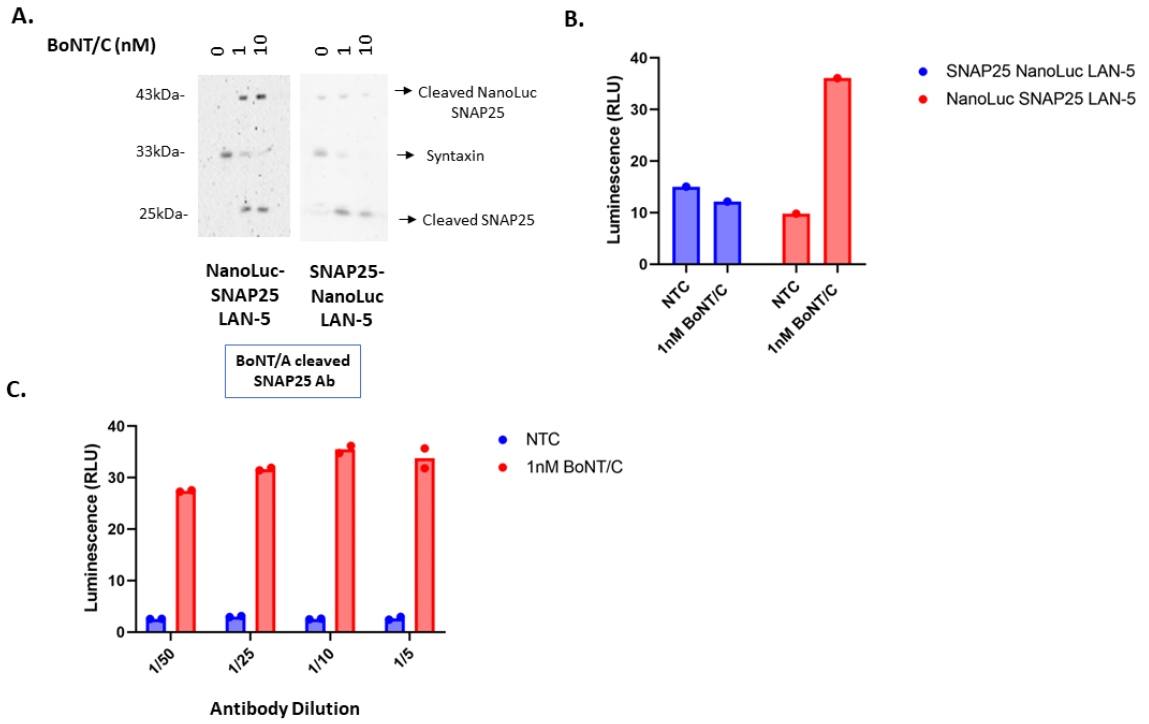

Figure 5.11 Cleaved NanoLuc SNAP25 was detectable by immunoblot but not effectively by one step ELISA.

A) *Immunoblot images showing the cleaved native SNAP25 and NanoLuc SNAP25 by BoNT/A cleaved SNAP25 Ab. BoNT/A cleaved SNAP25 Ab was added at 1:2000 dilution. Syntaxin antibody was added at 1:2000 dilution. Images were taken from ChemiDoc XRS.* ***B)*** *Bar chart showing NanoLuc SNAP25 detection using BoNT/A cleaved SNAP25 Ab at 1/10 dilution by one step ELISA after treatment with 1 nM BoNT/C.* ***C)*** *Bar chart showing NanoLuc SNAP25 detection with different dilutions of BoNT/A cleaved SNAP25 Ab by one step ELISA after treatment with 1 nM BoNT/C (n=2, ±experimental errors). Protein A plate was incubated with BoNT/A cleaved SNAP25 Ab with different dilution rates. The differentiated cells were treated with 1nM concentration of BoNT/C for 3 days. Cells were treated with the diluting agent (Opti-MEM, reduced serum media) as a no treatment control.*

Another cleaved SNAP25 antibody, a mouse monoclonal antibody which is specific for BoNT/C, was tested on N-term and C-term LAN-5 cell lines. However, the antibody did not work properly. It is because the antibody might have low affinity or be non-specific to the target. Another reason would be that the antibody might not be compatible with the methods of detection, which are ELISA and immunoblotting. The immunoblot image shows that only faint traces of cleaved NanoLuc SNAP25 and cleaved native SNAP25 were detected in N-term LAN-5 cells (Figure 5.12 A). Similar results were found for one-step ELISA tested on N-term NanoLuc SNAP25 LAN-5 cell lines. Although a difference was observed between treated and untreated cells, it was not significant because a very low level of signal was detected with BoNT/C antibody in treated cells (Figure 5.12 B). Moreover, the level of signal did not change with increasing concentrations of the antibody, indicating that the antibody affinity is very weak.

Protein A does not bind or weakly bind to immunoglobulins for some species, whereas another binding protein, Protein G, binds to immunoglobulins of most species but with a lower affinity (Page and Thorpe, 2009). Since the BoNT/C cleaved SNAP25 Ab is a mouse monoclonal antibody and Protein A shows low affinity for mouse immunoglobulins, Protein G was also examined to determine if it was more effective than Protein A in this case. However, the signal from Protein G plate was weaker than Protein A plate, confirming that the antibody has very low affinity for BoNT/C cleaved SNAP25 (Figure 5.12 C).

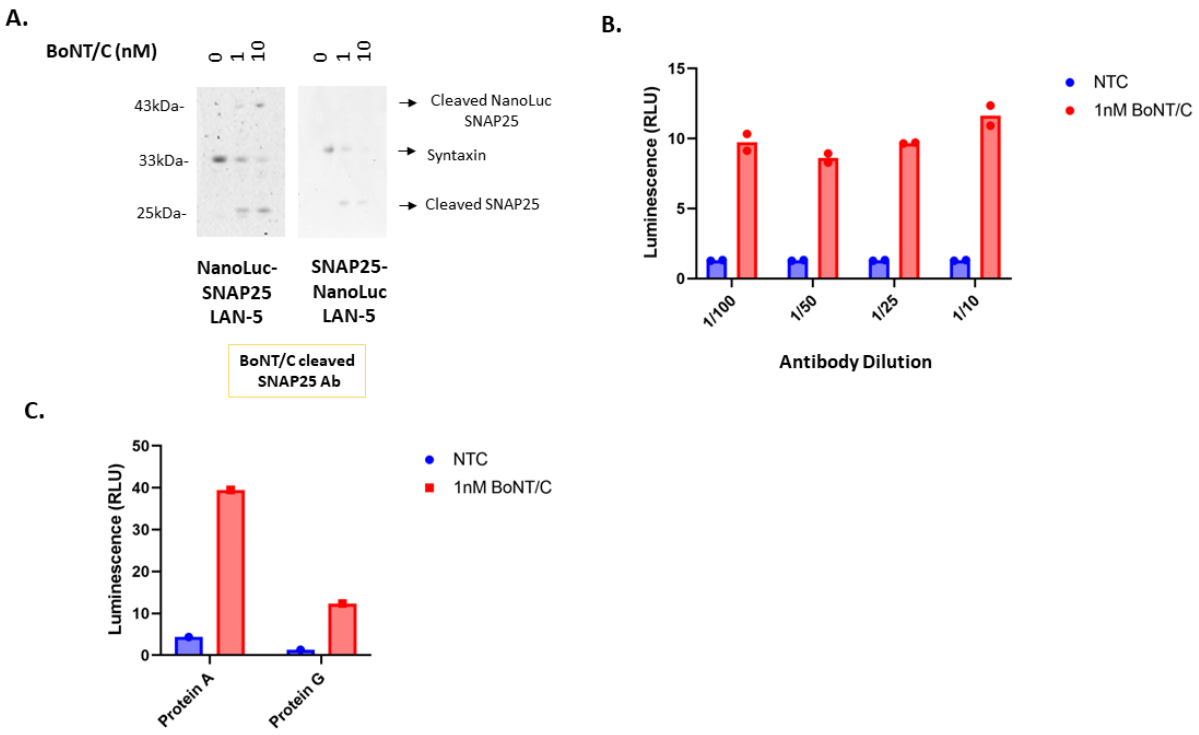

Figure 5.12 Mouse BoNT/C cleaved Ab did not detect efficiently cleaved SNAP25.

A) *Immunoblot images showing the cleaved native SNAP25 and NanoLuc SNAP25 by BoNT/C cleaved SNAP25 Ab. BoNT/C cleaved SNAP25 Ab was added at 1:2000 dilution. Syntaxin antibody was added at 1:2000 dilution. Images were taken from ChemiDoc XRS.* ***B)*** *Bar chart showing NanoLuc SNAP25 detection using BoNT/C cleaved SNAP25 Ab by one step ELISA (n=2, ±experimental errors). Protein A plate was incubated with BoNT/C cleaved SNAP25 Ab with different dilution rates.* ***C)*** *Bar chart showing NanoLuc SNAP25 detection by BoNT/C cleaved SNAP25 Ab in different protein plates. The plates were incubated with BoNT/C cleaved SNAP25 mouse monoclonal Ab at 1:10 dilution. The differentiated cells were treated with 1nM concentration of BoNT/C for 3 days. Cells were treated with the diluting agent (Opti-MEM, reduced serum media) as a no treatment control.*

Overall, the current one-step ELISA failed to detect BoNT/C activity effectively. However, NanoLuc SNAP25 LAN-5 cells are capable of being used for BoNT/C assays. In the presence of a strong affinity antibody for BoNT/C cleaved SNAP25, BoNT/C activity would increase significantly and a one-step ELISA would be successfully established for BoNT/C detection.

5.3 Discussion

For several reasons, cell-based assays are more effective than other assays. Apart from the mouse bioassay, they are the only test that enables the detection of all intoxication steps including binding, internalisation, translocation of the light chain, and cleavage of the target protein (Pellett et al., 2019). Moreover, most cell-based assays do not use animals, depending on the cell types. Additionally, the process is generally practical, requiring preparation of cells, incubation of the cells with toxins, and measuring the toxin activity (Pellett, 2013). Many cell-based assays have been developed for BoNT detection using a variety of cell lines and different endpoints.

In order to determine BoNT activity, one of the most specific endpoints is measuring cleaved SNARE, typically by western blotting or ELISA (Pellett, 2013). A substantial number of cell-based assays have been developed for the detection of BoNT/A using western blotting based on different types of cells, including primary neurons, mES-derived neurons, hiPSC-derived neurons, and continuous cell lines (Pellett et al., 2007, Kiris et al., 2011, Whitemarsh et al., 2012b, Hong et al., 2016). Although the western blot technique is the gold standard for many studies, it is time-consuming, highly variable, and only semi-quantitative. In comparison to western blot, ELISA has more advantages, such as being fully quantitative, reproducible, simpler, and cost-efficient (Kiris et al., 2014). ELISA also has the advantage of high-throughput screening and quality control validation, in contrast to western blot (Fernandez-Salas et al., 2012). Thus, ELISA has become more popular for cell-based assays and has been used for quantifying BoNT/A in a range of different cells (Fernandez-Salas et al., 2012, Yadirgi et al., 2017, Pellett et al., 2017). In this chapter, a novel cell-based assay for BoNT/A detection employing ELISA was described.

The first FDA approved cell-based assay employing ELISA to detect BoNT/A was developed by Fernandez Salas et al. (2012). For their sandwich ELISA based assay, they used two different SNAP25 antibodies, one for capturing cleaved SNAP25 and another that was tagged with a sulfo-tag for detection. Our one-step ELISA is slightly different from their sandwich ELISA and has more advantages in terms of the functional properties of the assay. The direct linkage of luciferase and SNAP25 in one-step ELISA may enable faster and more practical detection of BoNT/A activity because the one-step capture assays based on enzymatic reporters usually involve fewer wash steps and less incubation

time (Boutel et al., 2016, Rust et al., 2017). A comparison of two assays confirmed this finding. The sandwich ELISA assay requires overnight incubation of the lysate, whereas the one-step ELISA requires 1.5 hours of incubation of the lysate. Additionally, the NanoLuc enzyme reaction in a one-step ELISA takes five minutes as opposed to one hour with their antibody detection process.

However, even though our one-step ELISA is more efficient than the sandwich ELISA in terms of the assay process, the sandwich ELISA detected BoNT/A more sensitively than our assay. BoNT/A was detected at a level as low as 1.2 pM using differentiated SiMa cells in their assay while it was detected as low as 10 pM using differentiated LAN-5 cells in one-step ELISA. A variety of factors may contribute to the differences, such as the use of different types of cells, the differentiation time and media, the duration of treatment, and the specificity of the antibodies. Due to the fact that LAN-5 cells are more sensitive to BoNT/A than SiMa cells (Chapter 3, Table 3.1), SiMa cells are not the reason for higher sensitivity. Both assays have a similar differentiation time, but the medium components differ slightly. The SiMa cells were incubated with GT1b during differentiation, which may have increased the uptake of BoNT/A by the cells. It is also unlikely that the duration of BoNT/A treatment is the reason for the higher sensitivity since it is roughly the same in both assays. The main reason for more sensitive detection of BoNT/A would be the use of a more specific antibody in the sandwich ELISA. In their assay, the cleaved SNAP25 was captured strongly by a monoclonal antibody which was specific to only cleaved SNAP25 and did not show any cross-reactivity to intact SNAP25. However, our assay uses a polyclonal antibody to detect cleaved BoNT/A, which might have cross-reactivity or less binding affinity. In light of the fact that the affinity of antibodies to antigens plays a significant role in determining the sensitivity of an immunoassay, a highly specific and affinitive antibody would increase the signal significantly. Therefore, the main limitation of one-step ELISA for BoNT/A is currently the lack of a monoclonal antibody.

BoNT/A via ELISA was also detected in ES-derived- and hiPSC-derived neurons with the lowest detection of 0.02 U/well and EC50 value of 0.3 U/well, which allows more sensitive detection than SiMa and LAN-5 neuroblastomas (Pellett et al., 2017, Yadirgi et al., 2017). This significant rise in sensitivity resulted from the cell type because stem cell-derived neurons are much more sensitive to BoNT/A than continuous cell lines (Pellett, 2013). However, their maturation takes approximately 18 days and includes many steps, which limits their use in cell-based assays.

In addition to the detection of cleaved substrate, there are other endpoints that can be used to measure BoNT activity, including inhibition of neurotransmitter release and electrophysiological measurements (Pellett, 2013). BoNT/A was detected in SH-SY5Y neuroblastomas by measuring the inhibition of stimulated release of radiolabelled neurotransmitter with an IC50 of 5.56 ± 2.37 nM

(Purkiss et al., 2001). Similarly, neurosecretory vesicle release, which can be used to represent neurotransmitter release, was used to detect BoNT/A activity in SiMa neuroblastomas (Pathe-Neuschafer-Rube et al., 2015, Pathe-Neuschafer-Rube et al., 2018). The assay measured the inhibition of neurosecretory vesicle release, tagged with a reporter enzyme, by BoNT/A at concentrations as low as 1 pM. In a similar approach, blocking the release of pre-loaded FM-florescent dyes into synaptic vesicles in NT2 neurons upon BoNT/A treatment was also used to measure BoNT/A activity (Tegenge et al., 2012). Their assay measured BoNT/A activity at the lowest concentration of 66.67 pM.

Using inhibition of neurotransmitter release as an endpoint has an advantage since it does not limit the assay to a specific type of CNT, allowing for the detection of all serotypes with a single test. However, the inhibition of neurotransmitter release is not a very specific and direct endpoint in comparison to the detection of cleaved substrate. Furthermore, this endpoint is sensitive to a wide range of conditions affecting exocytosis and endocytosis. There are many potential factors, such as calcium and salt concentrations, ion channel inhibitors/activators, and temperatures that might affect exocytosis (Pellett et al., 2019). If pre-loaded dyes or radiolabelled neurotransmitters are used to measure exocytosis, the factors that impact endocytosis should also be considered.

Another significant endpoint is measuring the inhibition of synaptic transmission by BoNT, which serves as a surrogate for neurotransmitter paralysis in MBA. Using this endpoint, BoNT/A activity was measured at concentrations of varying from 0.005 pM to 1.67 pM in mES-derived neurons (Hubbard et al., 2015, Beske et al., 2016, Jenkinson et al., 2017). The sensitivity of this endpoint is significantly higher than substrate cleavage detected by western blotting for all tested CNTs (Beske et al., 2016). The loss of synaptic activity was detected with an IC50 of 0.05 pM, whereas cleaved SNAP25 was detected with an EC50 value of 0.71 pM for BoNT/A activity. Although it is a physiological endpoint of intoxication and very sensitive, many factors affect the endpoint measurement including ion and salt concentrations, temperature, inhibitors/inducers of signal transmission (Pellett et al., 2019). Additionally, it commonly requires the use of mES neurons, which makes the use of synaptic activity as an endpoint impractical.

Direct detection of cleaved substrate is generally the most common and more specific endpoint utilized in the current one-step ELISA assay. With the one-step ELISA, BoNT/A activity was measured by detecting cleaved SNAP25 in a practical and sensitive manner; however, the assay has some limitations depending on the method used. In order to have consistent protein concentration in cell lysates, the same number of cells need to be seeded per well because it is a concentration-dependent method. The challenge comes when the cells clump together and are not separated, resulting in an inaccurate cell count. For this reason, DC assays for determining protein concentration or a second

ELISA step for measuring control protein should be added to ensure the same amount of protein is loaded and normalize the results.

Either detection of a loading protein like beta actin or full-length SNAP25 could be used to get reliable results from an ELISA-based test. Recently, Nuss et al., (2010) developed a rabbit polyclonal BoNT/A cleavage-sensitive antibody that only recognizes full-length SNAP25, and developed an ELISA capture assay, which quantifies the amount of full-length SNAP25. Their capture ELISA could be used to measure the percentage of full-length SNAP25 in lysates, which would serve as a standard in ELISA-based tests.

In this study, Western blot and ELISA were performed in parallel for many experiments. The sensitivity of ELISA and western blotting for BoNT/A was not compared, contrary to other studies (Pellett et al., 2017). Because without having a control protein and normalisation of the results for ELISA, the comparison would be less reliable. In western blot, % SNAP25 cleavage was calculated by cleaved SNAP25 versus uncleaved SNAP25 or cleaved SNAP25 was normalised by a loading protein, Syntaxin. However, only cleaved SNAP25 was measured in ELISA. Due to this, it may not be possible to obtain a reliable result from the comparison.

The current one-step ELISA was unable to properly detect BoNT/C activity due to the lack of a specific BoNT/C cleaved SNAP25 antibody. However, it appears that, with more work, the current one-step ELISA has the potential to detect BoNT/C in a practical and sensitive manner. Detecting BoNT/C sensitively is crucial because it causes botulism in animals and is similarly dangerous for humans (Moura et al., 2011). A sensitive assay specific for BoNT/C detection is required for both diagnosis of botulism and validation of toxoid vaccines for animals. Therefore, modifying the assay for BoNT/C is something that needs to be done in future work.

All in all, with the development of sensitive and specific monoclonal antibodies for both BoNT/A and BoNT/C, the current sensitivity would improve significantly for BoNT/A and BoNT/C activity could be detectable in one-step ELISA. Additionally, having a standard to normalise the results would provide a more reliable and reproducible assay.

6 Chapter 6: General Discussion

In spite of the fact that BoNTs are extremely poisonous, they have been used for cosmetic purposes for many years (Patil et al., 2016). Moreover, very small amounts of BoNT can cause botulism, a rare but deadly disease. Therefore, they need to be tested in a sensitive manner and currently the most sensitive assay is the mouse bioassay (Adler et al., 2010). Additionally, potential residual TeNT activity needs to be tested for in produced TeNT vaccines, which is typically done using guinea pigs (Greenberg et al., 1943). Although animal tests are highly sensitive to detect CNTs, they have serious limitations such as being time-consuming, laborious, expensive, and most importantly requiring the sacrifice of many animals for one test. Therefore, there is a huge demand to develop a replacement assay for CNTs testing, and cell-based assays would be ideal candidates for their replacement for several reasons. They are generally capable of testing toxins in a faster, simpler, cheaper, and reproducible manner (Pellett et al., 2019). Moreover, cell-based assays reflect all of the steps of intoxication, which is essential for a replacement assay. However, *in vitro* cell based assays still cannot determine pharmacodynamic and pharmacokinetic properties of the toxins, which is an essential part of *in vivo* assay.

The major aim of this thesis is the development of replacement cell-based assays for detection of CNTs. Human SiMa neuroblastoma cells were previously tested and found to be sensitive to BoNT/A and BoNT/B detection (Fernandez-Salas et al., 2012, Rust et al., 2017). In my thesis, I continued investigating SiMa neuroblastoma as well as introducing LAN-5, a novel human neuroblastoma cell line for testing the activity of CNTs. According to my results, both SiMa and LAN-5 neuroblastomas are highly sensitive to detecting CNTs. SiMa was found to be more sensitive to BoNT/A detection than other continuous cell lines, PC12, Neuro-2a, and LA1-55n, SH-SY5Y (Purkiss et al., 2001, Fernandez-Salas et al., 2012). However, LAN-5 outperformed SiMa cells by detecting BoNT/A with the lowest concentration of 0.001 nM. Similarly, BoNT/DC activity was tested more sensitively in LAN-5 cells than in P19 and SiMa cells (Tsukamoto et al., 2012). SiMa and LAN-5 neuroblastomas can be differentiated within 3 days, which makes them more advantageous than most of the other continuous cell lines. For example, differentiation of SH-SY5Y neuroblastomas takes 18 days, and NG108-15 cells are differentiated at least for 5 days (Whitemarsh et al., 2012a, Shipley et al., 2016).

The limitation of SiMa and LAN-5 neuroblastoma cell lines is that they are not the most sensitive cells for the detection of CNTs. Primary neurons and stem cell-derived neurons (mouse ES-derived neurons and motor neurons, hiPSC-derived neurons) are considerably more sensitive than SiMa and LAN-5 neuroblastomas for BoNT/A and BoNT/B detection (Pellett et al., 2007, McNutt et al., 2011, Whitemarsh et al., 2012b). However, stem-cell-derived neurons and primary neurons have other

serious limitations that make them inadequate for a reproducible and fast cell-based assay. Their maturation takes about 2-3 weeks and has more maturation steps. Moreover, primary neurons and mouse-ES-derived neurons are not composed of homogenous neurons, so assay reproducibility is likely to be low. Culture handling is quite difficult for both primary neurons and mouse-ES-derived neurons. And animals must still be sacrificed animals in order to obtain primary neurons (Pellett, 2013, Kiris et al., 2014). On the other hand, SiMa and LAN-5 cells are easier to culture, differentiate quickly within 3 days, and are reproducible. As they are easy to manipulate, their sensitivity could be enhanced by the addition and transduction of desired receptors into the assays and the cells. Transduction of SYTII receptors to LAN-5 cells enhanced BoNT/B sensitivity significantly, as demonstrated in this study. Moreover, exogenous GT1b addition improved the sensitivity of LAN-5 cells to BoNT/A, BoNT/B and BoNT/C.

Although LAN-5 and SiMa are both appropriate cell lines for cell-based assays of CNTs, there are a few properties that make LAN-5 cells more favourable. The clumpy nature of SiMa cells makes them difficult to handle in cell culture and therefore difficult to differentiate, whereas LAN-5 cells are easier to culture and differentiate. Moreover, undifferentiated LAN-5 cells seem to already display some neuronal properties, such as neuronal processes, in contrast to undifferentiated SiMa cells. Later, it was also found that undifferentiated LAN-5 cells express the required receptors for CNT entry and they were sensitive enough to detect BoNT/A, BoNT/B, BoNT/C, and BoNT/DC. Furthermore, LAN-5 cells are slightly more sensitive than SiMa cells for the detection of BoNT/A, BoNT/C, BoNT/DC, and TeNT. Additionally, since SiMa cells have a patent issue, the majority of my research was conducted using human neuroblastoma LAN-5 cells.

In addition to neuroblastoma cells, a non-neuronal cell line, HeLa cells, was re-engineered to be sensitive to BoNT/B. After transduction of SYTII, BoNT/B cleaved VAMP2 was successfully detected in the cells, confirming that SYTII is an essential receptor for BoNT/B activity. These re-engineered HeLa cells are less sensitive than LAN-5 cells but offer faster and easier detection of BoNT/B because the differentiation step is not necessary. As a result, they may be used for detecting concentrated samples where highly effective detection of BoNT/B is not required.

An invaluable contribution of this research is the introduction of the novel cell line, LAN-5, into a cell-based assay platform for the detection of CNTs. Moreover, the sensitivity of one-step ELISA that was previously developed by Rust et al. (Rust et al., 2017) for BoNT/B detection was enhanced by using SYTII-NanoLuc VAMP2 LAN-5 cells. Furthermore, the one-step ELISA was modified for BoNT/A detection by generating NanoLuc SNAP25 LAN-5 cells, resulting in a novel ELISA cell-based assay for BoNT/A. The FDA approved sandwich ELISA assay, using SiMa cells, detects BoNT/A more sensitively

than the one-step ELISA (Fernandez-Salas et al., 2012). However, the one-step ELISA has more advantages in terms of its operating procedure and testing time. There are also a couple of potential ways to enhance the sensitivity of the one-step ELISA for BoNT/A in the future. First, since we are currently using a polyclonal BoNT/A cleaved Ab for the one-step ELISA, development of a monoclonal Ab could increase the specificity and sensitivity of the assay. Secondly, SV2 proteins could be transduced into LAN-5 cells to make the cells more sensitive to BoNT/A and improve sensitivity.

In conclusion, the new cell line, human LAN-5 neuroblastoma, is an appropriate candidate for replacement assays for sensitively detecting BoNT/A, BoNT/B, BoNT/C, BoNT/DC, and TeNT. The low sensitivity to BoNT/D could be improved by transduction of LAN-5 cells with SV2 receptors and exogenous addition of specific gangliosides for BoNT/D entry. For one-step ELISA detection of BoNT/D and BoNT/DC, NanoLuc VAMP2 LAN-5 cells could be employed after development of a specific antibody for BoNT/D cleavage. Similarly, developing a sensitive, BoNT/C cleaved SNAP25 specific antibody would allow NanoLuc SNAP25 LAN-5 cells to be used to detect BoNT/C via one-step ELISA. This thesis demonstrates that LAN-5 cells are suitable cells and one-step ELISA is convenient and fast method for CNT detection, showing them both together offers the development of replacement cell-based assays for most CNTs.

6.1 Future directions for clostridial neurotoxin testing

There is an increasing demand for both therapeutic and cosmetic use of BoNT. Thus, there is no doubt that CNTs and sensitive testing of CNTs will continue to be hot topics and a focus in the scientific area for quite some time to come. With the advancement of CNT research, the current understanding of CNT intoxication and pathways may be able to be improved in the near future (Kiris et al., 2014). There is a possibility that this might allow the identification of new areas of CNT use the has the potential to provide new therapeutic benefits and may also allow the further development of CNT testing. In light of the fact that cell-based assays offer many advantages, such as being practical, cheap, fast, and suitable for high-throughput screens, researchers will primarily work on developing a sensitive cell-based assay that replaces the mouse bioassay. Cell-based assays have improved significantly, especially for BoNT/A and BoNT/B serotypes in recent years since they are the most commonly used serotypes as pharmaceuticals (Fernandez-Salas et al., 2012, Rust et al., 2017). However, other BoNT serotypes may soon be used as therapeutic agents since there might be more patients who develop resistance to BoNT/A and BoNT/B and do not respond to them. Therefore, the focus will shift to other serotypes for sensitive cell-based tests.

In order to improve cell-based assays, it is expected that there will be a great deal of improvement mainly in three areas: cells, antibodies and immunoassay technologies. Advanced cellular models might be available through improved neuronal differentiation protocols and the generation of novel cell lines. With more efficient differentiation protocols, differentiation will be optimised and performed with a reduced number of steps in a shorter time period, making it more practical and easier to handle. Moreover, a number of novel cell lines will be generated by viral transduction of several CNT receptor proteins, resulting in more sensitive cell lines. Furthermore, most cell lines consist of heterogeneous subpopulations of cells, all of which are different in their sensitivity to CNTs. Therefore, characterisation of subpopulations on the basis of their levels of gene expression relative to CNTs and subsequent selection of the most sensitive subpopulation will be a central focus for each cell line used for CNT testing. As a result of homogeneous cell populations, more sensitive, reproducible and sustainable tests will be possible in the future. In addition to advances in the field of cells, technological developments in immunoassays as well as combining multiple immunoassays may improve CNT testing. It is also expected that antibody studies will contribute to the development of more efficient, specific-targeted antibodies targeted at CNT tests, which will lead to improved CNT detection in the future.

To conclude, it is expected that developments in cell, antibody and immunoassay technologies will improve cell-based assays for CNT testing and provide rapid and more sensitive detection of toxins, thus reducing the need for animals to be subjected to CNT testing in the future.

Appendix 1: Re-engineered botulinum molecules, called BiTox, can be detected sensitively in differentiated SiMa neuroblastomas

Introduction

Novel BoNT derivatives have been developed to treat a variety of medical conditions. As discussed in detail in section 1.3, the BiTox molecules are one type of these reengineered molecules, which are produced by reassembling the domains of CNTs using a 'stapling technique'. These molecules were tested in differentiated NanoLuc VAMP2 SiMa cells for their biological activity.

Material and methods

Reengineered toxins, BiTox molecules, were diluted with 0.4 % OG (Octyl β-D-glucopyranoside (OG) Sigma/ 08001), which helps SNARE complex formation, in Buffer A. Table A1.1 shows tested re-engineered BiTox molecules in differentiated NanoLuc VAMP2 SiMa cell line.

Toxins	Source	Supplier
BiTox/A; BiTox/AA	Recombinant	Expressed and purified by Dr Charlotte Leese
BiTox/C; BiTox/CC	Recombinant	Expressed and purified by Dr Charlotte Leese
BiTox/D; BiTox/DD	Recombinant	Expressed and purified by Dr Charlotte Leese
BiTox/E; BiTox/EE	Recombinant	Expressed and purified by Dr Charlotte Leese
Tet-Bot; 2x Tet-Bot	Recombinant	Expressed and purified by Dr Charlotte Leese

Table A1. 1 Details of toxins and reengineered BiTox molecules used.

Results

Re-engineered BiTox molecules were produced with either one binding domain or two binding domains (Figure A1.1 A). There are several different BiTox molecules named depending on which and binding domains serotype (Rbd) they were made with and how many copies of it they are carrying (Figure A1.1 B). However, all BiTox molecules have the proteolytic domain and translocation domain of BoNT/A (LcTd/A). These new molecules show lower paralysis activity than BoNT/A, which would be beneficial for migraine treatment. Therefore, these re-engineered molecules are candidate therapeutics for pain treatment, and they have to be tested to find safe doses before they can be used as medicines. Here, toxin activity of these molecules was tested in the differentiated NanoLuc VAMP2

SiMa cell line. As a result, differences in toxin potency were identified both among different BiTox molecules and between single and double versions of a BiTox molecule. Our results showed the differentiated NanoLuc VAMP2 SiMa cell line was sensitive enough to determine toxin activity and the differences between BiTox molecules.

Furthermore, CNT domains were examined in GFP-VAMP2 LAN-5 cells to see if the full toxin structure is required to see toxin activity. To demonstrate this, the neurotoxin domains, LcTd/A and Rbd/A, and full toxin, BoNT/A, were tested in differentiated LAN-5 cells. It was found that SNAP25 cleavage was not seen when the cells were treated with either LcTd/A or Rbd/A, while cleaved SNAP25 was detected when the cells were treated with BoNT/A. This means that a full toxin is required to see toxin activity (Figure A1.1 C).

A.

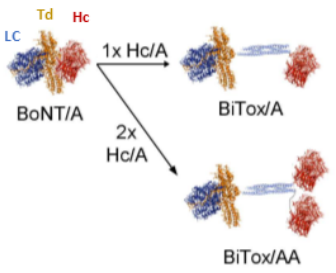

B.

BiTox molecules	Proteolytic domain (LC)-Translocation domain (Td)	Binding Domain (Hc)
BiTox-A	LcTd/A	1x Hc/A
BiTox-AA	LcTd/A	2x Hc/A
BiTox-C	LcTd/A	1x Hc/C
BiTox-CC	LcTd/A	2x Hc/C
BiTox-D	LcTd/A	1x Hc/D
BiTox-DD	LcTd/A	2x Hc/D
BiTox-E	LcTd/A	1x Hc/E
BiTox-EE	LcTd/A	2x Hc/E
Tet-Bot	LcTd/A	1x Hc/Tet
2xTet-Bot	LcTd/A	2x Hc/Tet

C.

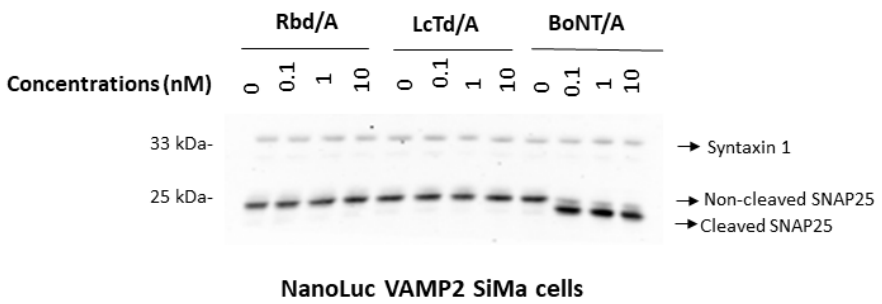

Figure A1. 1 BiTox molecules were reengineered by recombining the domains of CNTs.

A) *Schematic representation of reengineered BiTox molecules. Proteolytic-translocation domain of BoNT/A (Lc-Td/A) is reassembled with one binding domain of BoNT/A (1x HC/A) and two binding domains of BoNT/A (2x HC/A) forming BiTox/A and BiTox/AA, respectively. 3D image was created by Dr. Charlotte Leese.* ***B)*** *Table showing several BiTox molecules, which differ from each other by having different binding domain serotypes.* ***C)*** *Western blot result showing the proportion of cellular cleaved SNAP25 in differentiated GFP-VAMP2 LAN-5 neuroblastomas following treatment with titrated BoNT/A, LcTd/A and Rbd/A for 72 hrs. As no cleavage is seen with LcTd/A or Rbd/A, it can be concluded that the full toxin construct is required to see toxin activity.*

48-hr treatment is the ideal time to see higher activity of BiTox molecules and additional binding domain causes earlier onset of toxin activity based on BiTox-C and BiTox-CC results.

An ideal toxin treatment duration is important not only to get the highest efficiency, but also to get the result faster. Therefore, BiTox-C and BiTox-CC molecules were investigated to see when the toxin activity started at the earliest, and to determine the ideal duration of treatment. According to immunoblot result, cleaved SNAP25 was only seen when cells were treated with BiTox-C for 24-hr and 48-hr. SNAP25 was not detected when the treatment time was less than 24 hours (Figure A1.2 A). As for BiTox-CC, cleaved SNAP25 started to be observed after 6-hr treatment, showing that an additional receptor binding domain sped up the onset of toxin activity (Figure A1.2 B). As seen in the graph

(Figure A1.2 C), the cleaved amount of SNAP25 significantly increased from 6-hr treatment to 24-hr treatment for both BiTox-C and BiTox-CC molecules and continued to increase slightly after 48-hr. Therefore, the ideal treatment time was determined to be 48-hr for BiTox molecules, and all BiTox molecules were treated in the cells for 48-hr unless indicated.

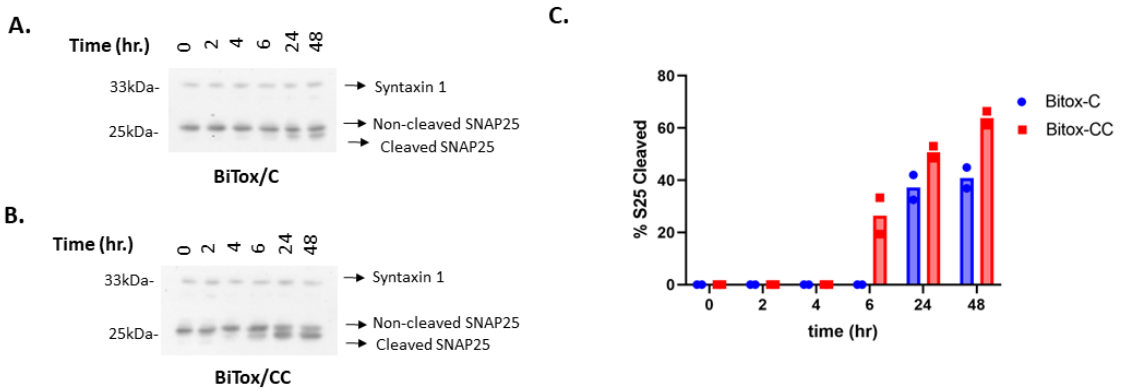

Figure A1. 2 Additional receptor binding domain causes earlier onset of toxin activity; 48-hr treatment is ideal to get better results.

A-B) *Representative immunoblots showing the proportion of cellular cleaved SNAP25 in differentiated SiMa neuroblastoma cells following application of BiTox-C and BiTox-CC molecules. The concentration of 2nM BiTox molecules were used to treat cells for 48-hours. Cells were treated with diluting agent (0.4% Octyl β-D-glucopyranoside buffer) as a no treatment control. Syntaxin antibody was used at 1:2000 dilution as a control. SNAP25 antibody was added at 1:4000 dilution to detect cleaved and uncleaved SNAP25. Images were taken using ChemiDoc XRS.* ***C)*** *Graph comparing the quantification of immunosignals, (n=2, experimental errors).*

Additional binding domain increases the toxin potency for most of BiTox molecules.

Single and double binding versions of BiTox molecules were tested in differentiated NanoLuc VAMP2 SiMa cells to determine the differences in toxin activities. The lowest concentrations that cleaved SNAP25 was observed at was 0.1 nM for BiTox-A and 0.001 nM for BiTox-AA (Figure A1.3 A-B). The amounts of cleaved SNAP25 were significantly increased at molecule concentrations of 0.1 nM, 0.01 nM, and 0.001 nM when the additional receptor binding was involved (Figure A1.3 C). The EC50 value of BiTox-AA was 0.037 nM (0.8070 R^2, 0.005587 to 0.2988 95%CI), which is considerably lower than the EC50 value of BiTox-A, 0.091 nM (0.8711 R^2, 0.02432 to 0.4071 95%CI).

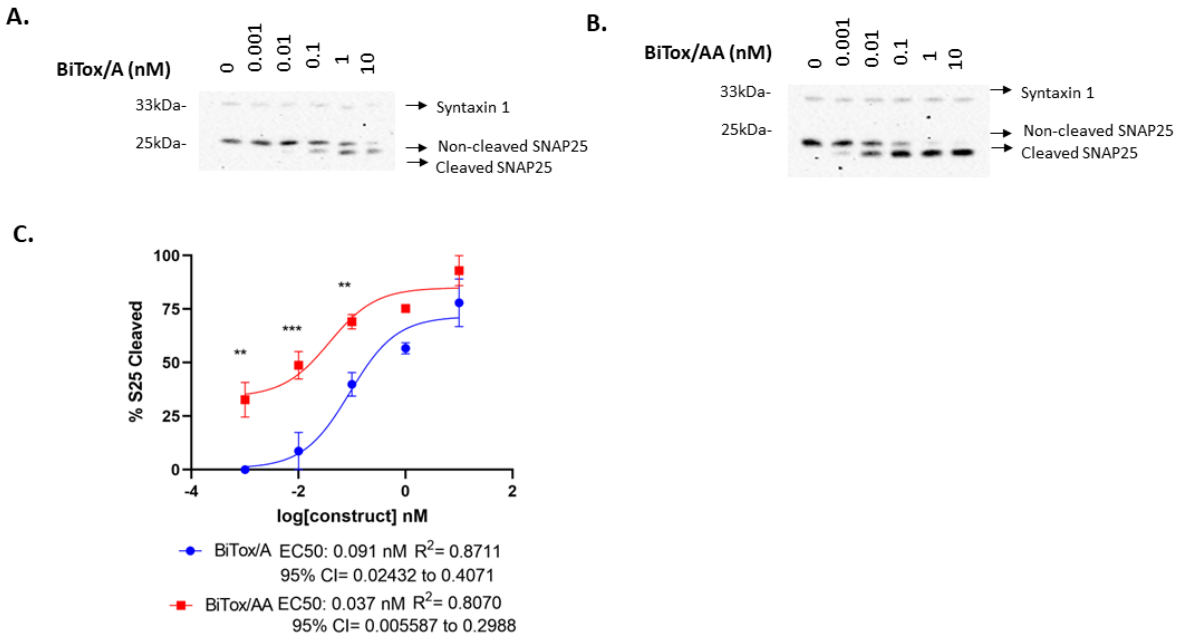

Figure A1. 3 BiTox-AA is significantly more potent than BiTox-A.

A-B) *Representative immunoblots showing the proportion of cellular cleaved SNAP25 in differentiated SiMa neuroblastoma cells following application of BiTox/A and BiTox/AA molecules. Toxins were titrated in 1:10 dilution and used to treat cells for 48-hours. Cells were treated with diluting agent (0.4% Octyl β-D-glucopyranoside buffer) as a no treatment control. Syntaxin antibody was used at 1:2000 dilution as a control. SNAP25 antibody was added at 1:4000 dilution to detect cleaved and uncleaved SNAP25 cleavage. Images were taken using ChemiDoc XRS.* ***C)*** *Graph comparing the quantification of immunosignals, (n=3, ± SEM). Multiple comparisons were examined by a two-way ANOVA analysis and alpha P values of <0.05 were considered statistically significant. **=P<0.01; ***=P<0.001.*

Regarding TetBot molecules, they showed significant toxin activity, similar to BiTox-A and BiTox-AA molecules. the lowest concentration cleaved SNAP25 was seen at was 0.1 nM for TetBot, whereas it 0.001 nM for 2xTetBot (Figure A1.4 A-B). The cleaved amount of SNAP25 was significantly higher for the double binding version at a concentration of 0.01 nM (Figure A1.4 C). Also, EC50 value decreased from 0.05 nM with 0.9035 R^2 and 0.01948 to 0.1751 95%CI (TetBot) to 0.006 nM with 0.6690 R^2 and unknown to 0.7412 95%CI (2xTetBot).

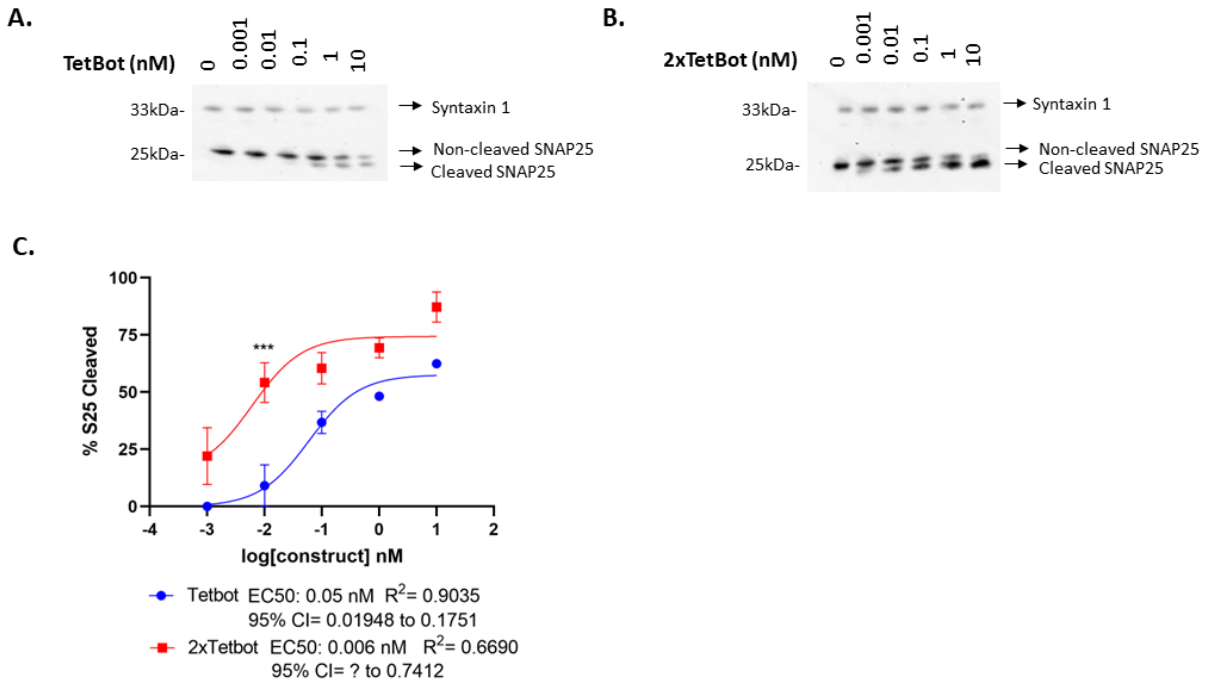

Figure A1. 4 2xTetBot is considerably more potent than TetBot.

A-B) *Representative immunoblots showing the proportion of cellular cleaved SNAP25 in differentiated SiMa neuroblastoma cells following application of TetBot and 2xTetBot molecules. Toxins were titrated in 1:10 dilution and used to treat cells for 48-hours. Cells were treated with diluting agent (0.4% Octyl β-D-glucopyranoside buffer) as a no treatment control. Syntaxin antibody was used at 1:2000 dilution as a control. SNAP25 antibody was added at 1:4000 dilution to detect cleaved and uncleaved SNAP25 cleavage. Images were taken using ChemiDoc XRS.* ***C)*** *Graph comparing the quantification of immunosignals, (n=3, ± SEM). Multiple comparisons were examined by a two-way ANOVA analysis and alpha P values of <0.05 were considered statistically significant. ***=P<0.001.*

BiTox-DD also showed more potency compared to its single domain version, BiTox-D (Figure A1.5 A-B). However, the toxin activity of both molecules was not high. For both molecules, a remarkable amount of SNAP25 cleavage was observed only at 10 nM and 1nM concentrations. No significance was observed between molecules but EC50 value decreased from 0.96 nM with 0.9401 R^2 and 0.2859 to 3.086 95%CI (BiTox-D) to 0.27 nM with 0.5770 R^2 and unknown 95%CI (BiTox-DD) (Figure A1.5 C).

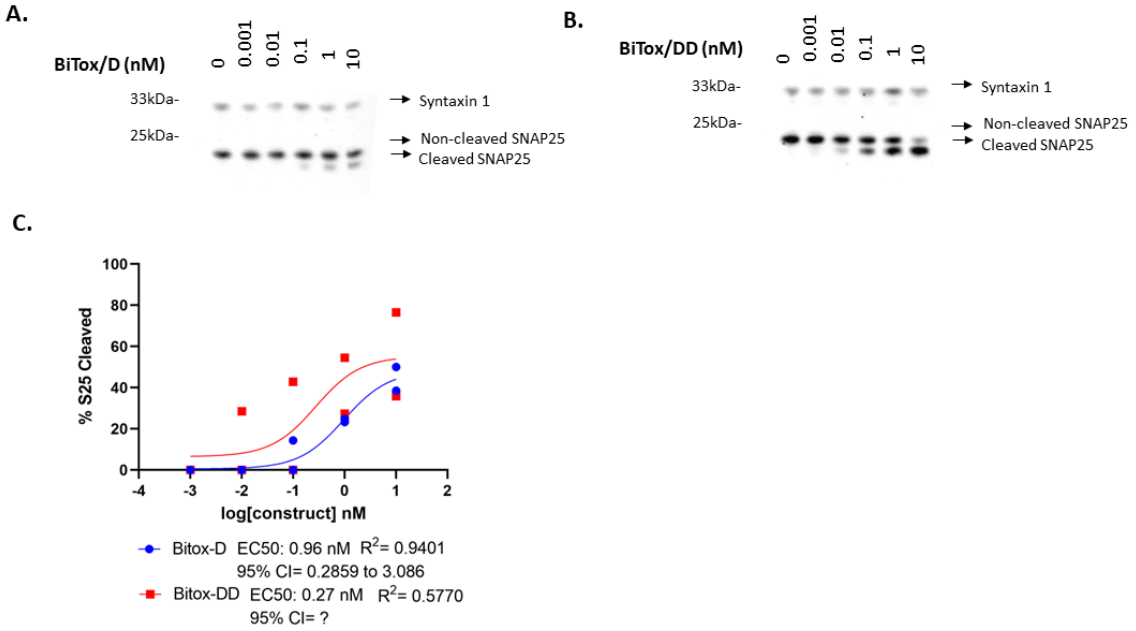

Figure A1. 5 BiTox-DD is more potent than BiTox-D.

A-B) *Representative immunoblots showing the proportion of cellular cleaved SNAP25 in differentiated SiMa neuroblastoma cells following application of BiTox-D and BiTox-DD molecules. Toxins were titrated in 1:10 dilution and used to treat cells for 48-hours. Cells were treated with diluting agent (0.4% Octyl β-D-glucopyranoside buffer) as a no treatment control. Syntaxin antibody was used at 1:2000 dilution as a control. SNAP25 antibody was added at 1:4000 dilution to detect cleaved and uncleaved SNAP25 cleavage. Images were taken using ChemiDoc XRS.* ***C)*** *Graph comparing the quantification of immunosignals, (n=2, experimental errors).*

When considering BiTox-C and BiTox-CC molecules, the double-bound version cleaved SNAP25 at concentrations of 1 nM and 0.1 nM, while the single-bound version only slightly cleaved SNAP25 at a concentration of 1 nM (Figure A1.6 A-B). Although neither molecules showed strong toxin activity, BiTox-CC was more effective than BiTox-CC.

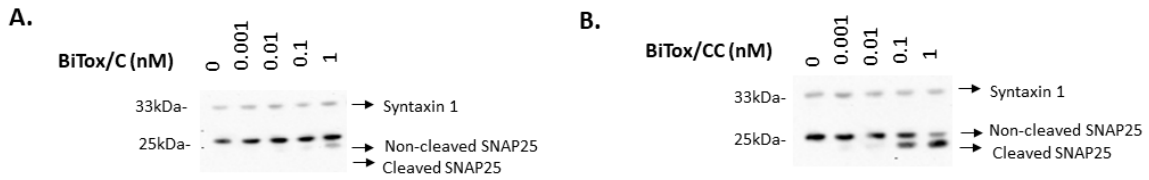

Figure A1. 6 BiTox-CC is more potent than BiTox-C.

A-B) *Representative immunoblots showing the proportion of cellular cleaved SNAP25 in differentiated SiMa neuroblastoma cells following application of BiTox-C and BiTox-CC molecules. Toxins were titrated in 1:10 dilution and used to treat cells for 48-hours. Cells were treated with diluting agent (0.4% Octyl β-D-glucopyranoside buffer) as a no treatment control. Syntaxin antibody was used at 1:2000 dilution as a control. SNAP25 antibody was added at 1:4000 dilution to detect cleaved and uncleaved SNAP25 cleavage. Images were taken using ChemiDoc XRS.*

For BiTox-E and BiTox-EE, no differences were observed between the single and double binding versions for toxin activity (Figure A1.7 A-B). This was an unusual result compared to the other BiTox molecules evaluated, as the double binding versions of each molecule showed stronger activity than the single binding versions. This may be explained by the fact that SiMa cells can only express protein receptors of the receptor binding site of BoNT/E in small amounts.

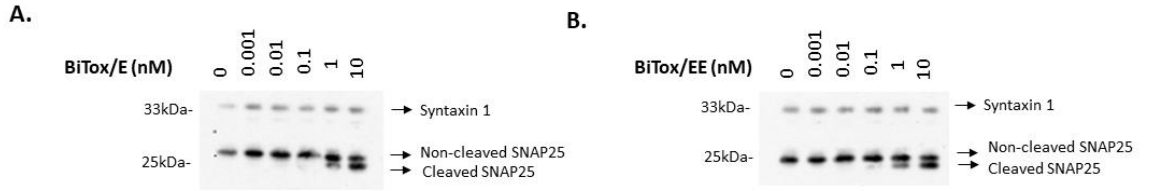

Figure A1. 7 BiTox-E and BiTox-EE have similar potency.

A-B) *Representative immunoblots showing the proportion of cellular cleaved SNAP25 in differentiated SiMa neuroblastoma cells following application of BiTox-E and BiTox-EE molecules. Toxins were titrated in 1:10 dilution and used to treat cells for 48-hours. Cells were treated with diluting agent (0.4% Octyl β-D-glucopyranoside buffer) as a no treatment control. Syntaxin antibody was used at 1:2000 dilution as a control. SNAP25 antibody was added at 1:4000 dilution to detect cleaved and uncleaved SNAP25 cleavage. Images were taken using ChemiDoc XRS.*

Conclusion

NanoLuc SiMa cell line is sensitive to detecting BiTox molecules as well as distinguishing the potency between single binding and double binding BiTox molecules. Moreover, it was successfully demonstrated that additional binding receptor resulted in an earlier onset of toxin activity, as well as enhancing the potency. Out of the Bitox molecules tested, the NanoLuc SiMa cell line was found to be most sensitive to BiTox-AA and 2xTetBot.

Appendix 2: Evaluating commercial human induced pluripotent stem cells (hiPSCs) for botulinum neurotoxins

Introduction

Human induced pluripotent stem cells (hiPSCs) were investigated for sensitivity to BoNTs. Commercial hiPSCs cells, grown in special media, were differentiated into sensory neurons for 8 days. The hiPSCs derived sensory neurons were characterised in terms of relative gangliosides, receptor proteins and target proteins, which are necessary for BoNT sensitivity. Followingly, they were tested for BoNT/A, BoNT/B, and BoNT/D sensitivity.

Material and methods

The plates, 96-well plates (Greiner bio-one, 655090) and 48-well plates (Thermo Fisher Scientific, 150687) were coated with 0.01 % Poly-l-ornithine (Sigma P3655, 10 mg/ml) and kept overnight at room temperature. The following day, after aspiration and rinsing with dH_2O, it was coated with 0.1 mL/cm2 Chrono^{TM} matrix 3, which is 1:100 diluted in PBS. The plate was covered with parafilm and incubated overnight at 4 C°. The following day, after cells (IPS-Chrono^{TM} sensory neurons, ANATOMIC) were thawed in DMEM/F12 media (Gibco), they were resuspended in maturation media (ChronoTM senso-MM), which was pre-warmed at room temperature. As the company recommends a cell density of 100.000 cells/cm2, the cells were counted accordingly and seeded twice more than required because half of the cells are expected to die within 1-2 weeks. Seeded cells were cultured at 37 C°, 5% CO_2, and 95% humidity. The brightfield image of the cells after cultured for 1 day is shown in Figure A2.1 A. After plating the cells, they were fed the maturation medium once every two days. The cells grew neurites and matured into sensory neurons after 8 days (Figure A2.1 B). After 8 days, some of the cells were incubated with BoNT/A, BoNT/B and BoNT/D for 3 days. The cells used for immunocytochemistry were treated with 1 nM concentration of the toxins. For western blot, the cells were treated with 10 nM concentration of the toxins by the addition of 50 µg/mL GT1b. After 3-day incubation of the toxins, the cells were collected for either western blotting or used for immunohistochemistry methods explained in detail in Chapter 2.

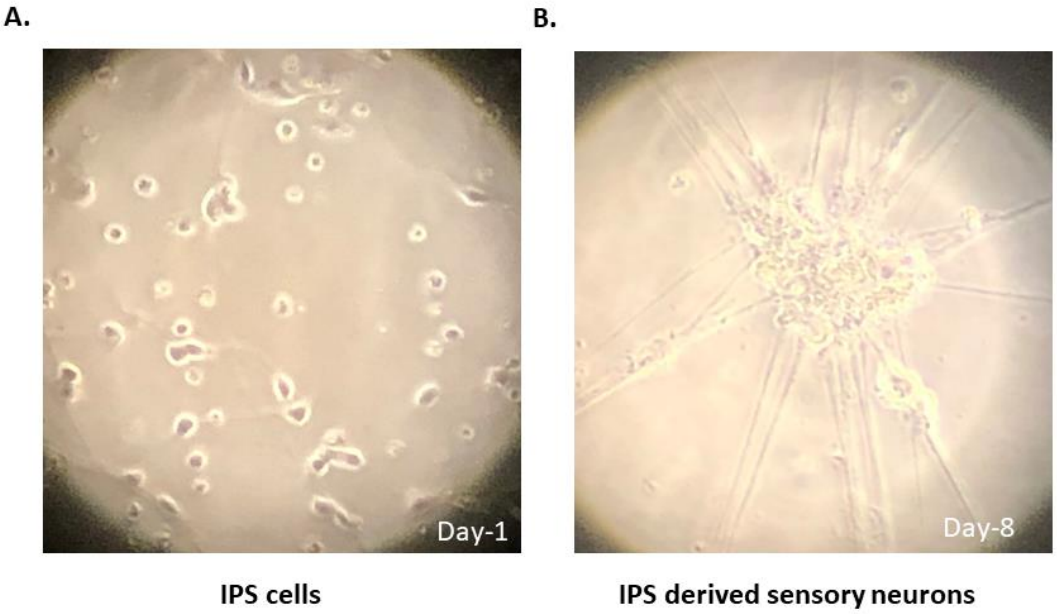

Figure A2. 1 HiPSCs were maturated into sensory neurons within 8 days.

A) *Brightfield image showing the cells after seeding for 1 day.* ***B)*** *Brightfield image showing the cells grew neurites and differentiated into sensory neurons after 8 days.*

Results

HiPSCs derived sensory neuron cells express gangliosides, receptor, and target proteins necessary for BoNT entry.

After maturation of hiPSCs to sensory neurons, the cells were characterised for specific target and receptor proteins, and gangliosides which are necessary for BoNT activity. SNAP25, the target protein of BoNT/A and BoNT/C, was extensively stained in the cells (Figure A2.2 A). VAMP2, the target protein of BoNT/B, BoNT/D, BoNT/DC, and TeNT was also detected in the cells (Figure A2.2 A). There was a significant level of GD2 and GT1b expression in the cells, while GD1a expression was very low (Figure A2.2 B). It was also found that SYTI and SV2-pan receptor proteins were expressed in the cells, but not SYTII (Figure A2.2 C).

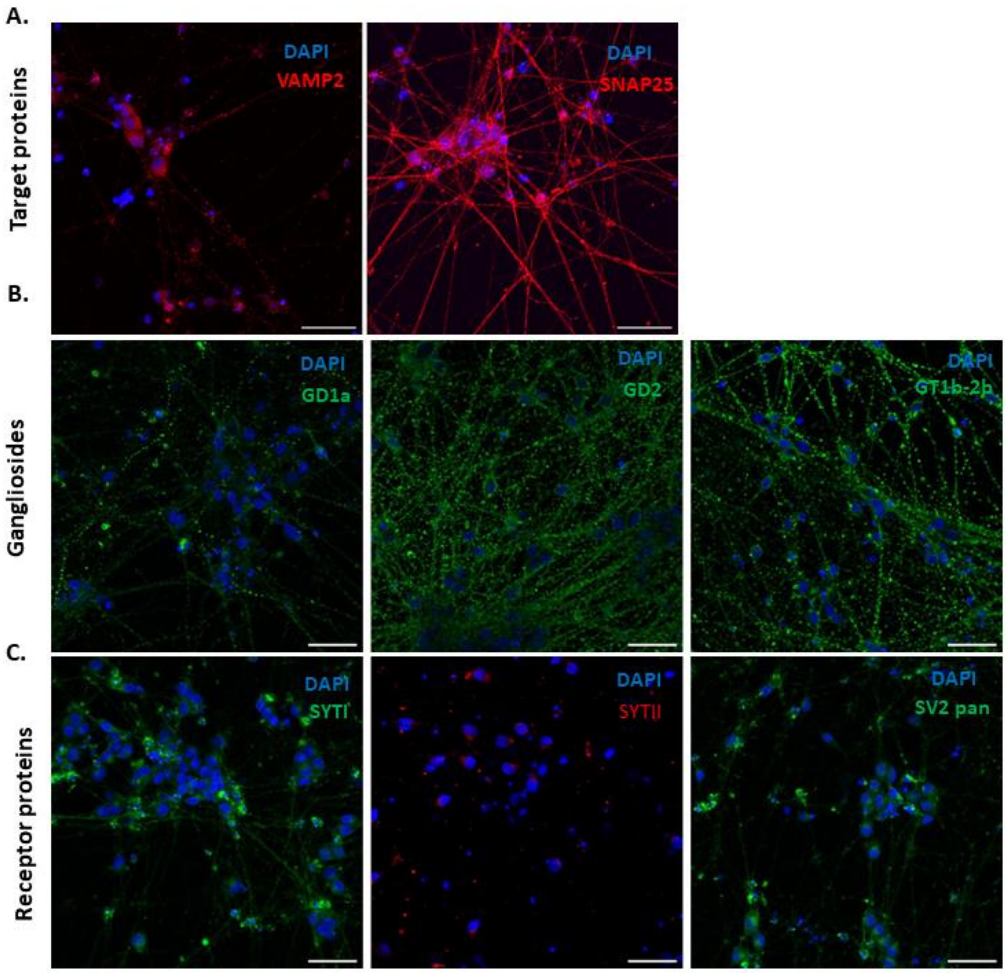

Figure A2. 2 HiPSCs-derived sensory neurons express most of the receptors and substrates necessary for BoNT activity.

A) *Immunofluorescence images showing the expression of substrates, SNAP25 (stained in red) and VAMP2 (stained in red). Rabbit SNAP25 Ab (in house) is used at 1:500 dilution. Rabbit VAMP2 Ab is used at 1:200 dilution. DAPI is used at 1:1000 dilution to see nucleus (stained in blue).* ***B)*** *Immunofluorescence images showing the expression of ganglioside receptors, GD1a (stained in green), GD2 (stained in green), GT1b-2b (stained in green). Mouse GD1a Ab is used at 5 µg/mL without permeabilization of the cells. Mouse GD2 Ab is used at 1:200 dilution without permeabilization of the cells. Mouse GT1b-2b Ab is used at 5 µg/mL without permeabilization of the cells.* ***C)*** *Immunofluorescence images showing the expression of receptor proteins, SYTI (stained in green), SYTII, SV2 pan (stained in green). Mouse SYTI Ab is used at 1:100 dilution. Rabbit SYTII Ab is used at 1:100 dilution. Mouse SV2-pan (detects A, B, C isoforms) Ab is used at 5 µg/mL. Images were taken with confocal microscope at 40x objective. All scale bars are 50 µm.*

HiPSCs-derived sensory neuron cells are sensitive to BoNT/A and BoNT/D but not BoNT/B.

Next, hiPSC-derived sensory neurons were tested against BoNT/A, BoNT/B and BoNT/D activity. Immunofluorescence images shows that cleaved SNAP25 (stained in red) is extensively detected in the cells following treatment with 1 nM BoNT/A (Figure A2.3 A). Immunoblot analysis confirmed the detection of cleaved SNAP25 in the cells treated with 10 nM BoNT/A and GT1b (Figure A2.3 B-C).

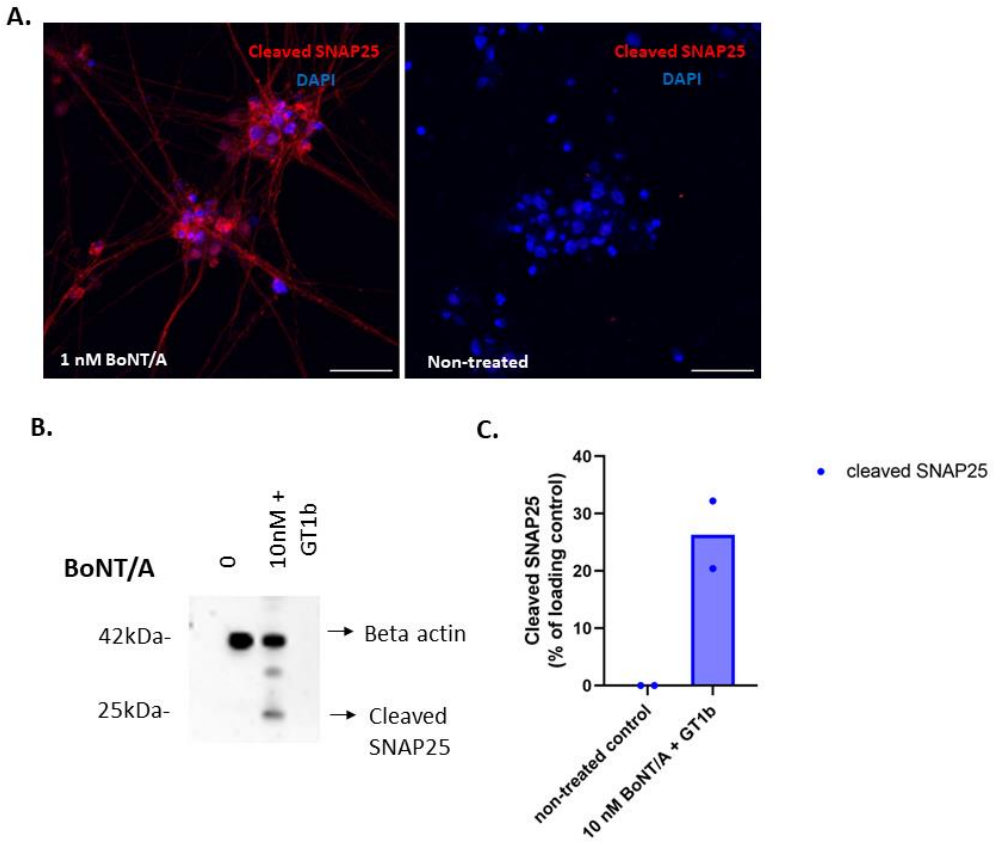

Figure A2. 3 HiPSCs-derived sensory neurons are sensitive to detect BoNT/A activity.

A) *Immunofluorescence image showing the cleaved SNAP25 (stained in red) in hiPSCs derived sensory neurons treated with 1 nM BoNT/A. Rabbit BoNT/A cleaved SNAP25 Ab (in house) is used at 1:5000 dilution. DAPI is used at 1:1000 dilution to see nucleus (stained in blue). Images were taken with confocal microscope at 40x objective. All scale bars are 50 µm.* ***B)*** *Western blot showing the proportion of cellular cleaved SNAP25 in hiPSCs derived sensory neurons following 3-day treatment with 10 nM BoNT/A and 50 µg/mL GT1b. Cells were treated with the diluting agent (Opti-MEM, reduced serum media) as a no treatment control. Rabbit BoNT/A cleaved SNAP25 Ab (in house) was added at 1:2000 dilution. Mouse beta-actin Ab was added at 1:1200 dilution as a loading control. Images were taken using ChemiDoc XRS.* ***C)*** *The graph shows the quantification of cleaved SNAP25 immunosignals (n=2, ±experimental errors).*

BoNT/B activity could not be detected in hiPSC-derived cells because endogenous VAMP2 is degraded when it is cleaved by the toxin in the cytosol (Pellizzari et al., 1998). Therefore, cleaved cytosolic VAMP2 wasn't detected by either immunocytochemistry or immunoblotting (Figure A2.4 A-B). SYTI and SYTII are the receptor proteins for BoNT/B entry. It is also possible that SYTII was not present in hiPSC-derived cells and that the SYTI receptor protein alone was insufficient to allow BoNT/B entry. When checking for sensitivity of hiPSC-derived sensory neurons to BoNT/B, either exogenous VAMP2 should be introduced to detect cleaved VAMP2 or total VAMP2 Ab should be used to detect VAMP2 disappearance. Endogenous cleaved vesicular VAMP2 does not disappear so BoNT/B activity could also be determined by using BoNT/B cleaved vesicular VAMP2 Ab.

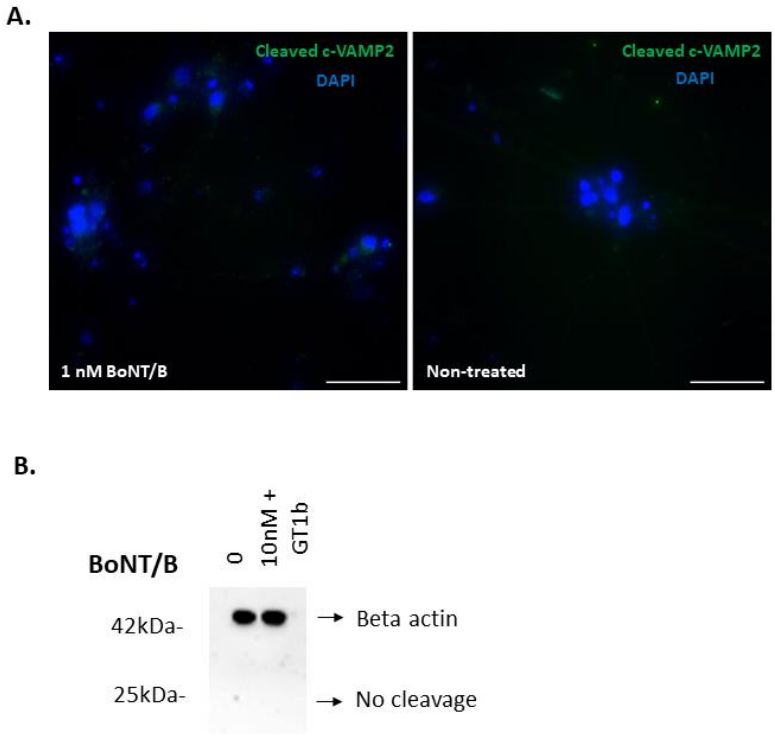

Figure A2. 4 BoNT/B activity could not be detected in hiPSC derived sensory neurons.

A) *Immunofluorescence images showing cleaved VAMP2 in hiPSCs derived sensory neurons after treatment with 1 nM BoNT/B. Mouse B151 Ab was used at 1:500 dilution to see BoNT/B cleaved cytosolic VAMP2. DAPI is used at 1:1000 dilution to see nuclei (stained in blue). Images were taken with confocal microscope at 40x objective. All scale bars are 50 µm.* ***B)*** *Western blot showing the proportion of cellular cleaved VAMP2 in hiPSCs derived sensory neurons following 3-day treatment with 10 nM BoNT/B and 50 µg/mL GT1b. Cells were treated with the diluting agent (Opti-MEM, reduced serum media) as a no treatment control. Rabbit monoclonal Ab (Genscript 2F7-1) was added at 1:2000 dilution to detect cleaved cytosolic VAMP2. Mouse beta-actin Ab was added at 1:1200 dilution as a loading control. Image was taken using ChemiDoc XRS.*

For BoNT/D activity, cleaved vesicular VAMP2 was successfully labelled on hiPSC-derived sensory neurons after treated with 1 nM BoNT/D (Figure A2.5 A). It was also confirmed by immunoblot results that cleaved vesicular VAMP2 was detected following treatment of the cells with 10 nM BoNT/D and GT1b (Figure A2.5 B-C).

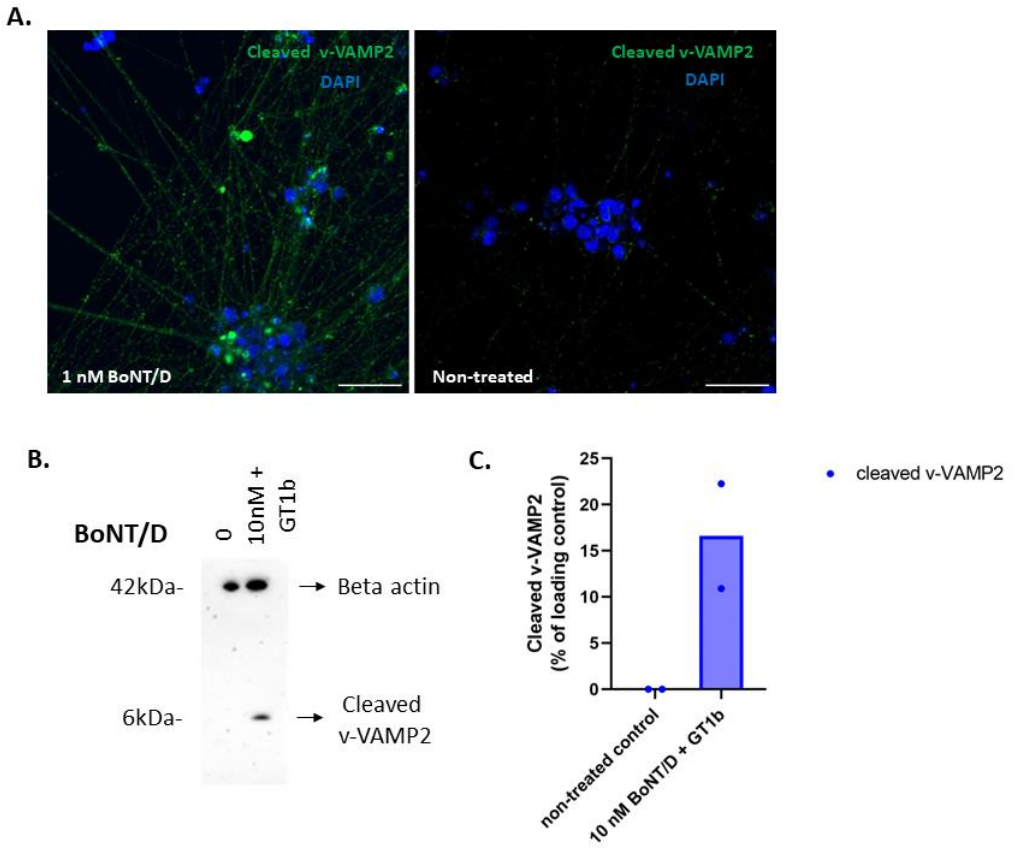

Figure A2. 5 HiPSCs-derived sensory neurons are sensitive to detect BoNT/D activity.

A) *Immunofluorescence image showing the cleaved vesicular VAMP2 (stained in green) in hiPSCs derived sensory neurons treated with 1 nM BoNT/D. Mouse monoclonal Ab (D27) was added at 1:500 dilution for vesicular VAMP2 cleavage detection. DAPI is used at 1:1000 dilution to see nucleus (stained in blue). Images were taken with confocal microscope at 40x objective. All scale bars are 50 µm.* ***B)*** *Western blot showing the proportion of cellular cleaved vesicular VAMP2 in hiPSCs derived sensory neurons following 3-day treatment with 10 nM BoNT/D and 50 µg/mL GT1b. Cells were treated with the diluting agent (Opti-MEM, reduced serum media) as a no treatment control. Mouse monoclonal Ab (D27) was added at 1:2000 dilution for vesicular VAMP2 cleavage detection. Mouse beta-actin Ab was added at 1:1200 dilution as a loading control. Images were taken using ChemiDoc XRS.* ***C)*** *The graph shows the quantification of cleaved v-VAMP2 immunosignals (n=2, ±experimental errors).*

Overall, hiPSC-derived neurons generated the required substrates and most of the receptors essential for BoNTs. Additionally, the cells are sensitive to BoNT/A and BoNT/D activity. For BoNT/B sensitivity, further tests must be performed.

Appendix 3: Immunoblot results of clostridial neurotoxins testing on NanoLuc VAMP2 SiMa, NanoLuc VAMP2 LAN-5, NanoLuc SNAP25 LAN-5 cells

NanoLuc VAMP2 SiMa cells were tested for the activity of BoNT/A, BoNT/B, BoNT/C, BoNT/D, BoNT/DC, and TeNT. Representative immunoblots and graphs are given below.

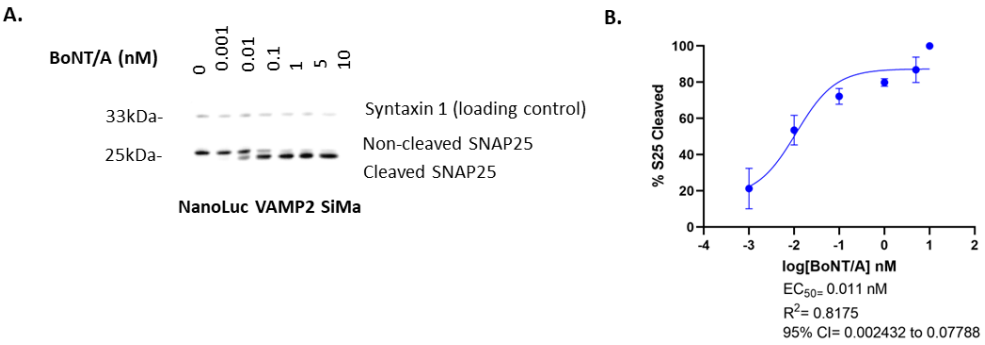

Figure A3. 1 BoNT/A activity was detected in differentiated NanoLuc VAMP2 SiMa cell line.

A) *Western blot showing the proportion of cleaved cellular SNAP25 in differentiated NanoLuc VAMP2 SiMa neuroblastomas following 3-day treatment with 1:10 titrated BoNT/A. Cells were treated with the diluting agent (Opti-MEM, reduced serum media) as a no treatment control. SNAP25 antibody was added at 1:3000 dilution. Syntaxin antibody was added at 1:2000 dilution as a control antibody. Image was taken using ChemiDoc XRS.* ***B)*** *Graph showing the quantification of cleaved SNAP25 immunosignals expressed as a percentage of total SNAP25 (N=3, ± S.E.M.).*

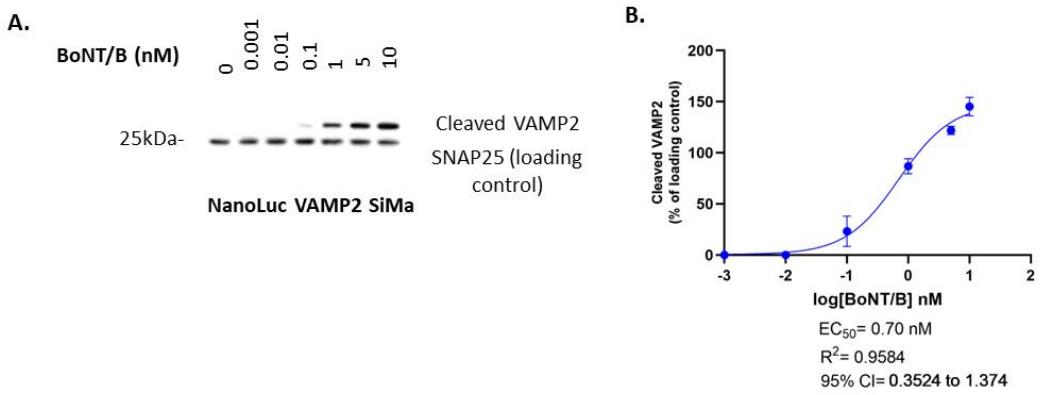

Figure A3. 2 BoNT/B activity was detected in differentiated NanoLuc VAMP2 SiMa cell line.

A) *Western blot showing the proportion of cleaved cytosolic VAMP2 in differentiated NanoLuc VAMP2 SiMa neuroblastomas following 3-day treatment with 1:10 titrated BoNT/B. Cells were treated with the diluting agent (Opti-MEM, reduced serum media) as a no treatment control. Rabbit monoclonal Ab (2F7-1) was added at 1:2000 dilution for cleaved cytosolic VAMP2 detection. SNAP25 antibody was added at 1:3000 dilution as a control antibody to detect uncleaved SNAP25. Images were taken using ChemiDoc XRS.* ***B)*** *Graph showing the quantification of cleaved cytosolic VAMP2 immunosignals (N=3, ± S.E.M.).*

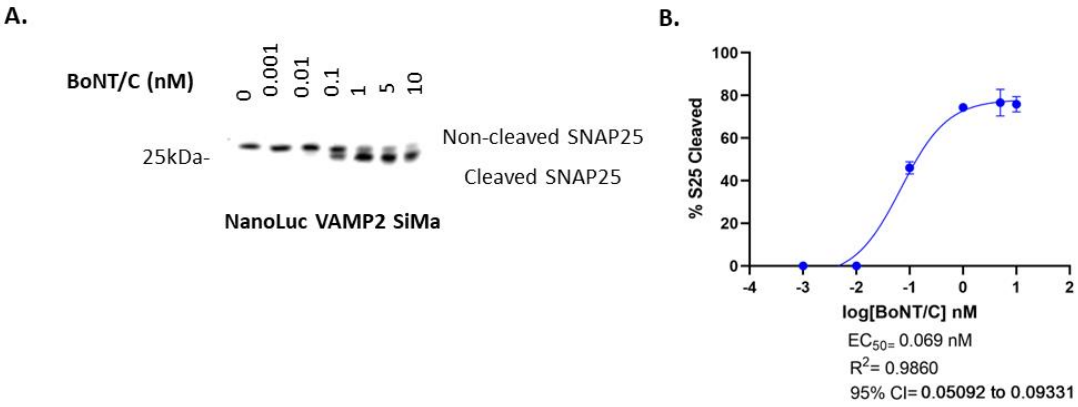

Figure A3. 3 BoNT/C activity was detected in differentiated NanoLuc VAMP2 SiMa cell line.

A) *Western blot showing the proportion of cleaved cellular SNAP25 in differentiated NanoLuc VAMP2 SiMa neuroblastomas following 3-day treatment with 1:10 titrated BoNT/C. Cells were treated with the diluting agent (Opti-MEM, reduced serum media) as a no treatment control. SNAP25 antibody was added at 1:3000 dilution. Syntaxin antibody was added at 1:2000 dilution. Image was taken using ChemiDoc XRS.* ***B)*** *Graph showing the quantification of cleaved SNAP25 immunosignals expressed as a percentage of total SNAP25 (N=3, ± S.E.M.).*

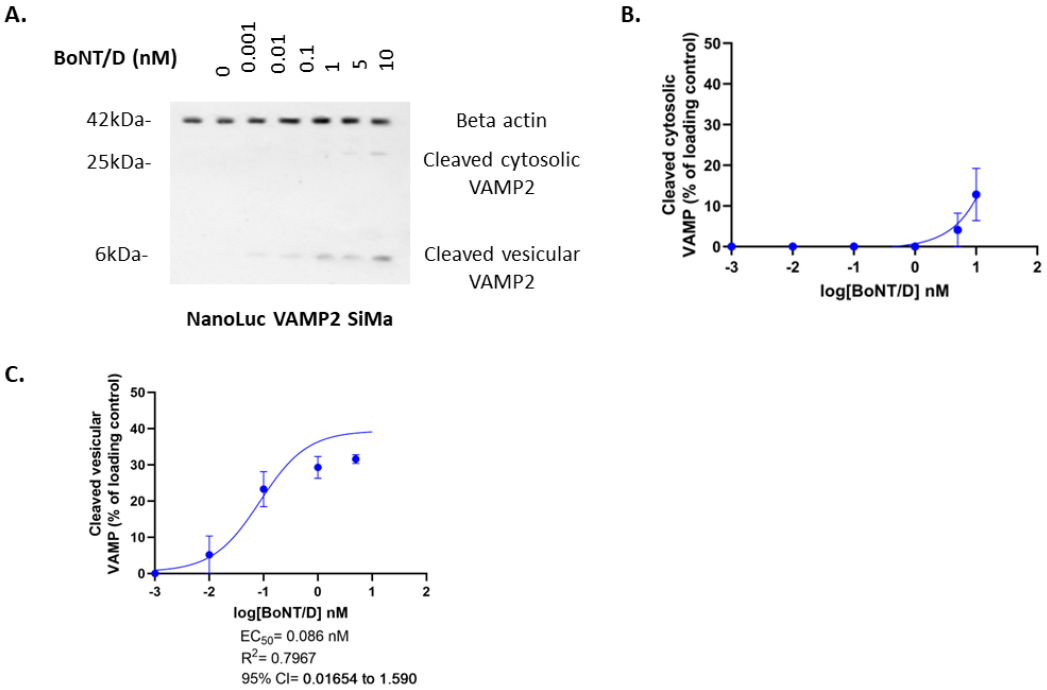

Figure A3. 4 BoNT/D activity was detected in NanoLuc VAMP2 SiMa cell line.

A) *Western blot showing the proportions of cleaved cytosolic and vesicular NanoLuc VAMP2 in differentiated NanoLuc VAMP2 SiMa neuroblastomas following 3-day treatment with 1:10 titrated BoNT/D. Cells were treated with the diluting agent (Opti-MEM, reduced serum media) as a no treatment control. Mouse monoclonal Ab (D27) was added at 1:2000 dilution for vesicular VAMP2 cleavage detection; D cleaved VAMP2 cytosolic rabbit polyclonal Ab was used at 1:2000 dilution for cytosolic VAMP2 cleavage detection. Mouse beta-actin Ab was added at 1:1200 dilution as a loading control. Images were taken using ChemiDoc XRS.* ***B)*** *Graph showing the quantification of cleaved cytosolic VAMP2 immunosignals (N=3, ± S.E.M.).* ***C)*** *Graph showing the quantification of cleaved vesicular VAMP2 immunosignals (N=3, ± S.E.M.).*

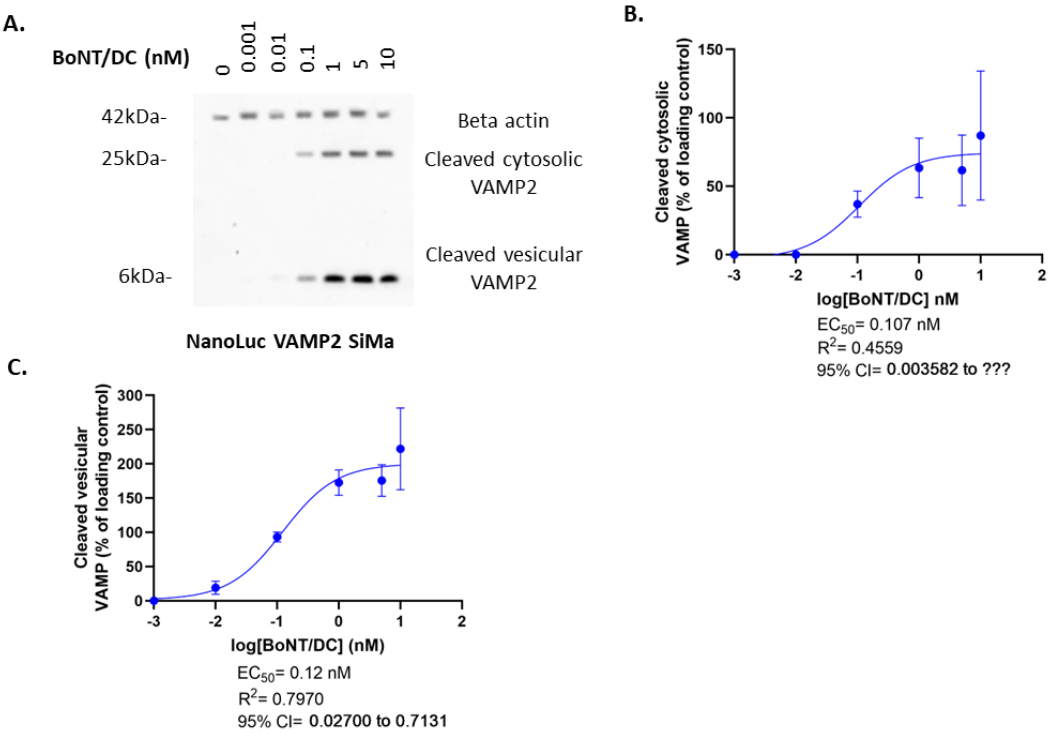

Figure A3. 5 BoNT/DC activity was detected in NanoLuc VAMP2 SiMa cell line.

A) *Western blot showing the proportions of cleaved cytosolic and vesicular NanoLuc VAMP2 in differentiated NanoLuc VAMP2 SiMa neuroblastomas following 3-day treatment with 1:10 titrated BoNT/DC. Cells were treated with the diluting agent (Opti-MEM, reduced serum media) as a no treatment control. Mouse monoclonal Ab (D27) was added at 1:2000 dilution for vesicular VAMP2 cleavage detection; D cleaved VAMP2 cytosolic rabbit polyclonal Ab was used at 1:2000 dilution for cytosolic VAMP2 cleavage detection. Mouse beta-actin Ab was added at 1:1200 dilution as a loading control. Images were taken using ChemiDoc XRS.* ***B)*** *Graph showing the quantification of cleaved cytosolic VAMP2 immunosignals (N=3, ± S.E.M.).* ***C)*** *Graph showing the quantification of cleaved vesicular VAMP2 immunosignals (N=3, ± S.E.M.).*

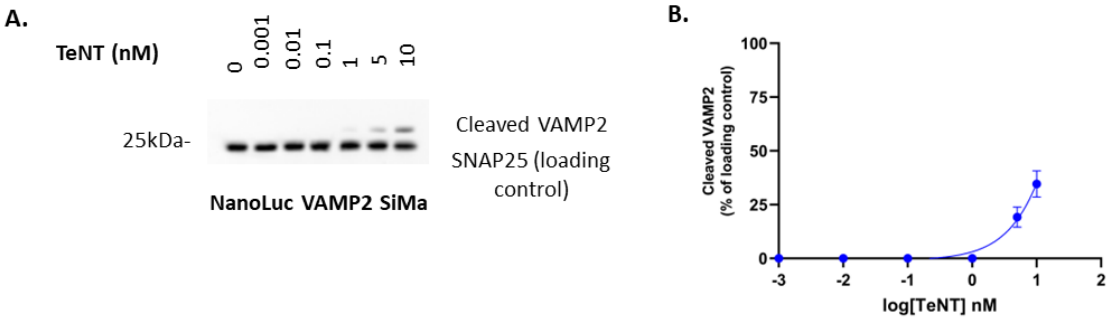

Figure A3. 6 TeNT activity was detected in differentiated NanoLuc VAMP2 SiMa cell line.

A) *Western blot showing the proportion of cleaved cytosolic VAMP2 in differentiated NanoLuc VAMP2 SiMa neuroblastomas following 3-day treatment with 1:10 titrated TeNT. Cells were treated with the diluting agent (Opti-MEM, reduced serum media) as a no treatment control. Rabbit monoclonal Ab (2F7-1) was added at 1:2000 dilution for cleaved cytosolic VAMP2 detection. SNAP25 antibody was added at 1:3000 dilution as a control antibody to detect uncleaved SNAP25. Images were taken using ChemiDoc XRS.* ***B)*** *Graph showing the quantification of cleaved cytosolic VAMP2 immunosignals (N=3, ± S.E.M.).*

NanoLuc VAMP2 LAN-5 cells were tested for the activity of BoNT/A, BoNT/C, BoNT/D. Representative immunoblots, and graphs are given below.

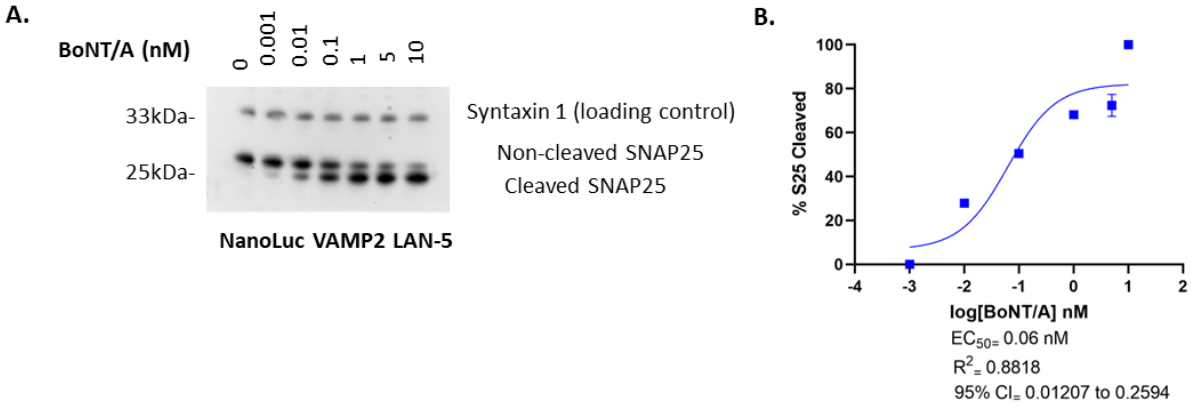

Figure A3. 7 BoNT/A activity was detected in differentiated NanoLuc VAMP2 LAN-5 cell line.

A) *Western blot showing the proportion of cleaved cellular SNAP25 in differentiated NanoLuc VAMP2 LAN-5 neuroblastomas following 3-day treatment with 1:10 titrated BoNT/A. Cells were treated with the diluting agent (Opti-MEM, reduced serum media) as a no treatment control. SNAP25 antibody was added at 1:3000 dilution. Syntaxin antibody was added at 1:2000 dilution as a control antibody. Image was taken using ChemiDoc XRS. C) Graph showing the quantification of cleaved SNAP25 immunosignals expressed as a percentage of total SNAP25 (N=3, ± S.E.M.).*

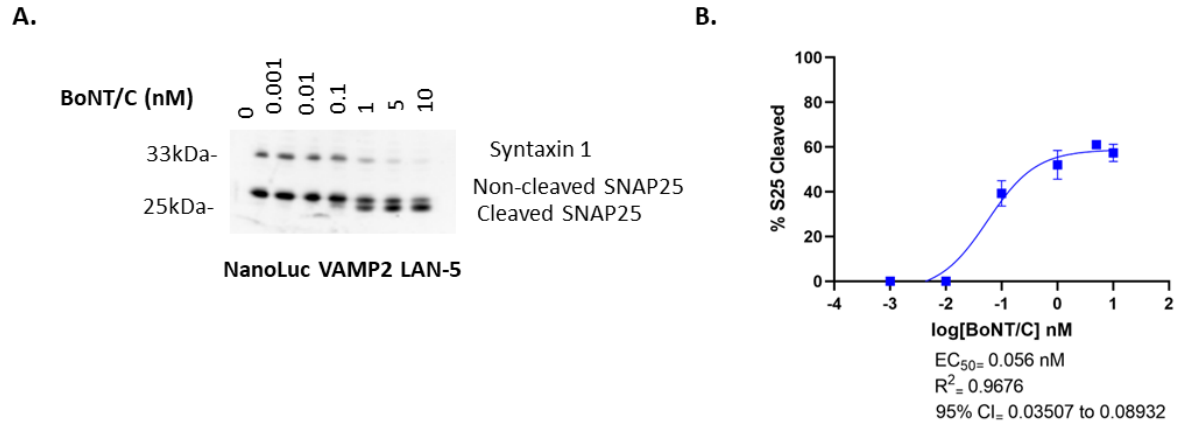

Figure A3. 8 BoNT/C activity was detected in differentiated NanoLuc VAMP2 LAN-5 cell line.

A) *Western blot showing the proportion of cleaved cellular SNAP25 in differentiated NanoLuc VAMP2 LAN-5 neuroblastomas following 3-day treatment with 1:10 titrated BoNT/C. Cells were treated with the diluting agent (Opti-MEM, reduced serum media) as a no treatment control. SNAP25 antibody was added at 1:3000 dilution. Syntaxin antibody was added at 1:2000 dilution. Image was taken using ChemiDoc XRS.* ***B)*** *Graph showing the quantification of cleaved SNAP25 immunosignals expressed as a percentage of total SNAP25 (N=3, ± S.E.M.).*

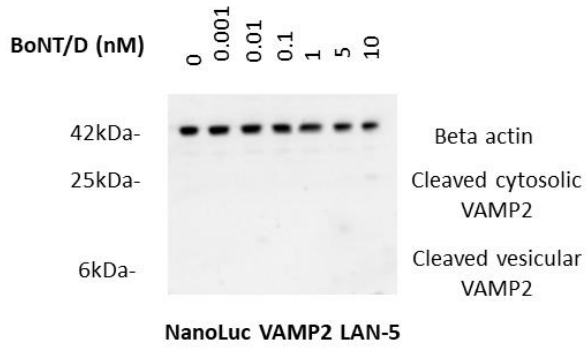

Figure A3. 9 BoNT/D activity was not detected in NanoLuc VAMP2 LAN-5 cell line.

Western blot showing the proportion of cleaved cytosolic and vesicular NanoLuc VAMP2 in differentiated NanoLuc VAMP2 LAN-5 neuroblastomas following 3-day treatment with 1:10 titrated BoNT/D. Cells were treated with the diluting agent (Opti-MEM, reduced serum media) as a no treatment control. Mouse monoclonal Ab (D27) was added at 1:2000 dilution for vesicular VAMP2 cleavage detection; D cleaved VAMP2 cytosolic rabbit polyclonal Ab was used at 1:2000 dilution for cytosolic VAMP2 cleavage detection. Mouse beta-actin Ab was added at 1:1200 dilution as a loading control. Images were taken using ChemiDoc XRS.

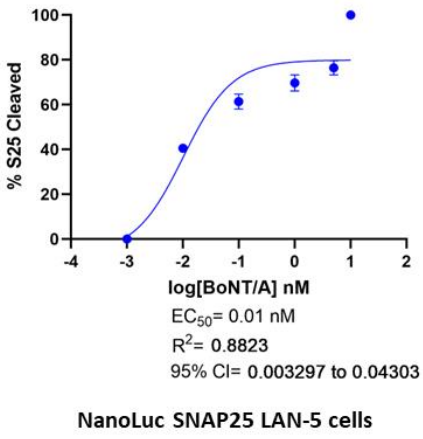

Figure A3. 10 Dose response curve of serial diluted BoNT/A in NanoLuc SNAP25 LAN-5 cell line.

Differentiated NanoLuc SNAP25 LAN-5 neuroblastomas were treated with 1:10 titrated BoNT/A for 3-days. Cells were treated with the diluting agent (Opti-MEM, reduced serum media) as a no treatment control. SNAP25 antibody was added at 1:3000 dilution. Syntaxin antibody was added at 1:2000 dilution. Graph showing the quantification of cleaved SNAP25 immunosignals expressed as a percentage of total SNAP25 (N=3, ± S.E.M.).

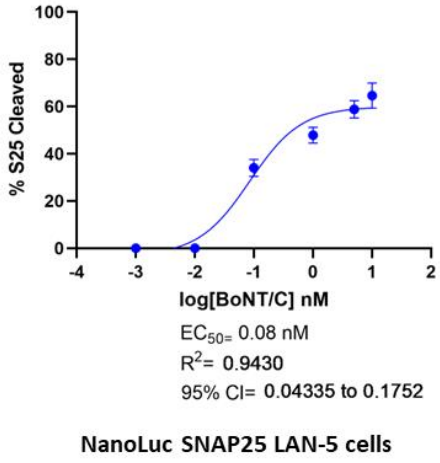

Figure A3. 11 Dose response curve of serial diluted BoNT/C in NanoLuc SNAP25 LAN-5 cell line.

Differentiated NanoLuc SNAP25 LAN-5 neuroblastomas were treated with 1:10 titrated BoNT/C for 3-days. Cells were treated with the diluting agent (Opti-MEM, reduced serum media) as a no treatment control. SNAP25 antibody was added at 1:3000 dilution. Syntaxin antibody was added at 1:2000 dilution. Graph showing the quantification of cleaved SNAP25 immunosignals expressed as a percentage of total SNAP25 (N=3, ± S.E.M.).

Appendix 4: Immunoblot results of clostridial neurotoxins testing on NanoLuc VAMP2 HeLa and SYTII-NanoLuc VAMP2 HeLa cells

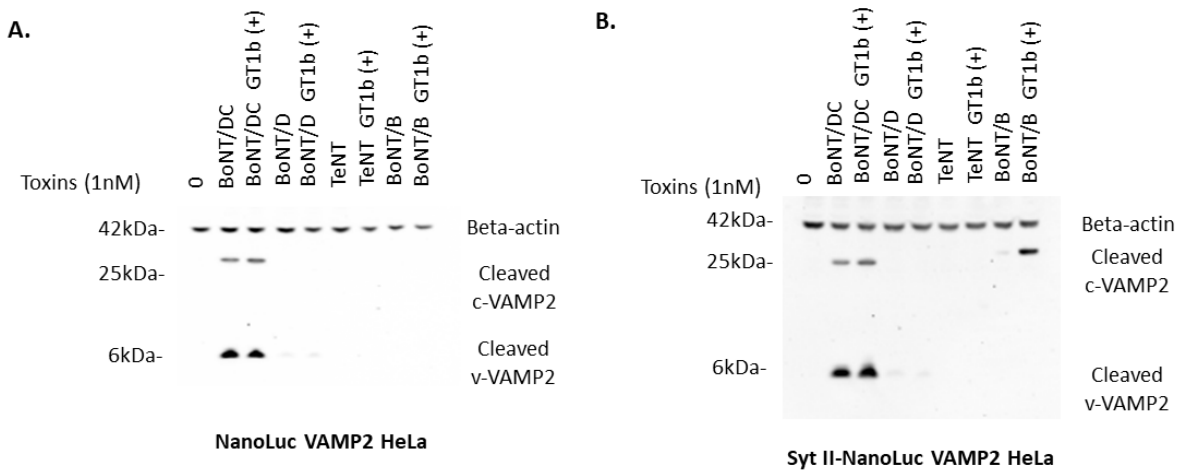

Figure A4. 1 Testing CNTs in NanoLuc VAMP2 HeLa and SYTII-NanoLuc VAMP2 HeLa cells.

A-B) *Immunoblot images showing the results of 1nM BoNT/B, TeNT, BoNT/D, BoNT/DC treated (A) NanoLuc VAMP2 HeLa and (B) SYTII-NanoLuc VAMP2 HeLa cells either with (+) or without (-) 50 µg/mL GT1b gangliosides for 3 days. Cells were treated with the diluting agent (Opti-MEM with 0.5% BSA) as a no treatment control. Rabbit monoclonal Ab (Genscript 2F7-1) was added at 1:2000 dilution to detect BoNT/B and TeNT cleaved cytosolic VAMP2. Mouse monoclonal Ab (Robert Koch D27) was added at 1:2000 dilution to detect BoNT/D and BoNT/DC cleaved vesicular VAMP2; rabbit polyclonal D cleaved VAMP cytosolic Ab was used at 1:2000 dilution to detect BoNT/D and BoNT/DC cleaved cytosolic VAMP2. Mouse beta-actin Ab was added at 1:1200 dilution as a loading control. Images were taken using ChemiDoc XRS.*

References

ADLER, S., BICKER, G., BIGALKE, H., BISHOP, C., BLUMEL, J., DRESSLER, D., FITZGERALD, J., GESSLER, F., HEUSCHEN, H., KEGEL, B., LUCH, A., MILNE, C., PICKETT, A., RATSCH, H., RUHDEL, I., SESARDIC, D., STEPHENS, M., STIENS, G., THORNTON, P. D., THURMER, R., VEY, M., SPIELMANN, H., GRUNE, B. & LIEBSCH, M. 2010. The Current Scientific and Legal Status of Alternative Methods to the LD50 Test for Botulinum Neurotoxin Potency Testing. *Atla-Alternatives to Laboratory Animals,* 38**,** 315-330.

ANDREOU, A. P., LEESE, C., GRECO, R., DEMARTINI, C., CORRIE, E., SIMSEK, D., ZANABONI, A., KOROLEVA, K., LLOYD, J. O., LAMBRU, G., DORAN, C., GAFUROV, O., SEWARD, E., GINIATULLIN, R., TASSORELLI, C. & DAVLETOV, B. 2021. DOUBLE-BINDING BOTULINUM MOLECULE WITH REDUCED MUSCLE PARALYSIS: EVALUATION IN IN VITRO AND IN VIVO MODELS OF MIGRAINE. *Toxicon,* 190**,** S5-S5.

BADE, S., RUMMEL, A., REISINGER, C., KARNATH, T., AHNERT-HILGER, G., BIGALKE, H. & BINZ, T. 2004. Botulinum neurotoxin type D enables cytosolic delivery of enzymatically active cargo proteins to neurones via unfolded translocation intermediates. *Journal of Neurochemistry,* 91**,** 1461-1472.

BEHRENSDORF-NICOL, H. A., BONIFAS, U., HANSCHMANN, K. M., KRAMER, B. & WEISSER, K. 2013. Binding and cleavage (BINACLE) assay for the functional in vitro detection of tetanus toxin: Applicability as alternative method for the safety testing of tetanus toxoids during vaccine production. *Vaccine,* 31**,** 6247-6253.

BEHRENSDORF-NICOL, H. A., BONIFAS, U., KEGEL, B., SILBERBACH, K., KRAMER, B. & WEISSER, K. 2010. In vitro determination of tetanus toxicity by to a ganglioside-binding step. *Toxicology in Vitro,* 24**,** 988-994.

BEHRENSDORF-NICOL, H. A., WILD, E., BONIFOS, U., KLIMEK, J., HANSCHMANN, K. M., KRAMER, B. & KEGEL, B. 2018. In vitro potency determination of botulinum neurotoxin serotype A based on its receptor-binding and proteolytic characteristics. *Toxicology in Vitro,* 53**,** 80-88.

BERCSENYI, K., SCHMIEG, N., BRYSON, J. B., WALLACE, M., CACCIN, P., GOLDING, M., ZANOTTI, G., GREENSMITH, L., NISCHT, R. & SCHIAVO, G. 2014. Nidogens are therapeutic targets for the prevention of tetanus. *Science,* 346**,** 1118-1123.

BERGES, J. A., FISHER, A. E. & HARRISON, P. J. 1993. A COMPARISON OF LOWRY, BRADFORD AND SMITH PROTEIN ASSAYS USING DIFFERENT PROTEIN STANDARDS AND PROTEIN ISOLATED FROM THE MARINE DIATOM THALASSIOSIRA-PSEUDONANA. *Marine Biology,* 115**,** 187-193.

BERNTSSON, R. P. A., PENG, L. S., DONG, M. & STENMARK, P. 2013a. Structure of dual receptor binding to botulinum neurotoxin B. *Nature Communications,* 4.

BERNTSSON, R. P. A., PENG, L. S., SVENSSON, L. M., DONG, M. & STENMARK, P. 2013b. Crystal Structures of Botulinum Neurotoxin DC in Complex with Its Protein Receptors Synaptotagmin I and II. *Structure,* 21**,** 1602-1611.

BESKE, P. H., BRADFORD, A. B., GRYNOVICKI, J. O., GLOTFELTY, E. J., HOFFMAN, K. M., HUBBARD, K. S., TUZNIK, K. M. & MCNUTT, P. M. 2016. Botulinum and Tetanus Neurotoxin-Induced Blockade of Synaptic Transmission in Networked Cultures of Human and Rodent Neurons. *Toxicological Sciences,* 149**,** 503-515.

BINZ, T. & RUMMEL, A. 2009. Cell entry strategy of clostridial neurotoxins. *Journal of Neurochemistry,* 109**,** 1584-1595.

BINZ, T., SIKORRA, S. & MAHRHOLD, S. 2010. Clostridial Neurotoxins: Mechanism of SNARE Cleavage and Outlook on Potential Substrate Specificity Reengineering. *Toxins,* 2**,** 665-682.

BLUM, F. C., CHEN, C., KROKEN, A. R. & BARBIERI, J. T. 2012. Tetanus Toxin and Botulinum Toxin A Utilize Unique Mechanisms To Enter Neurons of the Central Nervous System. *Infection and Immunity,* 80**,** 1662-1669.

BLUM, F. C., TEPP, W. H., JOHNSON, E. A. & BARBIERI, J. T. 2014. Multiple Domains of Tetanus Toxin Direct Entry into Primary Neurons. *Traffic,* 15**,** 1057-1065.

BORRIELLO, A., DELLA PIETRA, V., CRISCUOLO, M., OLIVA, A., TONINI, G. P., IOLASCON, A., ZAPPIA, V. & DELLA RAGIONE, F. 2000. p27(Kip1) accumulation is associated with retinoic-induced neuroblastoma differentiation: evidence of a decreased proteasome-dependent degradation. *Oncogene,* 19**,** 51-60.

BOUTEL, N., LOWE, P., BERGER, S., MALISSARD, M., ROBERT, A. & TESAR, M. 2016. NanoLuc Luciferase - A Multifunctional Tool for High Throughput Antibody Screening. *Frontiers in Pharmacology,* 7.

BRODEUR, G. M. 2003. Neuroblastoma: Biological insights into a clinical enigma. *Nature Reviews Cancer,* 3**,** 203-216.

BRUNGER, A. T., JIN, R. & BREIDENBACH, M. A. 2008. Highly specific interactions between botulinum neurotoxins and synaptic vesicle proteins. *Cellular and Molecular Life Sciences,* 65**,** 2296-2306.

BURKE, G. S. 1919. Notes on Bacillus botulinus. *Journal of Bacteriology,* 4**,** 555-571.

BUSINARO, R., LEONE, S., FABRIZI, C., SORCI, G., LAURO, G. M. & FUMAGALLI, L. 2006. S100B protects LAN-5 neuroblastoma cells against A beta amyloid-induced neurotoxicity via RAGE engagement at low doses but increases A beta amyloid neurotoxicity at high doses. *Journal of Neuroscience Research,* 83**,** 897-906.

CALLAWAY, J. E. 2004. Botulinum toxin type B (Myobloc((R))): Pharmacology and biochemistry. *Clinics in Dermatology,* 22**,** 23-28.

CAPES-DAVIS, A., THEODOSOPOULOS, G., ATKIN, I., DREXLER, H. G., KOHARA, A., MACLEOD, R. A. F., MASTERS, J. R., NAKAMURA, Y., REID, Y. A., REDDEL, R. R. & FRESHNEY, R. I. 2010. Check your cultures! A list of cross-contaminated or misidentified cell lines. *International Journal of Cancer,* 127**,** 1-8.

CHAI, Q., ARNDT, J. W., DONG, M., TEPP, W. H., JOHNSON, E. A., CHAPMAN, E. R. & STEVENS, R. C. 2006. Structural basis of cell surface receptor recognition by botulinum neurotoxin B. *Nature,* 444**,** 1096-1100.

CHEN, C., FU, Z. J., KIM, J. J. P., BARBIERI, J. T. & BALDWIN, M. R. 2009. Gangliosides as High Affinity Receptors for Tetanus Neurotoxin. *Journal of Biological Chemistry,* 284**,** 26569-26577.

CHEN, S. 2012. Clinical Uses of Botulinum Neurotoxins: Current Indications, Limitations and Future Developments. *Toxins,* 4**,** 913-939.

CHEN, Y. A. & SCHELLER, R. H. 2001. Snare-mediated membrane fusion. *Nature Reviews Molecular Cell Biology,* 2**,** 98-106.

CIRUELAS, K., MARCOTULLI, D. & BAJJALIEH, S. M. 2019. Synaptic vesicle protein 2: A multi-faceted regulator of secretion. *Seminars in Cell & Developmental Biology,* 95**,** 130-141.

COCCO, A. & ALBANESE, A. 2018. Recent developments in clinical trials of botulinum neurotoxins. *Toxicon,* 147**,** 77-83.

CONNAN, C. & POPOFF, M. R. 2017. Uptake of Clostridial Neurotoxins into Cells and Dissemination. *In:* BARTH, H. (ed.) *Uptake and Trafficking of Protein Toxins.* Cham: Springer International Publishing Ag.

DAVLETOV, B., BAJOHRS, M. & BINZ, T. 2005. Beyond BOTOX: advantages and limitations of individual botulinum neurotoxins. *Trends in Neurosciences,* 28**,** 446-452.

DONG, M., MASUYER, G. & STENMARK, P. 2019. Botulinum and Tetanus Neurotoxins. *Annual Review of Biochemistry, Vol 88,* 88**,** 811-837.

DONG, M., RICHARDS, D. A., GOODNOUGH, M. C., TEPP, W. H., JOHNSON, E. A. & CHAPMAN, E. R. 2003. Synaptotagmins I and II mediate entry of botulinum neurotoxin B into cells. *Journal of Cell Biology,* 162**,** 1293-1303.

DONG, M. & STENMARK, P. 2021. The Structure and Classification of Botulinum Toxins. *Botulinum Toxin Therapy,* 263**,** 11-33.

DRESSLER, D. & ELEOPRA, R. 2006. Clinical use of non-A botulinum toxins: Botulinum toxin type B. *Neurotoxicity Research,* 9**,** 121-125.

DUMAN, J. G. & FORTE, J. G. 2003. What is the role of SNARE proteins in membrane fusion? *American Journal of Physiology-Cell Physiology,* 285**,** C237-C249.

ELEGHEERT, J., BEHIELS, E., BISHOP, B., SCOTT, S., WOOLLEY, R. E., GRIFFITHS, S. C., BYRNE, E. F. X., CHANG, V. T., STUART, D. I., JONES, E. Y., SIEBOLD, C. & ARICESCU, A. R. 2018. Lentiviral transduction of mammalian cells for fast, scalable and high-level production of soluble and membrane proteins. *Nature Protocols,* 13**,** 2991-3017.

ELEOPRA, R., TUGNOLI, V., QUATRALE, R., ROSSETTO, O., MONTECUCCO, C. & DRESSLER, D. 2006. Clinical use of non-A botulinum toxins: Botulinum toxin type C and botulinum toxin type F. *Neurotoxicity Research,* 9**,** 127-131.

FERNANDEZ-SALAS, E., WANG, J., MOLINA, Y., NELSON, J. B., JACKY, B. P. S. & AOKI, K. R. 2012. Botulinum Neurotoxin Serotype a Specific Cell-Based Potency Assay to Replace the Mouse Bioassay. *Plos One,* 7.

FISCHER, A. & MONTAL, M. 2007. Crucial role of the disulfide bridge between botulinum neurotoxin light and heavy chains in protease translocation across membranes. *Journal of Biological Chemistry,* 282**,** 29604-29611.

FORAN, P. G., MOHAMMED, N., LISK, G. O., NAGWANEY, S., LAWRENCE, G. W., JOHNSON, E., SMITH, L., AOKI, K. R. & DOLLY, J. O. 2003. Evaluation of the therapeutic usefulness of botulinum neurotoxin B, C1, E, and F compared with the long lasting type A - Basis for distinct durations of inhibition of exocytosis in central neurons. *Journal of Biological Chemistry,* 278**,** 1363-1371.

FOTINOU, C., EMSLEY, P., BLACK, I., ANDO, H., ISHIDA, H., KISO, M., SINHA, K. A., FAIRWEATHER, N. F. & ISAACS, N. W. 2001. The crystal structure of tetanus toxin Hc fragment complexed with a synthetic GT1b analogue suggests cross-linking between ganglioside receptors and the toxin. *Journal of Biological Chemistry,* 276**,** 32274-32281.

GARDNER, A. P. & BARBIERI, J. T. 2018. Light Chain Diversity among the Botulinum Neurotoxins. *Toxins,* 10.

GERST, J. E. 1999. SNAREs and SNARE regulators in membrane fusion and exocytosis. *Cellular and Molecular Life Sciences,* 55**,** 707-734.

GREENBERG, L., MORRELL, C. A. & GIBBARD, J. 1943. The biological assay of tetanus-toxoid. *The journal of immunology : official journal of the American Association of Immunologists.,* 46**,** 333-340.

GUGLIELMI, L., CINNELLA, C., NARDELLA, M., MARESCA, G., VALENTINI, A., MERCANTI, D., FELSANI, A. & D'AGNANO, I. 2014. MYCN gene expression is required for the onset of the differentiation programme in neuroblastoma cells. *Cell Death & Disease,* 5.

HANSBAUER, E. M., SKIBA, M., ENDERMANN, T., WEISEMANN, J., STERN, D., DORNER, M. B., FINKENWIRTH, F., WOLF, J., LUGINBUHL, W., MESSELHAUSSER, U., BELLANGER, L.,

WOUDSTRA, C., RUMMEL, A., FACH, P. & DORNER, B. G. 2016. Detection, differentiation, and identification of botulinum neurotoxin serotypes C, CD, D, and DC by highly specific immunoassays and mass spectrometry. *Analyst,* 141**,** 5281-5297.

HEDELAND, M., MOURA, H., BAVERUD, V., WOOLFITT, A. R., BONDESSON, U. & BARR, J. R. 2011. Confirmation of botulism in birds and cattle by the mouse bioassay and Endopep-MS. *Journal of Medical Microbiology,* 60**,** 1299-1305.

HERREROS, J., NG, T. & SCHIAVO, G. 2001. Lipid rafts act as specialized domains for tetanus toxin binding and internalization into neurons. *Molecular Biology of the Cell,* 12**,** 2947-2960.

HJELM, H., HJELM, K. & SJOQUIST, J. 1972. PROTEIN A FROM STAPHYLOCOCCUS-AUREUS - ITS ISOLATION BY AFFINITY CHROMATOGRAPHY AND ITS USE AS AN IMMUNOSORBENT FOR ISOLATION OF IMMUNOGLOBULINS. *Febs Letters,* 28**,** 73-&.

HONG, W. S., PEZZI, H. M., SCHUSTER, A. R., BERRY, S. M., SUNG, K. E. & BEEBE, D. J. 2016. Development of a Highly Sensitive Cell-Based Assay for Detecting Botulinum Neurotoxin Type A through Neural Culture Media Optimization. *Journal of Biomolecular Screening,* 21**,** 65-73.

HUBBARD, K., BESKE, P., LYMAN, M. & MCNUTT, P. 2015. Functional Evaluation of Biological Neurotoxins in Networked Cultures of Stem Cell-derived Central Nervous System Neurons. *Jove-Journal of Visualized Experiments*.

HUMEAU, Y., DOUSSAU, F., GRANT, N. J. & POULAIN, B. 2000. How botulinum and tetanus neurotoxins block neurotransmitter release. *Biochimie,* 82**,** 427-446.

JENKINSON, S. P., GRANDGIRARD, D., HEIDEMANN, M., TSCHERTER, A., AVONDET, M. A. & LEIB, S. L. 2017. Embryonic Stem Cell-Derived Neurons Grown on Multi-Electrode Arrays as a Novel In vitro Bioassay for the Detection of Clostridium botulinum Neurotoxins. *Frontiers in Pharmacology,* 8**,** 1-14.

JIRASEK, T., MANDYS, V. & VIKLICKY, V. 2002. Expression of class III beta-tubulin in neuroendocrine tumours of gastrointestinal tract. *Folia Histochemica Et Cytobiologica,* 40**,** 305-309.

KARALEWITZ, A. P. A., KROKEN, A. R., FU, Z. J., BALDWIN, M. R., KIM, J. J. P. & BARBIERI, J. T. 2010. Identification of a Unique Ganglioside Binding Loop within Botulinum Neurotoxins C and D-SA. *Biochemistry,* 49**,** 8117-8126.

KIRIS, E., KOTA, K. P., BURNETT, J. C., SOLOVEVA, V., KANE, C. D. & BAVARI, S. 2014. Recent developments in cell-based assays and stem cell technologies for botulinum neurotoxin research and drug discovery. *Expert Review of Molecular Diagnostics,* 14**,** 153-168.

KIRIS, E., NUSS, J. E., BURNETT, J. C., KOTA, K. P., KOH, D. C., WANNER, L. M., TORRES-MELENDEZ, E., GUSSIO, R., TESSAROLLO, L. & BAVARI, S. 2011. Embryonic stem cell-derived motoneurons

provide a highly sensitive cell culture model for botulinum neurotoxin studies, with implications for high-throughput drug discovery. *Stem Cell Research,* 6**,** 195-205.

KORIAZOVA, L. K. & MONTAL, M. 2003. Translocation of botulinum neurotoxin light chain protease through the heavy chain channel. *Nature Structural Biology,* 10**,** 13-18.

KOSTRZEWA, R. M., KOSTRZEWA, R. A. & KOSTRZEWA, J. P. 2015. Botulinum neurotoxin: Progress in negating its neurotoxicity; and in extending its therapeutic utility via molecular engineering. Mini Review. *Peptides,* 72**,** 80-87.

KROKEN, A. R., KARALEWITZ, A. P. A., FU, Z. J., BALDWIN, M. R., KIM, J. J. P. & BARBIERI, J. T. 2011a. Unique ganglioside binding by botulinum neurotoxins C and D-SA. *Febs Journal,* 278**,** 4486-4496.

KROKEN, A. R., KARALEWITZ, A. P. A., FU, Z. J., KIM, J. J. P. & BARBIERI, J. T. 2011b. Novel Ganglioside-mediated Entry of Botulinum Neurotoxin Serotype D into Neurons. *Journal of Biological Chemistry,* 286**,** 26828-26837.

KUKREJA, R. & SINGH, B. R. 2015. The botulinum toxin as a therapeutic agent: molecular and pharmacological insights. *Research and Reports in Biochemistry,* 5**,** 173-183.

KUTSCHENKO, A., WEISEMANN, J., KOLLEWE, K., FIEDLER, T., ALVERMAN, S., BOSELT, S., ESCHER, C., GARDE, N., GINGELE, S., KAEHLER, S. B., KARATSCHAI, R., KRUGER, T. H. C., SIKORRA, S., TACIK, P., WEGNER, F., WOLLMANN, J., BIGALKE, H., WOHLFARTH, K. & RUMMEL, A. 2019. Botulinum neurotoxin serotype D - A potential treatment alternative for BoNT/A and B non-responding patients. *Clinical Neurophysiology,* 130**,** 1066-1073.

LACY, D. B. & STEVENS, R. C. 1999. Sequence homology and structural analysis of the clostridial neurotoxins. *Journal of Molecular Biology,* 291**,** 1091-1104.

LACY, D. B., TEPP, W., COHEN, A. C., DASGUPTA, B. R. & STEVENS, R. C. 1998. Crystal structure of botulinum neuro-toxin type A and implications for toxicity. *Nature Structural Biology,* 5**,** 898-902.

LAM, K. H. & JIN, R. S. 2015. Architecture of the botulinum neurotoxin complex: a molecular machine for protection and delivery. *Current Opinion in Structural Biology,* 31**,** 89-95.

LEW, M. F. 2002. Review of the FDA-approved uses of botulinum toxins, including data suggesting efficacy in pain reduction. *Clinical Journal of Pain,* 18**,** S142-S146.

LIEBSCH, M., GRUNE, B., SEILER, A., BUTZKE, D., OELGESCHLAGER, M., PIROW, R., ADLER, S., RIEBELING, C. & LUCH, A. 2011. Alternatives to animal testing: current status and future perspectives. *Archives of Toxicology,* 85**,** 841-858.

LIN, R. C. & SCHELLER, R. H. 2000. Mechanisms of synaptic vesicle exocytosis. *Annual Review of Cell and Developmental Biology,* 16**,** 19-49.

LUNDHOLT, B. K., SCUDDER, K. M. & PAGLIARO, L. 2003. A simple technique for reducing edge effect in cell-based assays. *Journal of Biomolecular Screening,* 8**,** 566-570.

MARIANO, V., NARDI, A., GRADASSI, S., DE SANTIS, P., ANNIBALLI, F., BILEI, S., SCHOLL, F., AURICCHIO, B., BIELLI, C., CULICCHI, M. & DE ROSA, G. L. C. 2019. A severe outbreak of botulism in cattle in Central Italy. *Veterinaria Italiana,* 55**,** 57-62.

MASUYER, G., CONRAD, J. & STENMARK, P. 2018. THE STRUCTURE OF THE TETANUS TOXIN REVEALS PH-MEDIATED DOMAIN DYNAMICS. *Toxicon,* 156**,** S78-S78.

MCNUTT, P., CELVER, J., HAMILTON, T. & MESNGON, M. 2011. Embryonic stem cell-derived neurons are a novel, highly sensitive tissue culture platform for botulinum research. *Biochemical and Biophysical Research Communications,* 405**,** 85-90.

MONTAL, M. 2009. Translocation of botulinum neurotoxin light chain protease by the heavy chain protein-conducting channel. *Toxicon,* 54**,** 565-569.

MONTECUCCO, C. 1986. HOW DO TETANUS AND BOTULINUM TOXINS BIND TO NEURONAL MEMBRANES. *Trends in Biochemical Sciences,* 11**,** 314-317.

MONTECUCCO, C. & SCHIAVO, G. 1995. Structure and function of tetanus and botulinum neurotoxins. *Quarterly Reviews of Biophysics,* 28**,** 423-472.

MOTA, G., GALATIUC, C., SJOQUIST, J. & GHETIE, V. 1983. A NON-DISSOCIABLE RABBIT IGG-PROTEIN-A COMPLEX. *Annales D Immunologie,* C134**,** 331-340.

MOURA, H., TERILLI, R. R., WOOLFITT, A. R., GALLEGOS-CANDELA, M., MCWILLIAMS, L. G., SOLANO, M. I., PIRKLE, J. L. & BARR, J. R. 2011. Studies on botulinum neurotoxins type/C1 and mosaic/DC using Endopep-MS and proteomics. *Fems Immunology and Medical Microbiology,* 61**,** 288-300.

MUNRO, P., KOJIMA, H., DUPONT, J. L., BOSSU, J. L., POULAIN, B. & BOQUET, P. 2001. High sensitivity of mouse neuronal cells to tetanus toxin requires a GPI-anchored protein. *Biochemical and Biophysical Research Communications,* 289**,** 623-629.

NAKAMURA, K., KOHDA, T., SETO, Y., MUKAMOTO, M. & KOZAKI, S. 2013. Improved detection methods by genetic and immunological techniques for botulinum C/D and D/C mosaic neurotoxins. *Veterinary Microbiology,* 162**,** 881-890.

NAKAMURA, K., KOHDA, T., SHIBATA, Y., TSUKAMOTO, K., ARIMITSU, H., HAYASHI, M., MUKAMOTO, M., SASAKAWA, N. & KOZAKI, S. 2012. Unique Biological Activity of Botulinum D/C Mosaic Neurotoxin in Murine Species. *Infection and Immunity,* 80**,** 2886-2893.

NAUMANN, M. & JOST, W. 2004. Botulinum toxin treatment of secretory disorders. *Movement Disorders,* 19**,** S137-S141.

NEPAL, M. R. & JEONG, T. C. 2020. Alternative Methods for Testing Botulinum Toxin: Current Status and Future Perspectives. *Biomolecules & Therapeutics,* 28**,** 302-310.

NING, B. T. & TANG, Y. M. 2012. Establishment of the cell line, HeLa-CD14, transfected with the human CD14 gene. *Oncology Letters,* 3**,** 871-874.

NISHIKI, T., TOKUYAMA, Y., KAMATA, Y., NEMOTO, Y., YOSHIDA, A., SATO, K., SEKIGUCHI, M., TAKAHASHI, M. & KOZAKI, S. 1996. The high-affinity binding of Clostridium botulinum type B neurotoxin to synaptotagmin II associated with gangliosides G(T1b)/G(D1a). *Febs Letters,* 378**,** 253-257.

NUSS, J. E., RUTHEL, G., TRESSLER, L. E., WANNER, L. M., TORRES-MELENDEZ, E., HALE, M. L. & BAVARI, S. 2010. Development of Cell-Based Assays to Measure Botulinum Neurotoxin Serotype A Activity Using Cleavage-Sensitive Antibodies. *Journal of Biomolecular Screening,* 15**,** 42-51.

PAGE, M. & THORPE, R. 2009. Purification of IgG Using Protein A or Protein G. *Protein Protocols Handbook, Third Edition***,** 1761-1763.

PASSALACQUA, M., PATRONE, M., PICOTTI, G. B., DELRIO, M., SPARATORE, B., MELLONI, E. & PONTREMOLI, S. 1998. Stimulated astrocytes release high-mobility group 1 protein, an inducer of LAN-5 neuroblastoma cell differentiation. *Neuroscience,* 82**,** 1021-1028.

PATHE-NEUSCHAFER-RUBE, A., NEUSCHAFER-RUBE, F., GENZ, L. & PUSCHEL, G. P. 2015. Botulinum Neurotoxin Dose-Dependently Inhibits Release of Neurosecretory Vesicle-Targeted Luciferase from Neuronal Cells. *Altex-Alternatives to Animal Experimentation,* 32**,** 297-306.

PATHE-NEUSCHAFER-RUBE, A., NEUSCHAFER-RUBE, F., HAAS, G., LANGOTH-FEHRINGER, N. & PUSCHEL, G. P. 2018. Cell-Based Reporter Release Assay to Determine the Potency of Proteolytic Bacterial Neurotoxins. *Toxins,* 10.

PATIL, S., WILLETT, O., THOMPKINS, T., HERMANN, R., RAMANATHAN, S., CORNETT, E. M., FOX, C. J. & KAYE, A. D. 2016. Botulinum Toxin: Pharmacology and Therapeutic Roles in Pain States. *Current Pain and Headache Reports,* 20.

PELLETT, S. 2013. Progress in Cell Based Assays for Botulinum Neurotoxin Detection. *Botulinum Neurotoxins,* 364**,** 257-285.

PELLETT, S., DU, Z. W., PIER, C. L., TEPP, W. H., ZHANG, S. C. & JOHNSON, E. A. 2011. Sensitive and quantitative detection of botulinum neurotoxin in neurons derived from mouse embryonic stem cells. *Biochemical and Biophysical Research Communications,* 404**,** 388-392.

PELLETT, S., TEPP, W. H., CLANCY, C. M., BORODIC, G. E. & JOHNSON, E. A. 2007. A neuronal cell-based botulinum neurotoxin assay for highly sensitive and specific detection of neutralizing serum antibodies. *Febs Letters,* 581**,** 4803-4808.

PELLETT, S., TEPP, W. H. & JOHNSON, E. A. 2019. Critical Analysis of Neuronal Cell and the Mouse Bioassay for Detection of Botulinum Neurotoxins. *Toxins,* 11.

PELLETT, S., TEPP, W. H., JOHNSON, E. A. & SESARDIC, D. 2017. Assessment of ELISA as endpoint in neuronal cell-based assay for BoNT detection using hiPSC derived neurons. *Journal of Pharmacological and Toxicological Methods,* 88**,** 1-6.

PELLETT, S., TEPP, W. H., SCHERF, J. M., PIER, C. L. & JOHNSON, E. A. 2015. Activity of botulinum neurotoxin type D (strain 1873) in human neurons. *Toxicon,* 101**,** 63-69.

PELLIZZARI, R., ROSSETTO, O., SCHIAVO, G. & MONTECUCCO, C. 1999. Tetanus and botulinum neurotoxins: mechanism of action and therapeutic uses. *Philosophical Transactions of the Royal Society of London Series B-Biological Sciences,* 354**,** 259-268.

PELLIZZARI, R., ROSSETTO, O., WASHBOURNE, P., TONELLO, F., NICOTERA, P. L. & MONTECUCCO, C. 1998. In vitro biological activity and toxicity of tetanus and botulinum neurotoxins. *Toxicology Letters,* 103**,** 191-197.

PENG, L. S., BERNTSSON, R. P. A., TEPP, W. H., PITKIN, R. M., JOHNSON, E. A., STENMARK, P. & DONG, M. 2012. Botulinum neurotoxin D-C uses synaptotagmin I and II as receptors, and human synaptotagmin II is not an effective receptor for type B, D-C and G toxins. *Journal of Cell Science,* 125**,** 3233-3242.

PENG, L. S., TEPP, W. H., JOHNSON, E. A. & DONG, M. 2011. Botulinum Neurotoxin D Uses Synaptic Vesicle Protein SV2 and Gangliosides as Receptors. *Plos Pathogens,* 7.

PIRAZZINI, M., ROSSETTO, O., ELEOPRA, R. & MONTECUCCO, C. 2017. Botulinum Neurotoxins: Biology, Pharmacology, and Toxicology. *Pharmacological Reviews,* 69**,** 200-235.

PIRAZZINI, M., TEHRAN, D. A., LEKA, O., ZANETTI, G., ROSSETTO, O. & MONTECUCCO, C. 2016. On the translocation of botulinum and tetanus neurotoxins across the membrane of acidic intracellular compartments. *Biochimica Et Biophysica Acta-Biomembranes,* 1858**,** 467-474.

PONZONI, M., CASALARO, A., LANCIOTTI, M., MONTALDO, P. G. & CORNAGLIAFERRARIS, P. 1992. THE COMBINATION OF GAMMA-INTERFERON AND TUMOR-NECROSIS-FACTOR CAUSES A RAPID AND EXTENSIVE DIFFERENTIATION OF HUMAN NEUROBLASTOMA-CELLS. *Cancer Research,* 52**,** 931-939.

PONZONI, M., LUCARELLI, E., CORRIAS, M. V. & CORNAGLIAFERRARIS, P. 1993. PROTEIN-KINASE-C ISOENZYMES IN HUMAN NEUROBLASTS - INVOLVEMENT OF PKCE IN CELL-DIFFERENTIATION. *Febs Letters,* 322**,** 120-124.

POPOFF, M. R. 2018. NEURONAL SELECTIVITY OF BOTULINUM NEUROTOXINS. *Toxicon,* 156**,** S93-S93.

PURKISS, J. R., FRIIS, L. M., DOWARD, S. & QUINN, C. P. 2001. Clostridium botulinum neurotoxins act with a wide range of potencies on SH-SY5Y human neuroblastoma cells. *Neurotoxicology,* 22**,** 447-453.

RASETTI-ESCARGUEIL, C., JONES, R. G. A., LIU, Y. & SESARDIC, D. 2009. Measurement of botulinum types A, B and E neurotoxicity using the phrenic nerve-hemidiaphragm: Improved precision with in-bred mice. *Toxicon,* 53**,** 503-511.

RASETTI-ESCARGUEIL, C. MACHADO, C.B., PRENETA-BLANC, R., FLECK R.A., SESARDIC D. 2011. Enhanced sensitivity to Botulinum type A neurotoxin of human neuroblastoma SH-SY5Y cells after differentiation into mature neuronal cells. *The Botulinum Journal,* 2(1), 30-48.

RASETTI-ESCARGUEIL, C. & POPOFF, M. R. 2022. Recent Developments in Botulinum Neurotoxins Detection. *Microorganisms,* 10.

REYNOLDS, C., TOMAYKO, M., DONNER, L., HELSON, L., SEEGER, R. C., TRICHE, T. J., and BRODEUR, G. 1988. Biological Classification of cell lines derived from human extra-cranial neural tumors. *Prog. Clin. Biolog. Res*. 271, 291-306.

RICKMAN, C. & DAVLETOV, B. 2003. Mechanism of calcium-independent synaptotagmin binding to target SNAREs. *Journal of Biological Chemistry,* 278**,** 5501-5504.

ROSSETTO, O. 2012. Biohazards of Botulinum Neurotoxins. *Toxicon,* 60**,** 99-99.

ROSSETTO, O., MEGIGHIAN, A., SCORZETO, M. & MONTECUCCO, C. 2013a. Botulinum neurotoxins. *Toxicon,* 67**,** 31-36.

ROSSETTO, O., SCORZETO, M., MEGIGHIAN, A. & MONTECUCCO, C. 2013b. Tetanus neurotoxin. *Toxicon,* 66**,** 59-63.

ROSSI, R., ARJMAND, S., BAERENTZEN, S. L., GJEDDE, A. & LANDAU, A. M. 2022. Synaptic Vesicle Glycoprotein 2A: Features and Functions. *Frontiers in Neuroscience,* 16.

RUMMEL, A. 2017. Two Feet on the Membrane: Uptake of Clostridial Neurotoxins. *Uptake and Trafficking of Protein Toxins,* 406**,** 1-37.

RUMMEL, A., BADE, S., ALVES, J., BIGALKE, H. & BINZ, T. 2003. Two carbohydrate binding sites in the H-cc-domain of tetanus neurotoxin are required for toxicity. *Journal of Molecular Biology,* 326**,** 835-847.

RUST, A., DORAN, C., HART, R., BINZ, T., STICKINGS, P., SESARDIC, D., PEDEN, A. A. & DAVLETOV, B. 2017. A Cell Line for Detection of Botulinum Neurotoxin Type B. *Frontiers in Pharmacology,* 8.

RUST, A., LEESE, C., BINZ, T. & DAVLETOV, B. 2016. Botulinum neurotoxin type C protease induces apoptosis in differentiated human neuroblastoma cells. *Oncotarget,* 7**,** 33220-33228.

SCARLATOS, A., WELT, B. A., COOPER, B. Y., ARCHER, D., DEMARSE, T. & CHAU, K. V. 2005. Methods for detecting botulinum toxin with applicability to screening foods against biological terrorist attacks. *Journal of Food Science,* 70**,** R121-R130.

SCHANTZ, E. J. & JOHNSON, E. A. 1992. PROPERTIES AND USE OF BOTULINUM TOXIN AND OTHER MICROBIAL NEUROTOXINS IN MEDICINE. *Microbiological Reviews,* 56**,** 80-99.

SCHENKE, M., SCHJEIDE, B. M., PUSCHEL, G. P. & SEEGER, B. 2020. Analysis of Motor Neurons Differentiated from Human Induced Pluripotent Stem Cells for the Use in Cell-Based Botulinum Neurotoxin Activity Assays. *Toxins,* 12.

SESARDIC, D., LEUNG, T. & DAS, R. G. 2003. Role for standards in assays of botulinum toxins: international collaborative study of three preparations of botulinum type A toxin. *Biologicals,* 31**,** 265-276.

SHASTRY, P., BASU, A. & RAJADHYAKSHA, M. S. 2001. Neuroblastoma cell lines - a versatile in vitro model in neurobiology. *International Journal of Neuroscience,* 108**,** 109-126.

SHIPLEY, M. M., MANGOLD, C. A. & SZPARA, M. L. 2016. Differentiation of the SH-SY5Y Human Neuroblastoma Cell Line. *Jove-Journal of Visualized Experiments*.

STAHL, A. M., RUTHEL, G., TORRES-MELENDEZ, E., KENNY, T. A., PANCHAL, R. G. & BAVARI, S. 2007. Primary cultures of embryonic chicken neurons for sensitive cell-based assay of botulinum neurotoxin: Implications for therapeutic discovery. *Journal of Biomolecular Screening,* 12**,** 370-377.

STAHL, C., UNGER, L., MAZUET, C., POPOFF, M., STRAUB, R. & FREY, J. 2009. Immune response of horses to vaccination with the recombinant Hc domain of botulinum neurotoxin types C and D. *Vaccine,* 27**,** 5661-5666.

STENMARK, P., DUPUY, J., IMAMURA, A., KISO, M. & STEVENS, R. C. 2008. Crystal structure of botulinum neurotoxin type a in complex with the cell surface co-receptor GT1b - Insight into the toxin-neuron interaction. *Plos Pathogens,* 4.

STERN, D., VON BERG, L., SKIBA, M., DORNER, M. B. & DORNER, B. G. 2018. Replacing the mouse bioassay for diagnostics and potency testing of botulinum neurotoxins - progress and challenges. *Berliner Und Munchener Tierarztliche Wochenschrift,* 131**,** 375-394.

STROTMEIER, J., GU, S. Y., JUTZI, S., MAHRHOLD, S., ZHOU, J., PICH, A., EICHNER, T., BIGALKE, H., RUMMEL, A., JIN, R. S. & BINZ, T. 2011. The biological activity of botulinum neurotoxin type C is dependent upon novel types of ganglioside binding sites. *Molecular Microbiology,* 81**,** 143-156.

STROTMEIER, J., LEET, K., VOLKER, A. K., MAHRHOLD, S., ZONG, Y. N., ZEISER, J., ZHOU, J., PICH, A., BIGALKE, H., BINZ, T., RUMMEL, A. & JIN, R. S. 2010. Botulinum neurotoxin serotype D attacks

neurons via two carbohydrate-binding sites in a ganglioside-dependent manner. *Biochemical Journal,* 431**,** 207-216.

STROTMEIER, J., WILLJES, G., BINZ, T. & RUMMEL, A. 2012. Human synaptotagmin-II is not a high affinity receptor for botulinum neurotoxin B and G: Increased therapeutic dosage and immunogenicity. *Febs Letters,* 586**,** 310-313.

SWAMINATHAN, S. & ESWARAMOORTHY, S. 2000. Structural analysis of the catalytic and binding sites of Clostridium botulinum neurotoxin B. *Nature Structural Biology,* 7**,** 693-699.

TAYLOR, K., GERICKE, C. & ALVAREZ, L. R. 2019. Botulinum Toxin Testing on Animals is Still a Europe-Wide Issue. *Altex-Alternatives to Animal Experimentation,* 36**,** 81-90.

TEGENGE, M. A., BOHNEL, H., GESSLER, F. & BICKER, G. 2012. Neurotransmitter Vesicle Release from Human Model Neurons (NT2) is Sensitive to Botulinum Toxin A. *Cellular and Molecular Neurobiology,* 32**,** 1021-1029.

TIAN, R. M., WIDEL, M. & IMANIAN, B. 2022. The Light Chain Domain and Especially the C-Terminus of Receptor-Binding Domain of the Botulinum Neurotoxin (BoNT) Are the Hotspots for Amino Acid Variability and Toxin Type Diversity. *Genes,* 13.

TSUKAMOTO, K., ARIMITSU, H., OCHI, S., NAKAMURA, K., TANAKA, Y., NUEMKET, N., TANIGUCHI, K., KOZAKI, S. & TSUJI, T. 2012. P19 embryonal carcinoma cells exhibit high sensitivity to botulinum type C and D/C mosaic neurotoxins. *Microbiology and Immunology,* 56**,** 664-672.

TSUKAMOTO, K., KOHDA, T., MUKAMOTO, M., TAKEUCHI, K., IHARA, H., SAITO, M. & KOZAKI, S. 2005. Binding of Clostridium botulinum type C and D neurotoxins to ganglioside and phospholipid - Novel insights into the receptor for clostridial neurotoxins. *Journal of Biological Chemistry,* 280**,** 35164-35171.

TURTON, K., CHADDOCK, J. A. & ACHARYA, K. R. 2002. Botulinum and tetanus neurotoxins: structure, function and therapeutic utility. *Trends in Biochemical Sciences,* 27**,** 552-558.

WANG, M., GU, X., HUANG, X., ZHANG, Q., CHEN, X. Z. & WU, J. 2019. STX1A gene variations contribute to the susceptibility of children attention-deficit/hyperactivity disorder: a case-control association study. *European Archives of Psychiatry and Clinical Neuroscience,* 269**,** 689-699.

WHITEMARSH, R. C. M., PIER, C. L., TEPP, W. H., PELLETT, S. & JOHNSON, E. A. 2012a. Model for studying Clostridium botulinum neurotoxin using differentiated motor neuron-like NG108-15 cells. *Biochemical and Biophysical Research Communications,* 427**,** 426-430.

WHITEMARSH, R. C. M., STRATHMAN, M. J., CHASE, L. G., STANKEWICZ, C., TEPP, W. H., JOHNSON, E. A. & PELLETT, S. 2012b. Novel Application of Human Neurons Derived from Induced Pluripotent Stem Cells for Highly Sensitive Botulinum Neurotoxin Detection. *Toxicological Sciences,* 126**,** 426-435.

WHITEMARSH, R. C. M., TEPP, W. H., BRADSHAW, M., LIN, G. Y., PIER, C. L., SCHERF, J. M., JOHNSON, E. A. & PELLETT, S. 2013. Characterization of Botulinum Neurotoxin A Subtypes 1 Through 5 by Investigation of Activities in Mice, in Neuronal Cell Cultures, and In Vitro. *Infection and Immunity,* 81**,** 3894-3902.

WILD, E., BONIFAS, U., KLIMEK, J., TROSEMEIER, J. H., KRAMER, B., KEGEL, B. & BEHRENSDORF-NICOL, H. A. 2016. In vitro potency determination of botulinum neurotoxin B based on its receptor-binding and proteolytic characteristics. *Toxicology in Vitro,* 34**,** 97-104.

YADIRGI, G., STICKINGS, P., RAJAGOPAL, S., LIU, Y. & SESARDIC, D. 2017. Immuno-detection of cleaved SNAP-25 from differentiated mouse embryonic stem cells provides a sensitive assay for determination of botulinum A toxin and antitoxin potency. *Journal of Immunological Methods,* 451**,** 90-99.

YEH, F. L., DONG, M., YAO, J., TEPP, W. H., LIN, G. Y., JOHNSON, E. A. & CHAPMAN, E. R. 2010. SV2 Mediates Entry of Tetanus Neurotoxin into Central Neurons. *Plos Pathogens,* 6.

YOWLER, B. C., KENSINGER, R. D. & SCHENGRUND, C. L. 2002. Botulinum neurotoxin A activity is dependent upon the presence of specific gangliosides in neuroblastoma cells expressing synaptotagmin I. *Journal of Biological Chemistry,* 277**,** 32815-32819.

YU, R. K., TSAI, Y. T., ARIGA, T. & YANAGISAWA, M. 2011. Structures, Biosynthesis, and Functions of Gangliosides-an Overview. *Journal of Oleo Science,* 60**,** 537-544.

ZHANG, C. M., IMOTO, Y., HIKIMA, T. & INOUE, T. 2021. Structural flexibility of the tetanus neurotoxin revealed by crystallographic and solution scattering analyses. *Journal of Structural Biology-X,* 5.

ZHANG, S. C., BERNTSSON, R. P. A., TEPP, W. H., TAO, L., JOHNSON, E. A., STENMARK, P. & DONG, M. 2017. Structural basis for the unique ganglioside and cell membrane recognition mechanism of botulinum neurotoxin DC. *Nature Communications,* 8.

ZHOU, S., CHEN, S., PEI, Y. A. & PEI, M. 2022. Nidogen: A matrix protein with potential roles in musculoskeletal tissue regeneration. *Genes & Diseases,* 9**,** 598-609.

ZUVERINK, M. & BARBIERI, J. T. 2018. Protein Toxins That Utilize Gangliosides as Host Receptors. *In:* SCHNAAR, R. L. & LOPEZ, P. H. H. (eds.) *Gangliosides in Health and Disease.* San Diego: Elsevier Academic Press Inc.